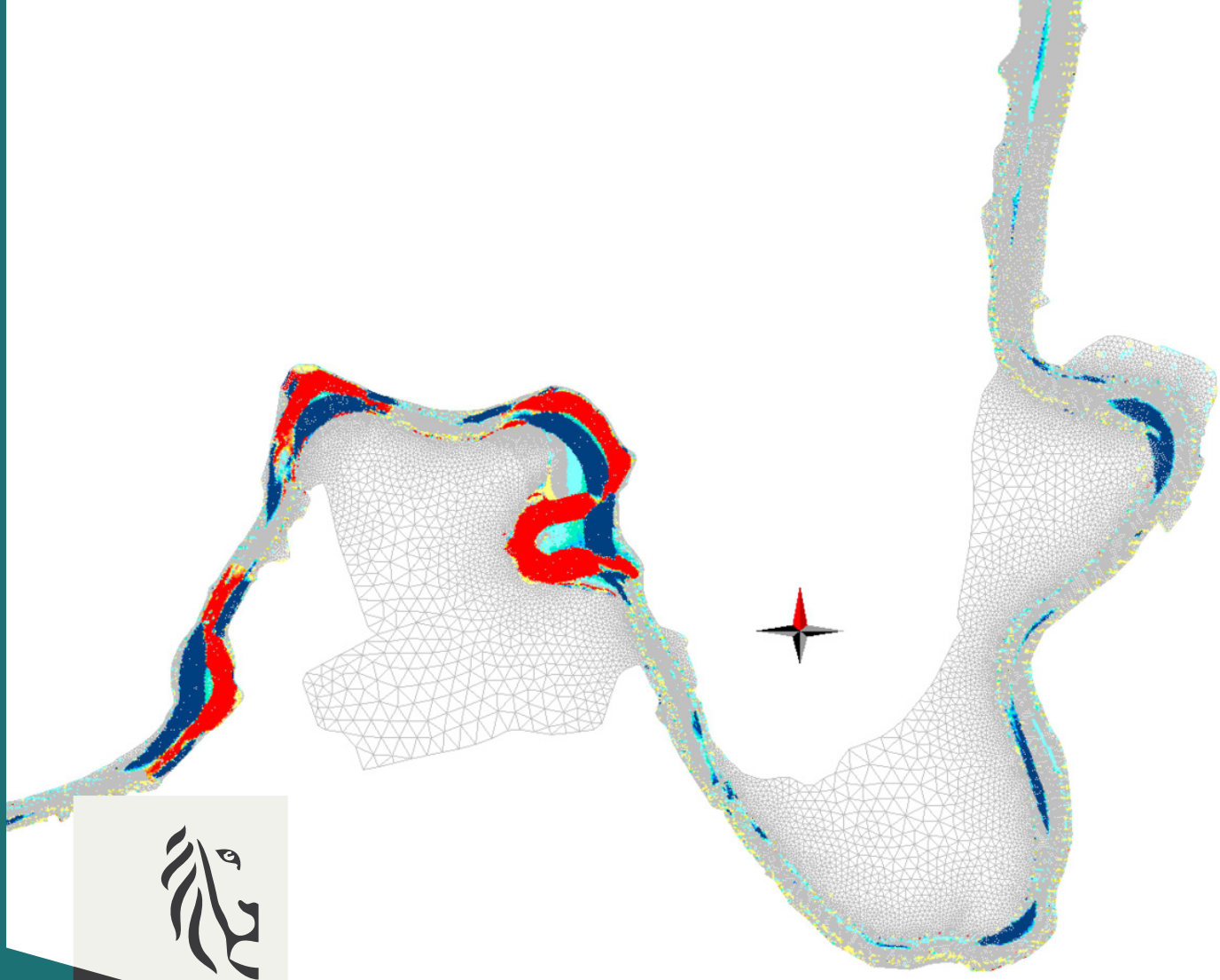

Flanders
State of
the Art

13_131_7
FHR reports

Integraal Plan Bovenzeeschelde

Sub report 7
Effect of B-alternatives on Hydrodynamics

DEPARTMENT
**MOBILITY &
PUBLIC
WORKS**

www.flandershydraulicsresearch.be

Integraal Plan Bovenzeeschelde

Sub report 7 – Effect of the B-alternatives on the Hydrodynamics

Hassan, W.; Maximova, T.; Bi, Q.; Smolders, S.; Vanlede, J.; Mostaert, F.

Flanders Hydraulics Research
Flanders State of the Art

Cover figure © The Government of Flanders, Department of Mobility and Public Works, Flanders Hydraulics Research

Legal notice

Flanders Hydraulics Research is of the opinion that the information and positions in this report are substantiated by the available data and knowledge at the time of writing.
The positions taken in this report are those of Flanders Hydraulics Research and do not reflect necessarily the opinion of the Government of Flanders or any of its institutions.
Flanders Hydraulics Research nor any person or company acting on behalf of Flanders Hydraulics Research is responsible for any loss or damage arising from the use of the information in this report.

Copyright and citation

© The Government of Flanders, Department of Mobility and Public Works, Flanders Hydraulics Research 2019
D/2018/3241/235

This publication should be cited as follows:

Hassan, W.; Maximova, T.; Bi, Q.; Smolders, S.; Vanlede, J.; Mostaert, F. (2019). Integraal Plan Bovenzeeschelde: Sub report 7 – Effect of the B-alternatives on the Hydrodynamics. Version 2.0. FHR Reports, 13_131_7. Flanders Hydraulics Research: Antwerp.

Reproduction of and reference to this publication is authorised provided the source is acknowledged correctly.

Document identification

Customer:	Flanders Hydraulics Research	Ref.:	WL2019R13_131_7
Keywords (3-5):	Scaldis-model, Scheldt estuary, Hydrodynamics, Telemac, Tidal Asymmetry		
Text (p.):	62	Appendices (p.):	78
Confidentiality:	☒ No	☒ Available online	

Author(s):	Hassan, W.; Maximova, T.; Bi, Q.

Control

	Name	Signature
Reviser(s):	Smolders, S.	Getekend door: Sven Smolders (Signature) Getekend op: 2019-02-11 12:58:24 +01:00 Reden: Ik keur dit document goed Sven Smolders
Project leader:	Vanlede, J.	Getekend door: Joris Vanlede (Signature) Getekend op: 2019-02-15 14:24:22 +01:00 Reden: Ik keur dit document goed Joris Vanlede

Approval

Head of Division:	Mostaert, F.	Getekend door: Frank Mostaert (Signature) Getekend op: 2019-02-18 08:47:05 +01:00 Reden: Ik keur dit document goed Frank Mostaert

CERTIFIED LR ISO 9001

Abstract

The Scaldis-model of the tidal Scheldt estuary is used to analyze the effects of several bathymetry alternatives (different alternatives of the Scheldt were studied under different boundary conditions). The alternatives are studied in a future reference situation (2050). The Scaldis model is calibrated for 2013 (Smolders et al., 2016). The implementation of the future reference situation (2050) is described in more detail in Smolders et al. (2017). This report describes the effect on the hydrodynamics of three alternatives (VaG, VaH, Chafing) in the bathymetry of the model.

The model results are analysed in terms of water levels, harmonic components, discharges, and tidal asymmetry. A first comparison between Scaldis-model results and the 1D-model from the “Bouwstenenonderzoek” (IMDC,2018) is also presented in this report.

Contents

Abstract III
Contents V
List of tables VIII
List of figures IX
1 Units and reference plane 1
2 Bathymetry 2
2.1 Bathymetry Updates from Scaldis_2013 to Scaldis_2050_REF 2
2.1.1 Sustainable bathymetry 2
2.1.2 Durme 4
2.1.3 Heusden 4
2.1.4 Groyne at Fort Filip 5
2.2 Bathymetry of alternatives 6
2.2.1 The VaG-alternative 6
2.2.2 The Chafing-alternative 6
2.2.3 The VaH-alternative 6
3 Hydrodynamic scenarios 7
3.1 Normal (QN) and Events (QE) discharge scenarios 7
3.2 Tidal range scenarios 8
3.3 Sea level rise scenarios 9
3.4 List of model runs 9
4 Methodology of determining hydrodynamic effect 11
4.1 Combination of 4QN+QE runs 11
4.2 Water Levels and Harmonic Components 11
4.3 Discharge 12
4.4 Tidal asymmetry 14
4.4.1 Tidal asymmetry associated with duration 15
4.4.2 Tidal asymmetry associated with the magnitudes of maximum flood and maximum ebb velocities 16
4.4.3 Interpretation 17
5 Results 18
5.1 Effect of VaG 18
5.1.1 Water levels 18
5.1.2 Harmonic components 20

5.1.3 Discharge 24
5.2 Effect of VaH 26
5.2.1 Water levels 26
5.2.2 Harmonic components 28
5.2.3 Discharge 32
5.2.4 Tidal asymmetry 33
5.3 Effect of Chafing 35
5.3.1 Water levels 35
5.3.2 Harmonic components 36
5.3.3 Discharge 40
5.3.4 Tidal asymmetry 41
6 Comparison between Scaldis and the 1D-model results 43
6.1 VAG alternative 43
6.2 Chafing alternative 52
7 Conclusions 59
8 References 62
Appendix 1: Difference in bathymetry alternatives A1
VaG vs Reference 2050 ..... A1
VaH vs Reference 2050 ..... A4
Chafing vs Reference 2050 ..... A7
Appendix 2: Effect of VaG A10
A0CH runs A10
Water levels A10
Harmonic components A11
Discharges A14
A0CL runs A15
Water levels A15
Harmonic components A16
Discharges A19
AplusCH runs A20
Water levels A20
Harmonic components A21
Discharges A24
AminCL runs A25
Water levels A25
Harmonic components A26
Discharges A29

Tidal asymmetry in runs with different boundary conditions A30
Appendix 3: Effect of VaH A33
A0CH runs A33
Water levels A33
Harmonic components A34
Discharges A37
A0CL runs A38
Water levels A38
Harmonic components A39
Discharges A42
AplusCH runs A43
Water levels A43
Harmonic components A44
Discharges A47
AminCL runs A48
Water levels A48
Harmonic components A49
Tidal asymmetry in runs with different boundary conditions A53
Appendix 4: Effect of Chafing A56
A0CH runs A56
Water levels A56
Harmonic components A57
Discharges A60
A0CL runs A61
Water levels A61
Harmonic components A62
Discharges A65
AplusCH runs A66
Water levels A66
Harmonic components A67
Discharges A70
AminCL runs A71
Water levels A71
Harmonic components A72
Discharges A75
Tidal asymmetry in runs with different boundary conditions A76

List of tables

Table 1 – Tidal range scenarios 8
Table 2 – List of different scenario runs 10
Table 3 – Comparison between Scaldis-model and the 1D-model, VaG alternative 44
Table 4 – Comparison between Scaldis-model and the 1D-model, VaG alternative. 52
Table 5 – Statistical parameters of HW, LW and complete time series of water levels A10
Table 6 – Statistical parameters of complete discharge time series VaG A0CH vs Reference A0CH A14
Table 7 – Statistical parameters of HW, LW and complete time series of water levels A15
Table 8 – Statistical parameters of complete discharge time series VaG A0CL vs Reference A0CL A19
Table 9 – Statistical parameters of HW, LW and complete time series of water levels A20
Table 10 – Statistical parameters of complete discharge time series VaG AplusCH vs Reference AplusCH. A24
Table 11 – Statistical parameters of HW, LW and complete time series of water levels A25
Table 12 – Statistical parameters of complete discharge time series VaG AminCL vs Reference AminCL ... A29
Table 13 – Statistical parameters of HW, LW and complete time series of water levels A33
Table 14 – Statistical parameters of complete discharge time series VaH A0CH vs Reference A0CH A37
Table 15 – Statistical parameters of HW, LW and complete time series of water levels A38
Table 16 – Statistical parameters of complete discharge time series VaH_A0CL vs Reference_A0CL A42
Table 17 – Statistical parameters of HW, LW and complete time series of water levels A43
Table 18 – Statistical parameters of complete discharge time series VaH AplusCH vs Reference AplusCH. A47
Table 19 – Statistical parameters of HW, LW and complete time series of water levels A48
Table 20 – Statistical parameters of complete discharge time series VaH AminCL vs Reference AminCL ... A52
Table 21 – Statistical parameters of HW, LW and complete time series of water levels A56
Table 22 – Statistical parameters of complete discharge time series Chafing A0CH vs Reference A0CH A60
Table 23 – Statistical parameters of HW, LW and complete time series of water levels A61
Table 24 – Statistical parameters of complete discharge time series Chafing A0CL vs Reference A0CL A65
Table 25 – Statistical parameters of HW, LW and complete time series of water levels A66
Table 26 – Statistical parameters of complete discharge time series Chafing AplusCH vs Reference AplusCH A70
Table 27 – Statistical parameters of HW, LW and complete time series of water levels (Chafing_AminCL - Reference_AminCL) A71
Table 28 – Statistical parameters of complete discharge time series Chafing AminCL vs Reference AminCL A75

List of figures

Figure 1 – Sustainable bathymetry, Upper Sea Scheldt and the Ringvaart (mTAW) 2
Figure 2 – Depth difference map of changes implemented in the sustainable bathymetry near Uitbergen (m) 3
Figure 3 – Depth difference map of changes implemented in the sustainable bathymetry near Wichelen (m) 3
Figure 4 – New bathymetry at Durme (mTAW) 4
Figure 5 – New bathymetry at Heusden (mTAW) 4
Figure 6 – Bathymetry near the groin at Fort Filip in Scaldis-model 2013 (mTAW) 5
Figure 7 – Bathymetry near the groin at Fort Filip in Scaldis-model 2050 (mTAW) 5
Figure 8 – Zones of the bathymetric analysis 6
Figure 12 – 10-year average tidal range between 1901 and 2010. (Kuijper, 2013) 8
Figure 13 – Location of cross-sections along the estuary until Liefkenshoek 13
Figure 14 – Location of cross-sections along the estuary from Liefkenshoek to Melle 14
Figure 15 – Bias of high water magnitude in VaG starting from Nieuwpoort 19
Figure 16 – Bias of high water magnitude in VaG starting from Antwerp 19
Figure 17 – Bias of low water magnitude in VaG 20
Figure 18 – Bias of complete water level time series in VaG 20
Figure 19 – Bias of Amplitude M2 in VaG 21
Figure 20 – Bias of Phase M2 in VaG 21
Figure 21 – Bias of Amplitude M4 in VaG 22
Figure 22 – Bias of Phase M4 in VaG 22
Figure 23 – Bias of Amplitude S2 in VaG 23
Figure 24 – Bias of Phase S2 in VaG 23
Figure 25 – ‘Signed’ relative RMSE of complete discharge time series of VaG alternative 24
Figure 26 – Effect on the tidal asymmetry (VaG vs Reference) 26
Figure 27 – Bias of high water magnitude in VaH 27
Figure 28 – Bias of low water magnitude in VaH 27
Figure 29 – Bias of complete water level time series in VaH 28
Figure 30 – Bias of Amplitude M2 in VaH 29
Figure 31 – Bias of Phase M2 in VaH 29
Figure 32 – Bias of Amplitude M4 in VaH 30
Figure 33 – Bias of Phase M4 in VaH 30
Figure 34 – Bias of Amplitude S2 in VaH 31
Figure 35 – Bias of Phase S2 in VaH 31

Figure 36 – 'Signed' relative RMSE of complete discharge time series of VaH alternative 32
Figure 37 – Effect on the tidal asymmetry (VaH vs Reference)..... 34
Figure 38 – Bias of high water magnitude in Chafing..... 35
Figure 39 – Bias of low water magnitude in Chafing..... 36
Figure 40 – Bias of complete water level time series in Chafing..... 36
Figure 41 – Bias of Amplitude M2 in Chafing 37
Figure 42 – Bias of Phase M2 in Chafing..... 37
Figure 43 – Bias of Amplitude M4 in Chafing 38
Figure 44 – Bias of Phase M4 in Chafing..... 38
Figure 45 – Bias of Amplitude S2 in Chafing..... 39
Figure 46 – Bias of Phase S2 in Chafing 39
Figure 47 – 'Signed' relative RMSE of complete discharge time series of Chafing alternative..... 40
Figure 48 – Effect on the tidal asymmetry (Chafing vs Reference) 42
Figure 49 – Relative changes of HW and LW (VaG vs Reference) as computed using the Scaldis-model (upper panel) and the 1D-model (lower panel) 47
Figure 50 – Relative changes of Tincrease and Tdecrease (VaG vs Reference) as computed using the Scaldis-model (upper panel) and the 1D-model (lower panel) 48
Figure 51 – Relative changes of Vmax flood and Vmax ebb (VaG vs Reference) as computed using the Scaldis-model (upper panel) and the 1D-model (lower panel) 49
Figure 52 – Relative changes of relative tidal amplitude (VaG vs Reference) as computed using the Scaldis-model (upper panel) and the 1D-model (lower panel) 50
Figure 53 – Relative changes of Tflood/Tebb (VaG vs Reference) as computed using the Scaldis-model (upper panel) and the 1D-model (lower panel) 51
Figure 54 – Relative changes of HW and LW (Chafing vs Reference) as computed using the Scaldis-model (upper panel) and the 1D-model (lower panel) 54
Figure 55 – Relative changes of Tincrease and Tdecrease (Chafing vs Reference) as computed using the Scaldis-model (upper panel) and the 1D-model (lower panel) 55
Figure 56 – Relative changes of Vmax flood and Vmax ebb (Chafing vs Reference) as computed using the Scaldis-model (upper panel) and the 1D-model (lower panel) 56
Figure 57 – Relative changes of relative tidal amplitude (Chafing vs Reference) as computed using the Scaldis-model (upper panel) and the 1D-model (lower panel) 57
Figure 58 – Relative changes of Tflood/Tebb (Chafing vs Reference) as computed using the Scaldis-model (upper panel) and the 1D-model (lower panel) 58
Figure 59 – Difference in bathymetry (VaG – Reference 2050) in zone 1..... A1
Figure 60 – Difference in bathymetry (VaG – Reference 2050) in zone 2..... A1
Figure 61 – Difference in bathymetry (VaG – Reference 2050) in zone 3..... A2
Figure 62 – Difference in bathymetry (VaG – Reference 2050) in zone 4..... A2
Figure 63 – Difference in bathymetry (VaG – Reference 2050) in zone 5..... A3
Figure 64 – Difference in bathymetry (VaG – Reference 2050) in zone 6..... A3
Figure 65 – Difference in bathymetry (VaH – Reference 2050) in zone 1..... A4

Figure 66 – Difference in bathymetry (VaH – Reference 2050) in zone 2 ..... A4
Figure 67 – Difference in bathymetry (VaH – Reference 2050) in zone 3 ..... A5
Figure 68 – Difference in bathymetry (VaH – Reference 2050) in zone 4 ..... A5
Figure 69 – Difference in bathymetry (VaH – Reference 2050) in zone 5 ..... A6
Figure 70 – Difference in bathymetry (VaH – Reference 2050) in zone 6 ..... A6
Figure 71 – Difference in bathymetry (Chafing – Reference 2050) in zone 1 ..... A7
Figure 72 – Difference in bathymetry (Chafing – Reference 2050) in zone 2 ..... A7
Figure 73 – Difference in bathymetry (Chafing – Reference 2050) in zone 3 ..... A8
Figure 74 – Difference in bathymetry (Chafing – Reference 2050) in zone 4 ..... A8
Figure 75 – Difference in bathymetry (Chafing – Reference 2050) in zone 5 ..... A9
Figure 76 – Difference in bathymetry (Chafing – Reference 2050) in zone 6 ..... A9
Figure 77 – M2 amplitude in VaG A0CH and Reference_A0CH A11
Figure 78 – M2 phase in VaG A0CH and Reference_A0CH A11
Figure 79 – M4 amplitude in VaG A0CH and Reference_A0CH A12
Figure 80 – M4 phase in VaG A0CH and Reference_A0CH A12
Figure 81 – S2 amplitude in VaG A0CH and Reference_A0CH A13
Figure 82 – S2 phase in VaG A0CH and Reference_A0CH A13
Figure 83 – M2 amplitude in VaG_A0CL and Reference_A0CL A16
Figure 84 – M2 phase in VaG_A0CL and Reference_A0CL A16
Figure 85 – M4 amplitude in VaG_A0CL and Reference_A0CL A17
Figure 86 – M4 phase in VaG_A0CL and Reference_A0CL A17
Figure 87 – S2 amplitude in VaG_A0CL and Reference_A0CL A18
Figure 88 – S2 phase in VaG_A0CL and Reference_A0CL A18
Figure 89 – M2 amplitude in VaG AplusCH and Reference AplusCH A21
Figure 90 – M2 phase in VaG AplusCH and Reference AplusCH A21
Figure 91 – M4 amplitude in VaG AplusCH and Reference AplusCH A22
Figure 92 – M4 phase in VaG AplusCH and Reference AplusCH A22
Figure 93 – S2 amplitude in VaG AplusCH and Reference AplusCH A23
Figure 94 – S2 phase in VaG AplusCH and Reference AplusCH A23
Figure 95 – M2 amplitude in VaG AminCL and Reference AminCL A26
Figure 96 – M2 phase in VaG AminCL and Reference AminCL A26
Figure 97 – M4 amplitude in VaG AminCL and Reference AminCL A27
Figure 98 – M4 phase in VaG AminCL and Reference AminCL A27
Figure 99 – S2 amplitude in VaG AminCL and Reference AminCL A28
Figure 100 – S2 phase in VaG AminCL and Reference AminCL A28
Figure 101 – Tidal asymmetry (Tincrease/Tdecrease water level) in VaG and Reference runs A30
Figure 102 – Tidal asymmetry (Tflood/Tebb) in VaG and Reference runs A30

Figure 103 – Tidal asymmetry (Vmax flood/Vmax ebb) in VaG and Reference runs A31
Figure 104 – Tidal asymmetry (based on V^3) in VaG and Reference runs A31
Figure 105 – Tidal asymmetry (based on V^4) in VaG and Reference runs A32
Figure 106 – M2 amplitude in VaH A0CH and Reference A0CH A34
Figure 107 – M2 phase in VaH A0CH and Reference A0CH A34
Figure 108 – M4 amplitude in VaH A0CH and Reference A0CH A35
Figure 109 – M4 phase in VaH A0CH and Reference A0CH A35
Figure 110 – S2 amplitude in VaH A0CH and Reference A0CH A36
Figure 111 - S2 phase in VaH A0CH and Reference A0CH A36
Figure 112 – M2 amplitude in VaH A0CL and Reference A0CL A39
Figure 113 – M2 phase in VaH A0CL and Reference A0CL A39
Figure 114 – M4 amplitude in VaH A0CL and Reference A0CL A40
Figure 115 – M4 phase in VaH A0CL and Reference A0CL A40
Figure 116 – S2 amplitude in VaH A0CL and Reference A0CL A41
Figure 117 – S2 phase in VaH A0CL and Reference A0CL A41
Figure 118 – M2 amplitude in VaH AplusCH and Reference AplusCH A44
Figure 119 – M2 phase in VaH AplusCH and Reference AplusCH A44
Figure 120 – M4 amplitude in VaH AplusCH and Reference AplusCH A45
Figure 121 – M4 phase in VaH AplusCH and Reference AplusCH A45
Figure 122 – S2 amplitude in VaH AplusCH and Reference AplusCH A46
Figure 123 – S2 phase in VaH AplusCH and Reference AplusCH A46
Figure 124 – M2 amplitude in VaH AminCL and Reference AminCL A49
Figure 125 – M2 phase in VaH AminCL and Reference AminCL A49
Figure 126 – M4 amplitude in VaH AminCL and Reference AminCL A50
Figure 127 – M4 phase in VaH AminCL and Reference AminCL A50
Figure 128 – S2 amplitude in VaH AminCL and Reference AminCL A51
Figure 129 – S2 phase in VaH AminCL and Reference AminCL A51
Figure 130 – Tidal asymmetry (T increase/Tdecrease water level) in VaH and Reference runs A53
Figure 131 – Tidal asymmetry (T flood/T ebb) in VaH and Reference runs A53
Figure 132 – Tidal asymmetry (V max flood/Vmax ebb) in VaH and Reference runs A54
Figure 133 – Tidal asymmetry (based on V^3) in VaH and Reference runs A54
Figure 134 – Tidal asymmetry (based on V^4) in VaH and Reference runs A55
Figure 135 – M2 amplitude in Chafing A0CH and Reference A0CH A57
Figure 136 - M2 phase in Chafing A0CH and Reference A0CH A57
Figure 137 – M4 amplitude in Chafing A0CH and Reference A0CH A58
Figure 138 – M4 phase in Chafing A0CH and Reference A0CH A58
Figure 139 – S2 amplitude in Chafing A0CH and Reference A0CH A59

Figure 140 – S2 phase in Chafing A0CH and Reference A0CH A59
Figure 141 – M2 amplitude in Chafing A0CL and Reference A0CL A62
Figure 142 – M2 phase in Chafing A0CL and Reference A0CL A62
Figure 143 – M4 amplitude in Chafing A0CL and Reference A0CL A63
Figure 144 – M4 phase in Chafing A0CL and Reference A0CL A63
Figure 145 – S2 amplitude in Chafing A0CL and Reference A0CL A64
Figure 146 – S2 phase in Chafing A0CL and Reference A0CL A64
Figure 147 – M2 amplitude in Chafing AplusCH and Reference AplusCH A67
Figure 148 – M2 phase in Chafing AplusCH and Reference AplusCH A67
Figure 149 – M4 amplitude in Chafing AplusCH and Reference AplusCH A68
Figure 150 – M4 phase in Chafing AplusCH and Reference AplusCH A68
Figure 151 – S2 amplitude in Chafing AplusCH and Reference AplusCH A69
Figure 152 – S2 phase in Chafing AplusCH and Reference AplusCH A69
Figure 153 – M2 amplitude in Chafing AminCL and Reference AminCL A72
Figure 154 – M2 phase in Chafing AminCL and Reference AminCL A72
Figure 155 – M4 amplitude in Chafing AminCL and Reference AminCL A73
Figure 156 – M4 phase in Chafing AminCL and Reference AminCL A73
Figure 157 – S2 amplitude in Chafing AminCL and Reference AminCL A74
Figure 158 – S2 phase in Chafing AminCL and Reference AminCL A74
Figure 159 – Tidal asymmetry (T increase/Tdecrease water level) in Chafing and Reference runs A76
Figure 160 – Tidal asymmetry (T flood/T ebb) in Chafing and Reference runs A76
Figure 161 – Tidal asymmetry (V max flood/Vmax ebb) in Chafing and Reference runs A77
Figure 162 – Tidal asymmetry (based on V^3) in Chafing and Reference runs A77
Figure 163 – Tidal asymmetry (based on V^4) in Chafing and Reference runs A78

1 Units and reference plane

Time is expressed in CET (Central European Time).

Depth, height, and water levels are expressed in meter, TAW (Tweede Algemene Waterpassing).

Bathymetry and water levels are positive above the reference plane.

The horizontal coordinate system is RD Paris.

2 Bathymetry

2.1 Bathymetry Updates from Scaldis_2013 to Scaldis_2050_REF

An overview of all bathymetry updates that were implemented in the 2013 Scaldis-model to make the 2050 model are presented in the next subsections. This information is taken from the report Scaldis 2050 (Smolders et al., 2017).

2.1.1 Sustainable bathymetry

The Sustainable Management Plan was developed for a sustainable management of the Upper Sea Scheldt and the Ringvaart. This plan focusses on maintaining the fairway with respect for the tidal nature. The designed bathymetry takes into account the needs for navigation and the characteristics of the river. The impact on the tidal nature is limited to specific areas. The hydrodynamic and morphological processes can develop to the extent that the safety and tidal nature are not endangered. The Management Plan aims to optimize the existing management efforts for navigation and protection of the riverbanks (IMDC, 2015).

The sustainable bathymetry is presented in Figure 1. The sustainable bathymetry only concerns bathymetry of the deeper part of the river channel. The de-embanked areas controlled reduced tide (CRT) and flood control areas (FCA) are today's situation based on Lidar 2013. The expected changes (until 2050) in the bathymetry were implemented in the Scaldis 2050 model (Smolders et al., 2017). To account for the fact that more FCA and CRT areas have become active in the Scaldis 2050 model, the inlet and outlet constructions of these areas are implemented in the model. Furthermore, the bed levels of the de-embanked areas and FCA with CRT were updated to account for sedimentation until 2050.

Figure 1 – Sustainable bathymetry, Upper Sea Scheldt and the Ringvaart (mTAW)

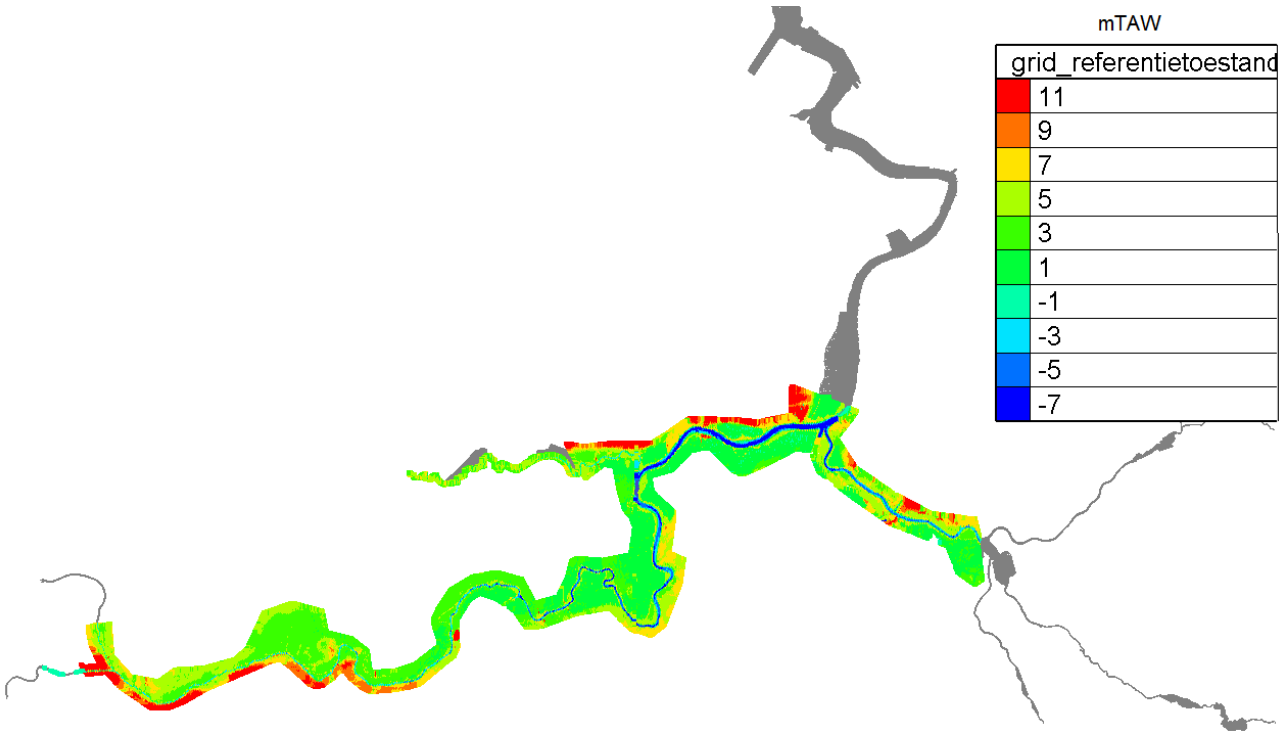

Information about the changes implemented in the sustainable bathymetry can be found in IMDC (2015). In this report, two examples are presented in Figure 2 and Figure 3.

Figure 2 – Depth difference map of changes implemented in the sustainable bathymetry near Uitbergen (m)

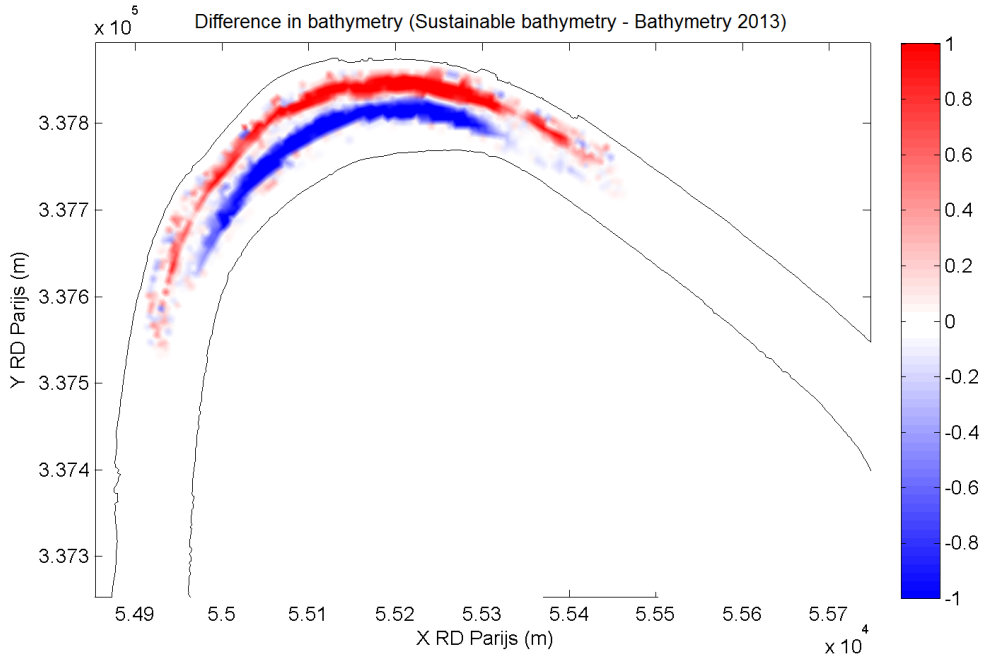

Figure 3 – Depth difference map of changes implemented in the sustainable bathymetry near Wichelen (m)

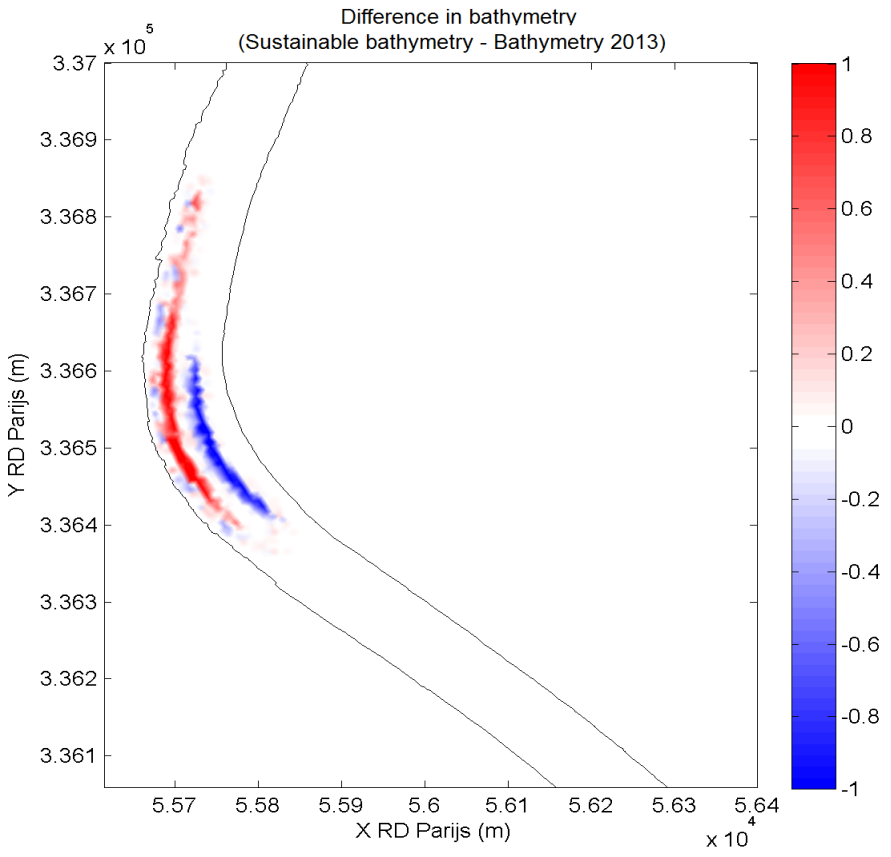

2.1.2 Durme

A new bathymetry is implemented in the Scaldis-model for the Durme as shown in Figure 4.

Figure 4 – New bathymetry at Durme (mTAW)

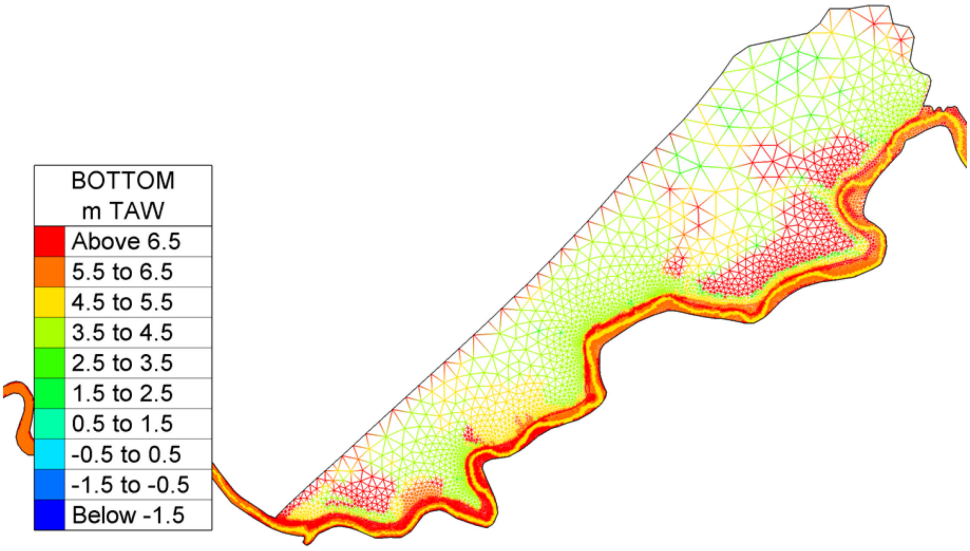

2.1.3 Heusden

Just north of the de-embankment of Heusden, a new sluice will prevent the full tide from penetrating further upstream (Figure 5). Like the FCA area with CRT, this sluice will get bypass culverts to allow part of the tide to pass and to encourage the development of fresh water tidal nature upstream in this tidal arm. A new bathymetry in this tidal arm is also implemented in the model.

Figure 5 – New bathymetry at Heusden (mTAW)

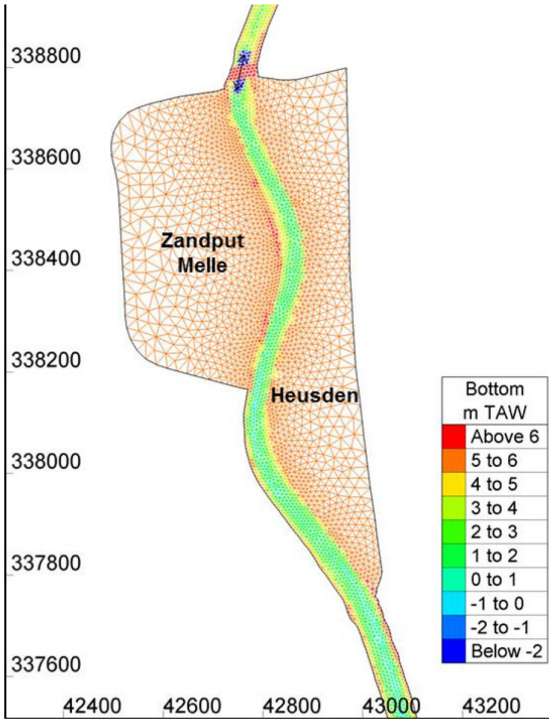

2.1.4 Groyne at Fort Filip

In the coming years, a nature area near Fort Filip is planned and will be made sustainable with the help of a groin. The groin will be constructed with a height of 3.5 m TAW. Sedimentation is expected in this area, so that tidal flats and marshes can develop.

The bathymetry of the area of interest in Scaldis 2013 and 2050 is presented in Figure 6 and Figure 7, respectively. The groin at Fort Filip is included in Scaldis 2050 based on the samples file c4_9422_zone1_kribbe+3.50_RD_TAW.xyz provided by Waterwegen & Zeekanaal of the Flemish government. The groin itself with the expected sedimentation was implemented. This means a single groin will not be visible in the model bathymetry (Figure 7). Different alternatives were tested using the SCALDIS-model. This bathymetry was chosen for future implementation. For more information and the different alternatives, we refer to Maximova et al. (2015).

Figure 6 – Bathymetry near the groin at Fort Filip in Scaldis-model 2013 (mTAW)

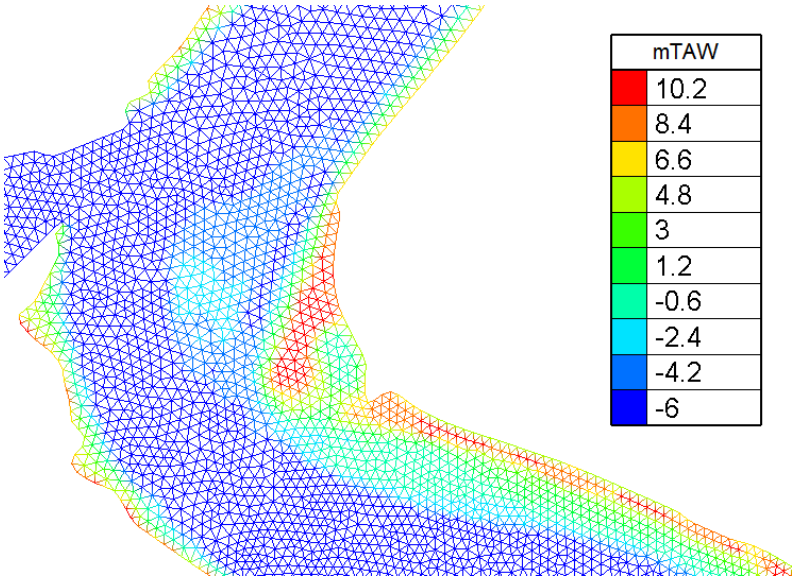

Figure 7 – Bathymetry near the groin at Fort Filip in Scaldis-model 2050 (mTAW)

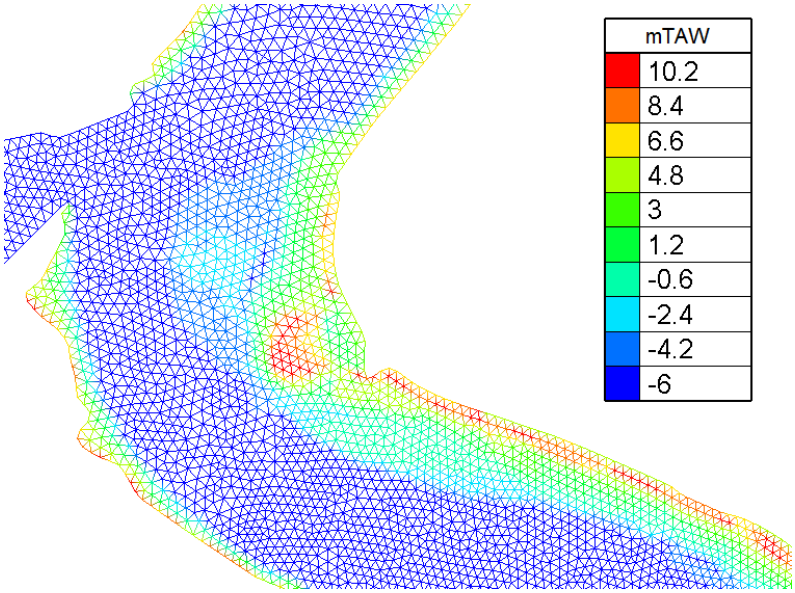

2.2 Bathymetry of alternatives

The B-alternatives have been defined in a preceding study (Bevaarbaarheid van de Boven-Zeeschelde en Zuidelijk vak Ringvaart voor klasse Va-schepen). The B-alternatives consist of three different potential designs

The implemented bathymetry in the Scaldis-model is based on the reference situation 2050. The bathymetry of the deeper part of the river channel of the B alternatives is based on the data provided by IMDC (May 2016) and is interpolated on top of the reference situation.

The differences between these three alternatives and the reference run 2050 are presented in Appendix 1 (Figure 56 to Figure 73) for the six different zones along Sea Scheldt. These six zones are shown in Figure 8.

Figure 8 – Zones of the bathymetric analysis

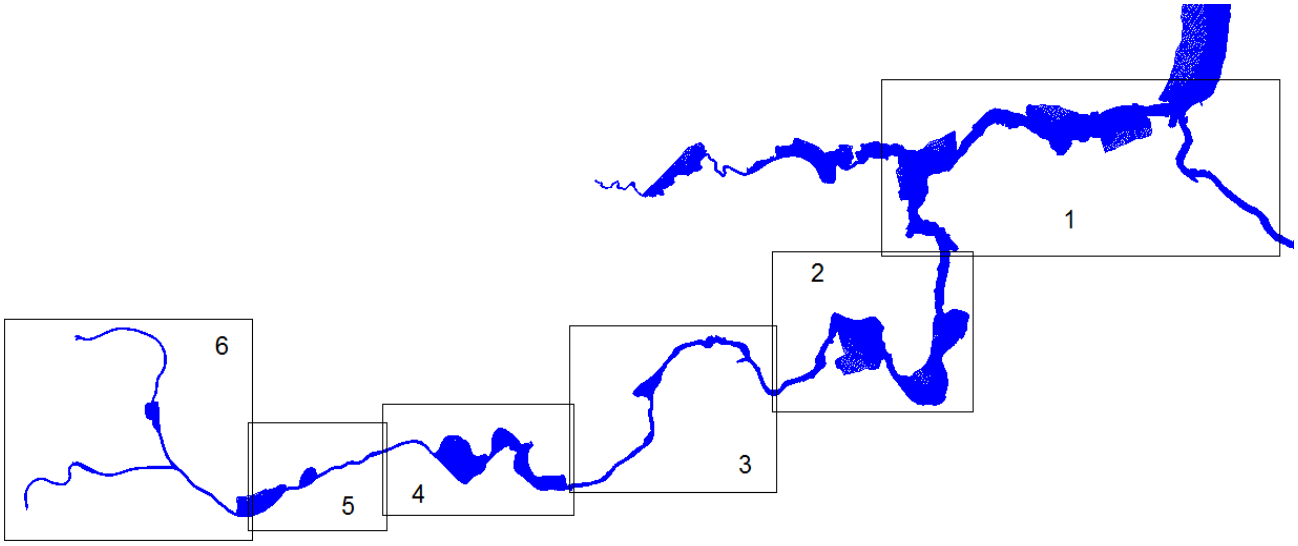

In the following section, a short overview is given of the zones where the most important changes take place.

2.2.1 The VaG-alternative

In the VaG-alternative, different bends are cut off and the navigation channel is also widened at a number of locations: the reclamation at Wijmeers, GOG-GGG Bergenmeersen (Uitbergen), GOG Scheldebroek, The Castle of the Dike and the Pottelbergse Schorren (Grembergen), the Groot Schoor near Vlassenbroek, the Vlassenbroekse Schorren, Uiterdijk, the Cramp and Sint-Amands. Additional modifications to the bathymetry of the Upper Sea Scheldt and the Ringvaart result in additional expansion of the navigation channel.

2.2.2 The Chafing-alternative

In the Chafing-alternative the bathymetry of different curves/bends is adjusted in the Sea Scheldt. For this alternative, the landboundary remains unchanged.

2.2.3 The VaH-alternative

The VaH-alternative combines the above alternatives with interventions by VaG up Wichelen and changes in the bathymetry of the SCHAAF alternative down Wichelen. This hybrid alternative makes maximum use of the existing channel.

3 Hydrodynamic scenarios

The Scaldis-model is used to evaluate the effects of different alternatives (specified bathymetry), under different scenarios (a range of boundary conditions to take into account climate change, sea level rise, increasing or decreasing tidal amplitude and high or low river discharge).

The resulting list of the scenario runs is presented in Table 2.

3.1 Normal (QN) and Events (QE) discharge scenarios

For the ecotope mapping, water level frequencies are required, especially the tails of the distribution of water levels over a year. The limitations on the calculation time (or cost) of the 3D hydrodynamic model forces the use of a different approach than calculating with very long time series.

The bulk of the distribution will be obtained by running the hydrodynamic model for a period of 3 months with a synthetic discharge boundary containing events with a return period equal to or smaller than ¼ year. This is the “normal” discharge scenario (**QN**). The downstream (tidal) boundary is a harmonic boundary without storm surge. The upstream boundary is a synthetic discharge boundary containing events with a return period equal to or smaller than 1/6 year (combined with QE (T1 & T1/2) this results in 6 exceedances of this discharge). The simulation period is 3 months.

Separately, a run of ca. 2 weeks will be run with a discharge timeseries that contains 3 discharge events with return periods of 1 year, ½ year and 1/3 year. Simultaneously, the downward boundary contains a storm surge period that is added to the harmonic signal. This is the “events” (**QE**) discharge scenario. The upstream boundary is a discharge time series that contains 2 discharge events with return periods of 1 year and 1/2 year. The simulation period is 20 days.

The water level distribution in specific points is obtained by adding the 4 x “normal” and 1 x “events” waterlevel scenarios.

The statistical techniques used to determine QN and QE boundary conditions for the 2013 and 2050 conditions are described in IMDC (2015). The implementation of the timeseries described in IMDC (2015) into the boundary conditions for Scaldis is described in chapter 6 of the Scaldis 2050 report (Smolders et al., 2017).

3.2 Tidal range scenarios

To establish the robustness of the predicted effects, the effects of changing the geometry of the Upper Sea Scheldt (the alternatives) is checked in a range of boundary conditions (the scenarios). Because the evolution of tidal range in the estuary is uncertain, a range of tidal amplitudes is considered.

The tidal range in the estuary has increased, and the tidal range maximum has moved upwards in the past decades.

Figure 9 – 10-year average tidal range between 1901 and 2010. (Kuijper, 2013)

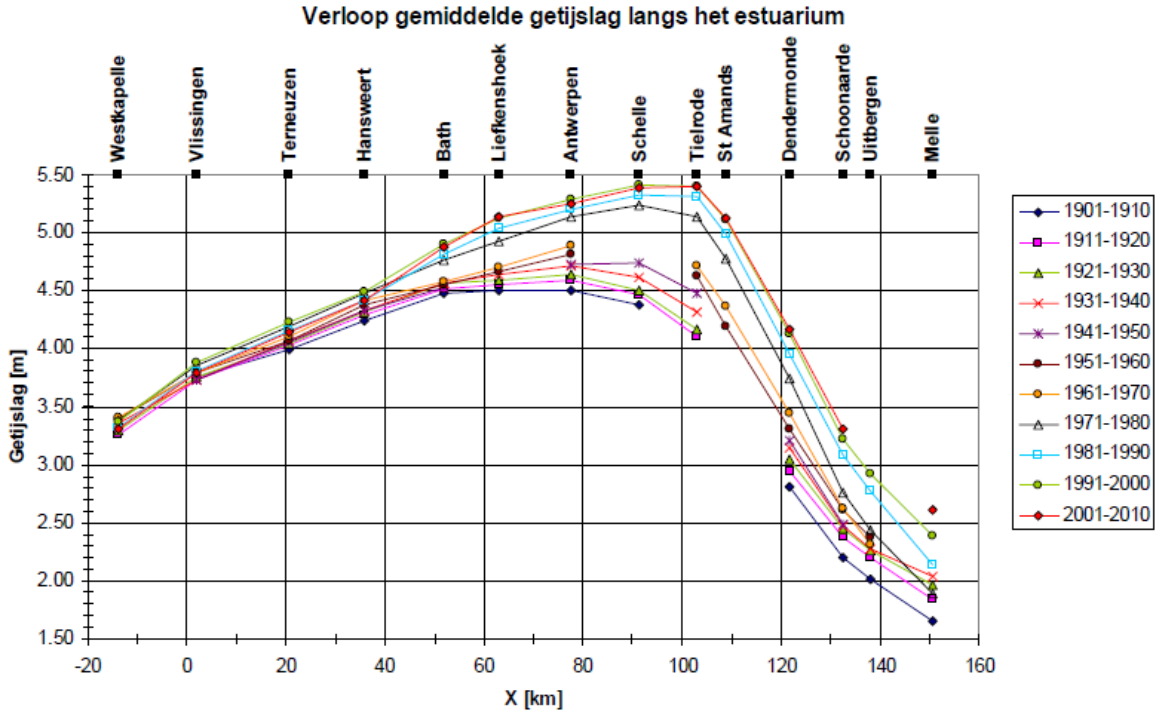

Three different tidal range scenarios A+, A0 and A- have been modeled. In these scenarios, the tidal amplitude at Schelle is equal to 5.70, 5.40 and 5.00 m, respectively, as shown in Table 1.

Table 1 – Tidal range scenarios

Scenario	Tidal amplitude at Schelle (m)
A+	5.70
A0	5.40 (current tidal range)
A-	5.00

The increase and decrease of the amplitude is enforced by changing the roughness in the Western Scheldt. By changing the roughness, the tidal propagation is influenced, without simulating specific measures in the downstream parts of the estuary (e.g. creating additional flooding areas, deepening, etc.)

3.3 Sea level rise scenarios

In KNMI (2014), climate scenarios for the Netherlands have been published for the climate around 2050 and 2085, for four climate change scenarios. The four scenarios are the combination of two extremes in global temperature rise ('moderate' M and 'warm' W) and the two possible atmospheric circulation pattern changes ('low' L and 'high' H). The combinations lead to scenarios indicated as WL, WH, GL and GH.

The climate prediction fork used in the present study could be approached as the extreme values in the four KNMI (2014) scenarios for Sea level rise in the North Sea coast in 2050:

- Scenarios GL, GH; **+15 cm** till + 30 cm (90% conf.int.)
- Scenarios WL, WH; + 20 cm till **+ 40 cm** (90% conf. int.)

The following sea level rise scenarios are modeled in Scaldis for 2050:

- The "low" scenario (**CL**, +15 cm in 2050);
- The "high" scenario (**CH**, +40 cm in 2050).

The downstream boundary conditions for year 2050 are increased with these values.

The tidal range scenario A+ is combined with the sea level rise CH. The tidal range scenario A- is combined with the sea level rise CL.

3.4 List of model runs

The overview of model runs is presented in Table 2. This table gives the various conditions of each model run, which includes the bathymetry alternative, discharge type, tidal amplitude and sea level rise scenario. The last column shows the duration of each run in days.

QN: normal discharge scenario.

QE: events discharge scenario.

(A0, A+, A-): Different tidal range scenarios.

(CL, CH): Sea level rise scenarios.

QN runs have a simulation period from 09/08/2050 22:00 to 12/11/2050 21:00 (95 days). The spin up period is 3 days from 09/08/2050 22:00 to 12/08/2050 22:00.

QE runs have a simulation period from 28/08/2050 11:00 to 17/09/2050 16:00 (20 days). The spin up period is 3 days from 28/08/2050 11:00 to 31/08/2050 11:00.

Table 2 – List of different scenario runs

Code	Year	Bathymetry (alternatives)	Discharge type	Amplitude correction	Sea level scenario	Duration of run [days]
2050_Reference_QN_A0CL	2050	Reference	QN	A0	CL	95
2050_Reference_QE_A0CL			QE			20
2050_Reference_QN_A0CH			QN		CH	95
2050_Reference_QE_A0CH			QE			20
2050_Reference_QN_AminCL			QN	A-	CL	95
2050_Reference_QE_AminCL			QE			20
2050_Reference_QN_AplusCH			QN	A+	CH	95
2050_Reference_QE_AplusCH			QE			20
2050_Chafing_QN_A0CL	2050	Chafing	QN	A0	CL	95
2050_Chafing_QE_A0CL			QE			20
2050_Chafing_QN_A0CH			QN		CH	95
2050_Chafing_QE_A0CH			QE			20
2050_Chafing_QN_AminCL			QN	A-	CL	95
2050_Chafing_QE_AminCL			QE			20
2050_Chafing_QN_AplusCH			QN	A+	CH	95
2050_Chafing_QE_AplusCH			QE			20
2050_VaH_QN_A0CL	2050	VaH	QN	A0	CL	95
2050_VaH_QE_A0CL			QE			20
2050_VaH_QN_A0CH			QN		CH	95
2050_VaH_QE_A0CH			QE			20
2050_VaH_QN_AminCL			QN	A-	CL	95
2050_VaH_QE_AminCL			QE			20
2050_VaH_QN_AplusCH			QN	A+	CH	95
2050_VaH_QE_AplusCH			QE			20
2050_VaG_QN_A0CL	2050	VaG	QN	A0	CL	95
2050_VaG_QE_A0CL			QE			20
2050_VaG_QN_A0CH			QN		CH	95
2050_VaG_QE_A0CH			QE			20
2050_VaG_QN_AminCL			QN	A-	CL	95
2050_VaG_QE_AminCL			QE			20
2050_VaG_QN_AplusCH			QN	A+	CH	95
2050_VaG_QE_AplusCH			QE			20

4 Methodology of determining hydrodynamic effect

The model results of the three alternatives (Chafing, VaH, and VaG) are presented in Chapter 5. The methodology to determine the hydrodynamic effects is described in the present chapter.

The used parameters include water levels, harmonic components, discharges, and tidal asymmetry. Effects are quantified at various locations along the estuary.

4.1 Combination of 4QN+QE runs

For the ecotope mapping, water level frequencies are required, especially the tails of the distribution based on a full year. To limit the calculation time (or cost) of the 3D hydrodynamic model a different approach (than calculating with very long time series) is used (IMDC/INBO/UA/WL, 2015).

The hydrodynamic model is run for a period of 3 months with a synthetic discharge boundary containing events with a return period equal to or smaller than 1/6 year. This is the “normal” discharge scenario (**QN**). The downstream (tidal) boundary is a harmonic boundary without a storm surge.

A shorter run (“events” discharge scenario) of about 20 days (**QE**) is run with a discharge time series that contains 2 discharge events with return periods of 1 year and 1/2 year. The downstream boundary contains a storm surge period additional to the harmonic signal. The surge was determined by IMDC in a statistical similar way as the precipitation signal, based on measurements of the last +/-40 years (Vlissingen).

The combination of 4 x “normal” and 1 x “events” discharge scenario produces an output for water levels, flow velocities and discharges that is statistically representative for one year.

It is worth to mention that the combination of 4QN+QE runs as a synthetic year is not suitable for harmonic analysis. It works well for analysis of exceedance frequencies of water levels, but makes little sense for performing an harmonic analysis on this synthetic timeseries. The synthetic time series is not a continuous sine signal anymore, therefore, classic harmonic analysis fails. Instead, the “normal” discharge scenario (QN) runs are used for the harmonic analysis since their simulation period is the longest, and best suited to obtain harmonic components.

4.2 Water Levels and Harmonic Components

The effects of each alternative on the flow hydrodynamics are quantified by the bias in high water, low water and complete time series of water levels, relative RMSE of discharges and with harmonic analysis of the vertical tide. All statistical parameters introduced in the report show the differences between bathymetry alternatives and the reference one. Definitions of the used statistical parameters are described as follows:

The reference time series is presented as x and the time series that is subject to the test as y .

The **mean** values of the time series are represented by $\bar{x}$ (reference) and $\overline{y}$ (subject to test).

$$\bar{x} = \frac{1}{N}\sum_{i=1}^{N} x_i$$
$$\bar{y} = \frac{1}{N}\sum_{i=1}^{N} y_i$$

Where N is the length of the time series.

The **bias** is the difference between the mean of the tested and the reference time series.

$$bias = \bar{y} - \bar{x}$$

The **root mean square error** (RMSE) is defined as:

$$RMSE = \sqrt{\frac{\sum_{i=1}^{N}(x_i - y_i)^2}{N}}$$

Corresponding time series will result in RMSE values close to zero. An important, extra source of information is the **unbiased root mean square error** or **$RMSE_0$**. If the tested time series shows apart from a constant offset (bias) to the reference time series no other differences in its signal, the $RMSE_0$ will be zero, while both bias and RMSE will be non-zero. If x and y are time series of a tidal signal (water level, current), an $RMSE_0$ value of zero means that both signals are equal in phasing and amplitude. This does not imply there is no constant bias between both.

$$RMSE_0 = \sqrt{\frac{\sum_{i=1}^{N}\left[(x_i - y_i) - (\bar{x} - \bar{y})\right]^2}{N}}$$

The harmonic analysis in this report is focused on the major components M2, M4 and S2 and it is based solely on the “normal” discharge scenario (QN) runs.

4.3 Discharge

Discharges are analyzed at various cross-sections along the estuary. The locations of these cross-sections are presented along the estuary in Figure 10 (from the mouth to Liefkenshoek) and in Figure 11 (from Liefkenshoek to Melle).

Statistical parameters are computed for complete flow discharge time series of all alternatives. Values of Bias, RMSE and RRMSE (relative RMSE) of discharges at various locations along the Scheldt estuary are used for the comparison between the three alternatives.

The differences in discharges are analyzed relative to the value of each discharge at a certain location. The value of flow discharge changes relative to the value in the reference runs. The sign of ‘signed’ relative RMSE is the same as the sign of bias and it shows if discharges increase or decrease at a certain cross-section.

The computed ‘Signed’ relative RMSE of complete discharge time series (for different alternatives under various scenarios) are presented between R3 Zimmermangeul and Melle.

Figure 10 – Location of cross-sections along the estuary until Liefkenshoek

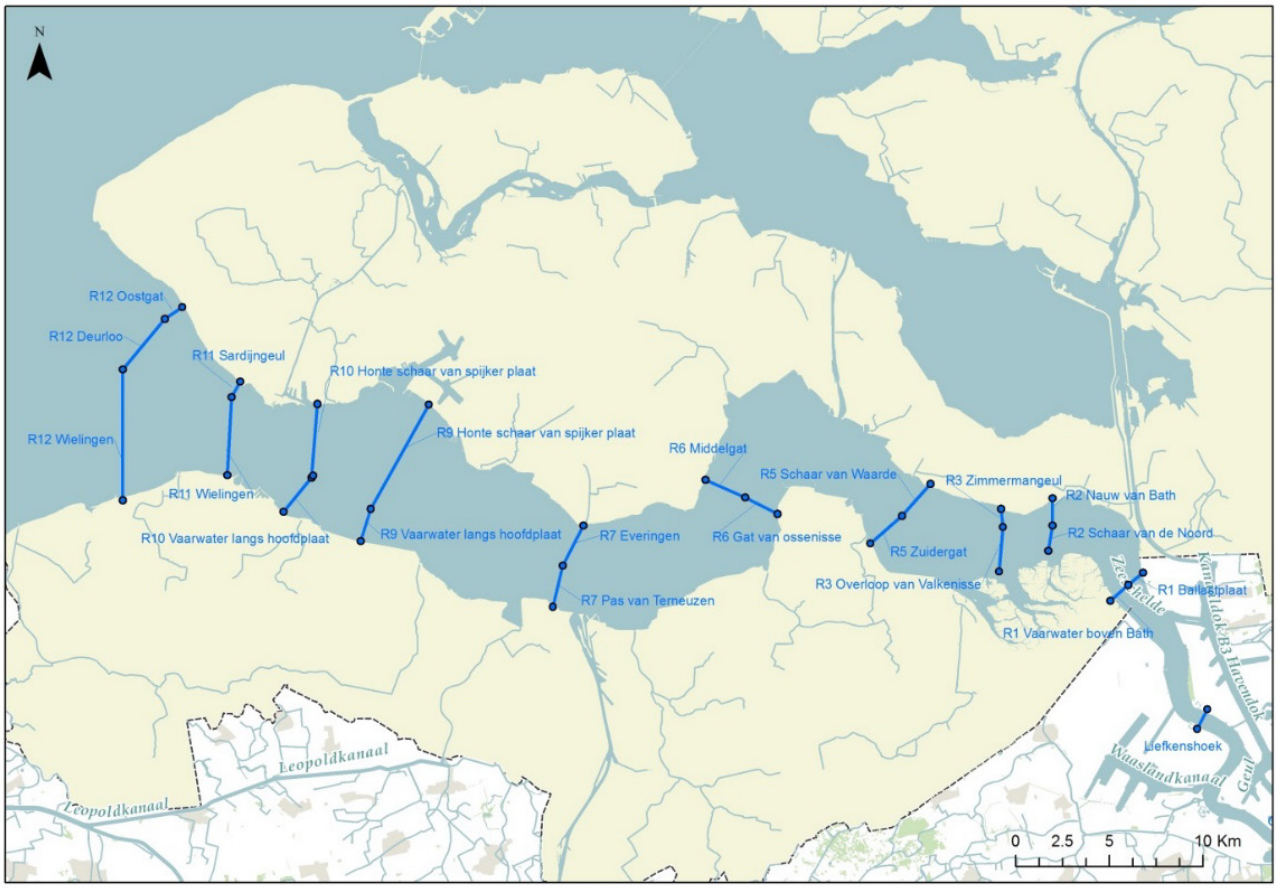

Figure 11 – Location of cross-sections along the estuary from Liefkenshoek to Melle

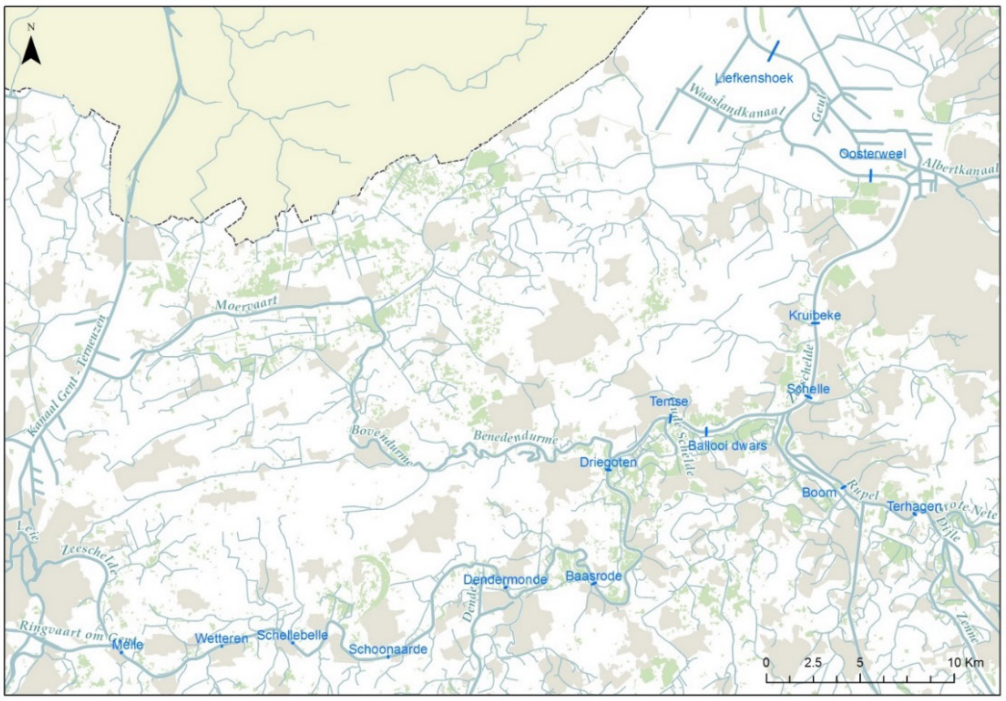

4.4 Tidal asymmetry

Hydrodynamic processes (tides, wind waves, density driven currents and wind induced currents) drive sediment transports and steer morphological developments. Various studies describe tide residual currents in estuaries resulting from tidal asymmetries (Steijn & Van der Spek, 2005; Van der Werf & Brière, 2013; Tonnon & van der Werf, 2014) which are partly confirmed by measured bed forms (Erkens, 2003).

Tidal asymmetry is an important parameter for predicting and understanding sediment transport behavior in an estuary, due to the non-linear relation between flow velocity and sediment transport (Van de Kreeke and Robaczewska, 1993; Wang et al., 1999). An estuary (or a part of it) is called ebb dominant or flood dominant depending on the direction of asymmetry. It is possibly a principal factor influencing the sediment exchange between the ebb tidal delta and the estuary, as well as between the various parts of the estuary (Wang et al., 1999; Friedrichs, 2011).

The asymmetry of the vertical tide is often described by the difference or ratio between the duration of rising tide (flood) and falling tide (ebb).

Similarly, horizontal tidal asymmetry is flood-dominant if the flood flow is stronger, while horizontal asymmetry is ebb dominant if the ebb flow is stronger.

Furthermore, the difference in duration of the slack water periods after high and low tide is another indicator for horizontal tidal asymmetry as the deposition of fine (suspended) sediment is closely related to the settling time of particles (e.g. Dronkers, 1986).

Finally, tidal asymmetry can also be characterized by the relative contribution of different tidal constituents to the tidal signal, as the amplitude ratios and phase differences between the principal constituents and their overtides or compound tides are indicators for the strength and nature of the tidal asymmetry (e.g. Friedrichs and Aubrey, 1988; Parker, 1984; Wang et al., 1999, 2002).

There are clearly many ways of quantifying asymmetry. In the present study, five different ratios for tidal asymmetry are used. The first two parameters are related to duration and the last three are related to

current velocities. All ratios are calculated in such a way that >1 is flood dominant, and <1 is ebb dominant. Note that an ebb dominance in duration, will be a flood dominance in velocities, because there is an inverse relation between both.

4.4.1 Tidal asymmetry associated with duration

Tidal duration asymmetry (the difference in the duration and/or amplitude of rising and falling tide) can arise from distortion of the tide in shallow water or from the interaction of astronomical tidal constituents (Parker, 1991). Physically, the crest of the tidal wave (High Water) propagates faster than the trough (Low Water), so within the embayment there is a shorter period of rising water (from LW to HW) than falling tide. HW propagation may be slowed if the intertidal volume of adjacent shoals is large relative to channel volume, resulting in a longer period of rising water (Fortunato and Oliveira, 2005).

Velocity skew is the asymmetrical distribution of ebb and flood tidal flow over a tidal cycle. This skew can be a local phenomenon caused by bathymetry, as in the case of water flow around a headland, or in channels with segregated flood/ebb conduits (van Veen et al., 2005). On a system-wide scale, shoaling bathymetry contributes to skewed velocities through the distortion of the surface tide, which results in differences between the duration of rising and falling water (Boon and Byrne, 1981).

Based on the tidal duration two different asymmetry parameters are used to analyze and to evaluate the effects of each bathymetry alternative. These two parameters are described as follows:

Tidal asymmetry of the duration (time) of rising and falling tide:

$$\frac{T_{\text{increase}}}{T_{\text{decrease}}}$$

$T_{increase}$ = time required within the tidal cycle to change water level from LW to HW;

$T_{decrease}$ = time required within the tidal cycle to change water level from HW to LW.

This parameter indicates the relative relation between the duration of rising and falling tide during a full tidal cycle. This ratio gives an indication of the shape of the tidal cycle.

This parameter can be different at various locations along the estuary, based on the hydrodynamic conditions at each location. It is important to mention that this parameter has no relation to the duration of the two phases (flood and ebb) of the tidal cycle.

Tidal asymmetry based on duration of *flood-period and ebb-period* :

$$\frac{T_{\text{flood}}}{T_{\text{ebb}}}$$

T_{flood} = duration of flood flow during the tidal cycle;

T_{ebb} = duration of ebb flow during the tidal cycle.

This parameter quantifies tidal asymmetry based on the horizontal tide (velocities). It is important to note that this parameter has no direct connection with the previous parameter which is related to asymmetry of the vertical tide.

4.4.2 Tidal asymmetry associated with the magnitudes of maximum flood and maximum ebb velocities

The above two tidal asymmetry parameters are based on tidal variations of water levels (vertical tide) and not the current velocities (horizontal tide), while the sediment transport is linked to the currents. The following three forms of the tidal asymmetry, which have been used in the present study, are based on the current flow velocities.

Tidal asymmetry of the maximum current flow velocities during flood and ebb phases:

One way to look at tidal asymmetry is to look at the difference in peak flood/ebb shear stresses (Dronkers, 1986; Friedrichs and Aubrey, 1988). This type of asymmetry is associated with a difference in the magnitude between maximum flood and ebb velocities. For example, if the maximum flood velocity exceeds the ebb velocity, a residual sediment transport in flood direction is likely to occur, and vice versa.

This tidal asymmetry parameter is based on maximum velocity during flood and maximum velocity during ebb within the tidal cycle.

Averaged cross-sectionally averaged velocities are computed by dividing the discharge at a certain cross-section by the wet area of this cross-section (V= Discharge (Q) / wet area (A)).

$$\frac{V_{\max flood}}{V_{\max ebb}}$$

$V_{maxflood}$ = maximum cross-sectionally averaged velocity during flood phase;

V_{maxebb} = maximum cross-sectionally averaged velocity during ebb phase.

Tidal asymmetry calculated based on the velocity as proxy for *the transport of fine sediments (~V^4)*

The horizontal sediment flux of mud is assumed to scale with the product of the saturation condition and the flow velocity, i.e. with V^4 (e.g. Winterwerp, 2001). According to Winterwerp (2001), when the flow velocity decreases slightly, sediment (mud) starts to settle, creating a two-layer fluid system close to the bed. At the interface between the two layers, vertical turbulent mixing is damped strongly, decreasing the sediment carrying capacity in the upper part of the flow. This results in a catastrophic collapse of the vertical turbulence field and the vertical sediment concentration profile. The suspended sediment concentration of cohesive sediment just prior to this collapse is denoted by the term "saturation concentration" to distinguish it from the equilibrium concentration for sand.

$$\frac{\frac{1}{T_{\text{flood}}}\int^{\text{flood duration}} V^4 dt}{\frac{1}{T_{\text{ebb}}}\int^{\text{ebb duration}} V^4 dt}$$

T_{flood} = duration of flood flow during the tidal cycle;

T_{ebb} = duration of ebb flow during the tidal cycle.

Current velocity V is calculated as a cross-sectional averaged velocity:

$$V = \frac{Q}{A}$$

With Q the time-varying discharge at location x along the river/estuary, and A the time-varying wet cross-section at the same location. T_{flood} and T_{ebb} are the duration of the flood flow and ebb flow period, respectively.

Tidal asymmetry calculated based on the velocity as proxy for *the transport of sand (~V^3)*:

$$\frac{\frac{1}{T_{\text{flood}}}}{\frac{1}{T_{\text{ebb}}}}\left|\frac{\int^{\text{flood duration}} V^3 dt}{\int^{\text{ebb duration}} V^3 dt}\right|$$

4.4.3 Interpretation

If the values of these five tidal asymmetry parameters (calculated with the formulas described above) are smaller than 1, the estuary or part of the estuary is ebb-dominant. Values bigger than 1 means that the estuary is flood-dominant. It is important to state that these different forms of tidal asymmetry are not directly related to each other. An estuary can be flood dominant for one of the tidal asymmetry forms but ebb dominant for another form.

All the above tidal asymmetry parameters were calculated at different stations/locations in the Sea Scheldt for different alternatives (Chafing, VaH and VaG) and presented in chapter 5.

5 Results

The model results of the three alternatives Chafing, VaH, and VaG are compared with the reference situation to investigate the effect of each bathymetry on the hydrodynamics in the estuary. Model runs are done with four different hydrodynamic boundary conditions (A0CH, A0CL, AplusCH and AminCL), see also Table 2 for a complete overview of all runs.

In this chapter, the effects of the alternatives on water levels, harmonic components, discharges, and tidal asymmetry are presented at various locations along the estuary. Each subsection presents the effect of one alternative on the flow hydrodynamics by introducing Bias values of high water, low water, complete time series of water levels, relative RMSE of discharges and harmonic analysis. All statistical parameters introduced in the report show the differences between bathymetry alternatives and the reference one.

Methods to quantify the effects are described in chapter 4.

The result of the VaG alternative is discussed in section 7.1. The results of VaH and Chafing alternatives are presented in subsections 5.2 and 5.3, respectively.

5.1 Effect of VaG

5.1.1 Water levels

The water level biases of model results (HW, LW, and complete time series) of the VaG alternative with various scenarios (A0CH, A0CL, AminCL, and AplusCH) are presented in Figure 12 to Figure 15. In Figure 12 the model results of HW bias at all measuring points starting from Nieuwpoort to Melle are presented to show that the VaG alternative has almost no effects on results downstream of Antwerp (and in the North Sea). The bathymetry of VaG alternative has the maximum changes compared to VaH and Chafing alternatives. Therefore, in this report the water level results are presented and discussed only upstream of Antwerp, where significant changes can be observed, for all alternatives as shown in Figure 13 to Figure 15.

Water levels bias results show that the VaG alternative has a clear effect on water levels, i.e. in the order of centimeters. The maximum water level changes (rising of HW) are taking place in the Upper Sea Scheldt with maximum values < 0.15 m (upstream of Sint-Amands). Significant change in results can be observed between Sint-Amands and Dendermonde and upstream of Dendermonde due to the large changes in bathymetry between these two locations (see Figure 57). These sudden changes in water levels can be explained by the implemented modifications between the two locations (shortening and removing part of the estuary). The adjusted part includes the existing strong meandering between Sint-Amands and Dendermonde. These modifications lead to general reduction of the flow resistance and consequently, water can propagate into the upstream part of the estuary easier and faster.

Results of HW levels show a general reduction downstream of Dendermonde (< 0.05 m) and an increase of levels starting from Dendermonde in the upstream direction (see, Figure 13), With maximum value of 0.13 m at Dendermonde. The LW results (Figure 14) show exactly the opposite behavior compare to HW results, with an increase (< 0.05 m) downstream of Dendermonde and a strong reduction of water level (< 0.27 m) in the upstream direction.

These water level changes (HW) along the estuary show that the VaG alternative leads to reduction of HW levels in the downstream part and an increase in the upstream part of the estuary. LW levels show the opposite behavior compare to HW, general reduction in the upstream part and an increase of levels in the downstream part. This change in behavior around Dendermonde can be claimed to the changes in VaG bathymetry and its effects on reducing flow resistance at this location as explained above.

In the VaG alternative tidal amplitudes increase in the upper part of the estuary (upstream of Sint-Amands), with a maximum value of 0.4 m. In the downstream part, tidal amplitudes decrease up to 0.08 m.

The statistical parameters of HW, LW and complete time series of water levels of all model runs (under different scenarios) are presented in Appendix 2. Table 5 includes (VaG_A0CH - Reference_A0CH), Table 7 (VaG_A0CL - Reference_A0CL), Table 9 (VaG_AplusCH - Reference_AplusCH) and Table 11 (VaG_AminCL - Reference_AminCL).

Figure 12 – Bias of high water magnitude in VaG starting from Nieuwpoort

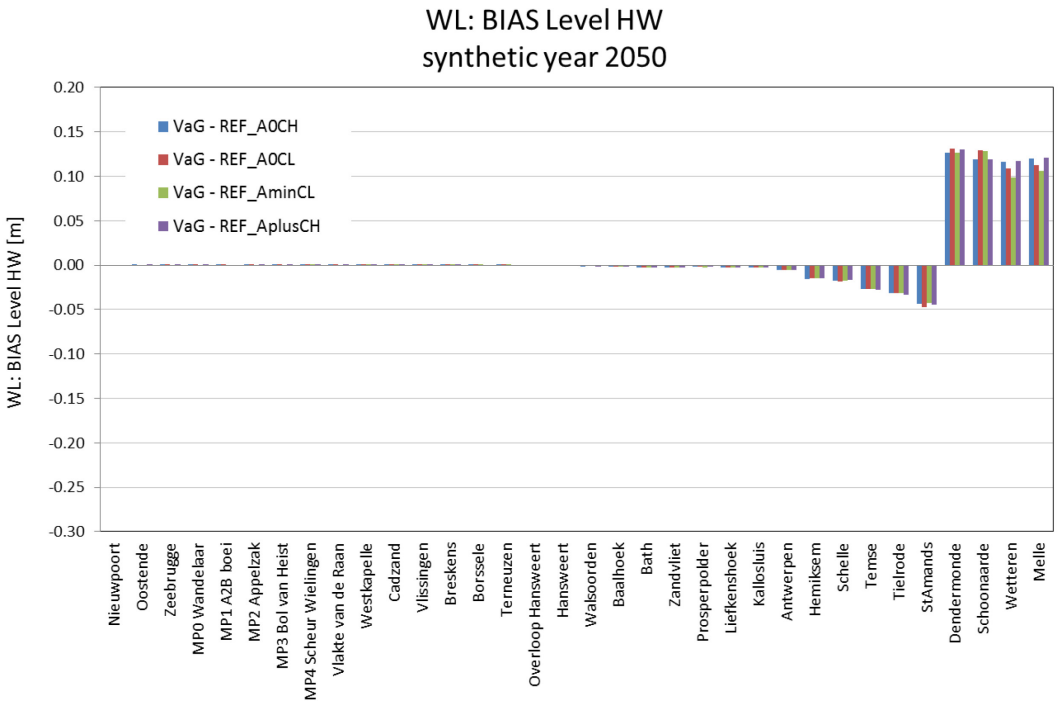

Figure 13 – Bias of high water magnitude in VaG starting from Antwerp

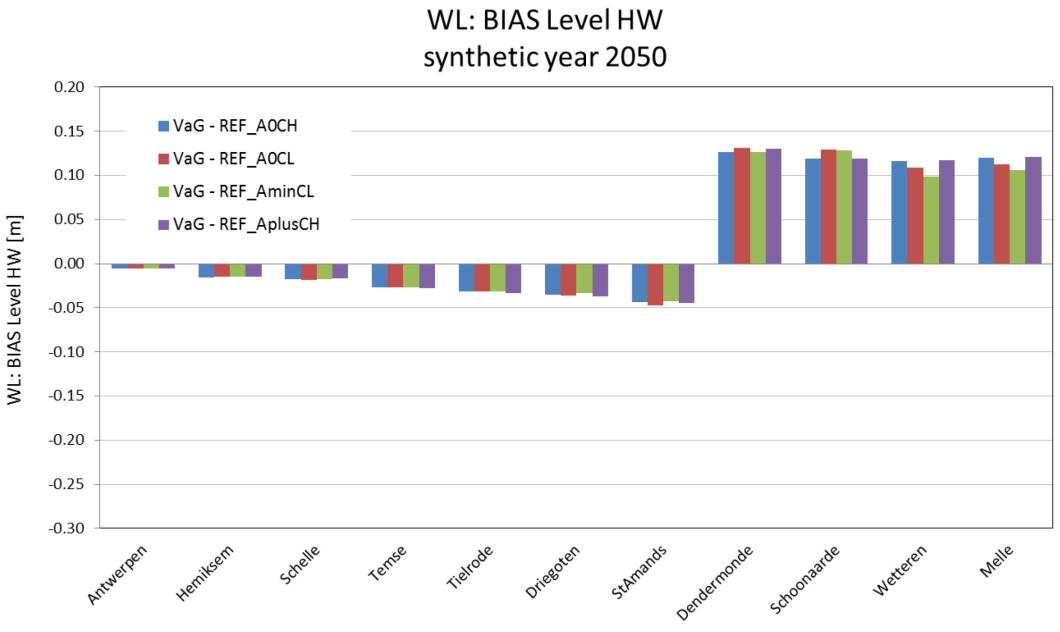

Figure 14 – Bias of low water magnitude in VaG

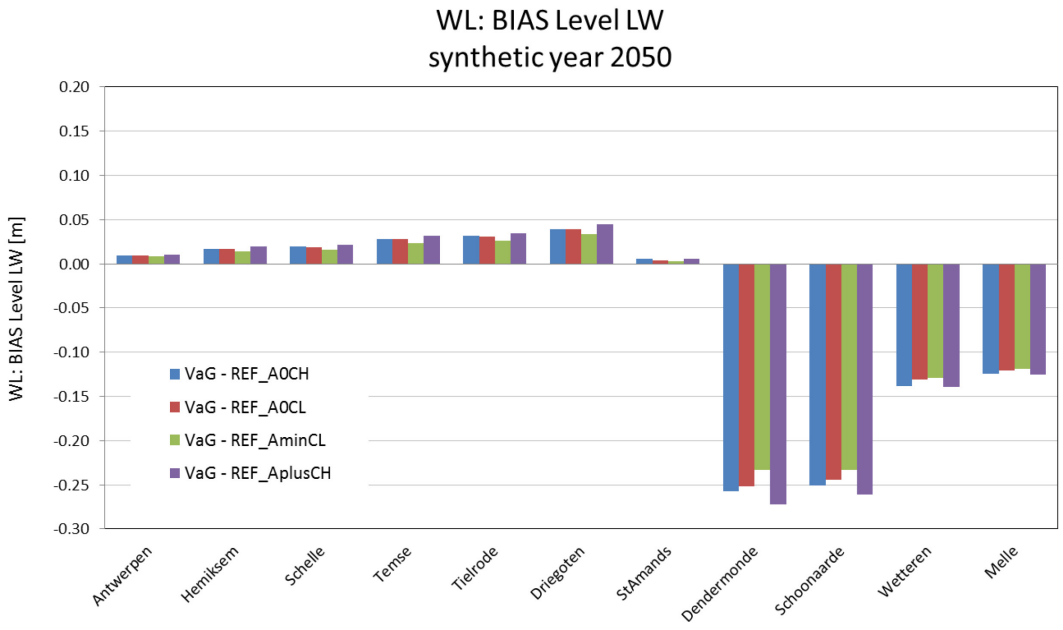

Figure 15 – Bias of complete water level time series in VaG

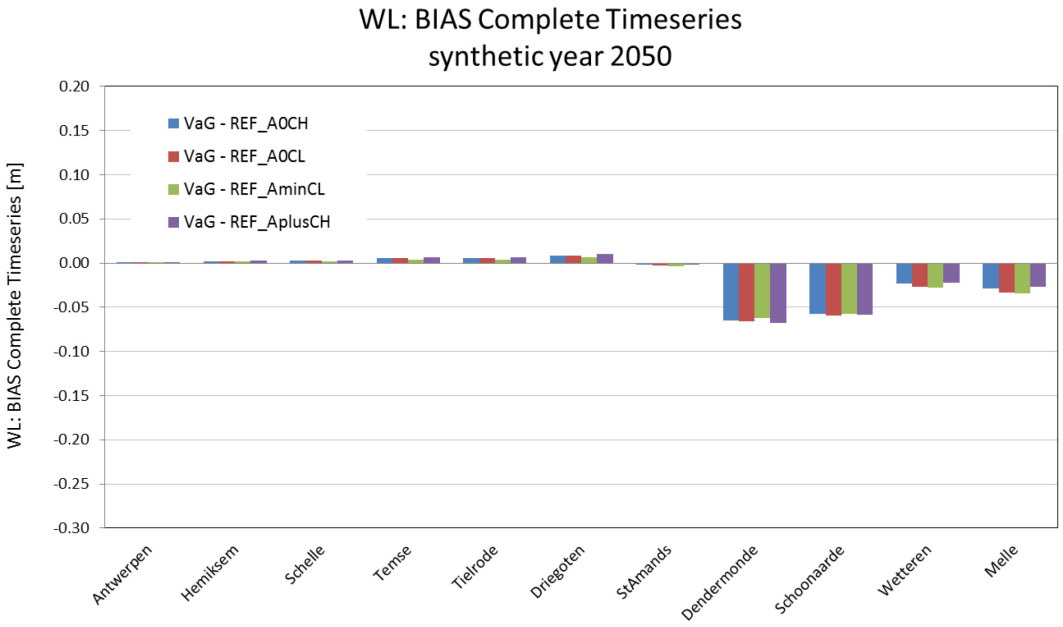

5.1.2 Harmonic components

The computed Bias values of tidal amplitudes and phases of M2, M4 and S2 are presented in Figure 16 to Figure 21 of VaG alternative (under various scenarios), respectively. Note that different scales of y-axis are used to clarify the results in these figures.

The results at different locations along the estuary (from Antwerp to Melle) show that VaG alternative has some effects on the harmonic components (M2, M4 and S2) of the tide, especially in the upstream part of Sint-Amands. These effects are smaller than 0.17 m (M2), 0.022 m (M4) and 0.048 m (S2). The maximum Bias values of phases (< 6.5°) of different tidal components are always taking place upstream of Sint-Amands for M2, M4 and S2.

It is important to state that the interaction of the M2 and M4 tides is one of the main drivers of the residual sediment transport. The variability in residual sediment transport can be estimated based on this interaction. This transport can vary along the different locations of the estuary based on this variability of interaction between the two components (M2 and M4 amplitudes). This interaction between M2 and M4 are not investigated further in the present hydrodynamic study.

Details of harmonic analysis of VaG alternative are presented in combination with the reference situation in Figure 74 to Figure 97 in Appendix 2. Amplitudes and phases of M2, M4 and S2 are presented for all model runs under various hydraulic scenarios.

Figure 16 – Bias of Amplitude M2 in VaG

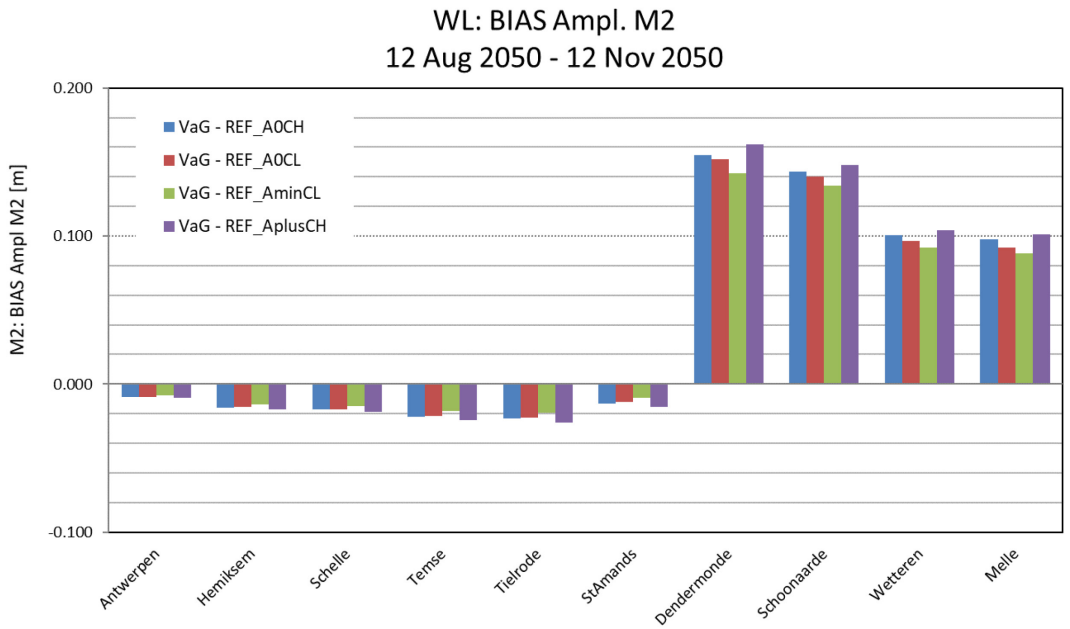

Figure 17 – Bias of Phase M2 in VaG

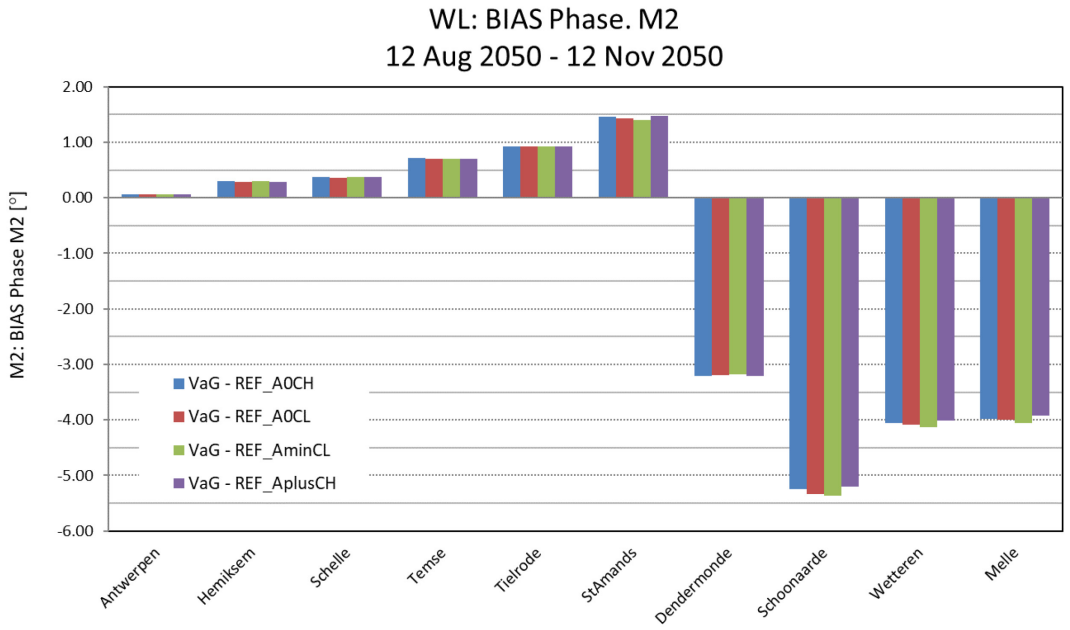

Figure 18 – Bias of Amplitude M4 in VaG

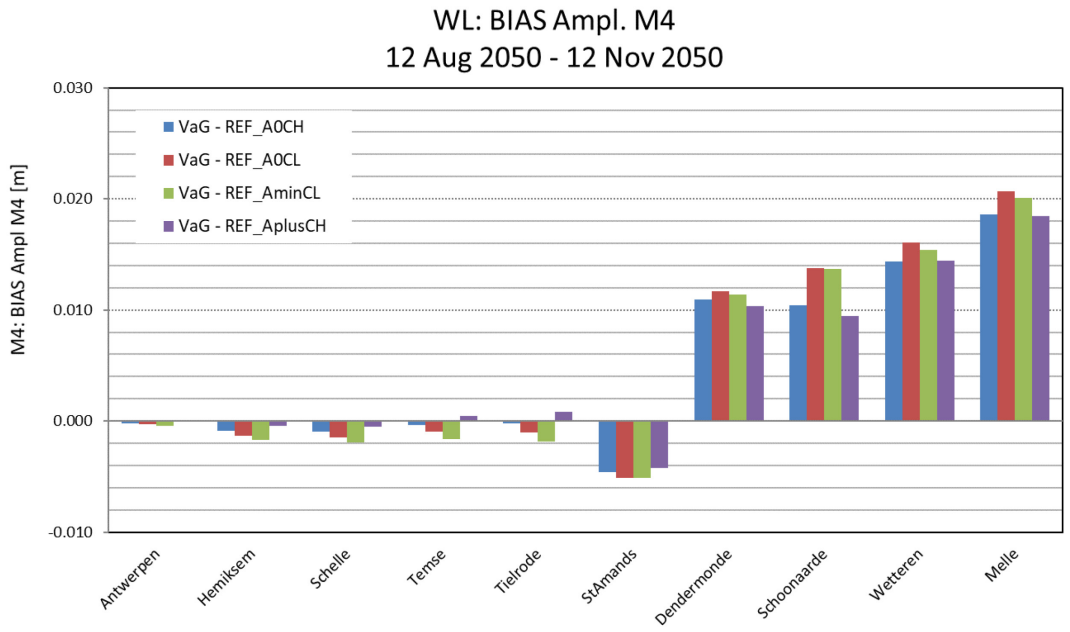

Figure 19 – Bias of Phase M4 in VaG

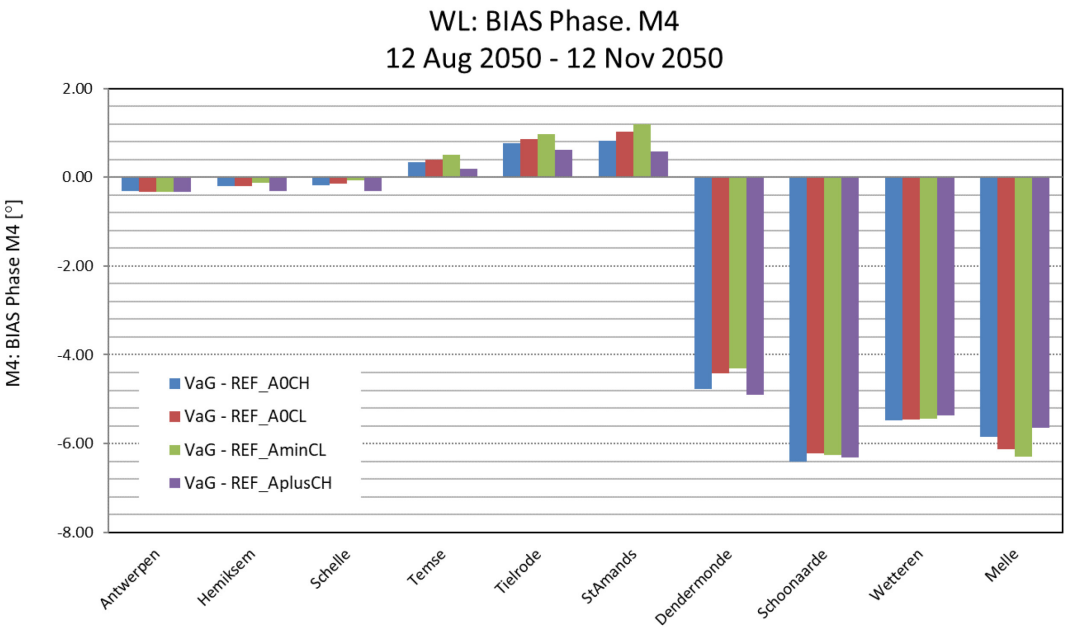

Figure 20 – Bias of Amplitude S2 in VaG

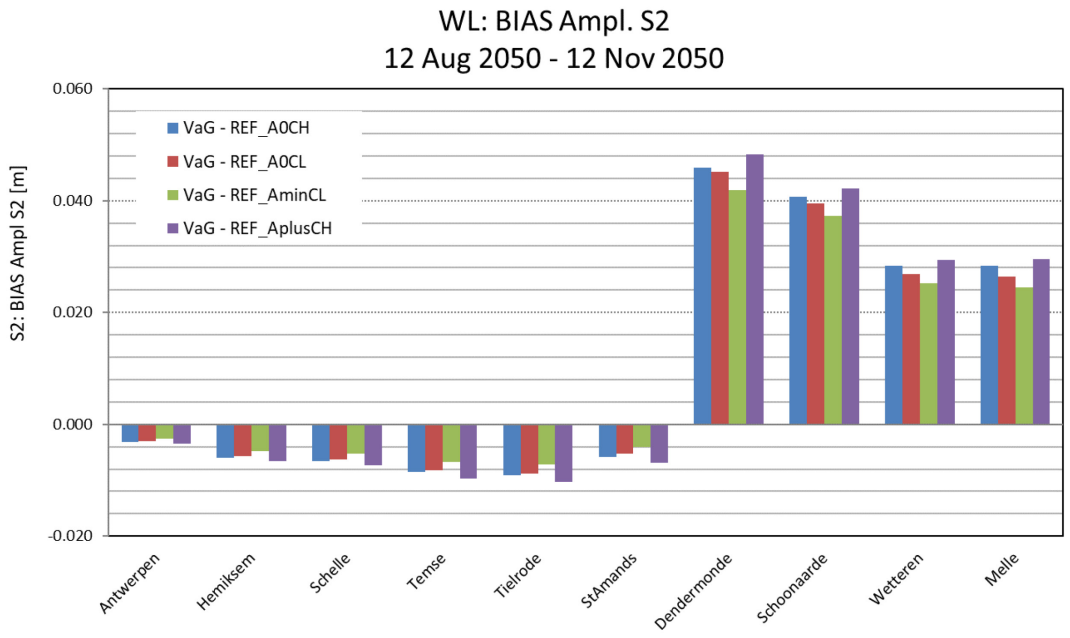

Figure 21 – Bias of Phase S2 in VaG

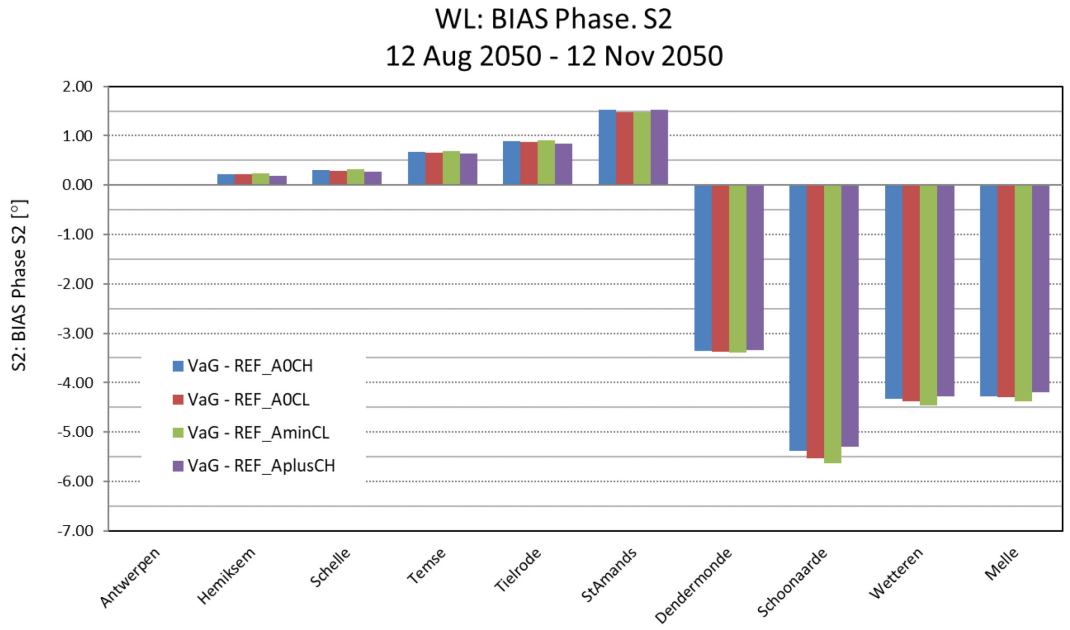

5.1.3 Discharge

The predicted flow discharges are analyzed at various cross-sections along the estuary. The locations of these cross-sections are presented along the estuary in Figure 10 (from the mouth to Liefkenshoek) and in Figure 11 (from Liefkenshoek to Melle).

Statistical parameters of complete flow discharge time series of all VaG model runs are presented in Appendix 2. Table 6, Table 8, Table 10 and Table 12 introduce values of Bias, RMSE and RRMSE (relative RMSE) of discharges at various locations along the Scheldt estuary.

Flow discharges in the downstream part (starting from the mouth) of Western Scheldt are significantly higher than upstream part. Therefore, the differences in discharges are analyzed relative to the value of each discharge at a certain location. Figure 22 ('signed' relative RMSE) shows the value of flow discharge changes relative to the value in the reference runs. The sign of 'signed' relative RMSE is the same as the sign of bias and it shows if discharges increase or decrease at a certain cross-section.

The computed 'Signed' relative RMSE of complete discharge time series for VaG alternative (under various scenarios) are presented between R3 Zimmermangeul and Melle in Figure 22. Discharges are slightly reduced downstream of Liefkenshoek (RRMSE < 0.01). On the other hand, RRMSE are increased in the upstream direction starting from Liefkenshoek to Melle. The highest values are observed between Melle and Dendermonde (RRMSE < 0.16). Besides, a sharp increase in RRMSE values can be noticed between Schelle (< 0.02) and Dendermonde (> 0.15). The VaG alternative has a clear effect on flow discharge starting from Schelle. Water level changes (increase) and increased flow velocities might explain the increased discharges. The effects of using different scenarios have a limited influence on the results.

Figure 22 – 'Signed' relative RMSE of complete discharge time series of VaG alternative

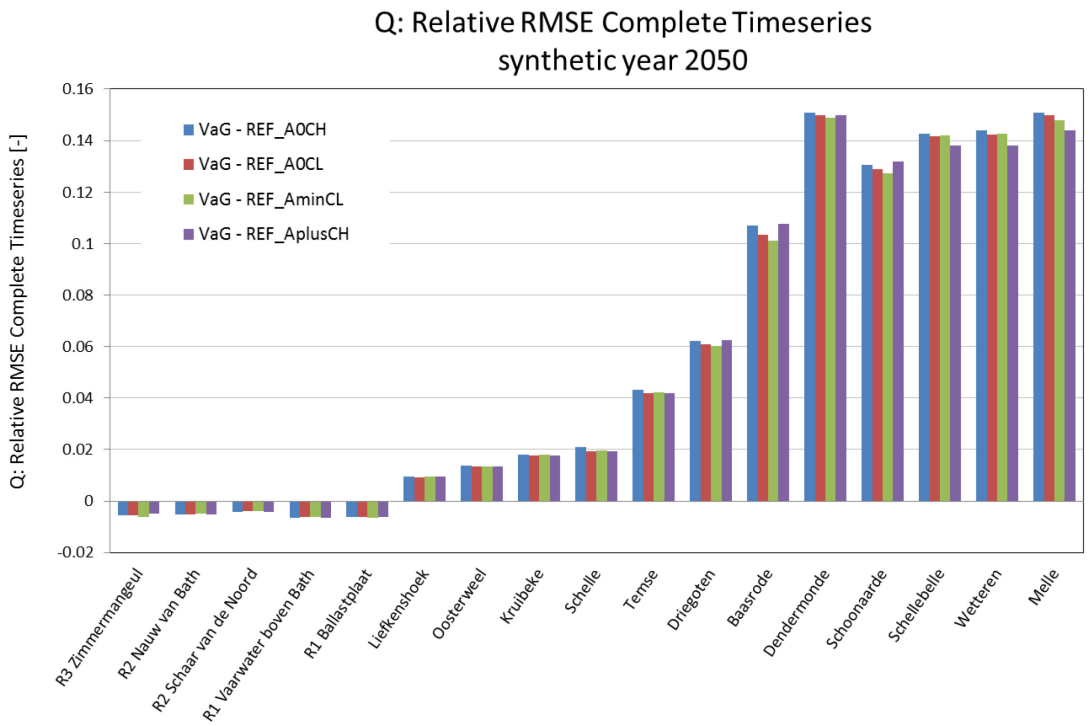

Tidal asymmetry

The values of tidal asymmetry itself are presented in Appendix 2 in Figure 98 to Figure 102. These figures show the tidal asymmetry of the VaG alternative and the reference (between Liefkenshoek and Melle) with four different scenarios (A0CH, AOCL, AminCL and AplusCH). Tidal asymmetry values smaller than 1 mean that the estuary is ebb dominant at a certain location along the estuary. The first two types of the tidal asymmetry (calculated as $T_{increase}/T_{decreaseWL}$ and T_{flood}/T_{ebb}) show that the estuary is ebb dominant upstream Liefkenshoek (Figure 98 and Figure 99). The tidal asymmetry reduced gradually from about 0.85 - 0.9 at Liefkenshoek to about 0.45 – 0.6 at Melle.

The third type of the tidal asymmetry ($V_{max\ flood}/V_{max\ ebb}$) varies from more than 1.2 at Liefkenshoek to more than 1.3 at Schelle, as shown in Figure 100. It has the smallest value (about 0.9) at Baasrode. At Schoonaarde and Schellebelle the tidal asymmetry is about 1 and it is about 0.8 at Melle. The tidal asymmetry values of V^3 and V^4 are presented in Figure 101 and Figure 102, respectively.

Figure 23 shows the effects of changes in the bathymetry on the tidal asymmetry of the VaG alternative in the Sea Scheldt from Liefkenshoek to Melle (the bathymetry is different in these alternatives upstream the location indicated by the vertical grey line in the plots). There are 5 subplots in Figure 23. Each subplot shows the difference in tidal asymmetry calculated based on one of the formulas described in chapter 4.4. A negative value means that the VaG alternative becomes more ebb dominant than the reference situation at a certain location. On the other hand, a positive value means that a VaG alternative becomes more flood dominant (or less ebb dominant).

In VaG alternative (Figure 23) the tidal asymmetry ($T_{increase}/T_{decrease}$) becomes slightly more flood dominant at Baasrode (by 2%) and upstream Schellebelle and slightly more ebb dominant at Schoonaarde. The second type of the tidal asymmetry (T_{flood}/T_{ebb}) increases at Dendermonde (maximum increase of 4%) and more upstream (by 1.5 - 3%). The tidal asymmetry ($V_{max\ flood}/V_{max\ ebb}$) increases by 4 to 5% at Baasrode and upstream Schellebelle. It decreases by 1 to 3% between Dendermonde and Schoonaarde. A bigger decrease is calculated in A0CL and AminCL alternatives. The values of tidal asymmetry calculated based on V^3 and V^4 have two peaks between Liefkenshoek and Melle. The maxima are observed at Schelle and between Schoonaarde and Wetteren. Most of maximum values are smaller than 1 (ebb dominant), except for scenario VaG AminCL (V^3 and V^4) and scenario VaG A0CL and VaG AminCL (V^4) which are bigger than 1 (flood dominant). The tidal asymmetry (calculated based on V^3 and V^4) reaches a minimum values at Baasrode and Melle.

The biggest effects are calculated for the last two types of the tidal asymmetry. The asymmetry found based on V^3 increases by about 8% at Baasrode in VaG alternatives, it decreases by about 8% between Dendermonde and Schoonaarde and it increases again upstream Schellebelle by 5 to 15%. The increase is slightly bigger in A0CL and AminCL runs. The changes in the tidal asymmetry calculated based on V^4 are bigger than the effects on the asymmetry found based on V^3. The asymmetry decreases by 10% at Schoonaarde and it increases by about 20% at Wetteren.

Figure 23 – Effect on the tidal asymmetry (VaG vs Reference).

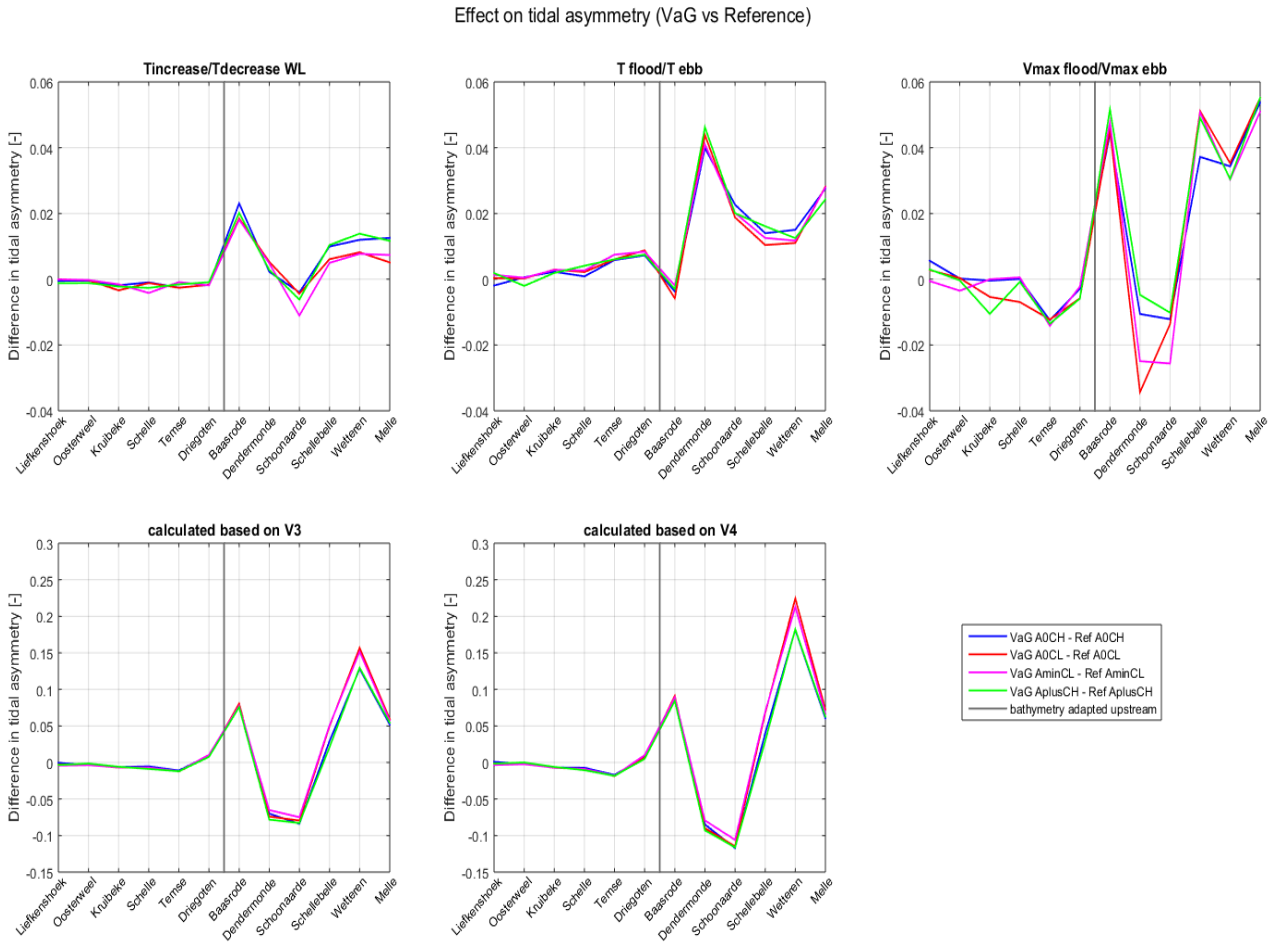

5.2 Effect of VaH

5.2.1 Water levels

The model results for water level bias of VaH alternative with various boundary conditions (A0CH, A0CL, AminCL and AplusCH) are presented in Figure 24 to Figure 26 of HW, LW and complete time series, respectively. The presented results are limited to the locations in the upstream part of the estuary (from Antwerp to Melle) as discussed before in subsection 5.1.1. It is clear from the results that the VaH alternative has a limited/small effect (order of centimeters) on water levels. The maximum water level changes are taking place at Melle with maximum values < 0.05 m (Figure 25).

The maximum bias of HW is very limited at all the presented locations which have a maximum values < 0.02 m, as shown in Figure 24. The LW bias results (Figure 25) show somewhat higher values at Melle and Wetteren with an increase of < 0.05 m. the VaH alternative results in a much smaller effect on water levels with a maximum change of tidal amplitude in the downstream part of Dendermonde (< 0.025 m). Tidal amplitudes are increased upstream of Dendermonde with a maximum value of 0.06 m at Melle.

These water level results of VaH alternative are much smaller than previous results of VaG alternative, which are presented in subsection 5.1.1. These results are expected by keeping in mind that the bathymetry of VaH alternative have less changes compare to VaG alternative.

The statistical parameters of HW, LW and complete time series of water levels of all model runs are presented in Appendix 3. In this appendix Table 13 includes (VaH_A0CH - Reference_A0CH), Table 15 (VaH_A0CL - Reference_A0CL), Table 17 (VaH_AplusCH - Reference_AplusCH) and Table 19 (VaH_AminCL - Reference_AminCL).

Figure 24 – Bias of high water magnitude in VaH

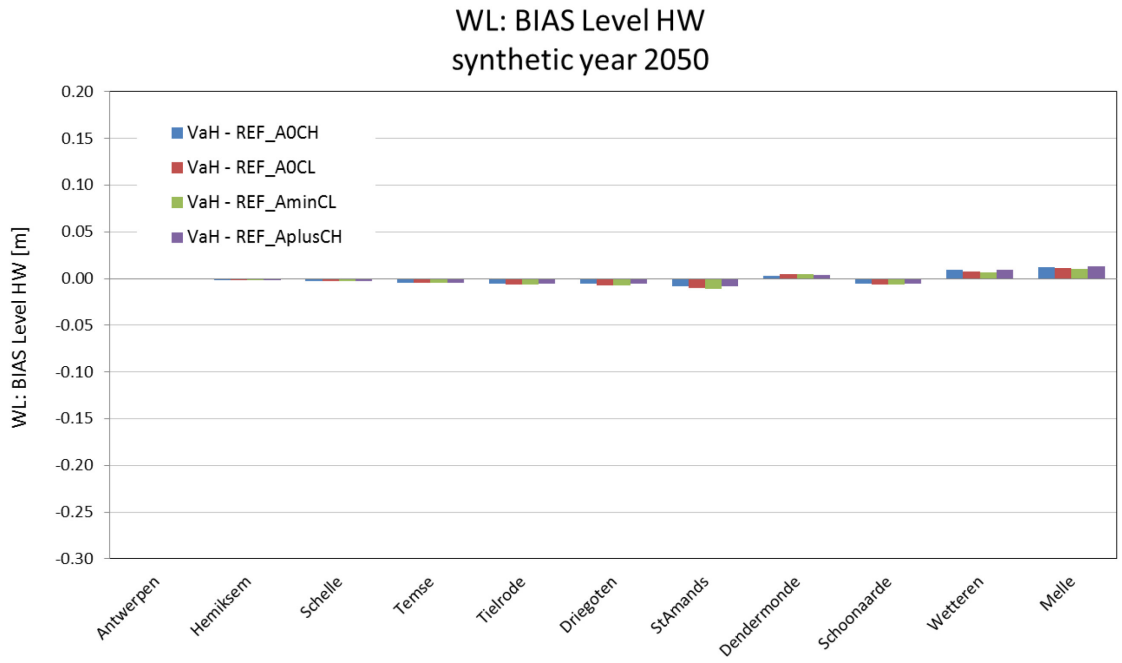

Figure 25 – Bias of low water magnitude in VaH

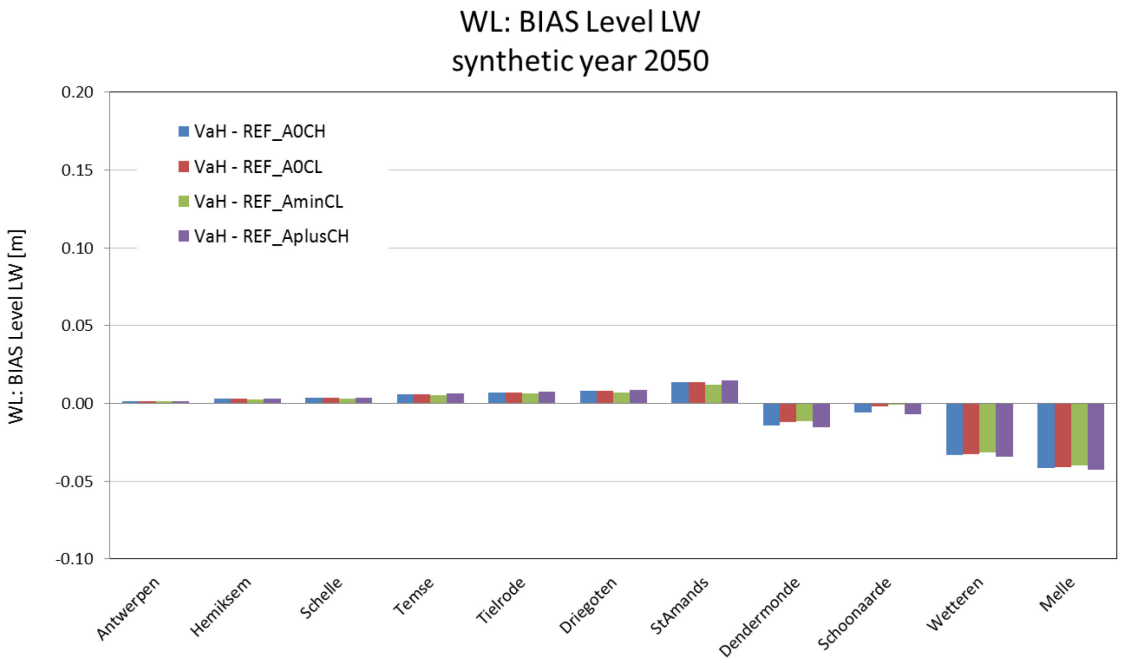

Figure 26 – Bias of complete water level time series in VaH

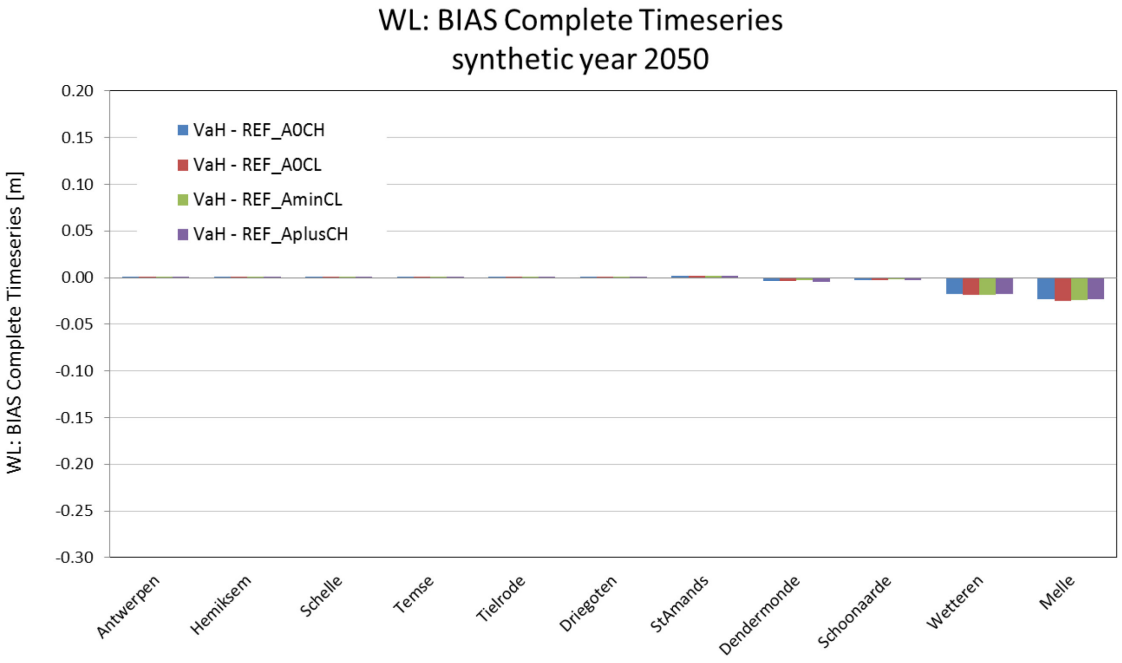

5.2.2 Harmonic components

The computed bias values of amplitudes and phases of M2, M4 and S2 are presented in Figure 27 to Figure 32 of VaH alternative under various scenarios. Note the different scales of y-axis used in these figures to clarify the results.

The results at different locations along the estuary show that the VaH alternative has no clear effects on the harmonic components (M2, M4 and S2) of the tide. These effects are smaller than 0.02 m (M2), 0.008 m (M4) and 0.006 m (S2). The maximum phase difference (< 1.8°) of different tidal components always occurs upstream of Sint-Amands for M2, M4 and S2.

Details of harmonic analysis of VaH alternative are presented in combination with the reference situation in Figure 103 to Figure 126 in Appendix 3. Amplitudes and phases of M2, M4 and S2 are presented for all model runs of various hydraulic scenarios.

Figure 27 – Bias of Amplitude M2 in VaH

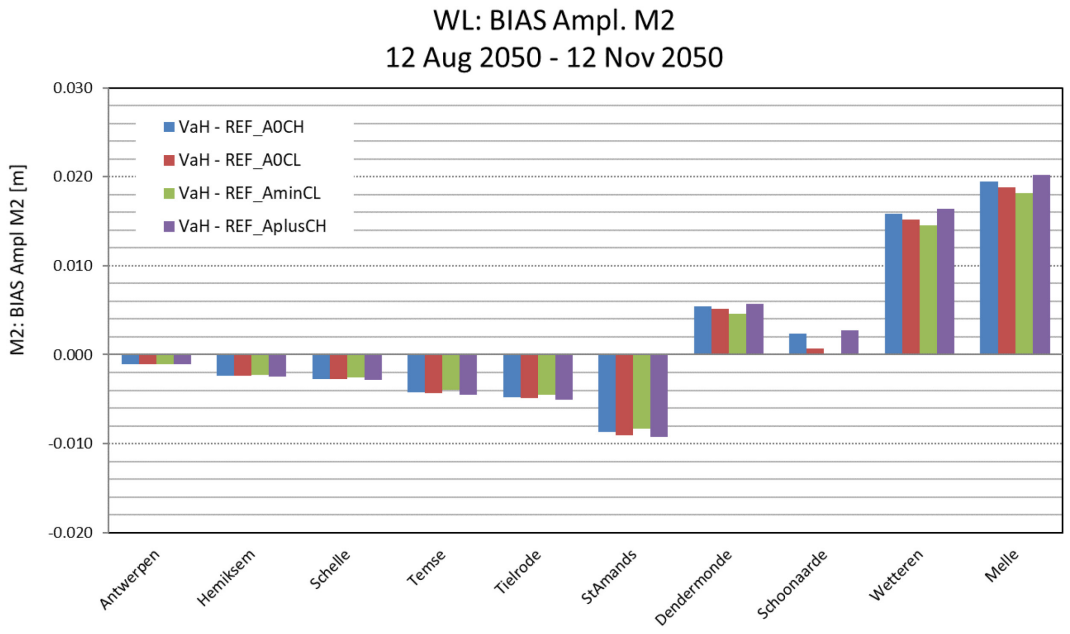

Figure 28 – Bias of Phase M2 in VaH

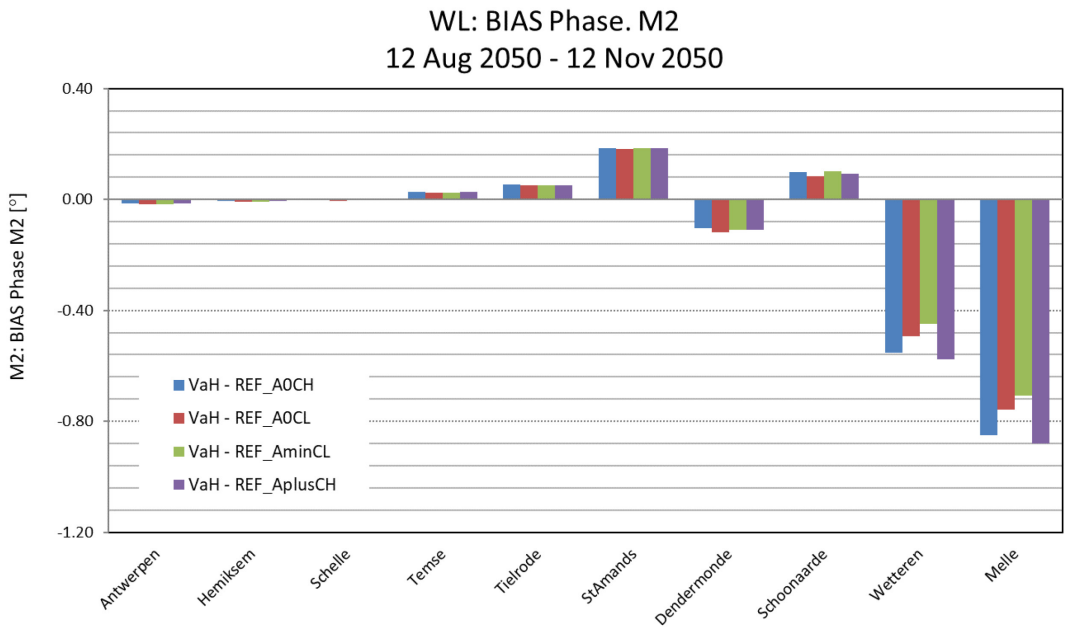

Figure 29 – Bias of Amplitude M4 in VaH

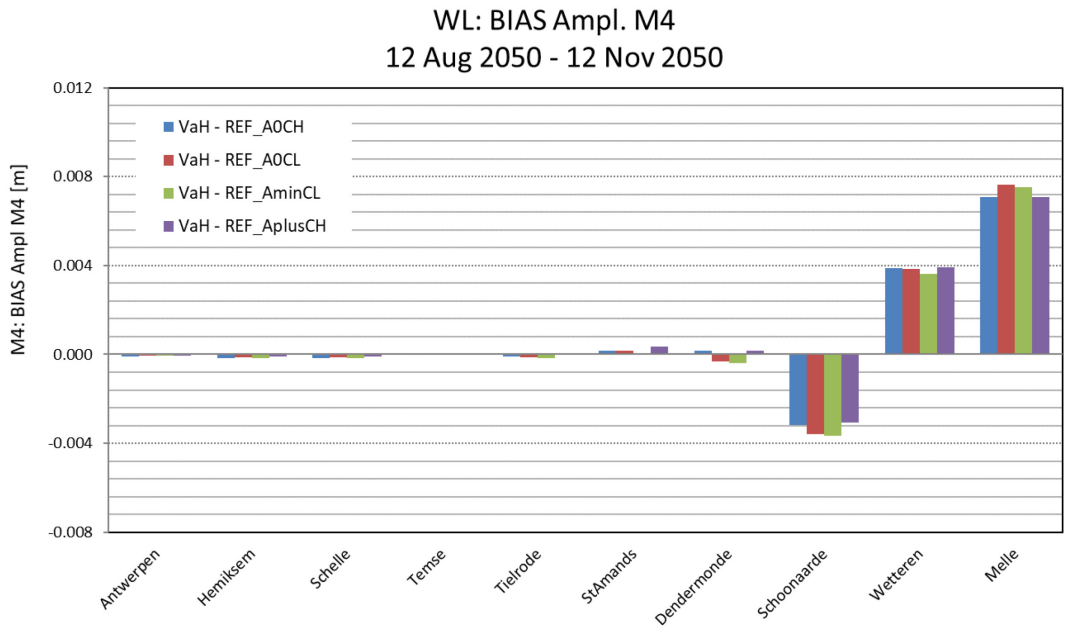

Figure 30 – Bias of Phase M4 in VaH

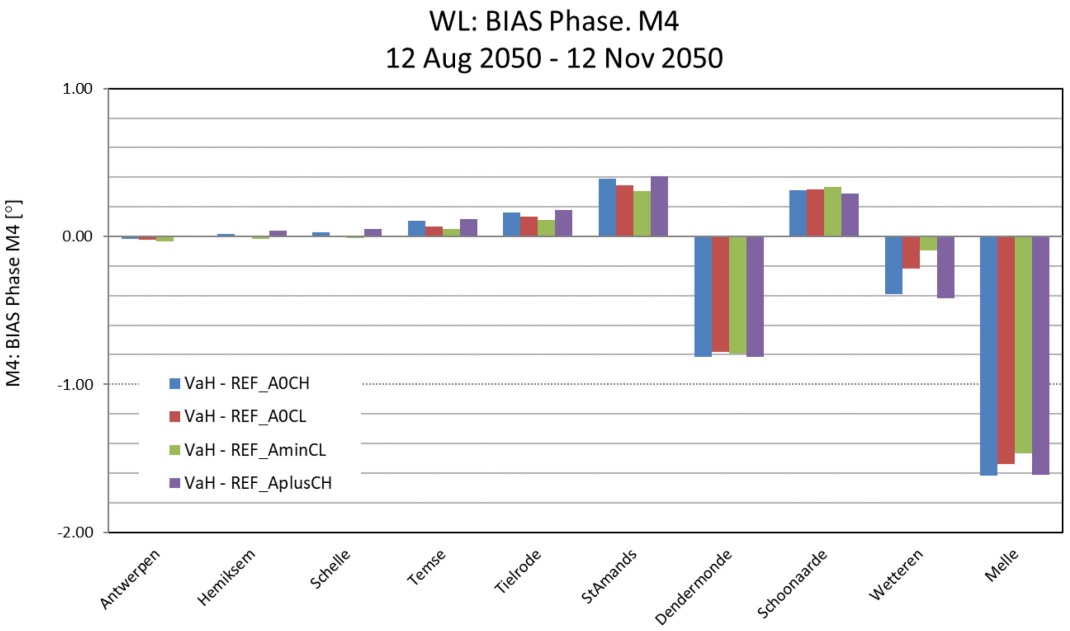

Figure 31 – Bias of Amplitude S2 in VaH

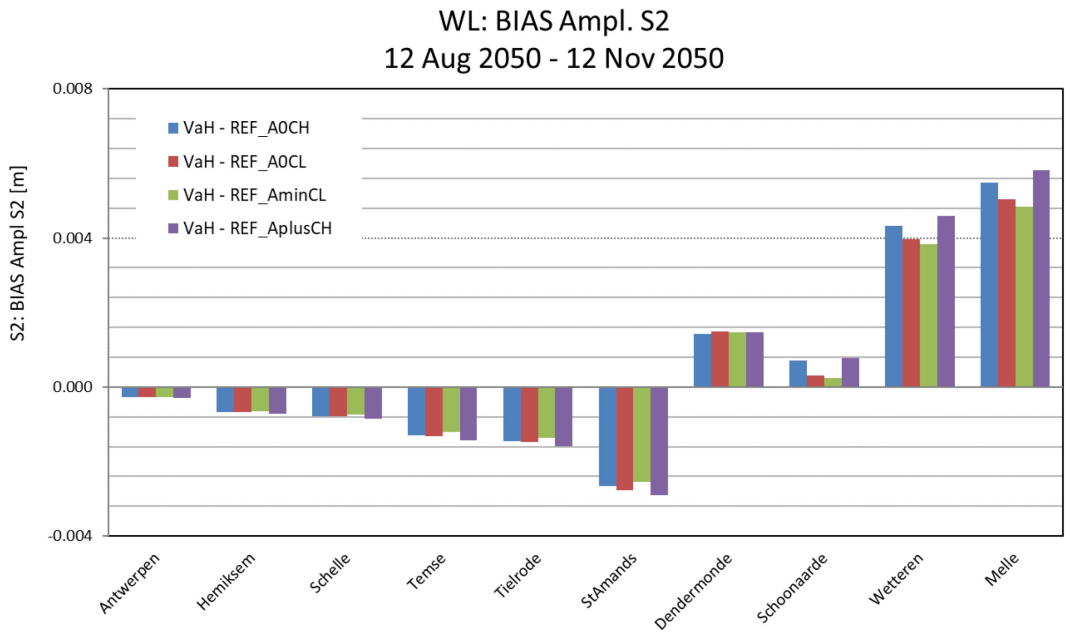

Figure 32 – Bias of Phase S2 in VaH

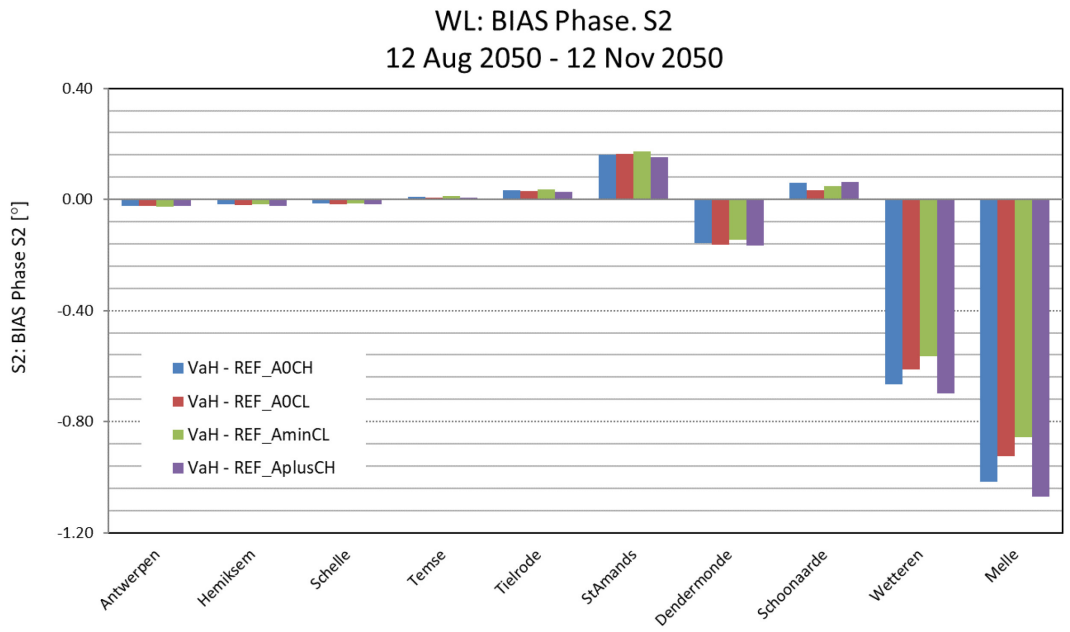

5.2.3 Discharge

Statistical parameters of complete flow discharge time series of all VaH model runs are presented in Appendix 3. In this appendix Table 14, Table 16, Table 18 and Table 20 introduce values of Bias, RMSE and RRMSE of discharges at various locations along the estuary.

Similar results as presented for the VaG alternative (5.1.3) are computed and presented herein for VaH alternative. Figure 33 ('signed' relative RMSE) shows the value of changes relative to the value of discharges in the corresponding reference runs. The sign of 'signed' relative RMSE is the same as the sign of bias and it shows if discharges increase or decrease at each cross-section.

The computed RRMSE values of the complete discharge time series of the VaH alternative (under various scenarios) are presented in Figure 33, between R3 Zimmermangeul and Melle. Results show that changes in discharges downstream of Schelle can be ignored (RRMSE < 0.005) and most of changes are taking place upstream of Schelle. The RRMSE values are increased in the upstream direction until its maximum value at Melle (< 0.06). Again these discharge results of VaH alternative are smaller than the effects of VaG alternative, which has more changes in bathymetry.

Figure 33 – 'Signed' relative RMSE of complete discharge time series of VaH alternative

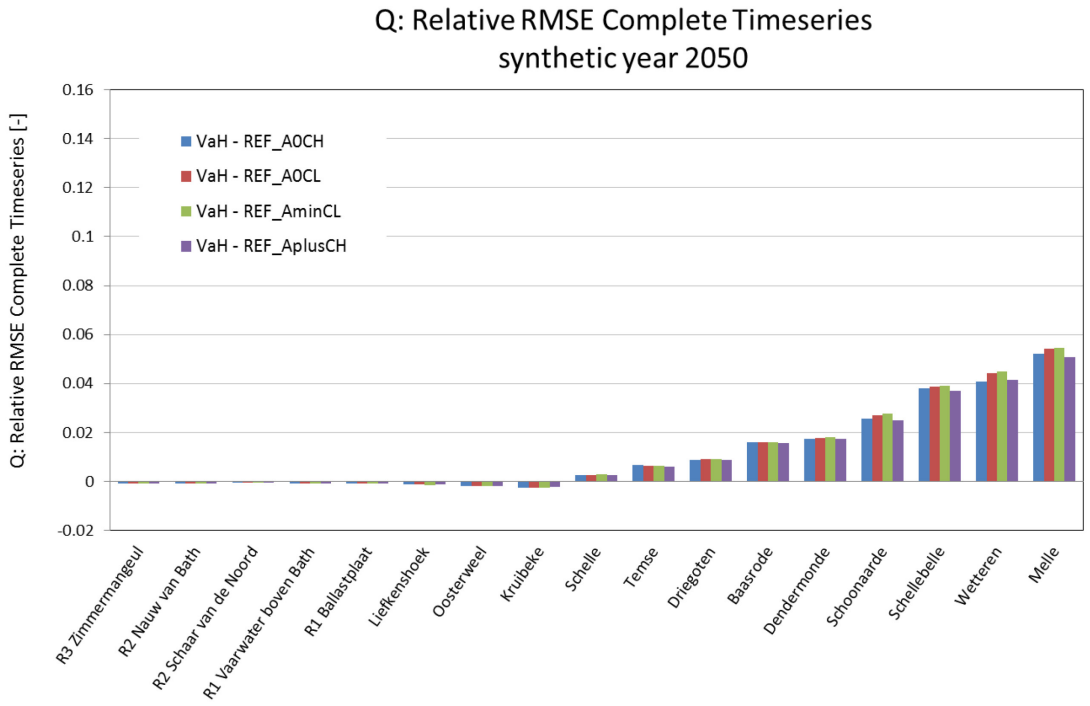

5.2.4 Tidal asymmetry

The values of tidal asymmetry itself are presented in Appendix 3 in Figure 127 to Figure 131. Values smaller than 1 means that the estuary is ebb dominant at a certain location. Two first types of the tidal asymmetry (calculated as $T_{increase}/T_{decrease}$ and T_{flood}/T_{ebb}) show that the estuary is ebb dominant upstream of Liefkenshoek. The tidal asymmetry reduced gradually from about 0.85 – 0.95 at Liefkenshoek to 0.45 – 0.6 at Melle. The third type of the tidal asymmetry ($V_{max\ flood}/V_{max\ ebb}$) varies from more than 1.2 at Liefkenshoek to more than 1.3 at Schelle. It has the smallest value (about 0.9) at Baasrode. At Schoonaarde and Schellebelle the tidal asymmetry is about 1 and it is about 0.7 at Melle.

Figure 34 shows the effects of changes in the bathymetry in VaH alternative model runs in the Sea Scheldt from Liefkenshoek to Melle (the bathymetry is different in these runs upstream the location indicated by the grey vertical line in the plots). There are 5 subplots are presented in Figure 34, each subplot shows the difference in tidal asymmetry calculated based on one of the formulas described in chapter 4.4. Negative values of difference in the plot means that the VaH alternative is more ebb dominant than Reference at a certain location. A positive value means that the VaH alternative is more flood dominant (or less ebb dominant).

Generally, results show that the effect of VaH bathymetry on the tidal asymmetry (Figure 34) is much smaller than the effect of VaG (see chapter 5.1.4). In VaH model runs the tidal asymmetry ($T_{increase}/T_{decrease}$) increases by less than 1% at Schellebelle and Wetteren. The second type of the tidal asymmetry (T_{flood}/T_{ebb}) increases upstream Schellebelle by 0.5 to 2%. The tidal asymmetry parameter ($V_{max\ flood}/V_{max\ ebb}$) increases by 1 to 2% upstream Baasrode in A0CH and AplusCH runs. In A0CL and AminCL runs this parameter increases only at Baasrode and upstream Schoonaarde and it decreases at Dendermonde by less than 1%.

The values of tidal asymmetry calculated based on V^3 and V^4 have two peaks between Liefkenshoek and Melle. The peaks are observed at Baasrode and between Dendermonde and Wetteren. Most of values are smaller than 1 (ebb dominant). The tidal asymmetry parameters (calculated based on V^3 and V^4) reaches a minimum at Dendermonde, Wetteren and Melle.

The biggest effects of VaH alternative are calculated for the last two types of the tidal asymmetry. The asymmetry found based on V^3 increases by about 1% at Baasrode and by 3 to 4% at Schoonaarde and Schellebelle in VaH runs. The increase is slightly bigger in A0CL and AminCL runs compare to other runs. The changes in the tidal bathymetry calculated based on V^4 are bigger than the effects on the asymmetry found based on V^3. The asymmetry increases by about 4 to 6% at Schoonaarde and Schellebelle.

Figure 34 – Effect on the tidal asymmetry (VaH vs Reference)

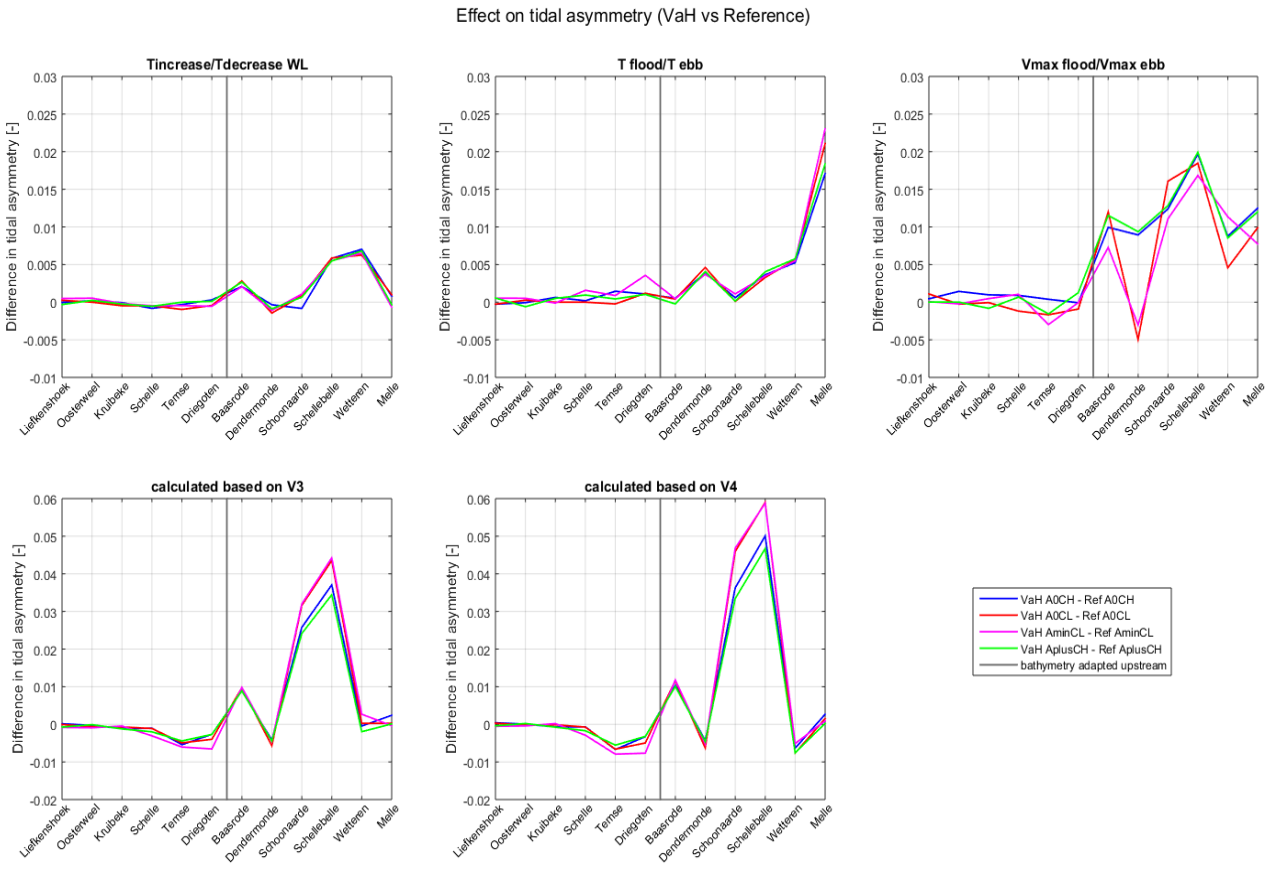

5.3 Effect of Chafing

5.3.1 Water levels

The model results of water level bias of Chafing alternative with various boundary conditions (A0CH, A0CL, AminCL and AplusCH) are presented in Figure 35 to Figure 37 of HW, LW and complete time series, respectively. The presented results are limited to the locations in the upstream part of the estuary (from Antwerp to Melle) as discussed before in subsection 7.1.1.

The Chafing alternative has very limited effect on water levels (in order of centimeters). The maximum changes are taking place upstream of Schelle.

The maximum bias of HW is very limited at all locations with maximum values < 0.015 m, as shown in Figure 35. The LW bias results (Figure 36) show somewhat higher values at Dendermonde with an increase of < 0.03 m. The Chafing alternative results in a much smaller effect on water levels with a maximum change of tidal amplitude in the downstream part of Dendermonde (< 0.025 m at Sint-Amands). Tidal amplitudes are increased upstream of Dendermonde with a maximum value < 0.035 m at Dendermonde.

It is important to state also that water level results of Chafing alternative as expected are much smaller than previous results of VaG alternative, which are presented in subsection 5.1.1. VaG alternative has more changes in bathymetry compare to Chafing alternative.

The statistical parameters of HW, LW and complete time series of water levels of all model runs are presented in Appendix 3. Table 21 presents (Chafing_A0CH - Reference_A0CH), Table 23 (Chafing_A0CL - Reference_A0CL), Table 25 (Chafing_AplusCH - Reference_AplusCH) and Table 27 (Chafing_AminCL - Reference_AminCL).

Figure 35 – Bias of high water magnitude in Chafing

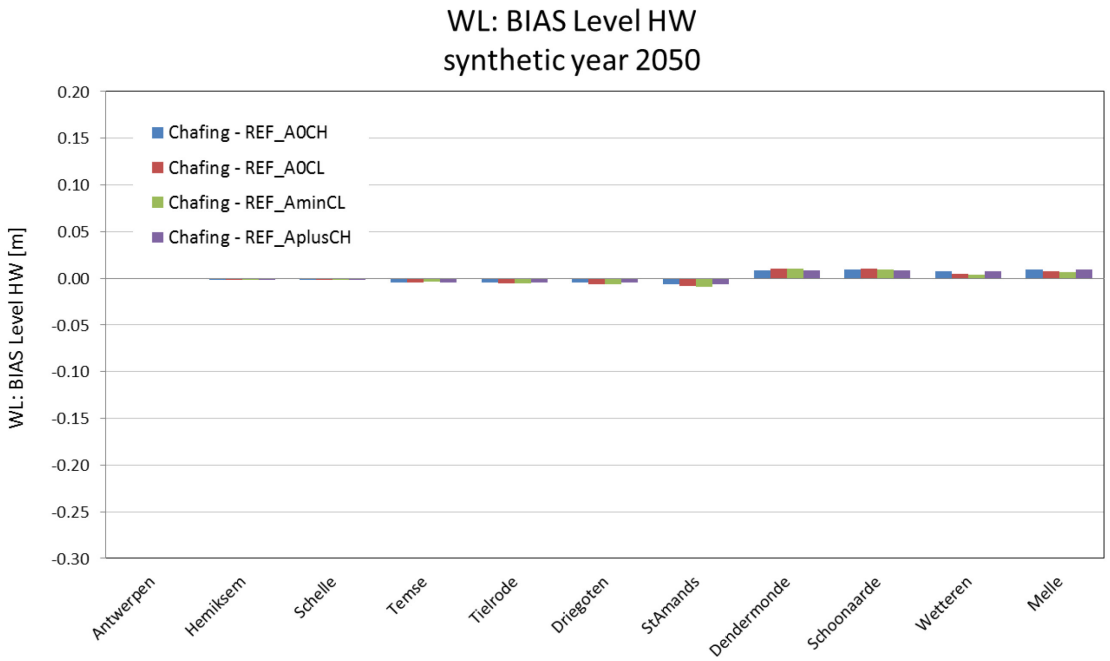

Figure 36 – Bias of low water magnitude in Chafing

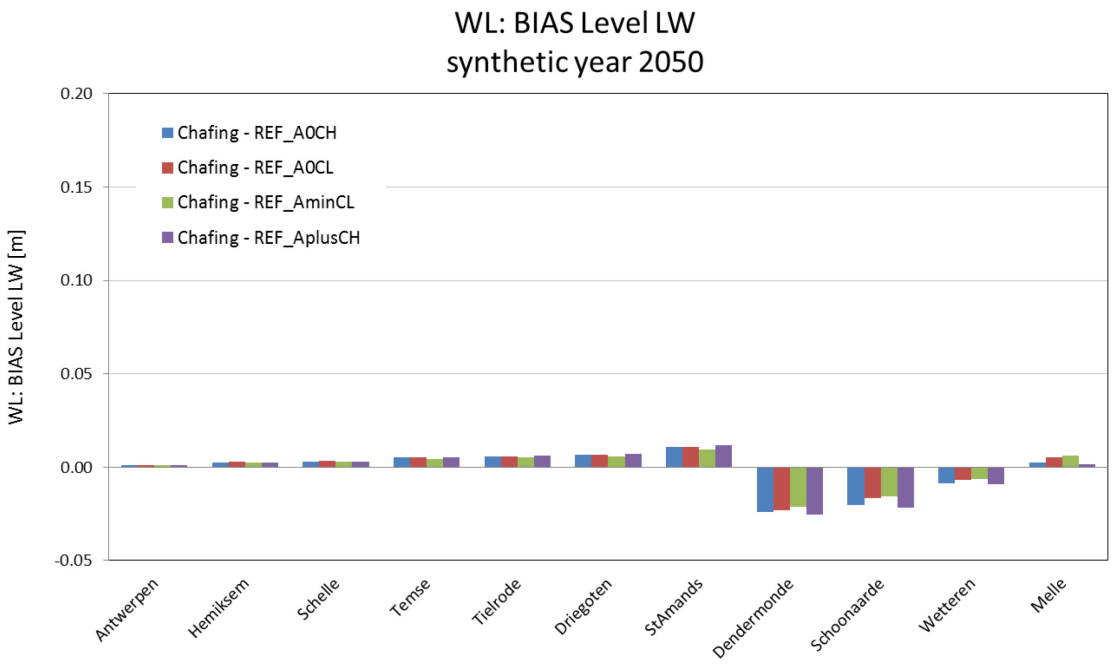

Figure 37 – Bias of complete water level time series in Chafing

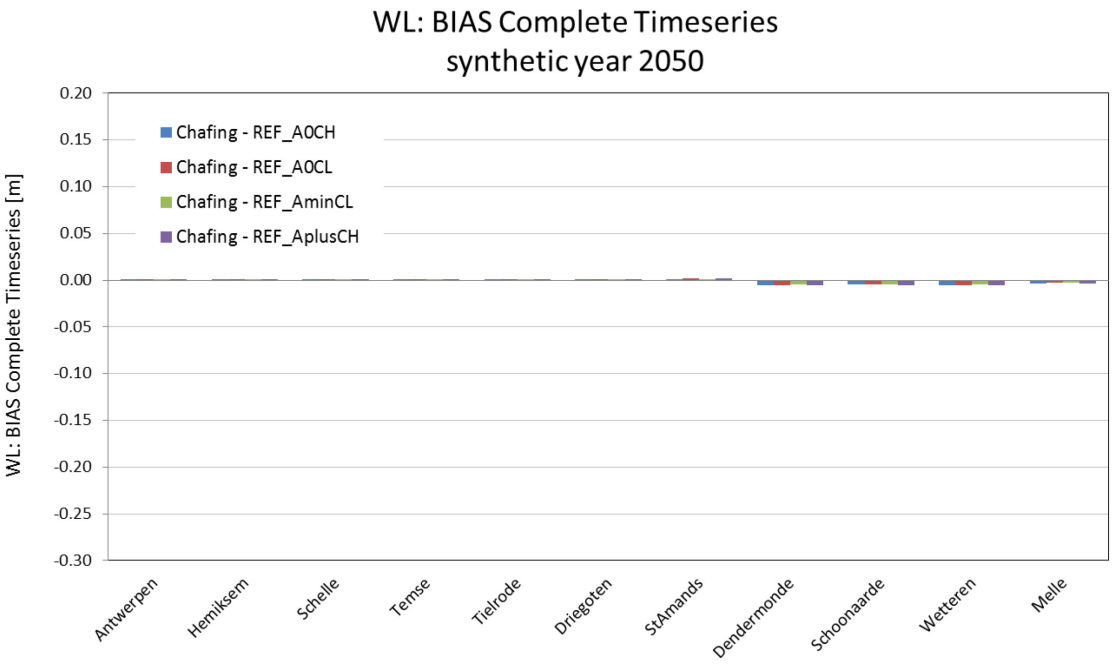

5.3.2 Harmonic components

The computed Bias values of amplitudes and phases of M2, M4 and S2 are presented in Figure 38 to Figure 43 of Chafing alternative (under various scenarios), respectively.

The results at different locations along the estuary show that Chafing alternative has no clear effects on the harmonic components (M2, M4 and S2) of the tide. These effects are smaller than 0.014 m (M2), 0.006 m (M4) and 0.004 m (S2). The maximum Bias values of phases (< 0.7°) of different tidal components are always taking place upstream of Sint-Amands for M2, M4 and S2.

Details of harmonic analysis of Chafing alternative are presented in combination with the reference situation in Figure 132 to Figure 155 in Appendix 4. Amplitudes and phases of M2, M4 and S2 are presented for all model runs. Results of Chafing alternative shows some effects on the harmonic components (M2, M4 and S2) of the tide.

Figure 38 – Bias of Amplitude M2 in Chafing

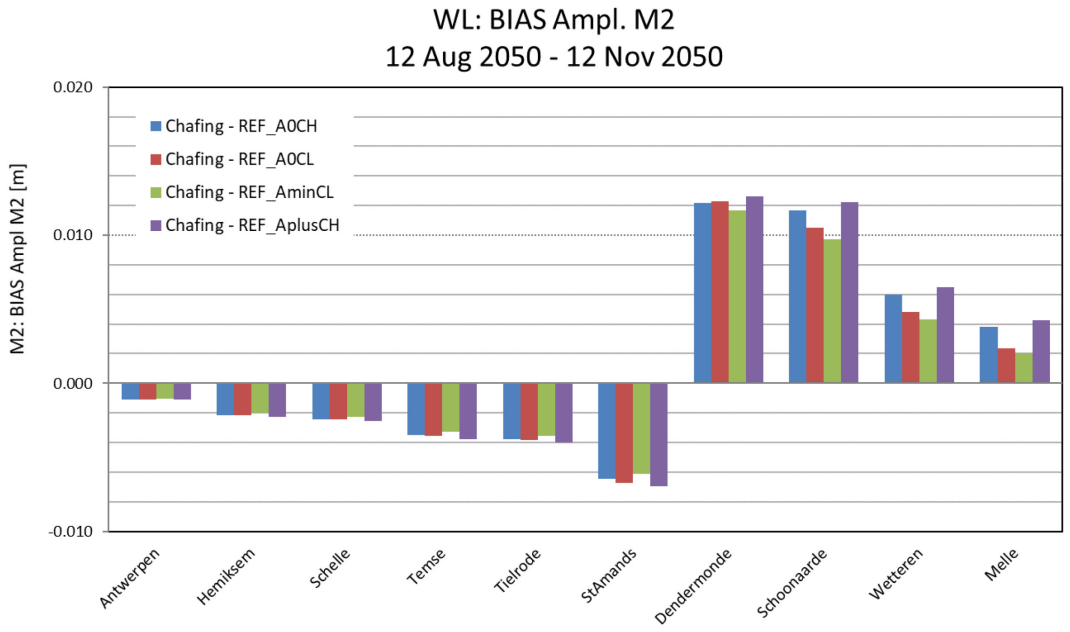

Figure 39 – Bias of Phase M2 in Chafing

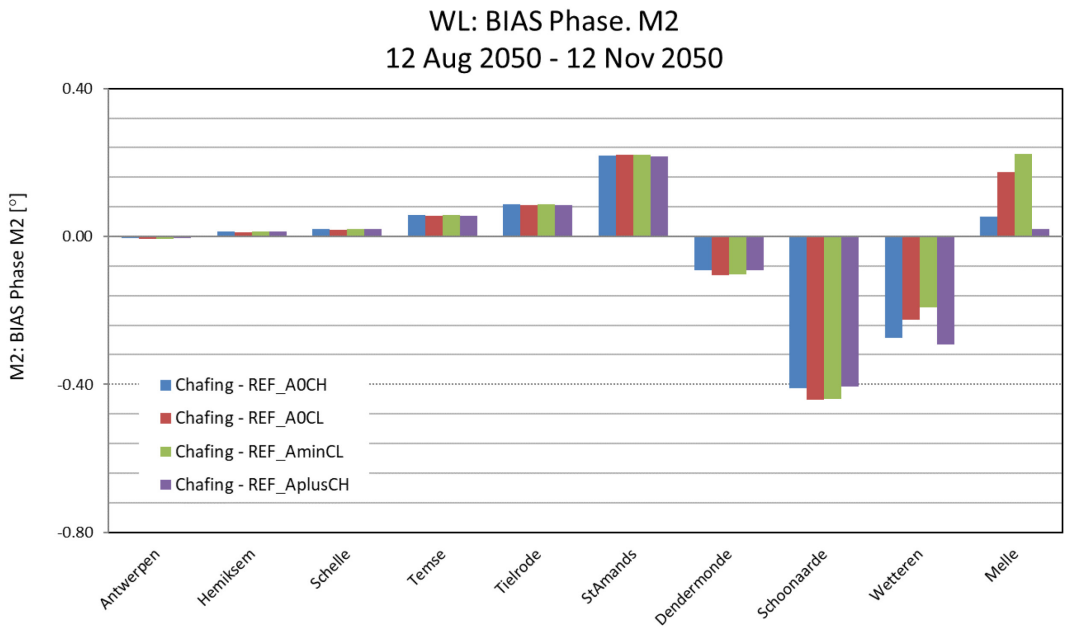

Figure 40 – Bias of Amplitude M4 in Chafing

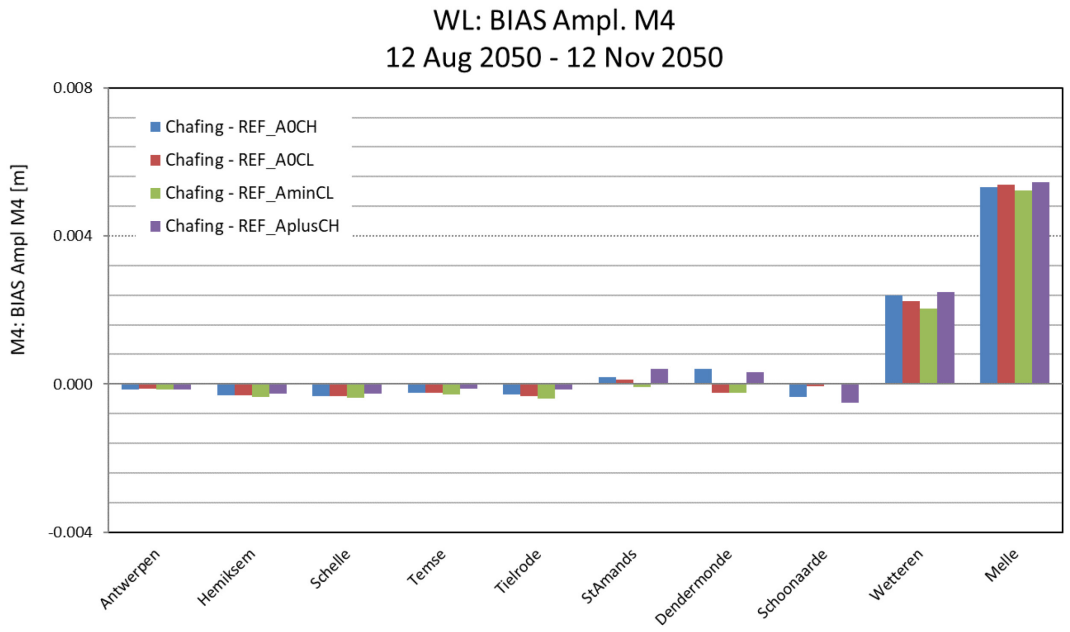

Figure 41 – Bias of Phase M4 in Chafing

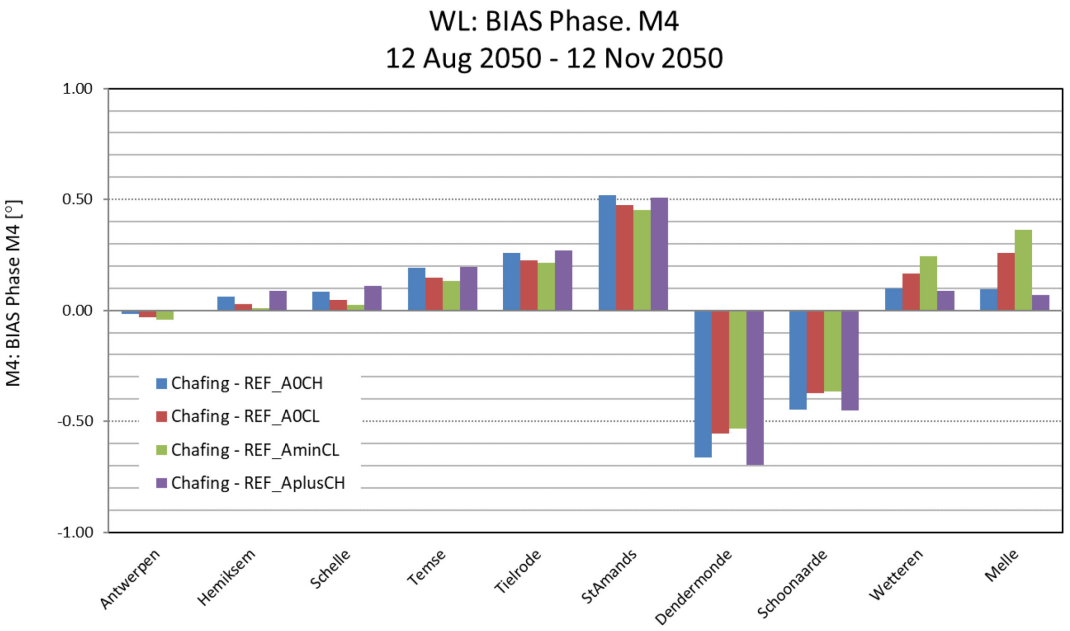

Figure 42 – Bias of Amplitude S2 in Chafing

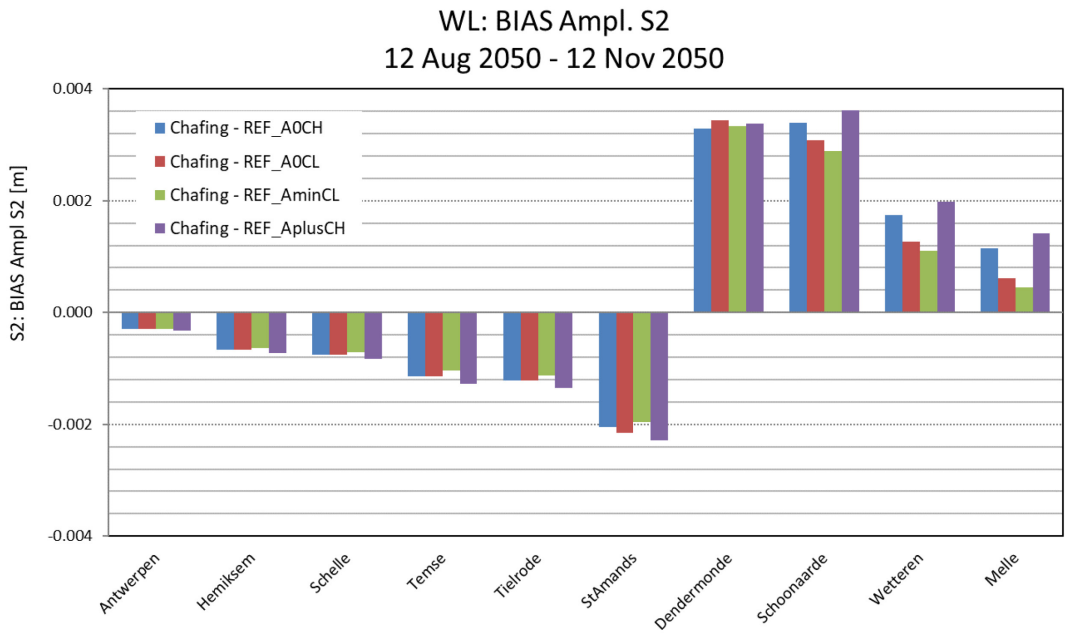

Figure 43 – Bias of Phase S2 in Chafing

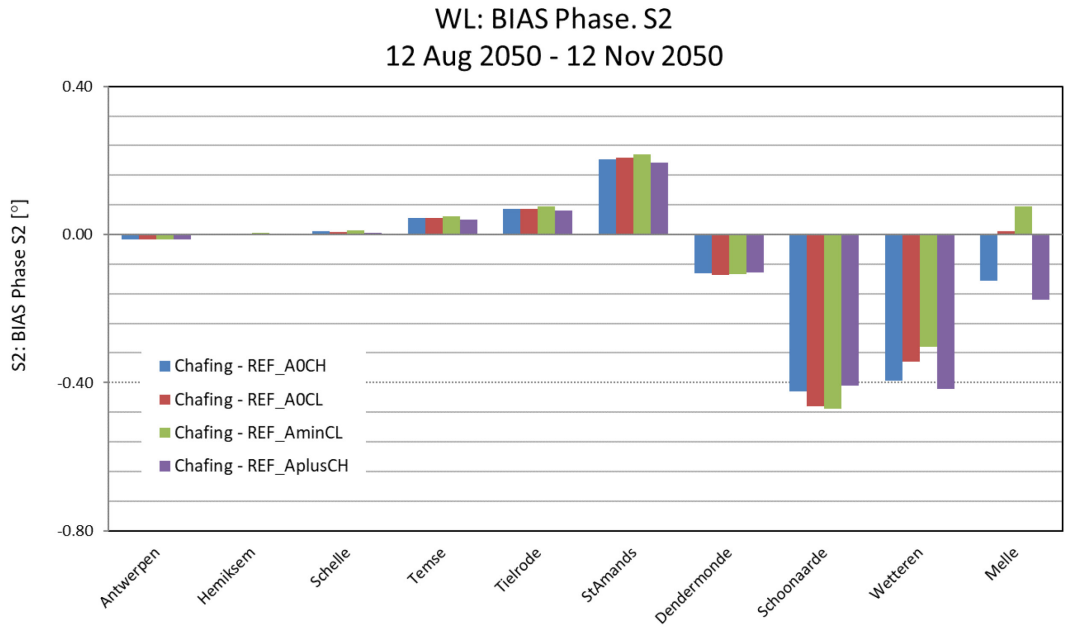

5.3.3 Discharge

Statistical parameters of the discharge complete time series for all Chafing model runs are presented in Appendix 4. In this appendix Table 22, Table 24, Table 26 and Table 28 introduce values of Bias, RMSE and RRMSE of discharges at various locations along the estuary.

Computed values of RRMSE of Chafing alternative are presented herein which are similar to presented results of VaG alternative (subsection 5.1.3). Figure 44 ('signed' relative RMSE) shows the value of changes relative to the value of discharges in the corresponding reference runs at each cross-section.

The computed RRMSE values of complete discharge time series of the VaH alternative (under various scenarios) are presented in Figure 44, between R3 Zimmermangeul and Melle. Results show that changes in discharges downstream of Schelle can be ignored (RRMSE < 0.005) and most of changes are taking place upstream of Schelle. The RRMSE values are increased in the upstream direction until its maximum value at Melle (< 0.04). It is important to stat that these discharge results of Chafing alternative are much smaller than the effects of VaG alternative, which has more changes in bathymetry compare to the Chafing alternative.

Figure 44 – 'Signed' relative RMSE of complete discharge time series of Chafing alternative

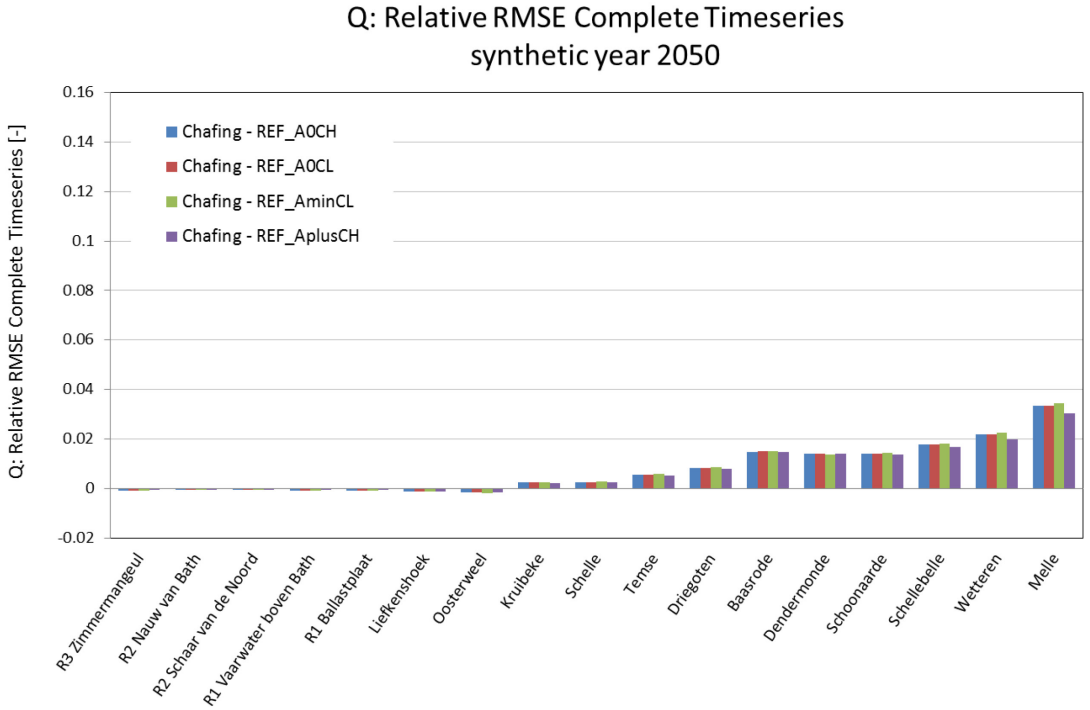

5.3.4 Tidal asymmetry

The values of tidal asymmetry itself are presented in Appendix 4 in Figure 156 to Figure 160. Values smaller than 1 mean that the estuary is ebb dominant at a certain location. Two first types of the tidal asymmetry (calculated as $T_{increase}/T_{decrease}$ and T_{flood}/T_{ebb}) show that the estuary is ebb dominant upstream Liefkenshoek. The tidal asymmetry reduced gradually from about 0.85 – 0.95 at Liefkenshoek to 0.45 – 0.6 at Melle. The third type of the tidal asymmetry ($V_{max\ flood}/V_{max\ ebb}$) varies from more than 1.2 at Liefkenshoek to more than 1.3 at Schelle. It has the smallest value (about 0.9) at Baasrode. At Schoonaarde and Schellebelle the tidal asymmetry is about 1 and it is about 0.7 at Melle.

Figure 45 shows the effects of the bathymetry changes in Chafing alternative runs in the Sea Scheldt from Liefkenshoek to Melle (the bathymetry changes in these runs are upstream the location indicated by the grey vertical line in the plots). There are 5 subplots in each figure; each subplot shows the difference of the tidal asymmetry parameters calculated based on one of the formulas described in chapter 4.4. Negative values of the difference in the plot mean that the Chafing alternative is more ebb dominant than reference situation at a certain location. Positive values mean that the Chafing alternative is more flood dominant (or less ebb dominant).

The effect of Chafing alternative bathymetry on the tidal asymmetry is much smaller than the effect of VaG alternative (see chapter 5.1.4). In Chafing alternative runs the changes in tidal asymmetry ($T_{increase}/T_{decrease}$) are smaller than 1%. The second type of the tidal asymmetry (T_{flood}/T_{ebb}) increases by 1 to 1.5% at Melle. The tidal asymmetry ($V_{max\ flood}/V_{max\ ebb}$) increases by 0.5 to 1% at Baasrode. The changes upstream are different in A0CH, A0CL, AminCL and AplusCH runs (Figure 45). At most locations the differences are smaller than 1%.

The values of tidal asymmetry calculated based on V^3 and V^4 have two peaks between Liefkenshoek and Melle. The maximums are observed at Schelle and Schoonaarde. Most of maximum values are smaller than 1 (ebb dominant), except for scenario Chafing AminCL (V^3) and scenario Chafing A0CL and Chafing AminCL (V^4) which are bigger than 1 (flood dominant). The tidal asymmetry (calculated based on V^3 and V^4) is minimum at Baasrode and Melle.

The biggest effects are calculated for two last types of the tidal asymmetry parameters. The asymmetry parameter based on V^3 increases by about 1% at Baasrode and Melle and by 1 to 2% at Schoonaarde and Schellebelle in Chafing alternative runs. This parameter decreases by 0.5 to 1 % at Dendermonde and Wetteren. The asymmetry parameter calculated based on V^4 increases by about 1.5 to 2% at Schoonaarde and Schellebelle. It decreases by 1% at Dendermonde and 2% at Wetteren.

Figure 45 – Effect on the tidal asymmetry (Chafing vs Reference)

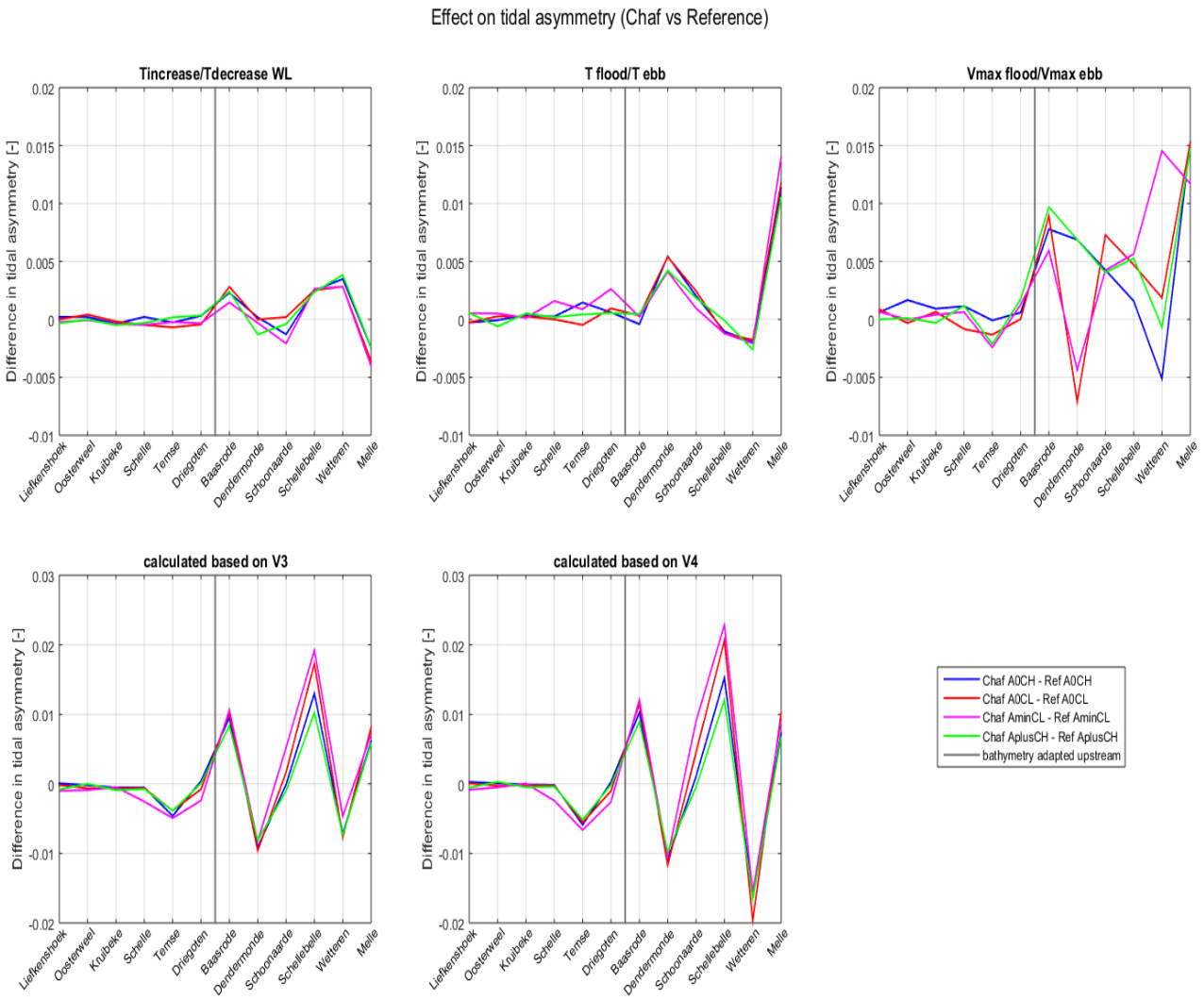

6 Comparison between Scaldis and the 1D-model results

This chapter presents a comparison between the 1D-model of the “Bouwstenenonderzoek” (IMDC,2017) and the Scaldis (3D) model of FHR results, using 5 different parameters. These parameters include Tincrease and Tdecrease, Tflood/Tebb, Vmax flood and Vmax ebb, HW and LW and Relative tidal amplitude. The first three parameters are described before in section 4.4. The last two parameters are presented in this chapter only to compare the results with the 1D-model.

The model comparisons are limited to VaG and Chafing alternatives, which are computed with the 1D-model. The following subsections introduce the differences of each parameter with the references of each B alternatives (VaG and Chafing), which have been carried out by both the 1D and 3D models.

6.1 VAG alternative

Table 3 presents comparison between the Scaldis 3D model and the 1D-model results as presented in Figure 46 to Figure 50.

All presented figures for the Scaldis-model intercomparison, in this chapter, are based on using the distances of each location starting from Vlissingen (0 km).

Table 3 – Comparison between Scaldis-model and the 1D-model, VaG alternative

Parameter	1D-model	Scaldis 3D-model
HW and LW (m) Figure 46	Almost no changes in the first 60 km (Liefkenshoek) upstream the mouth. LW shows positive values between 20 km (Terneuzen) and 120 km (Dendermonde). This means that LW rises between these 2 locations. Starting from 120 km (Dendermonde) LW is sharply reduced (negative values) in the upstream direction to 155 km (Melle). HW values are reduced in the downstream part between 20 km and 144 km (Wetteren), where it starts to sharply increase with positive value at Melle (155 km). Maximum values of HW and LW takes place at 2 locations, Dendermonde (120 km) and at Melle (155 km). LW has 2 peaks (+0.05) and (< -0.15) m at Dendermonde. HW has 2 peaks (-0.05) at Dendermonde and (+0.11) m at Melle.	Almost no changes in the first 60 km (Liefkenshoek) upstream the mouth. LW are increased between Liefkenshoek (40 km) and Baasrode (115 km) followed by a clear reduction (negative values) in the upstream direction between Baasrode (115 km) and Melle (155). Similar to the 1D-model, HW shows opposite behavior compare to LW changes. Negative values (with gradual reduction) between Liefkenshoek (60 km) and Baasrode (115 km) are followed by sharp increase (positive values) between Baasrode (115 km) and Melle (155 km). Maximum values of HW and LW are taking place at Dendermonde (120 km). LW has maximum values of 0.4 and -0.3 m and HW has maximum values of 0.12 and -0.03 m.
	Generally, the 1D-model and the Scaldis-model showed more or less the same evolution for HW and LW variation along the estuary. Both models are able to predict correctly the opposite behavior of HW and LW changes. <u>The main differences between the two models can be observed upstream of Dendermonde (120 km)</u>. HW and LW in the 1D-model are increasing continuously until Melle (155 km). On the other hand, the Scaldis-model shows the highest values (HW and LW) at Dendermonde (120 km) which are followed by variations in the upstream direction. The LW level in Melle (155 km) experiences a strong drop of approximately 0.34 m in the 1D-model. This drop is present at Dendermonde in the Scaldis-model (0.3 m).	
Tincrease and Tdecrease (min) Figure 47	Between Oosterweel (70 km) and Dendermonde (120 km) Tincrease and Tdecrease have a very small values < 2 min. Tincrease shows small negative values and Tdecrease shows positive values. This indicates that the period of rising tide is slightly reduced and the period of falling tide is slightly increased. Upstream of Dendermonde (120 km) Tincrease is increased (positive values) and Tdecrase is reduced until Melle (155 km). These changes in values means that the time of rising water level is increased and the duration of falling tide is reduced in the upstream part.	For Tincrease, positive values are more dominant between Driegoten (100 km) and Melle (155 km) with only one negative value at Schoonaarde (130 km). Tdecrease shows opposite behavior at the same locations. Maximum values of Tdecrase and Tincrease are fluctuating upstream of Driegoten (105 km), unlike the 1-D model. Maximum values of Tincrese are observed at Baasrode, 110 km (+6 min) and at Melle (+3.8 min). Tincrease results indicate that the time of water rising from LW to HW is increased in the upstream part.

	Maximum values of Tincrease (+6 min) and Tdecrease (-6 min) are observed at Melle.	Maximum values of Tdecrease are equal to -5.7 min at Schoonaarde (130 km) and -4 min at Melle. Values of Tdecrease show that the duration of falling tide is reduced.
	Changes of Tincrease and Tdecrease in the upstream part of the estuary show some differences between the two model results. The 1D-model shows a continues increase of both values until Melle (155) while the Scaldis-model shows the highest value at Dendermonde (120 km) and is followed by variations in the upstream direction. The results of the two models are similar in the downstream part of the estuary.	
Vmax flood and Vmax ebb (m/s) Figure 48	No significant effects on maximum ebb and flood velocities downstream of Oosterweel (70 km). Upstream of Oosterweel (70 km) Vmax ebb has positive values with maximum value > 0.16 m/s at Wetteren (140 km). Vmax flood has negative values over the same distance with maximum value < -0.16 m/s at Wetteren (140 km).	Similar to the 1D-model, there are no significant effects on velocities downstream of Oosterweel (70 km). Upstream of Oosterweel Vmax ebb has positive values with maximum value = 0.15 m/s at Dendermonde (120 km) and a maximum negative value = -0.1 m/s at Wetteren (140 km). Vmax flood has negative values over the same distance with maximum value = -0.12 m/s at Dendermonde (120 km) and maximum positive value = 0.09 m/s at Wetteren (140 km).
	Both models show a similar evolution of the maximum ebb and maximum flood velocities. The maximum velocities increase with respect to the reference. The greatest differences are expected close to Dendermonde, where the ebb velocity increases by almost 20 cm/s, and the flood velocity increases by approx. 17 cm/s. Afterwards, the difference with the reference decreases again. The ebb and flow rates react in an equal way to both models except at Wetteren (140 km). The predicted velocity values are within the same range. The maximum velocities of the Scaldis-model can be observed at Dendermonde (120 km) while in the 1D-model at (140 km).	
Relative tidal amplitude Figure 49	No change in the relative tidal amplitude downstream of Oosterweel (70 km). Negative values are taking place between Oosterweel (70 km) and Dendermonde (120 km) with a maximum value = -0.02. Strong increase with positive values occurs upstream of Dendermonde (120 km) with a maximum value of 0.1 at Melle (155 km).	Similar to the 1D-model, no changes occurs downstream of Oosterweel (70 km). Negative values are taking place between Oosterweel and Baasrode (110 km) with maximum value equal to -0.05. Upstream of Baasrode (115 km) positive values are taking place to Melle (155 km) with maximum value equal to +0.4 at Dendermonde (120 km).
	Although both models are able to show more or less the same trend along the estuary, the Scaldis-model predicts higher values than the 1D-model. This indicates that the Scaldis-model is more sensitive to bathymetry changes in the estuary. The maximum value of the Scaldis-model are taking place at Dendermonde (120 km) and is followed by small fluctuations in the upstream direction to Melle (155 km). Meanwhile, The 1D-model values are increased continuously in the upstream direction.	

Tflood/Tebb Figure 50	Differences with the reference are negative between Oosterweel at 70 km and Dendermonde at 120 km. Maximum negative value is located at 115 km (Baasrode), which is > -0.01. Upstream of Dendermonde (120 km) differences show sharp increase with positive values with a maximum value > 0.03 at Melle (155 km).	Most of values are very close to zero downstream of Schelle (90 km). Upstream of Schelle (90 km) results show a positive increase with fluctuation along the distance to Melle (155 km). The value at Temse (100 km) is positive and at Baasrode (115 km) is negative. Upstream of Baasrode all differences are positive. The maximum positive value is observed at 120 km (Dendermonde) (+0.045 m) and a maximum negative value are located at (105 km) Baasrode (- 0.01 m).
	The two models showed more or less the same trend in the downstream part of the estuary. Starting from Temse (100 km) and upstream part results are deviated from each other. The Scaldis-model predicts a maximum value at Dendermonde (120 km) and smaller values upstream of it. The 1D-model shows a continues increase upstream of Dendermonde (120 km). Results of the two models are in the same range of magnitudes between -0.01 and 0.045.	

Figure 46 – Relative changes of HW and LW (VaG vs Reference) as computed using the Scaldis-model (upper panel) and the 1D-model (lower panel)

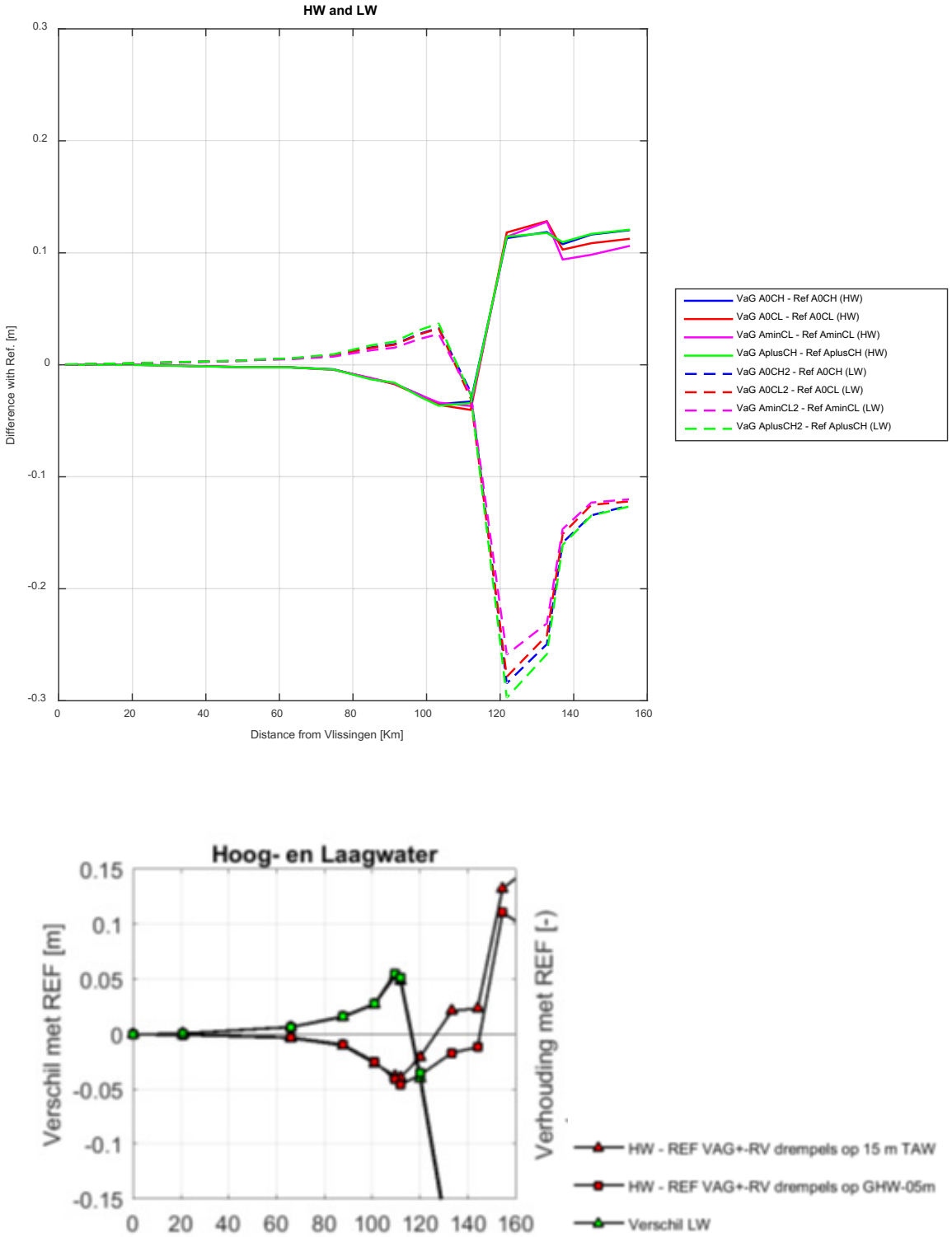

Figure 47 – Relative changes of Tincrease and Tdecrease (VaG vs Reference) as computed using the Scaldis-model (upper panel) and the 1D-model (lower panel)

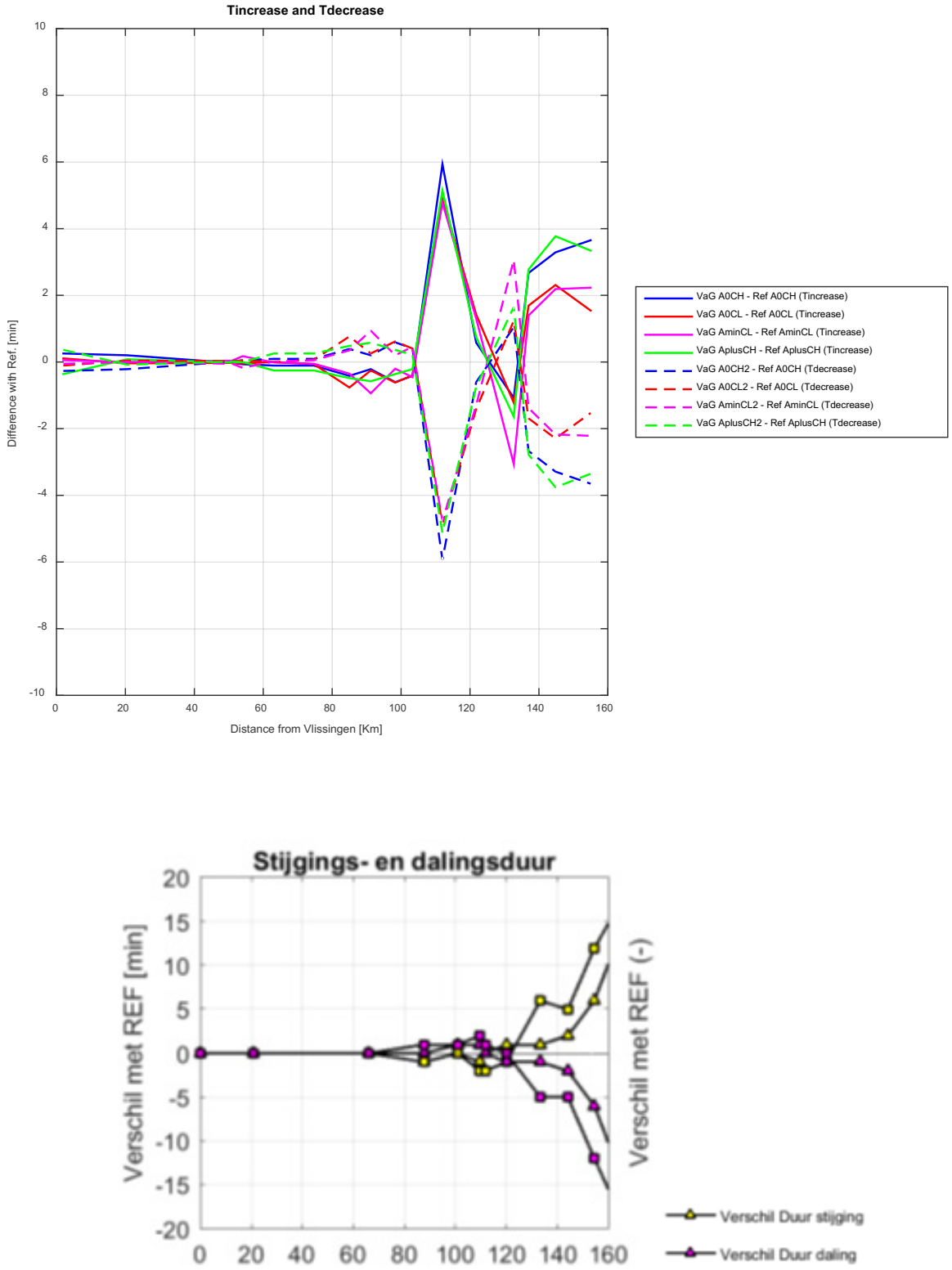

Figure 48 – Relative changes of Vmax flood and Vmax ebb (VaG vs Reference) as computed using the Scaldis-model (upper panel) and the 1D-model (lower panel)

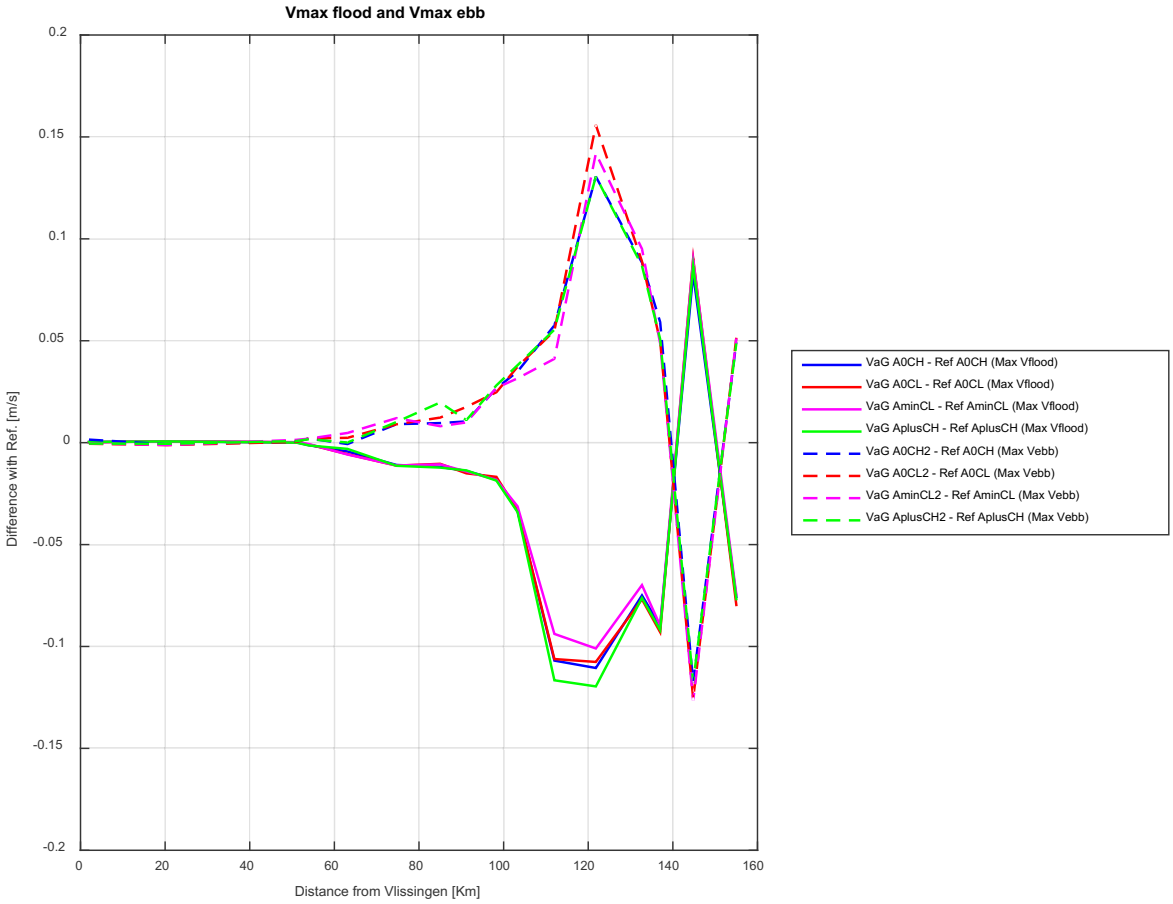

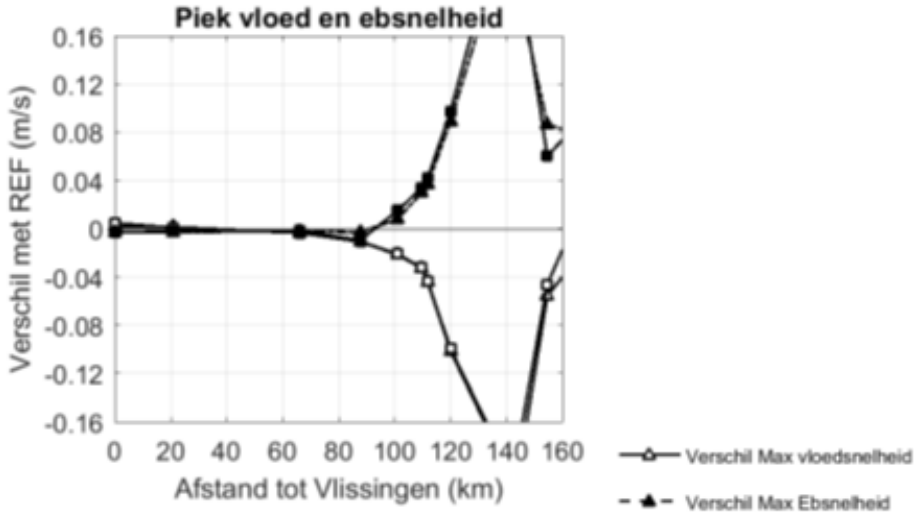

Figure 49 – Relative changes of relative tidal amplitude (VaG vs Reference) as computed using the Scaldis-model (upper panel) and the 1D-model (lower panel)

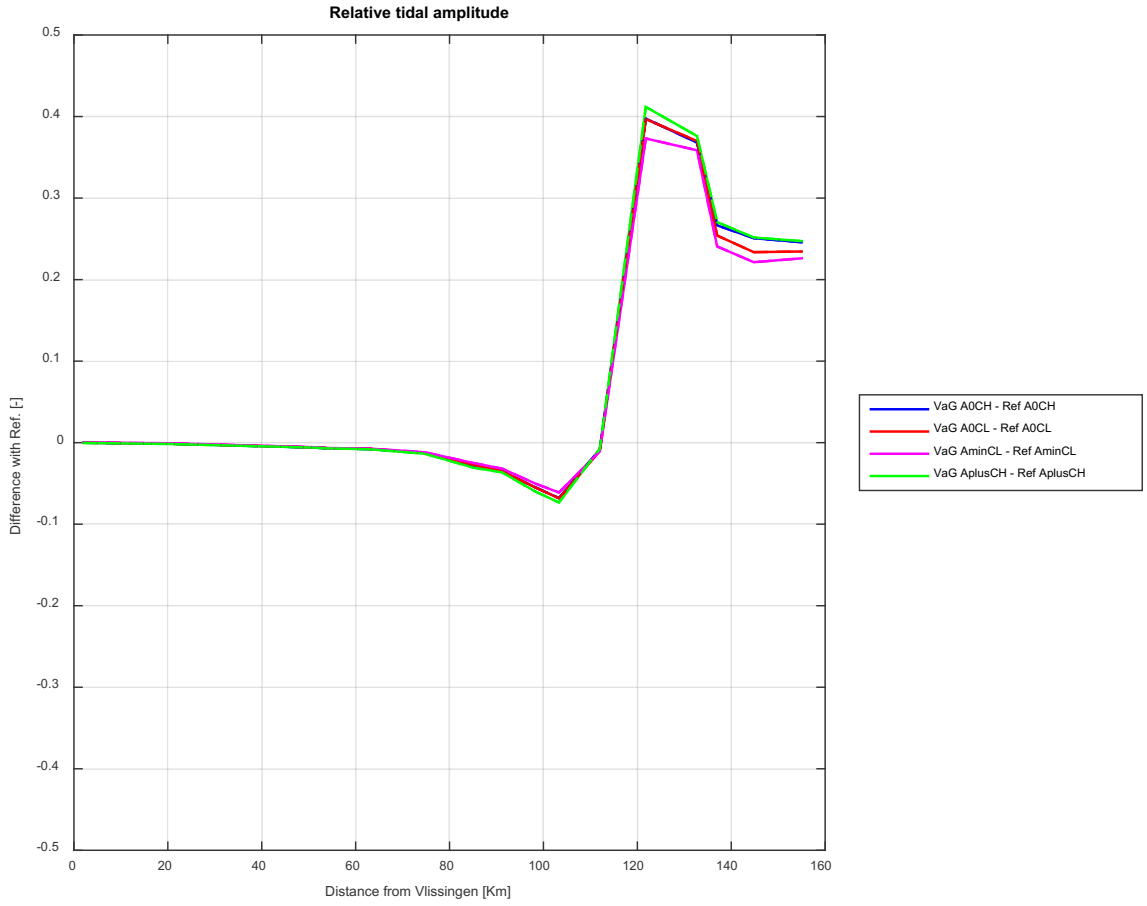

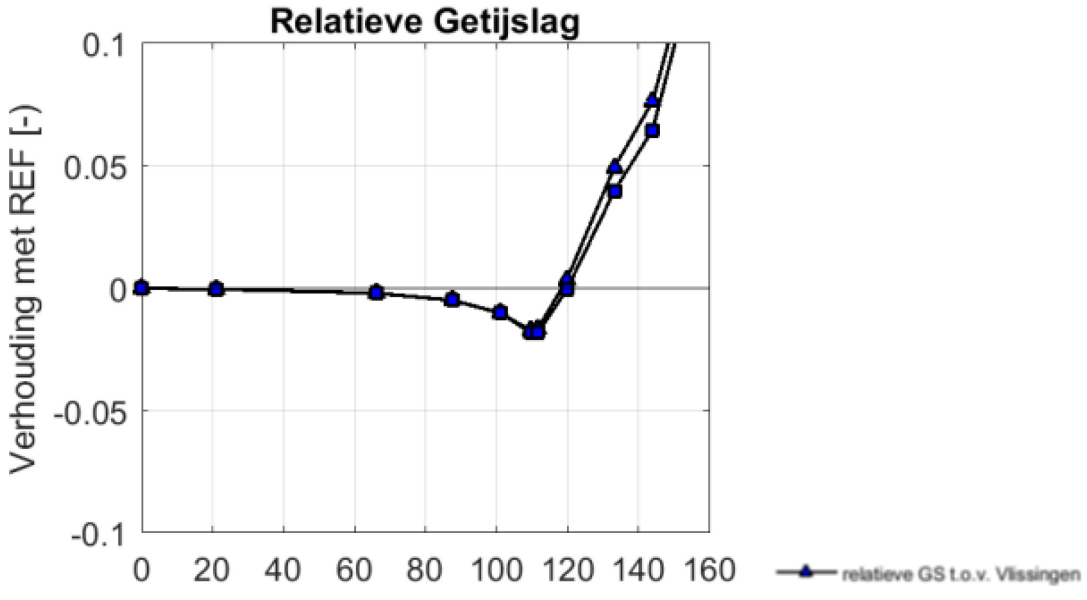

Figure 50 – Relative changes of Tflood/Tebb (VaG vs Reference) as computed using the Scaldis-model (upper panel) and the 1D-model (lower panel)

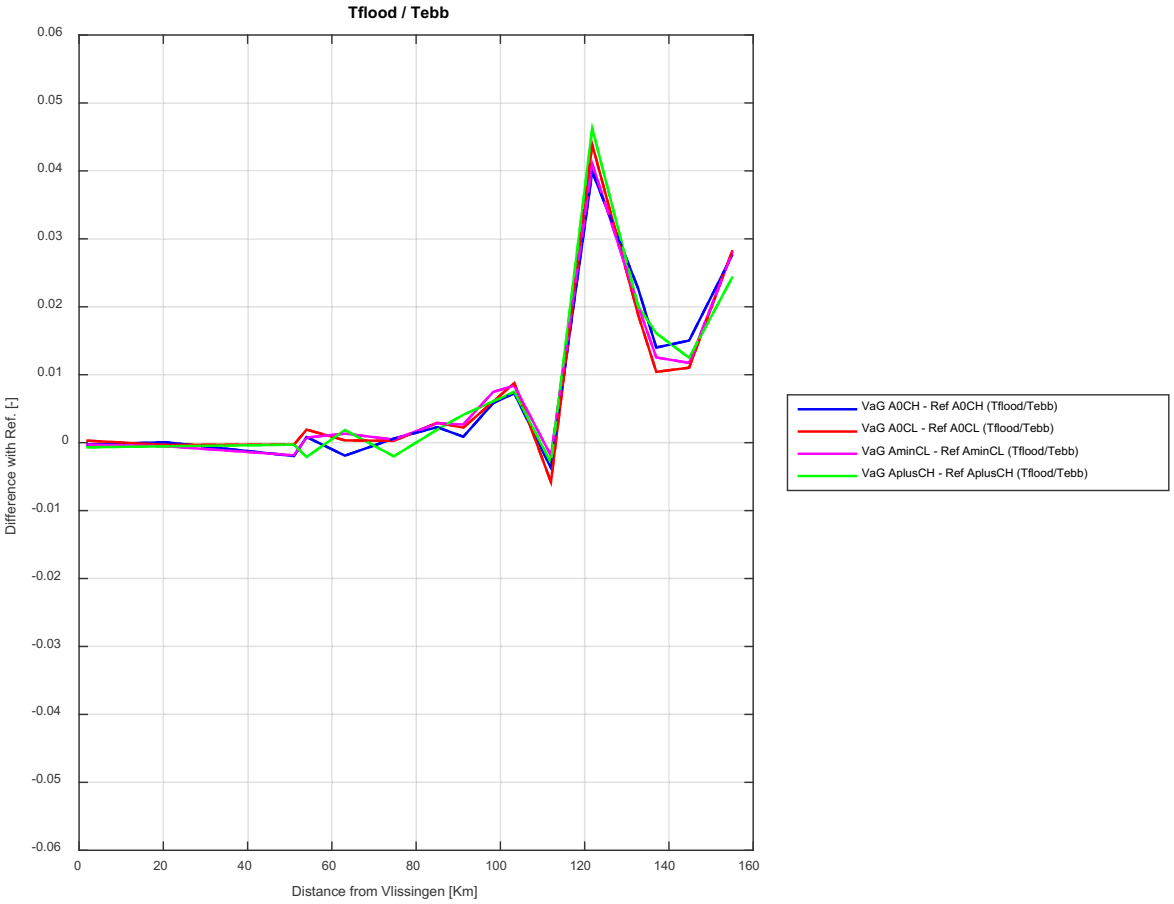

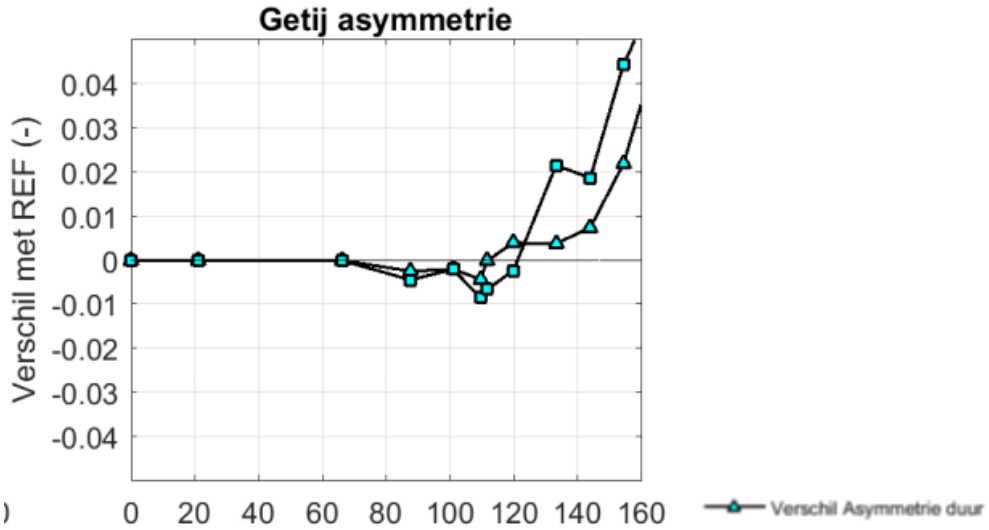

6.2 Chafing alternative

Table 4 presents comparison between the Scaldis 3D model and the 1D-model results as presented in Figure 51 to Figure 55.

Table 4 – Comparison between Scaldis-model and the 1D-model, VaG alternative.

Parameter	1D-model	SCALDIS 3D model
HW and LW (m) Figure 51	Almost no changes in the downstream part of the estuary from the mouth until Oosterweel (70 km). LW shows an increase of values between Oosterweel (70 km) and Schoonaarde (130 km). Starting from Schoonaarde (130 km) LW has a reduction in values to Melle (155 km). HW shows a general reduction with negative values between Oosterweel (70 km) and Melle (155 km), where it returns close to zero with a positive value. Maximum difference between HW and LW takes place at 2 locations, Dendermonde (120 km) and at Melle (155 km), 0.14 m and 0.12 m, respectively. These predicted values are much larger that the predictions of the Scaldis-model.	Similar to the 1D-model, no changes at the same locations downstream of Oosterweel (70 km). Similar to the 1D-model LW shows an increased values between Oosterweel (70 km) and Baasrode (110 km) followed by reduction of values between Dendermonde and Melle (155 km). HW shows similar behavior in the downstream part, compare to the 1D-model. HW values are reduced until Dendermonde (120 km). Along the distance positive values are observed upstream of Dendermonde (120 km). Maximum difference between HW and LW takes place at 2 locations, Baasrode at 110 km (0.02 m) and Dendermonde at 120 km (0.03 m). These values are much smaller that the 1D-model results.
	Both model results are identical in the downstream part until Oosterweel (70 km). In general the two models show more or less the same trend. The predicted changes in HW and LW values are not in the same range the 1D-model predicted maximum changes of about 0.14 m, while the Scaldis-model shows maximum range of about 0.03 m. The Chafing alternative has smaller effects on water level changes compare to VaG alternative, as presented in Table 3.	
Tincrease and Tdecrease (min) Figure 52	Positive values of Tdecrease are observed between Oosterweel (70 km) and Wetteren (144 km). Meanwhile negative values of Tincrease are occurred at the same locations. At Melle (155 km) Tdecrase and Tincrease changed its signs from positive to negative and vice versa. Maximum values of Tdecrease are observed at Schelle (90 km) with 2 min and at Melle (155 km) with -5 min. Maximum changes of Tincrease are equal	For Tdecrease, positive values are more dominant between Driegoten (100 km) and Wetteren (144 km) with only one negative value at Schoonaarde (130 km). Along the estuary we can observe opposite behavior of both Tincrease and Tdecrease, which are similar to the 1D-model. Similar to the 1D-model Tdecrase and Tincrease changed its signs from positive to negative and vice versa. Maximum values of Tdecrease is observed at Wetteren (1 min) and at Melle (-1 min). Maximum change of Tincrease is equal to

	to (-3 min) at 90 km and 5 min at Melle.	0.5 min at Schoonaarde (130 km) and 1 min at Melle (155 km).
	Both models show opposite behavior of Tincrease and Tdecrease. The predicted values of the Scaldis-model (± 1 min) are in general smaller than the 1D-model (± 5 min). The Scaldis-model results show more fluctuation around the zero (no change) compare to the 1D-model.	
Vmax flood and Vmax ebb (m/s) Figure 53	No significant effects on the predicted velocities downstream of Driegoten (100 km). Upstream of Driegoten (100 km) Vmax ebb has increased with positive values, which have a maximum value of 0.08 m/s at Wetteren (140 km). Vmax flood are reduced (negative values) over the same distance with maximum value = -0.1 m/s at Wetteren (140 km).	Similar to the 1D-model, no significant effects on the predicted flow velocities downstream of Driegoten (100 km). Upstream of Driegoten (100 km) Vmax ebb is increased (positive values) with a maximum value about 0.03 m/s at Wetteren (140 km). Vmax flood shows opposite behavior with general reduction (negative values) over the same interval with a maximum value of about -0.03 m/s at Wetteren (140 km).
	It is clear from the results that both models show exactly the same behavior along the estuary. Vmax ebb is increased and Vmax flood is reduced in the upstream part of the estuary with respect to the reference situation. On the other hand the predicted flow velocities by the Scaldis-model (about 0.03 m/s) are much smaller than the 1D-model (about 0.1 m/s).	
Relative tidal amplitude Figure 54	No change in the relative tidal amplitude downstream of Oosterweel (70 km). Reduction of values is taking place between Oosterweel (70 km) and Wetteren (144 km). Only positive value occurs at Melle (155 km).	Similar to the 1D-model, no changes occurs downstream of Oosterweel (70 km). Reduction of values is taking place between Oosterweel (70 km) and Baasrode (110 km). Upstream of Baasrode (110 km) positive values are taking place towards Melle (155 km).
	Results of the two models are in the same range of values. Both models show reduction in values until Dendedrmonde (120 km). The Scaldis-model shows increased values upstream of Dendermonde (120 km), while the 1D-model has one positive value at Melle (155 km).	
Tflood/Tebb Figure 55	Differences have negative values between Oosterweel (70 km) and Schoonaarde (140 km). Only at Melle (155 km) the difference is increased with a positive value. Maximum values are located at 90 km (Schelle) and at 155 km (Melle), which are equal to (-0.01) and (+0.019), respectively.	Most of values have positive values and are very close to zero downstream of Baasrode (110 km). Differences show two maximum values at Dendermonde (120 km) and at Melle (155 km), which are equal to 0.005 and 0.01, respectively.
	Both models predict the same range of values. Both models are identical in the downstream part (from 0 to 70 km). The Scalids-model shows an opposite behavior compare to the 1D-model results (between Oosterweel (70 km) and Schoonaarde (137 km)). The Scaldis-model has positive values and the 1D-model shows negative values. At the location of Melle (155 km) both model are in agreement with positive values, which indicate an increase of Tflood or a reduction in Tebb.	

Figure 51 – Relative changes of HW and LW (Chafing vs Reference) as computed using the Scaldis-model (upper panel) and the 1D-model (lower panel)

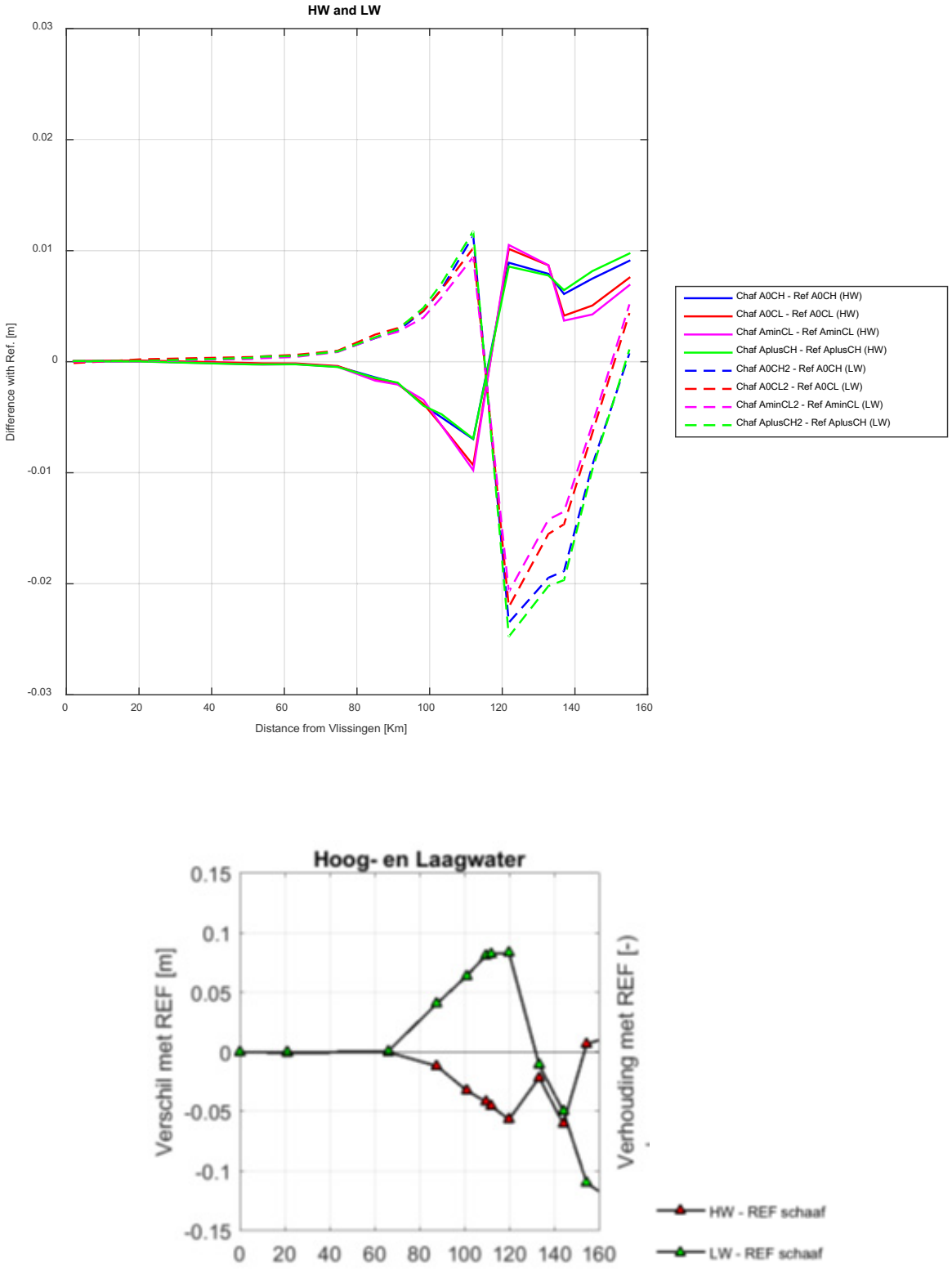

Figure 52 – Relative changes of Tincrease and Tdecrease (Chafing vs Reference) as computed using the Scaldis-model (upper panel) and the 1D-model (lower panel)

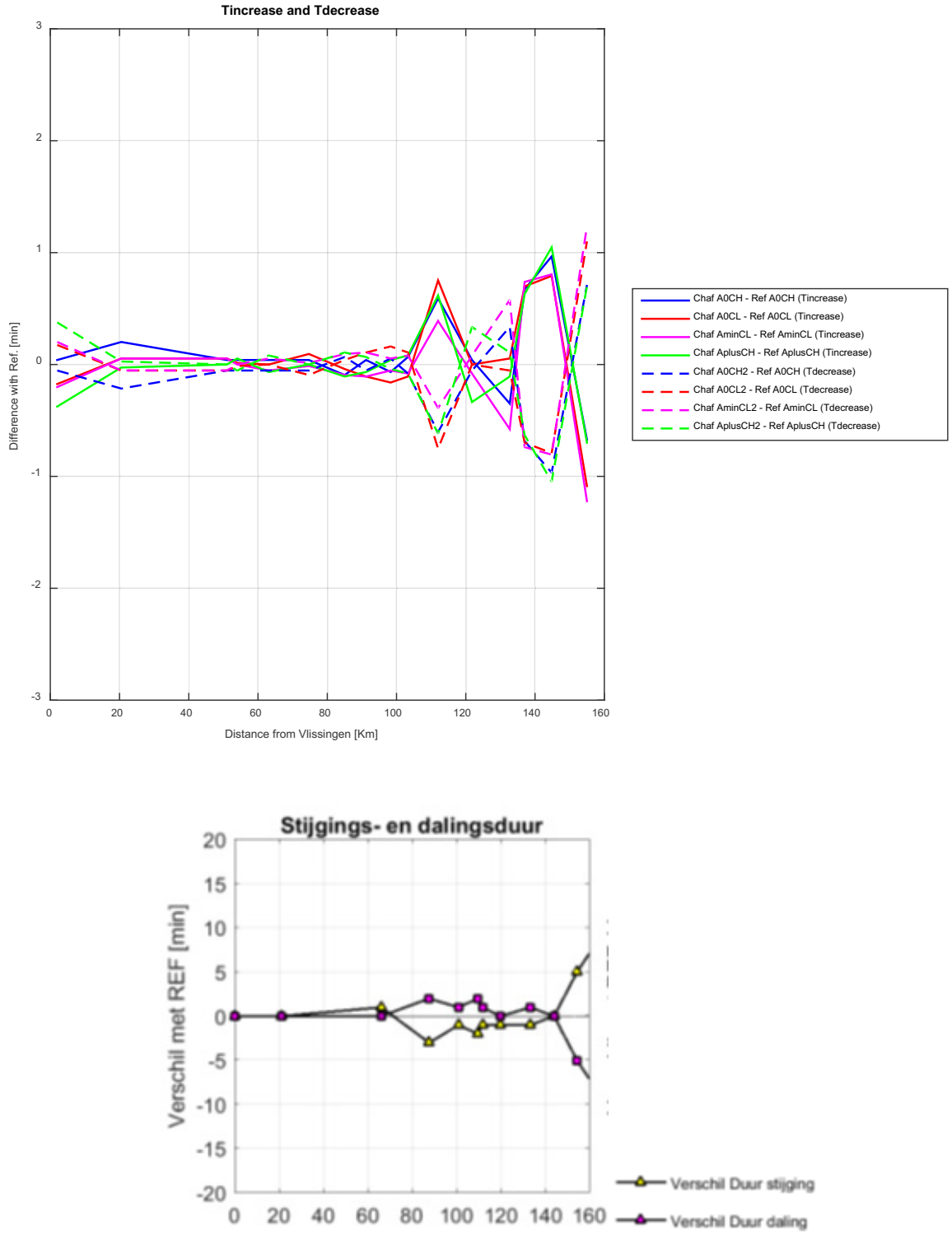

Figure 53 – Relative changes of Vmax flood and Vmax ebb (Chafing vs Reference) as computed using the Scaldis-model (upper panel) and the 1D-model (lower panel)

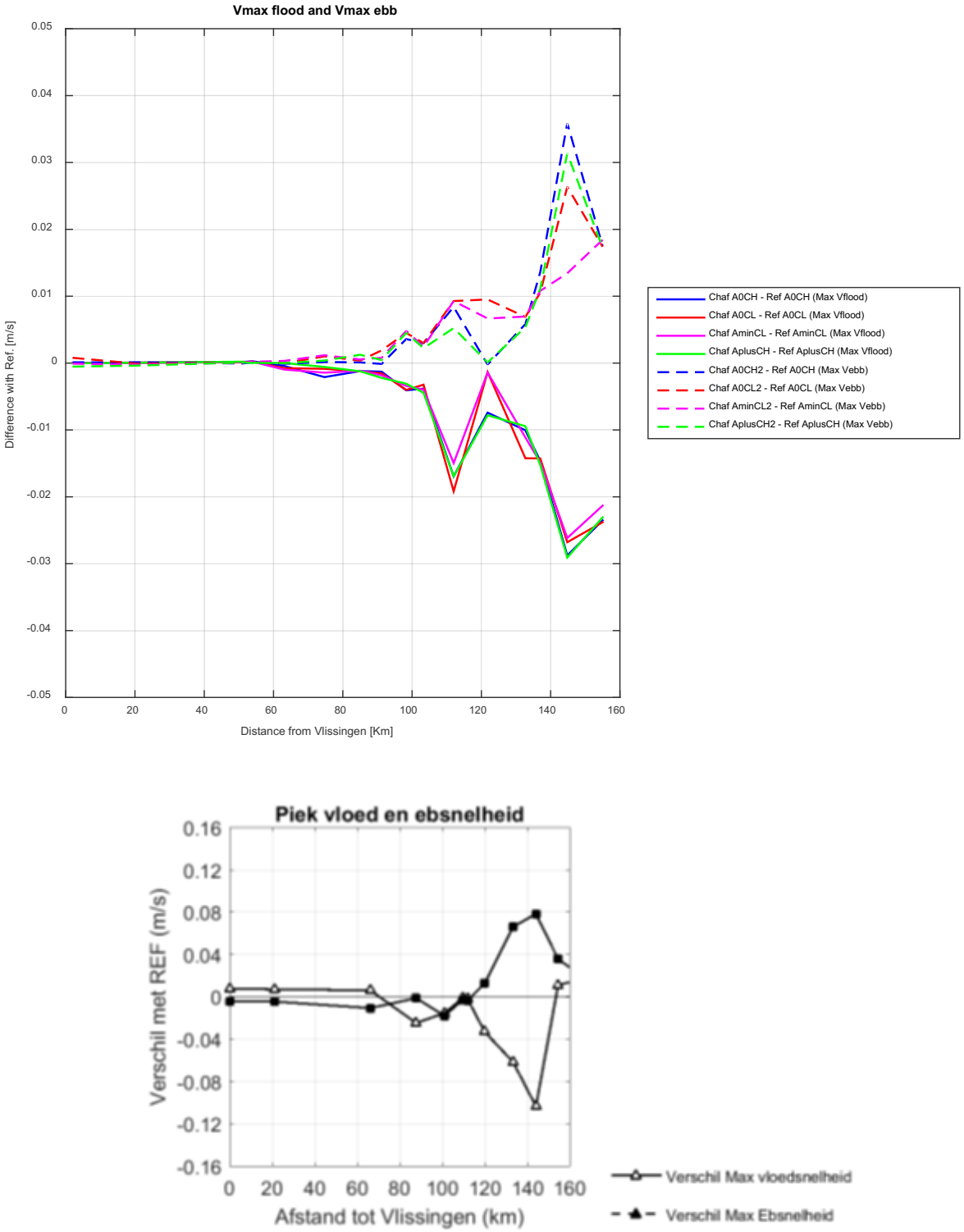

Figure 54 – Relative changes of relative tidal amplitude (Chafing vs Reference) as computed using the Scaldis-model (upper panel) and the 1D-model (lower panel)

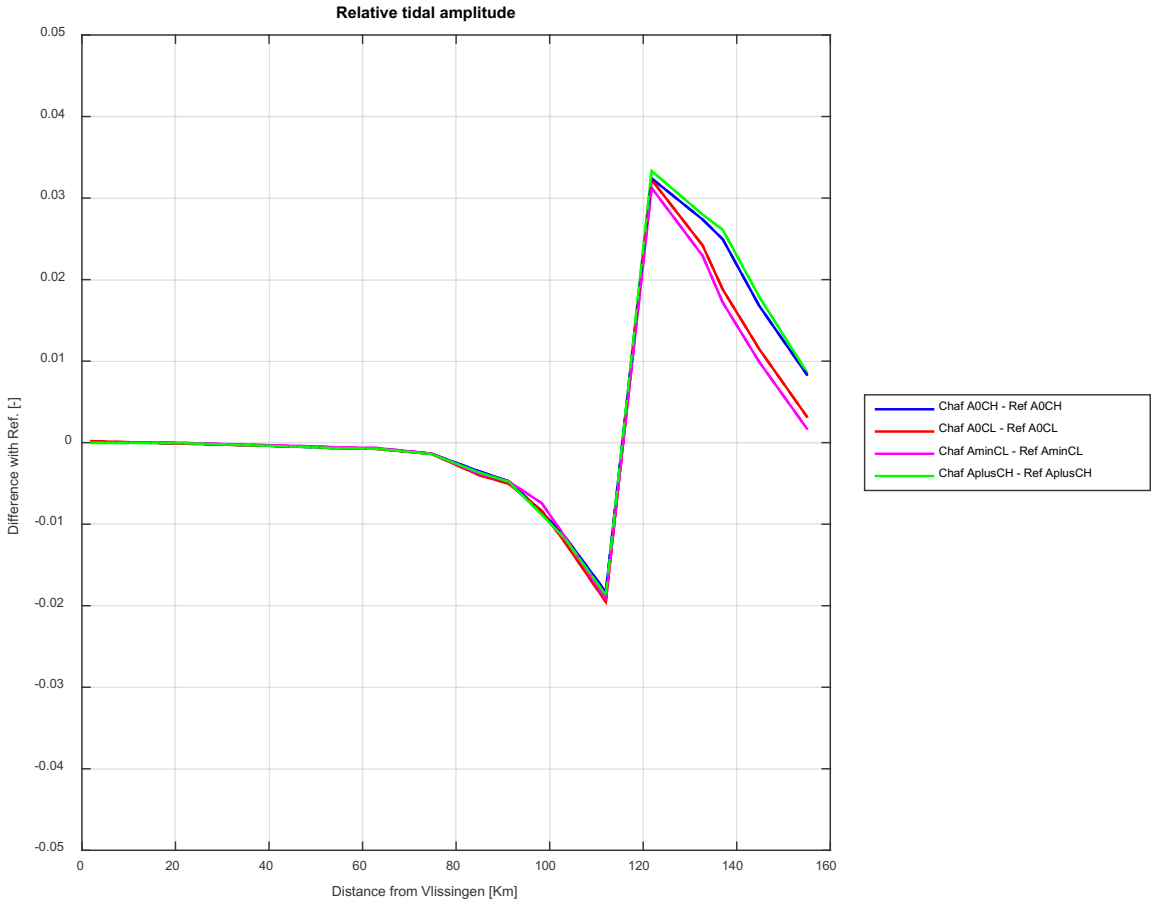

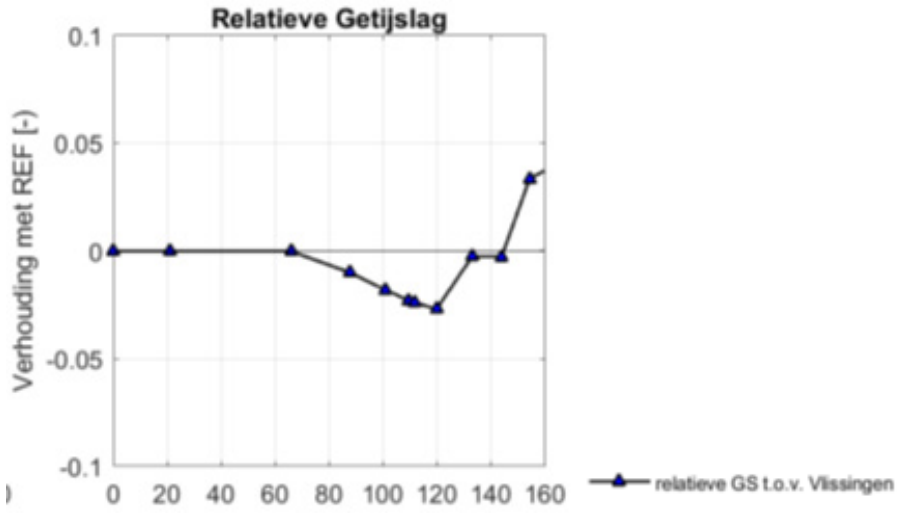

Figure 55 – Relative changes of Tflood/Tebb (Chafing vs Reference) as computed using the Scaldis-model (upper panel) and the 1D-model (lower panel)

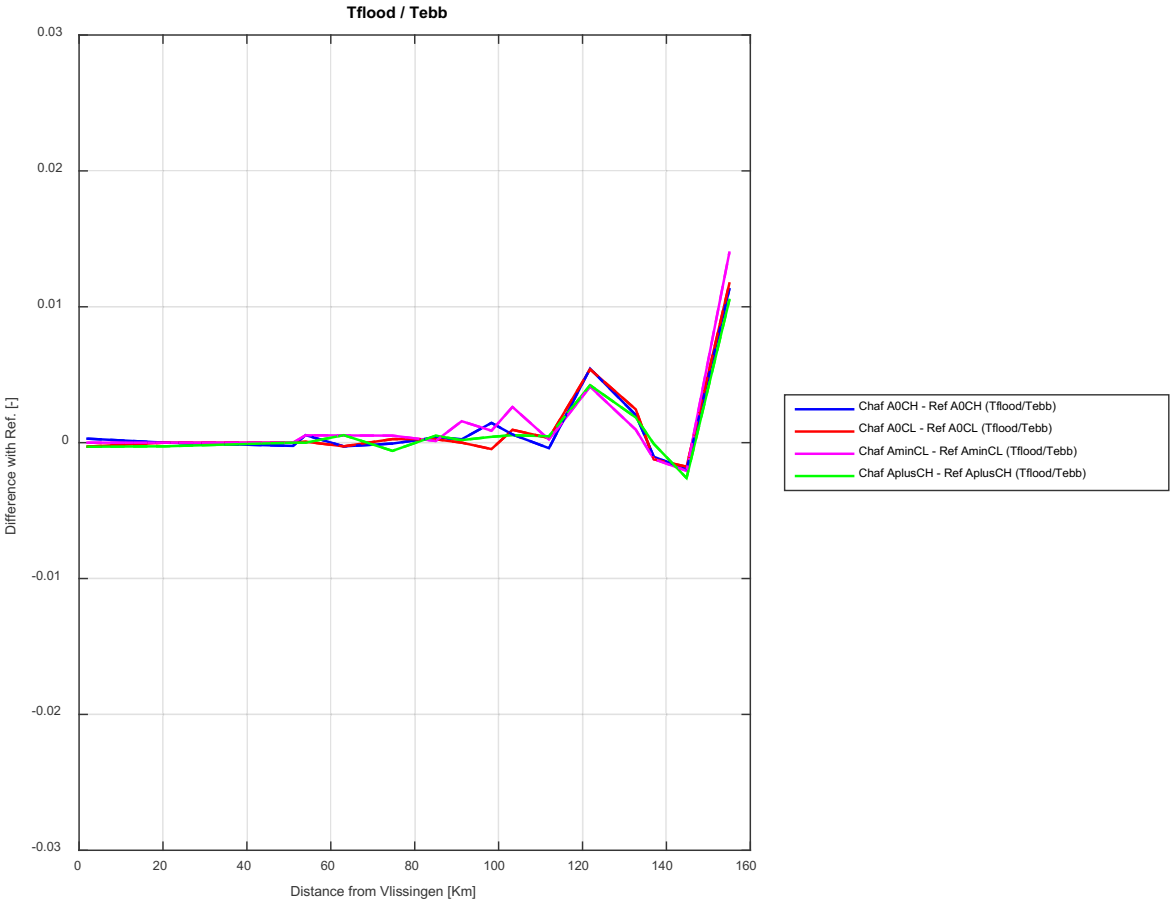

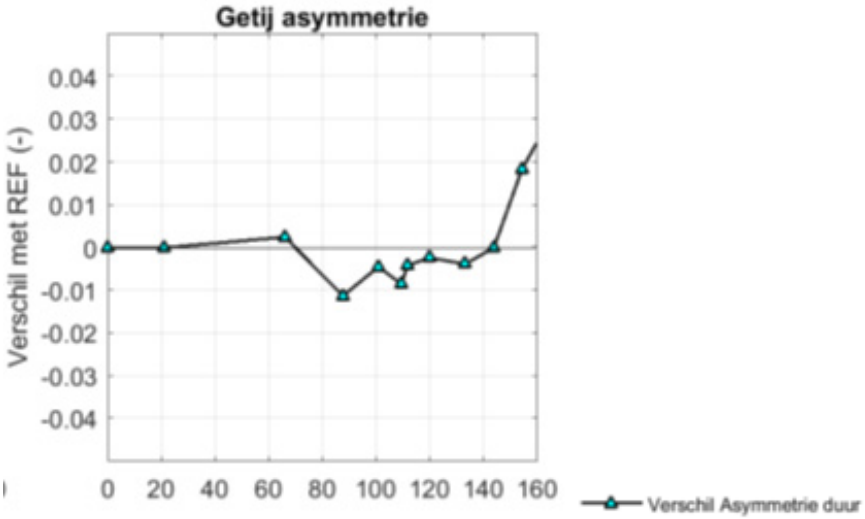

7 Conclusions

This report presents a detailed analysis is done of the expected effect of implementing three different bathymetry alternatives (VaG, VaH and Chafing) in the Scheldt estuary. The alternatives are introduced in section 2.2.

The reference year for this comparison is 2050. In order to take into account the uncertainty in quantifying the autonomous development of the estuary between 2013 and 2050, the effects are calculated using four different hydrodynamic scenarios for the boundary conditions (A0CH, A0CL, AplusCH and AminCL). The hydrodynamic scenarios are described in chapter 2.2.1.

The intercomparison between these various alternatives is done based on differences in water levels, harmonic components, flow discharge and tidal asymmetry. The main conclusions can be summarized as follows:

- The VaG alternative has the largest effect on the various hydrodynamic parameters, compared to the VaH and Chafing alternatives. VaG alternative has a significant effect, on water levels (in order of centimeters), on discharges and the tidal asymmetry. Most of the effects are taking place in the upper part of the estuary;
- The water level changes along the estuary show that the VaG alternative leads to reduction of HW levels in the downstream part and an increase in the upstream part. LW levels show an opposite behavior compared to HW. This change in behavior can be claimed to the large changes in VaG alternative bathymetry compared to the reference situation and its effects on reducing flow resistance. We can conclude from the comparison between the VaG alternative and the reference situation that tidal amplitudes are increased in the upper part of the estuary (upstream of Sint-Amands), with a maximum value of 0.4 m. In the downstream part, tidal amplitudes are reduced with a maximum value of about 0.08 m;
- For the VaH alternative the HW changes are very limited at all locations in the estuary, with a maximum value < 0.02 m. The LW results have somewhat higher values at Melle and Wetteren with an increase of < 0.05 m. Moreover, the VaH alternative has a much smaller effect on water level in the downstream part of Dendermonde with a maximum change of tidal amplitude < 0.025 m. Tidal amplitudes are increased upstream of Dendermonde with a maximum value of 0.06 m at Melle. These water level results of the VaH alternative are much smaller than the results of the VaG alternative. VaH results are expected to be smaller, by keeping in mind that the bathymetry of the VaH alternative has less modifications compared to the VaG alternative;
- Water level results of Chafing and VaH alternatives are quite similar, the maximum bias of HW is very limited at all locations with a maximum value < 0.015 m. The LW shows somewhat higher values at Dendermonde with an increase of < 0.03 m. In addition, the Chafing alternative has much smaller effects on water levels with a maximum change of tidal amplitude in the downstream part of Dendermonde (< 0.025 m at Sint-Amands). Tidal amplitudes are increased upstream of Dendermonde with a maximum value < 0.035 m at Dendermonde. The water level changes for the Chafing alternative are much smaller than for the VaG alternative, as can be expected. The VaG alternative has more changes in bathymetry compare to Chafing and VaH alternatives;
- The harmonic components analysis at different locations along the estuary (from Antwerp to Melle) shows that the VaG alternative has some effects on M2, M4 and S2 of the tide, especially in the upstream part of Sint-Amands. These effects are smaller than 0.17 m (M2), 0.022 m (M4) and 0.048 m (S2). The maximum Bias values of phases (< 6.5°) of different tidal components are always taking place upstream of Sint-Amands;
- The VaH alternative has no clear effects on the harmonic components. The effects are smaller than 0.02 m (M2), 0.008 m (M4) and 0.006 m (S2). The maximum bias values of phases (< 1.8°) is located

upstream of Sint-Amands for M2, M4 and S2 components. Similar small effects on tidal components are observed for the Chafing alternative. These effects are smaller than 0.014 m (M2), 0.006 m (M4) and 0.004 m (S2). The maximum bias values of phases (< 0.7°) of different components are also taking place upstream of Sint-Amands;

- Results of flow discharges of the various B-alternatives along the estuary show that in the VaG alternative, discharges are slightly reduced downstream of Liefkenshoek (RRMSE < 0.01) and are increased in the upstream direction starting from Liefkenshoek to Melle. The highest values are observed between Melle and Dendermonde (RRMSE < 0.16). The effect of using different scenarios has a limited influence on the results;
- The VaH alternative shows that changes in the discharge that occur downstream of Schelle can be ignored (RRMSE < 0.005) and that most important changes are taking place upstream of Schelle. The RRMSE values are increased in the upstream direction until its maximum value at Melle (RRMSE < 0.06). In addition, the Chafing alternative shows small values downstream of Schelle (RRMSE < 0.005) and most of the changes are taking place upstream of Schelle. The RRMSE values are increased in the upstream direction until the highest value at Melle (< 0.04). Again, these discharge results of VaH and Chafing alternatives are smaller than the effects of the VaG alternative, which has more changes in bathymetry.

There are many ways of quantifying tidal asymmetry using various parameters. In the present study, five different asymmetry parameters have been used to study the effects of B-alternatives on tidal flow (as described in section 4.4). The main conclusions can be listed as follows:

- In general, all asymmetry parameters point to an ebb dominant system upstream, with ratios < 1.
- In the VaG alternative, the V^3 tidal asymmetry parameter increases by about 8% at Baasrode and it decreases by about 8% between Dendermonde and Schoonaarde and it increases again upstream Schellebelle by 5 to 15%. This increase is slightly bigger in A0CL and AminCL runs. The V^4 tidal asymmetry parameter decreases by 10% at Schoonaarde and increases by about 20% at Wetteren. As shown in appendix 2, these changes are due to the upstream migration of the V^3 and V^4 asymetry patterns.
- Generally, the effect of the VaH bathymetry on the tidal asymmetry is much smaller than the effect of the VaG alternative. The biggest effects of the VaH alternative on tidal asymmetry are found for V^3, which increases by about 1% at Baasrode and by 3 to 4% at Schoonaarde and Schellebelle. The increase is slightly bigger in A0CL and AminCL runs compared to other runs;
- The effect of the Chafing alternative on the tidal asymmetry is much smaller than the effect of the VaG alternative.

The Scaldis-model results are compared with the results of a 1D-model, presented in the Bouwstenenonderzoek (IMDC, 2017). This comparison as presented in Chapter 6. The two models show a good agreement at various locations along the estuary, especially in the downstream part (downstream of Antwerp). On the other hand, the model results deviate at several locations in the upstream part. The main results of the comparison are presented as follows:

- Results of both models agree that the VaG alternative has the largest effect on the flow dynamics in the upstream part of the estuary. VaH and Chafing alternatives have smaller effects at the same locations;
- All B-alternatives show a decrease in the HW levels in the downstream part of the estuary and an increased HW level in upstream direction. The LW levels rise in the downstream part and decreases in the upstream direction.
- Generally, the predictions of the Scaldis-model of water levels and flow velocities have smaller magnitudes compare to the 1D-model predictions, for the Chafing alternative. For the VaG alternative the two models show a better agreement;
- All B-alternatives increase the flood duration in the upward part. Because of that the duration asymmetry T_flood/T_ebb decreases.

A part of the differences between the two models can be attributed to the differences in implementation of FCA, wetlands and depoldering. There are also differences in the physics that is taken into account in both models, which has an impact on how effects are calculated. More research is needed to disentangle both sources of the differences in effects.

The differences in model results between the 1D model and the 3D model show the importance in a careful integration of the results of the Bouwstenenonderzoek (done with the 1D model in IMDC, 2017) with the evaluation of the B-alternatives (done with the 3D model in this report)

8 References

Boon, J. D., and R. J. Byrne (1981). On basin hypsometry and the morphodynamic response of coastal inlet systems, Mar. Geol., 40, 27–48.

Claessens, J., and Meyvis, L. (1994). Overzicht van de tijwaarnemingen in het Zeescheldebekken gedurende het decennium 1981-1990. Antwerpse Zeehavendienst: Antwerpen. 108 pp.

Coen L., Vanlede J., Verwaest T. & Mostaert F. (2016). Integraal Plan Boven-Zeeschelde - Veiligheidstoets B- en C-alternatieven: Deelrapport 2 - Veiligheidstoets B-alternatieven. Versie 4.0. Waterbouwkundig Laboratorium, WL Rapporten, 14_176_2.

Dronkers, J. (1986), Tidal asymmetry and estuarine morphology, Neth. J. Sea Res., 20, 117–131

Fortunato, A. B., and A. Oliveira (2005), Influence of intertidal flats on tidal asymmetry, J. Coastal Res., 21, 1062–1067.

Friedrichs, C. T., and D. G. Aubrey (1988), Non-linear tidal distortion in shallow well-mixed estuaries: A synthesis, Estuarine Coastal Shelf Sci., 27, 521–545.

Friedrichs, C. L. (2011). Tidal flat morphodynamics: A synthesis, in Treatise on Estuarine and Coastal Science, vol. 3, Estuarine and Coastal Geology and Geomorphology, edited by J. D. Hansom and B. W. Fleming, pp. 137–170, Elsevier, Amsterdam, Netherlands.

IMDC/INBO/UA/WL (2015). Modelling instruments for Integrated Plan Upper Sea Scheldt. I/NO/11448/14.165/DDP.

IMDC (2015). Bepalen van randvoorwaarden voor de referentiesituatie (2050) m.b.t. debiet en waterstand. I/NO/11448/15.128/TFR/.

IMDC (2017). Integraal Plan Boven-Zeeschelde; Bouwstenenonderzoek. I/RA/11448/17.006/INE

Kuijper, K., Lescinski, J. & Taal, M. (2013). Data-analysis water levels, bathymetry Western Scheldt. Project Instandhouding vaarpassen Schelde Milieuvergunningen terugstorten baggerspecie (I/RA/11387/12.105/GVH).

Maximova, T., Smolders, S., Schramkowski, G., Verwaest, T., Mostaert, F. (2015). Verkennende studie kribben Fort Filip: Deelrapport II. aanvullende scenario's. Versie 1.0. WL Rapporten, 15_042. Waterbouwkundig Laboratorium: Antwerpen, België.

Parker, B. B. (1991), The relative importance of the various nonlinear mechanisms in a wide range of tidal interactions, in Tidal Hydrodynamics, edited by B. B. Parker, pp. 237–268, John Wiley, New York.

Smolders, S., Maximova, T., Vandenbruwaene, W., Coen, L., Vanlede, J., Verwaest, T., Mostaert, F. (2017). Integraal Plan Bovenzeeschelde: Deelrapport 5 – Scaldis 2050. Version 4.0. FHR Reports, 13_131_5. Flanders Hydraulics Research: Antwerp, Belgium..

Smolders, S., Maximova, T., Vanlede, J., Plancke, Y., Verwaest, T., Mostaert, F. (2016). Integraal Plan Bovenzeeschelde: Subreport 1 – SCALDIS: a 3D Hydrodynamic Model for the Scheldt Estuary. Version 5.0. WL Rapporten, 13_131. Flanders Hydraulics Research: Antwerp, Belgium.

van Veen, J., A. J. F. van derSpek, M. J. F. Stive, and T. Zitman (2005). Ebb and flood channel systems in the Netherlands tidal waters, J. Coastal Res., 21, 1107–1120, doi:10.2112/04-0394.1.

Wang, Z. B., Jeuken, C., & De Vriend, H. J. (1999). Tidal asymmetry and residual sediment transport in estuaries. Deltares (WL).

Winterwerp, J.C. (2001). Stratification Effects by cohesive and noncohesive sediment. J. Geophys. Res. 106: 559–574.

Appendix 1: Difference in bathymetry alternatives

VaG vs Reference 2050

Figure 56 – Difference in bathymetry (VaG – Reference 2050) in zone 1

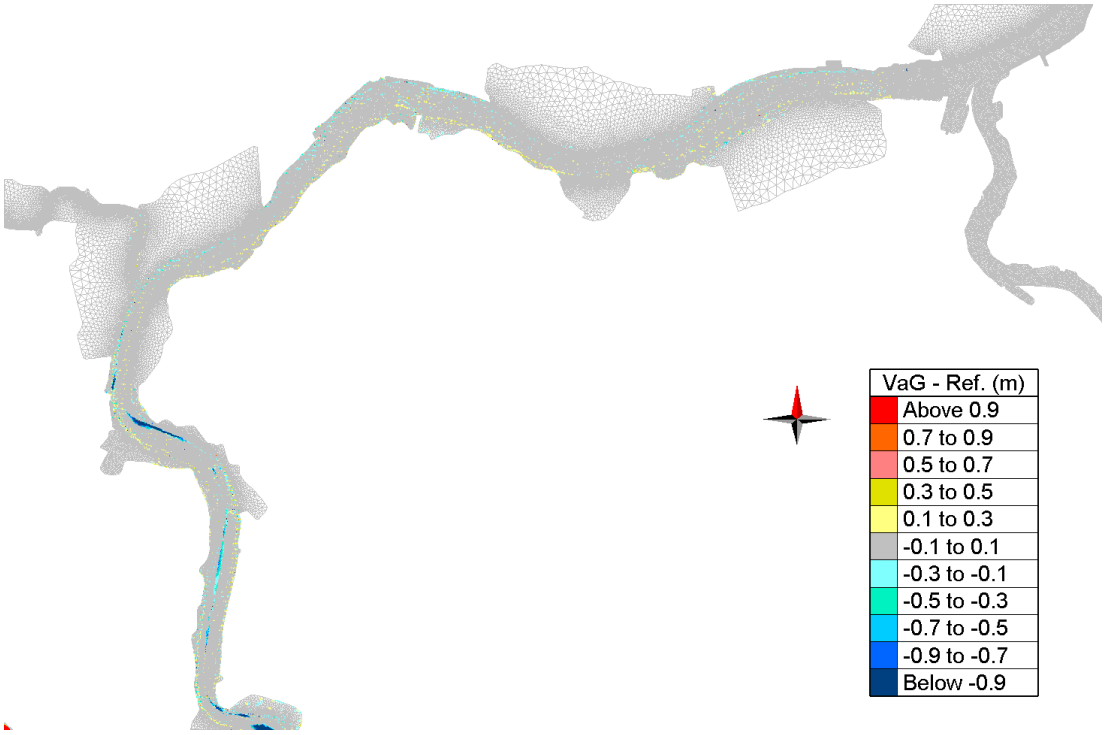

Figure 57 – Difference in bathymetry (VaG – Reference 2050) in zone 2

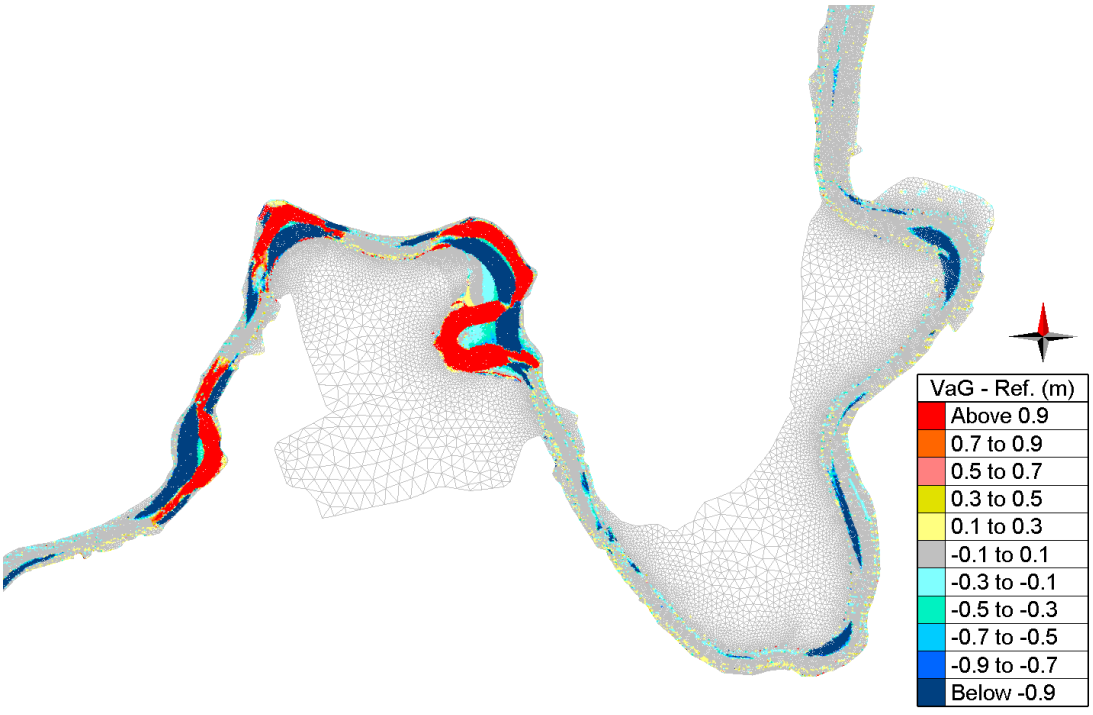

Figure 58 – Difference in bathymetry (VaG – Reference 2050) in zone 3

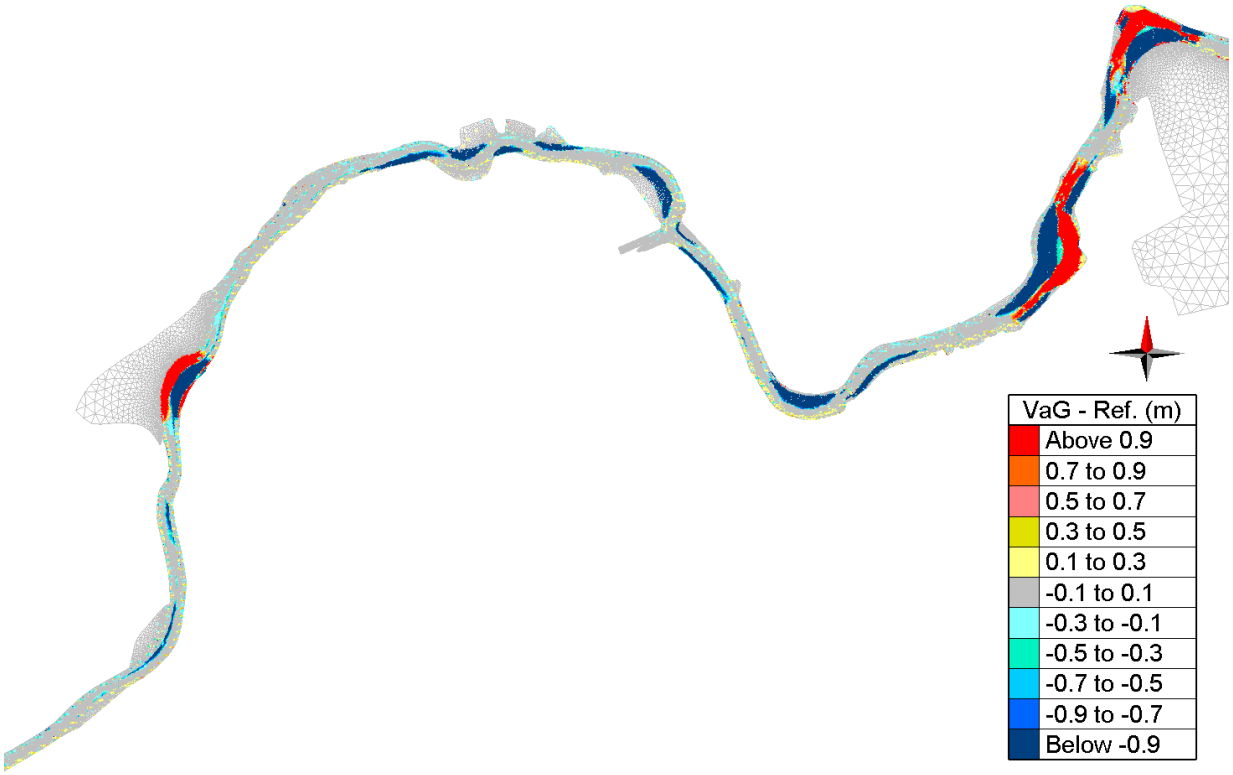

Figure 59 – Difference in bathymetry (VaG – Reference 2050) in zone 4

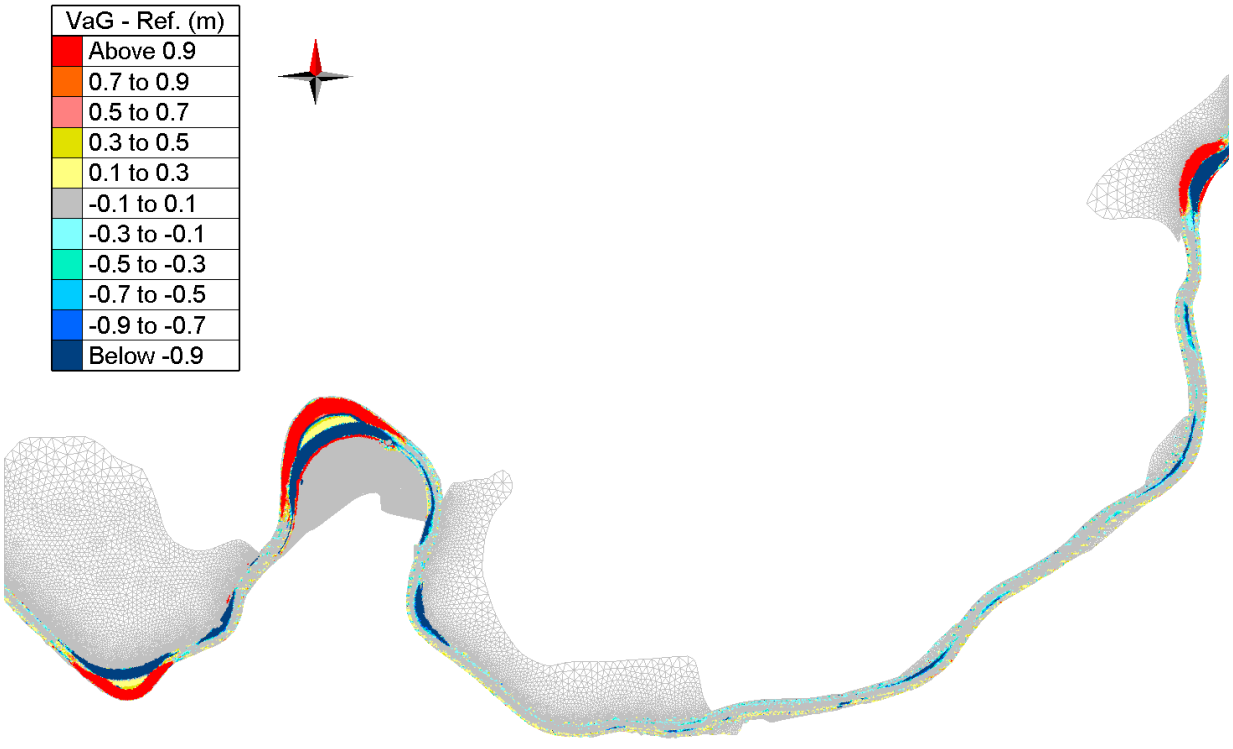

Figure 60 – Difference in bathymetry (VaG – Reference 2050) in zone 5

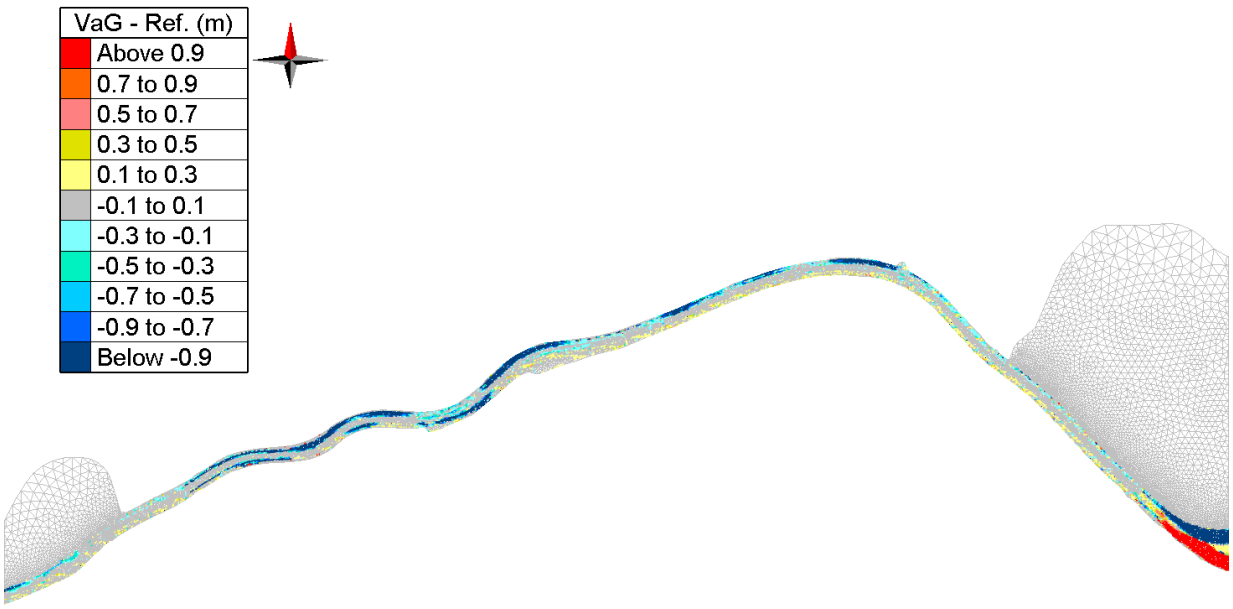

Figure 61 – Difference in bathymetry (VaG – Reference 2050) in zone 6

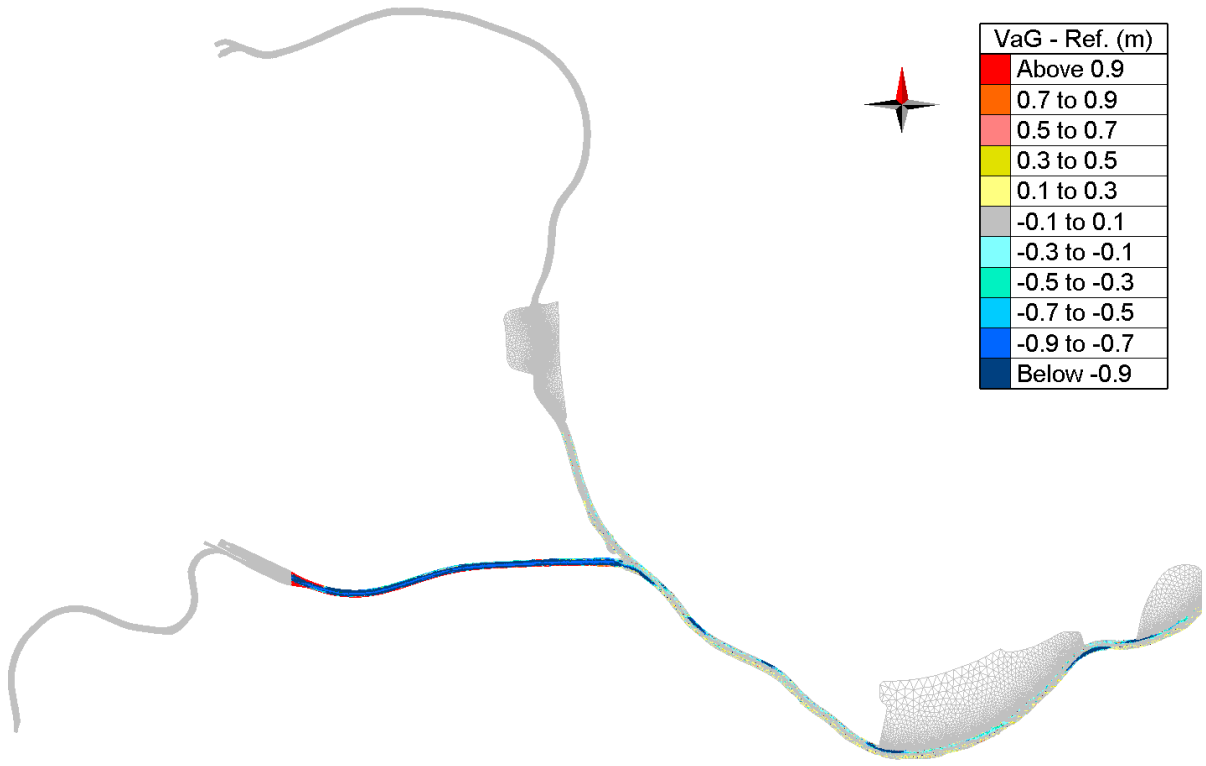

VaH vs Reference 2050

Figure 62 – Difference in bathymetry (VaH – Reference 2050) in zone 1

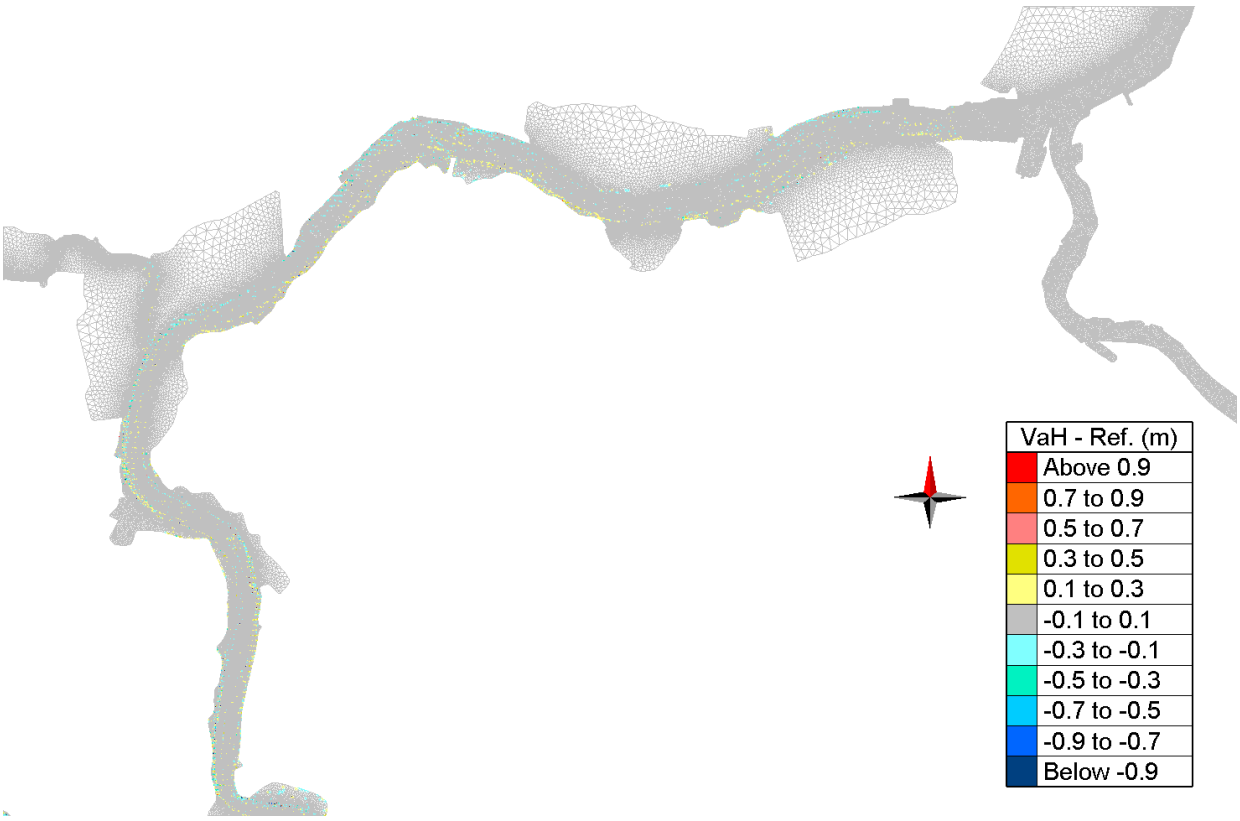

Figure 63 – Difference in bathymetry (VaH – Reference 2050) in zone 2

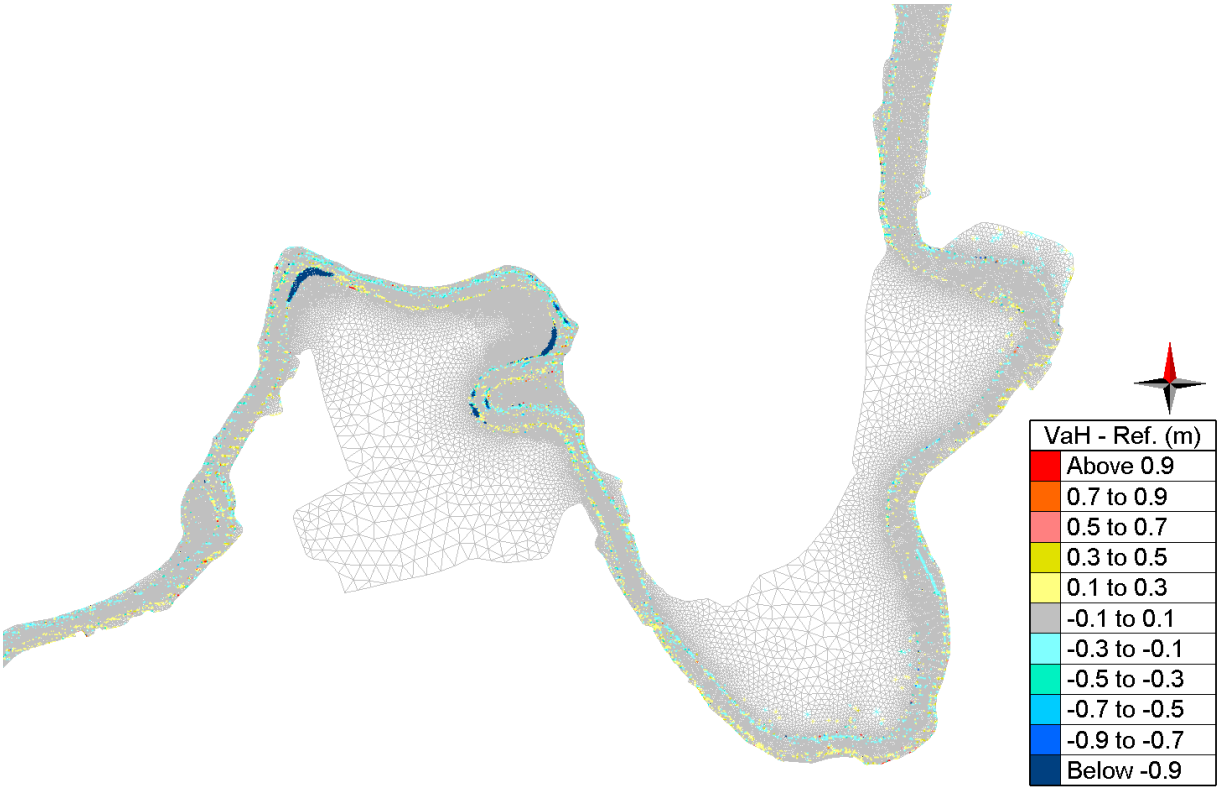

Figure 64 – Difference in bathymetry (VaH – Reference 2050) in zone 3

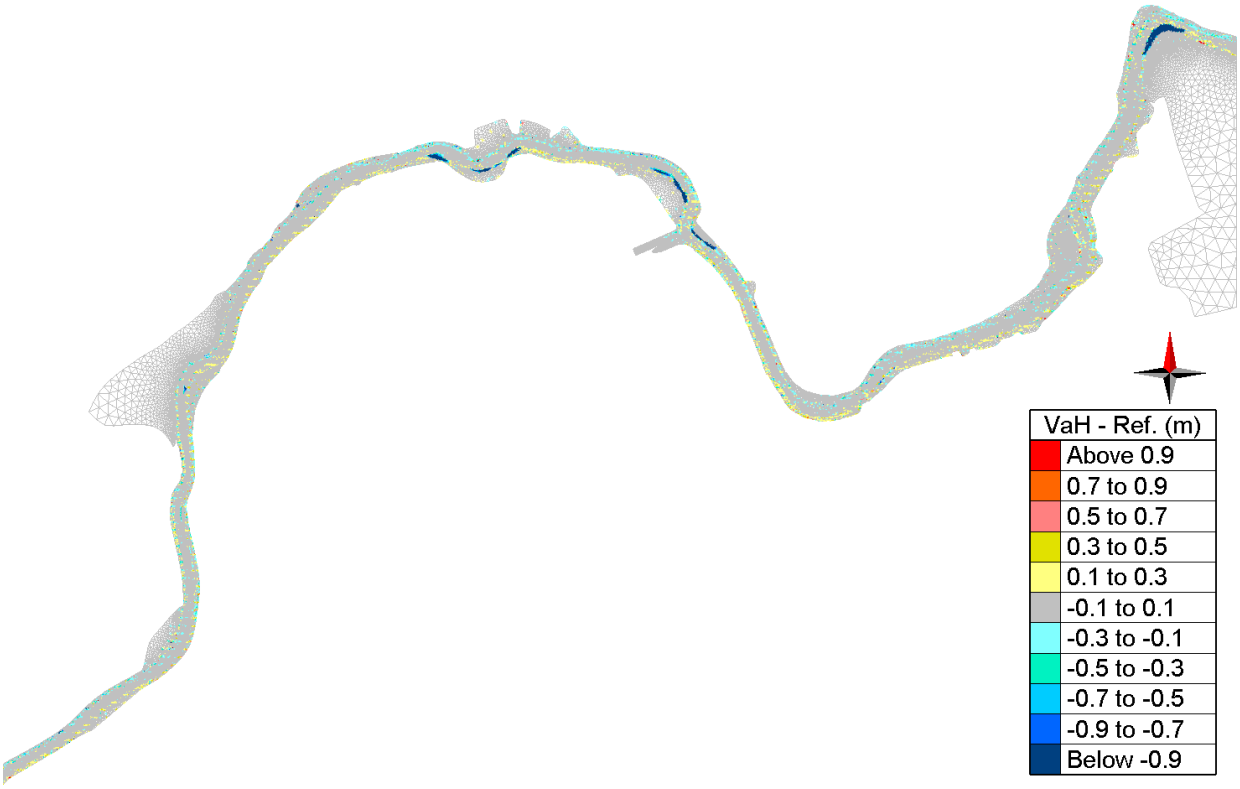

Figure 65 – Difference in bathymetry (VaH – Reference 2050) in zone 4

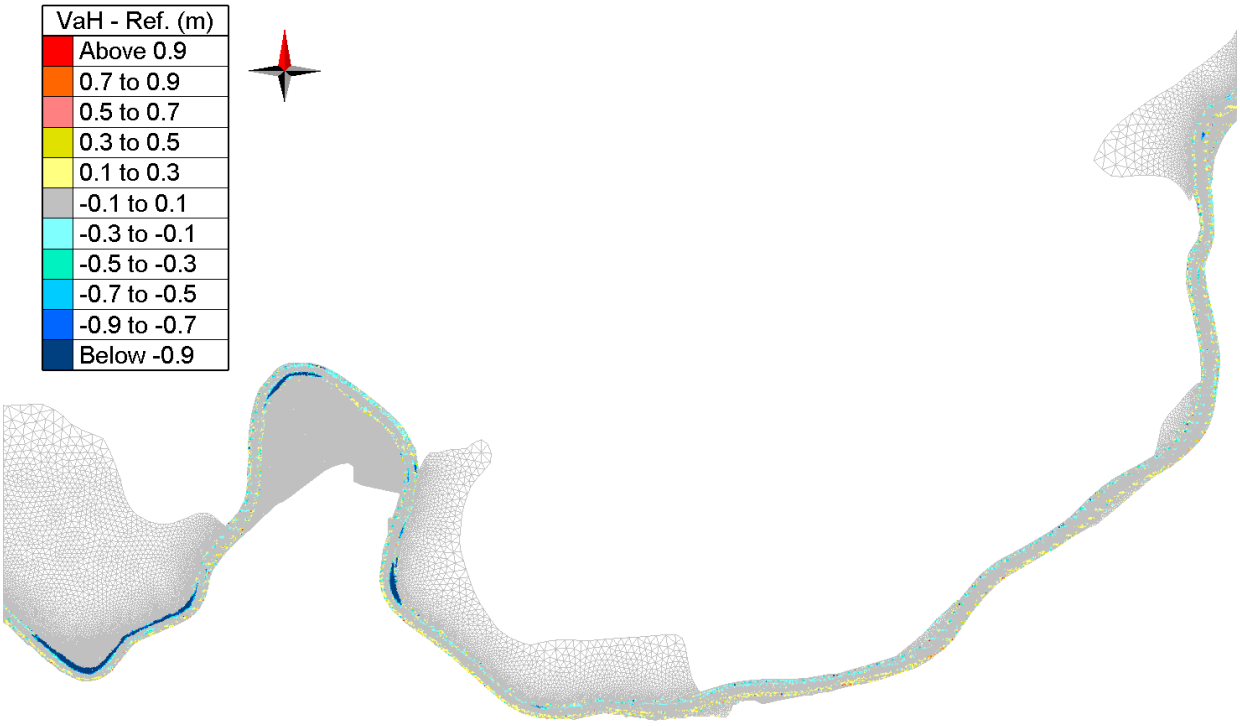

Figure 66 – Difference in bathymetry (VaH – Reference 2050) in zone 5

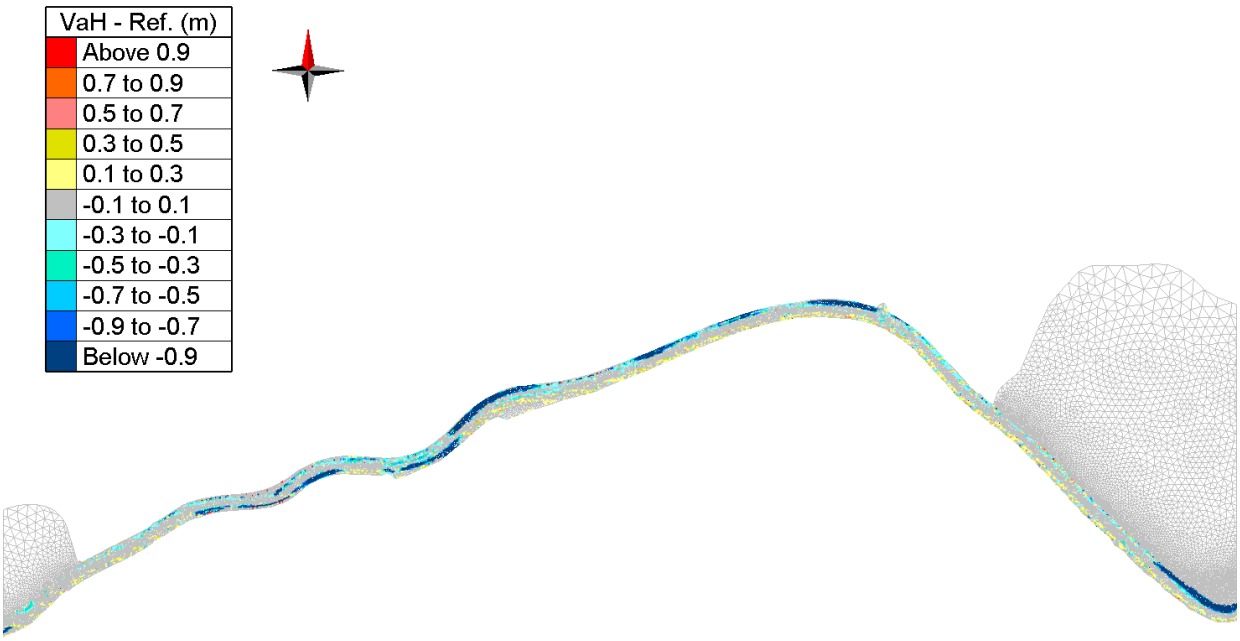

Figure 67 – Difference in bathymetry (VaH – Reference 2050) in zone 6

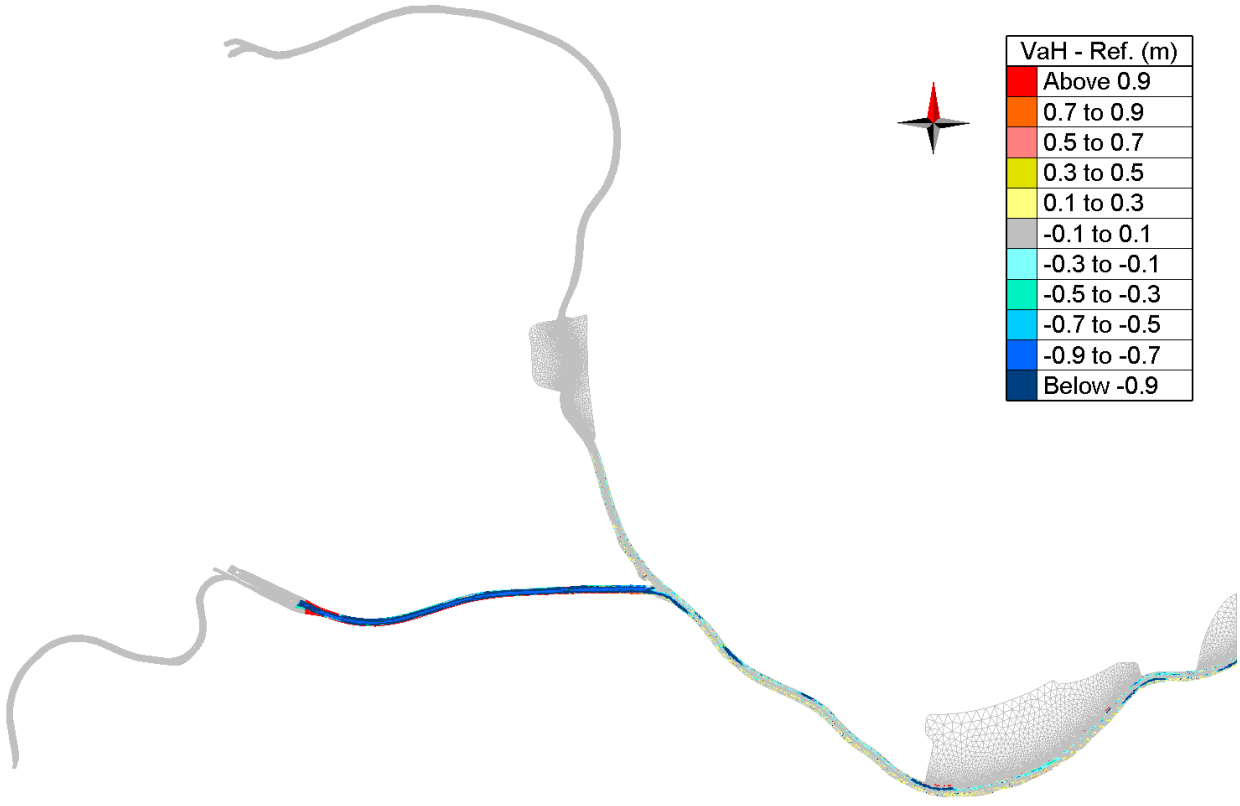

Chafing vs Reference 2050

Figure 68 – Difference in bathymetry (Chafing – Reference 2050) in zone 1

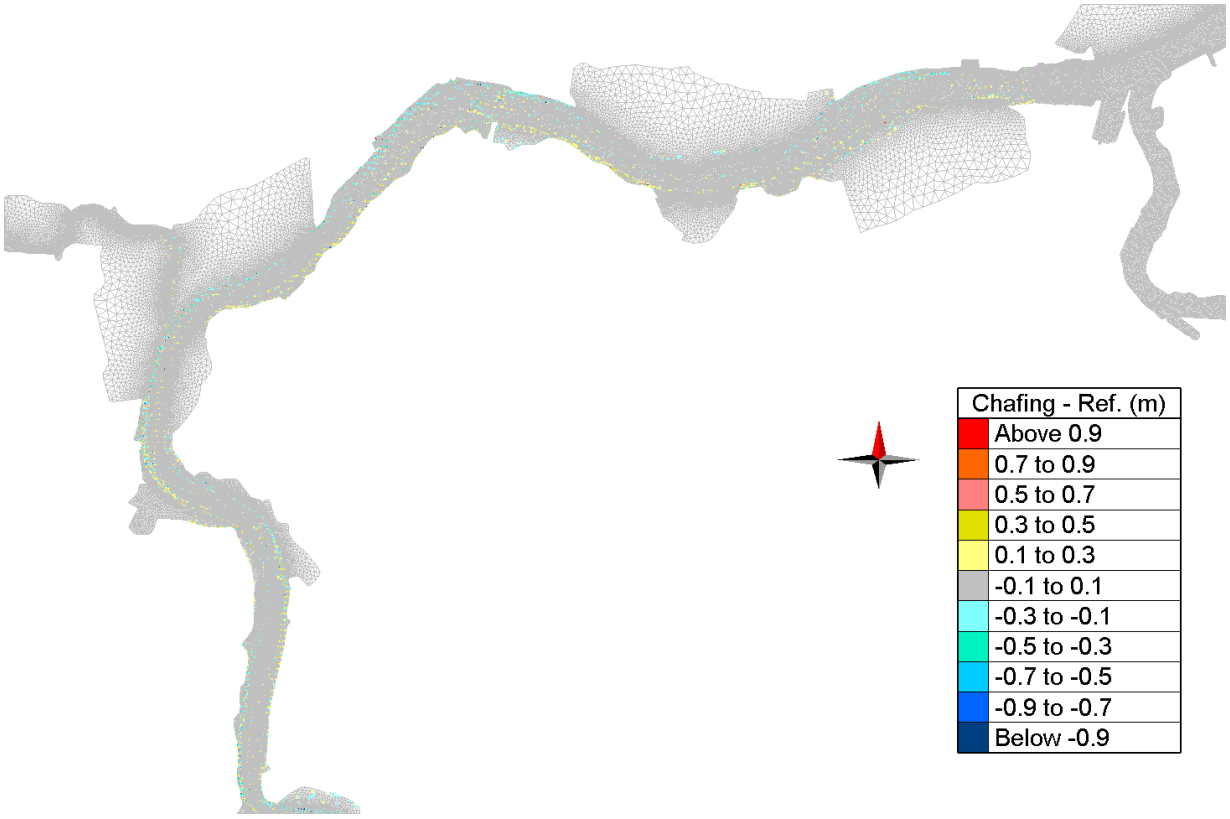

Figure 69 – Difference in bathymetry (Chafing – Reference 2050) in zone 2

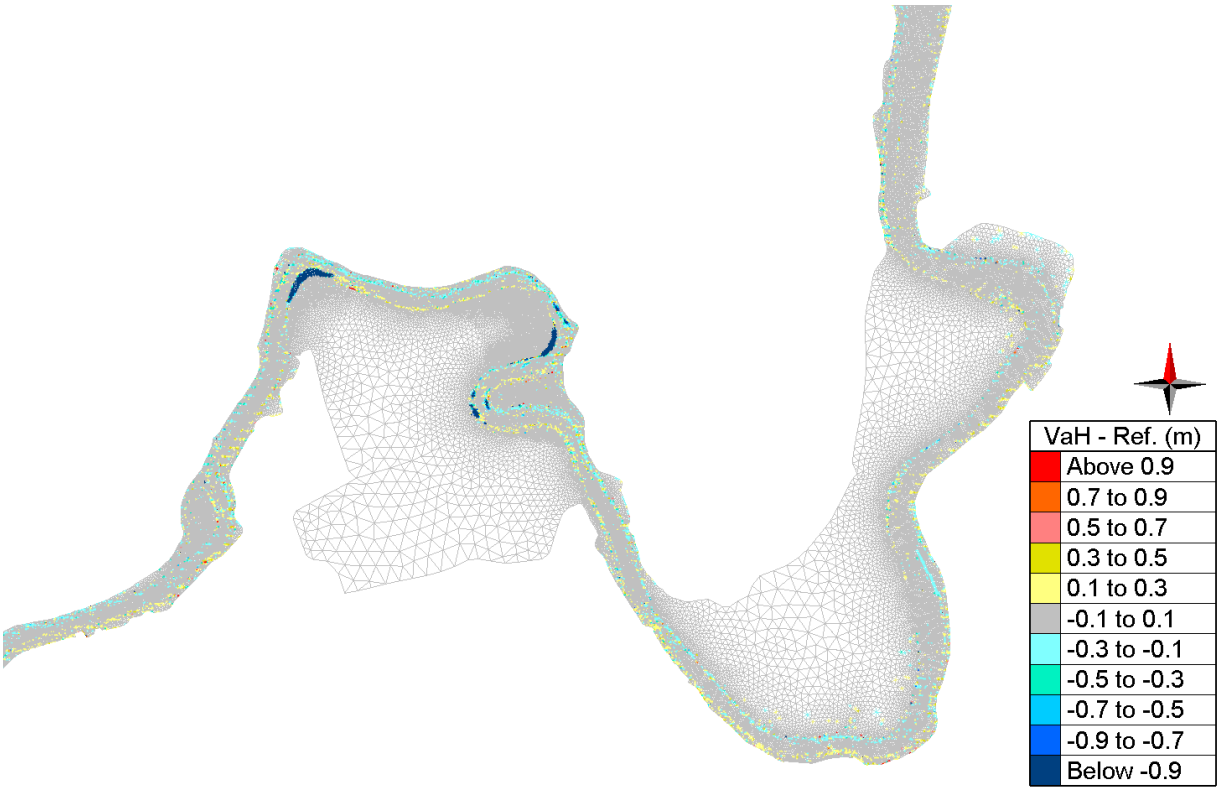

Figure 70 – Difference in bathymetry (Chafing – Reference 2050) in zone 3

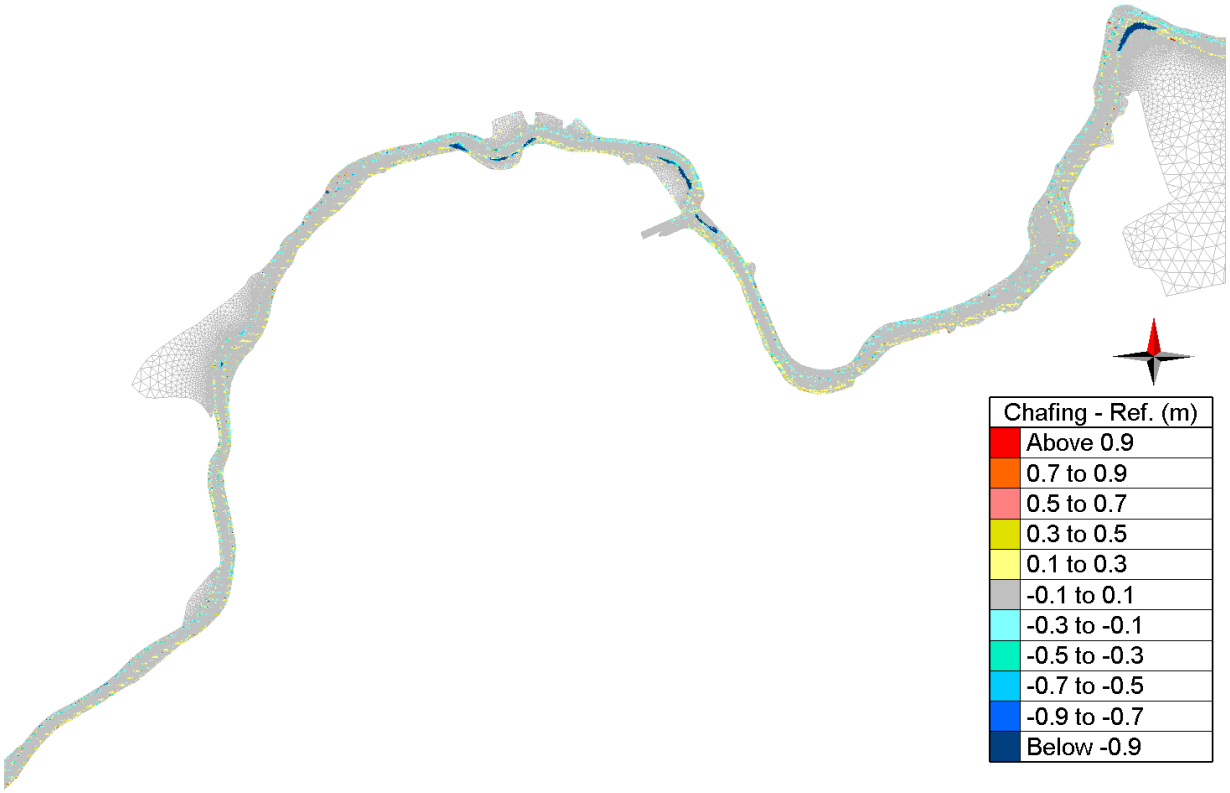

Figure 71 – Difference in bathymetry (Chafing – Reference 2050) in zone 4

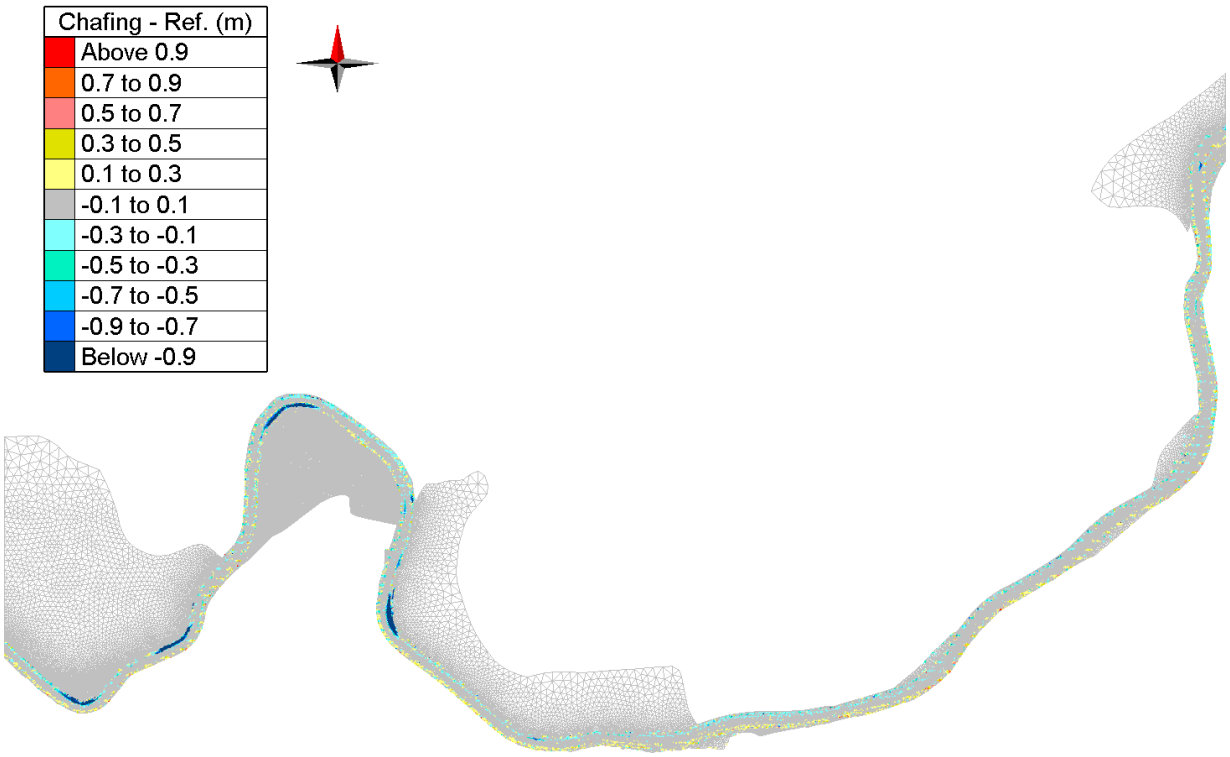

Figure 72 – Difference in bathymetry (Chafing – Reference 2050) in zone 5

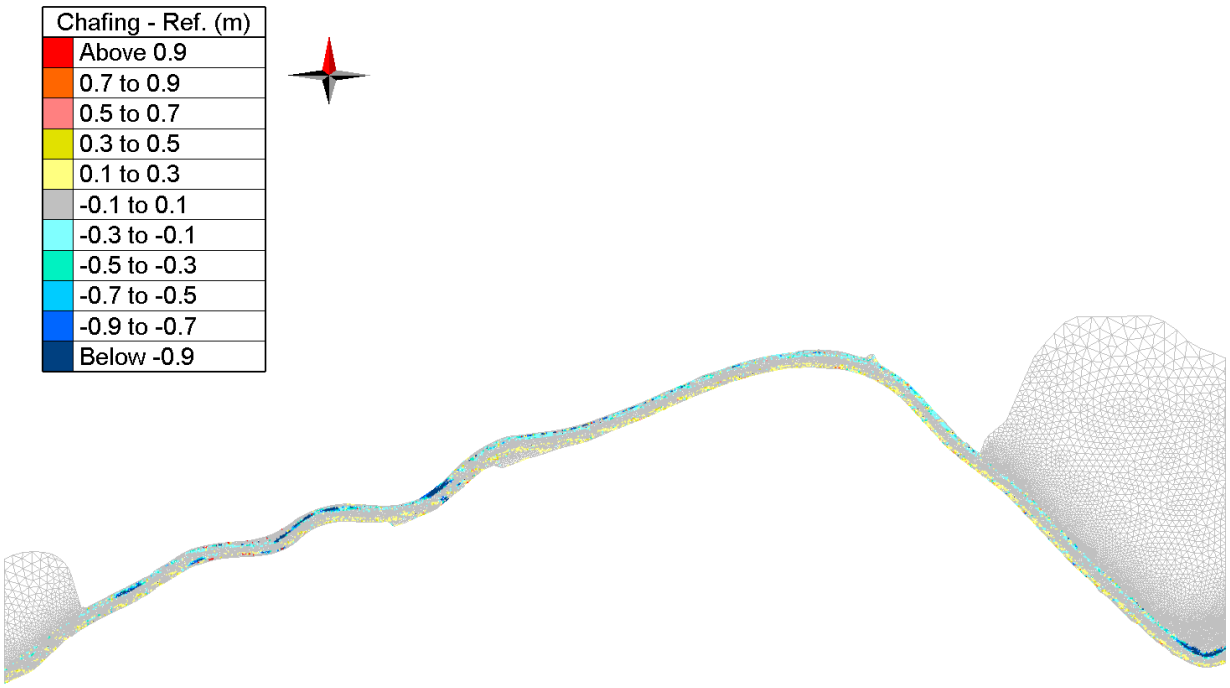

Figure 73 – Difference in bathymetry (Chafing – Reference 2050) in zone 6

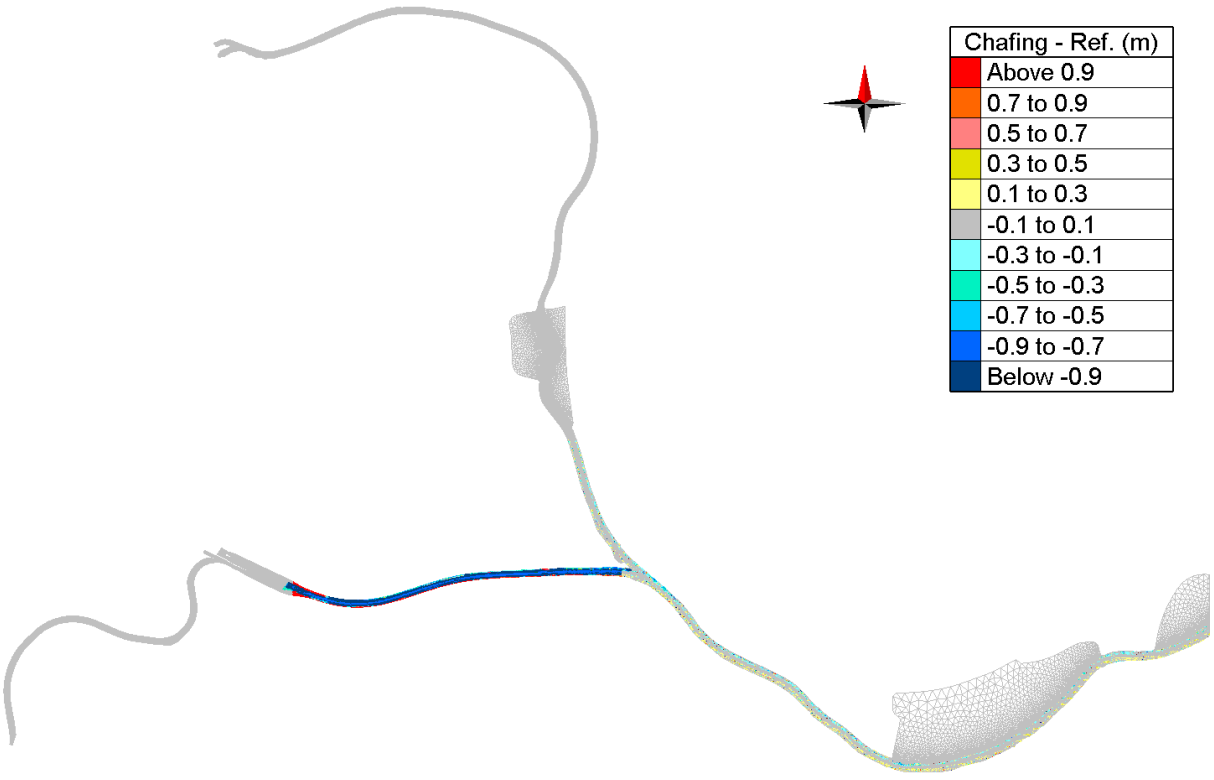

Appendix 2: Effect of VaG

A0CH runs

Water levels

Table 5 – Statistical parameters of HW, LW and complete time series of water levels (VaG_A0CH - Reference_A0CH)

Stations	Complete Time Series			HW			LW		
	BIAS	RMSE	RMSE_0	BIAS	RMSE	RMSE_0	BIAS	RMSE	RMSE_0
	[m]			[m]			[m]		
Bath	0.000	0.003	0.003	-0.002	0.002	0.000	0.004	0.004	0.000
Zandvliet	0.000	0.004	0.004	-0.002	0.002	0.000	0.005	0.005	0.001
Prosperpolder	0.000	0.003	0.003	-0.002	0.002	0.000	0.005	0.005	0.001
Liefkenshoek	0.000	0.004	0.004	-0.002	0.002	0.000	0.006	0.006	0.001
Kallosluis	0.001	0.005	0.005	-0.003	0.003	0.000	0.007	0.007	0.001
Antwerpen	0.001	0.008	0.008	-0.006	0.006	0.001	0.010	0.010	0.002
Hemiksem	0.002	0.016	0.016	-0.015	0.016	0.002	0.017	0.018	0.003
Schelle	0.003	0.019	0.019	-0.017	0.017	0.002	0.020	0.020	0.004
Temse	0.005	0.029	0.029	-0.026	0.027	0.004	0.028	0.029	0.006
Tielrode	0.006	0.035	0.035	-0.032	0.032	0.006	0.031	0.032	0.007
StAmands	-0.002	0.045	0.045	-0.043	0.044	0.008	0.006	0.007	0.005
Dendermonde	-0.065	0.161	0.147	0.127	0.127	0.014	-0.257	0.259	0.035
Schoonaarde	-0.057	0.167	0.156	0.120	0.121	0.016	-0.251	0.252	0.025
Wetteren	-0.023	0.112	0.110	0.116	0.118	0.022	-0.138	0.139	0.007
Melle	-0.029	0.111	0.107	0.120	0.123	0.025	-0.124	0.125	0.009

Harmonic components

Figure 74 – M2 amplitude in VaG A0CH and Reference_A0CH

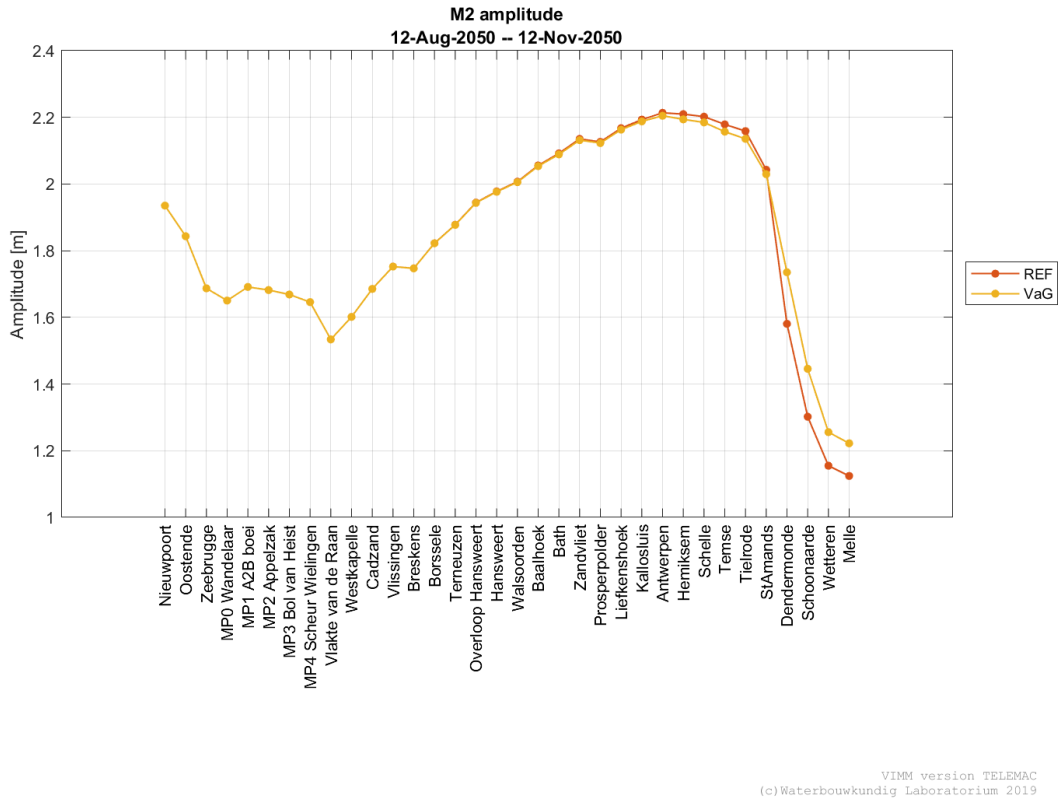

Figure 75 – M2 phase in VaG A0CH and Reference_A0CH

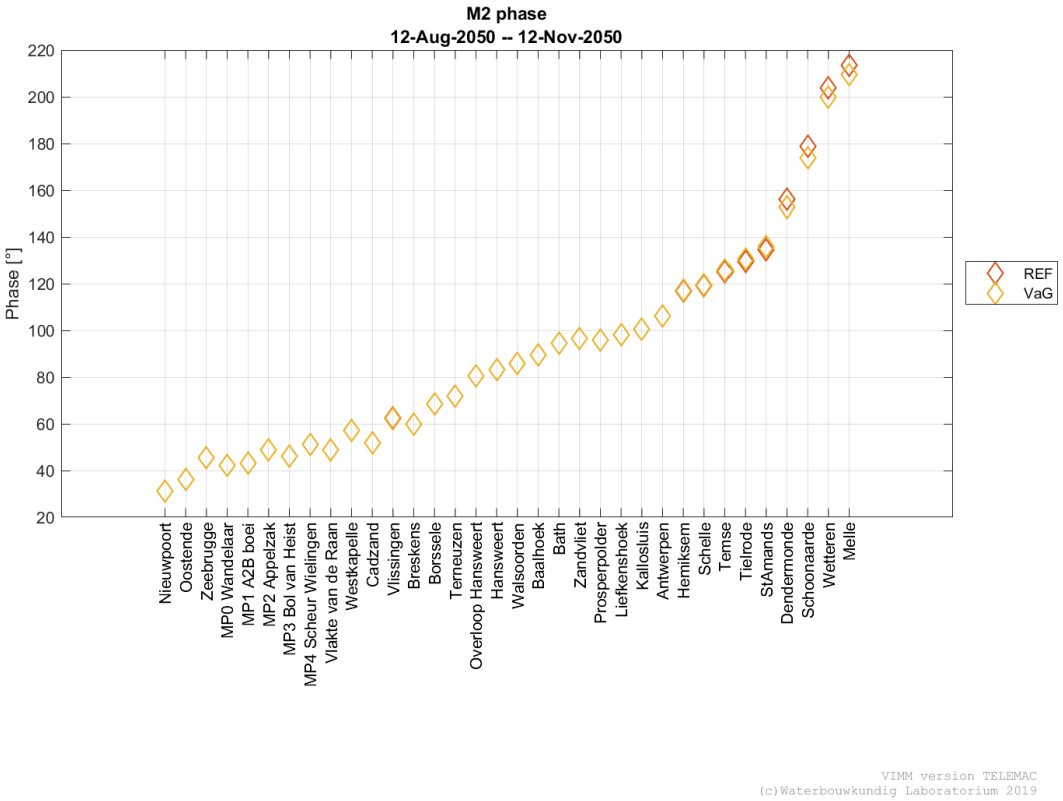

Figure 76 – M4 amplitude in VaG A0CH and Reference_A0CH

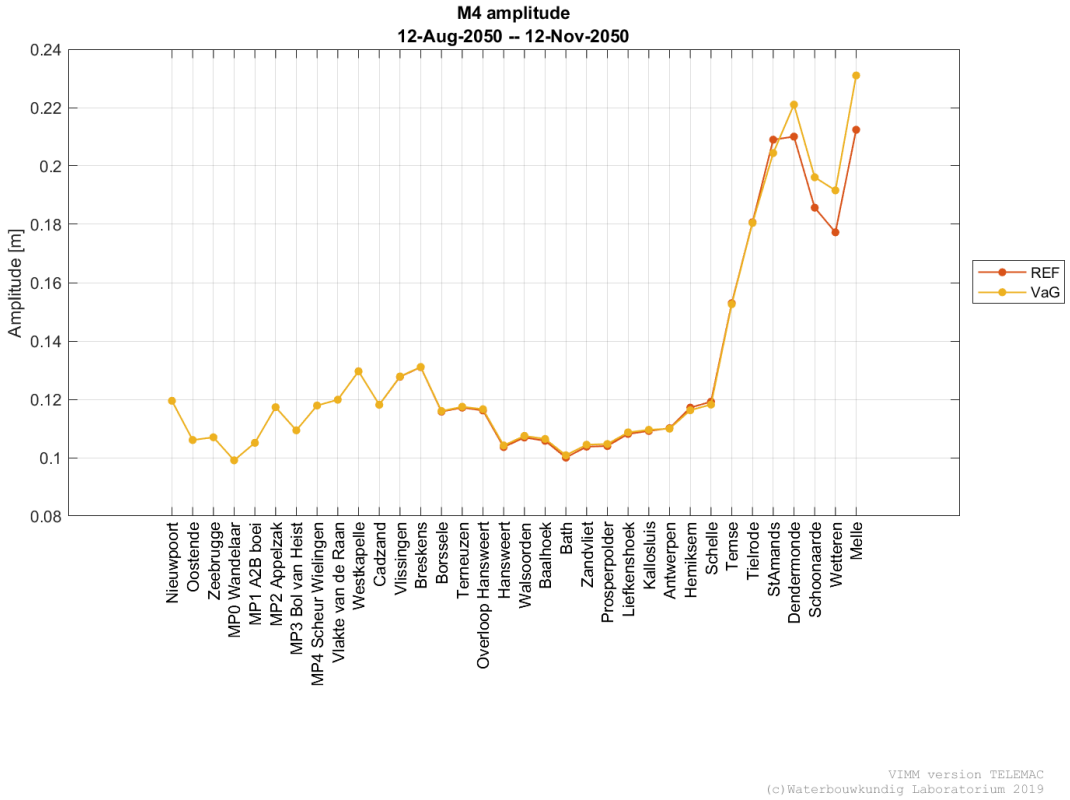

Figure 77 – M4 phase in VaG A0CH and Reference_A0CH

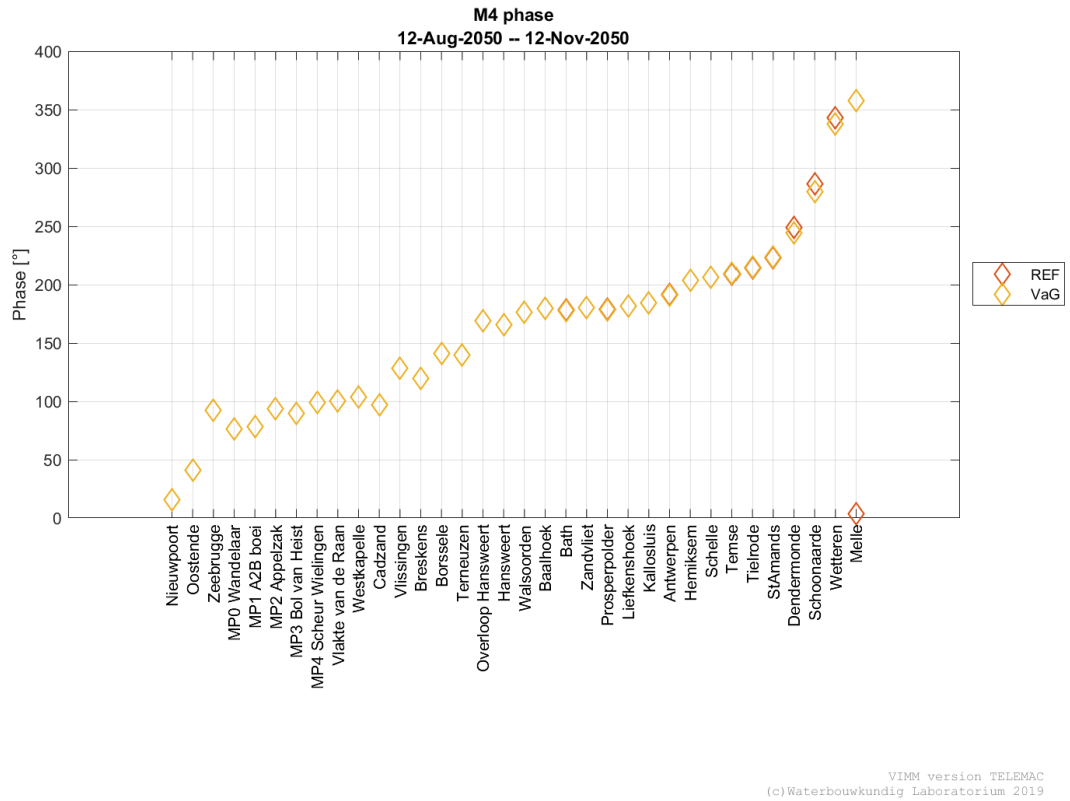

Figure 78 – S2 amplitude in VaG A0CH and Reference_A0CH

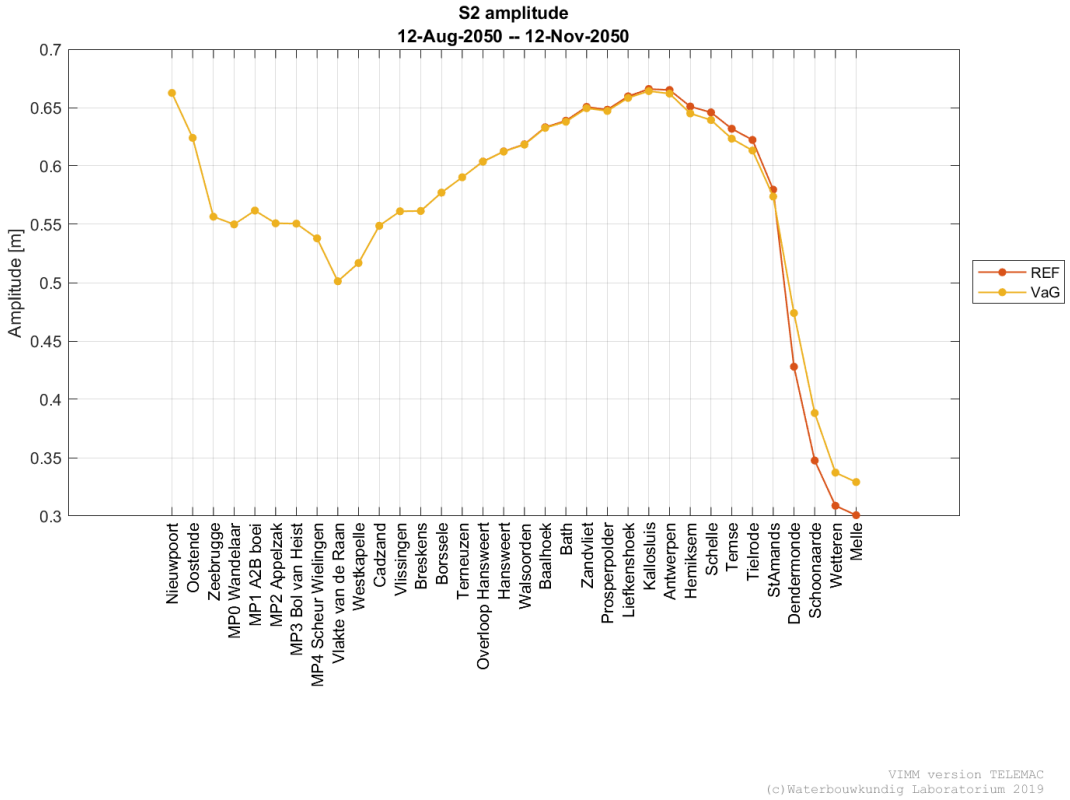

Figure 79 – S2 phase in VaG A0CH and Reference_A0CH

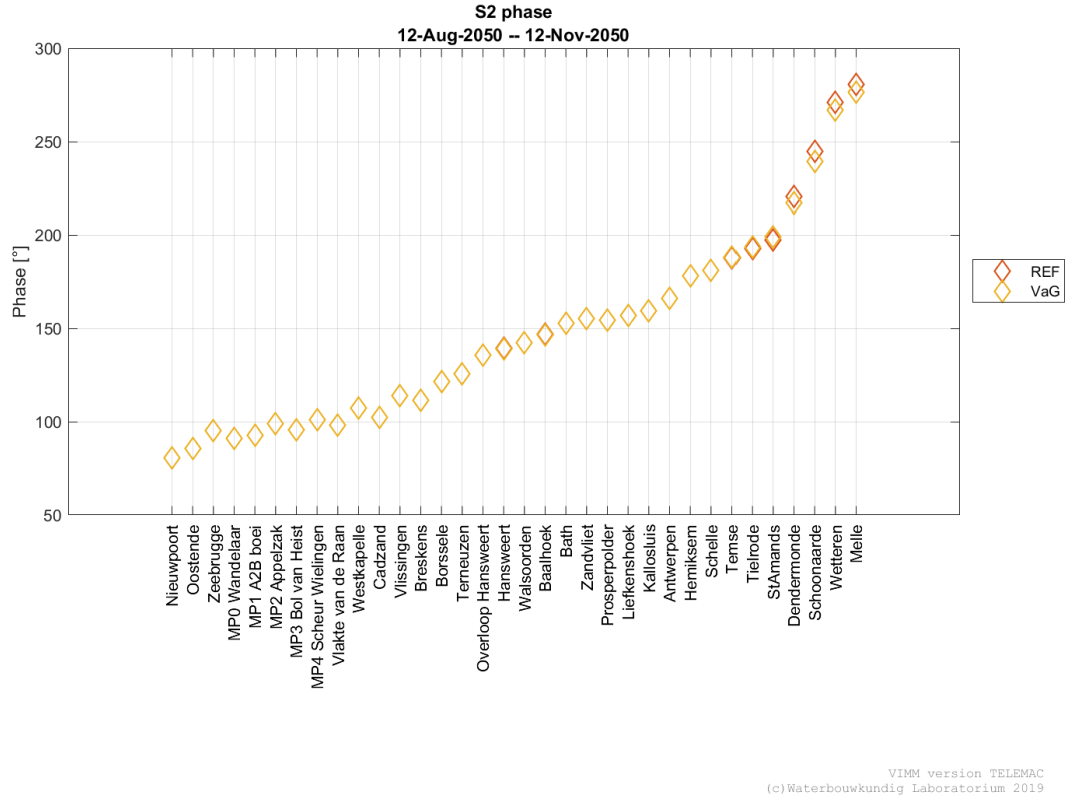

Discharges

Table 6 – Statistical parameters of complete discharge time series VaG A0CH vs Reference A0CH

Stations	VaG - Ref		
	BIAS TS	RMSE TS	RRMSE TS
	[m³/s]	[m³/s]	[-]
R3 Overloop van Valkenisse	-18.37	56.72	0.00
R3 Zimmermangeul	-0.98	3.84	0.01
R2 Nauw van Bath	-7.28	31.41	0.01
R2 Schaar van de Noord	-7.50	30.05	0.00
R1 Vaarwater boven Bath	-7.33	56.14	0.01
R1 Ballastplaat	-0.75	7.54	0.01
Liefkenshoek	2.29	62.35	0.01
Oosterweel	13.82	61.74	0.01
Kruibeke	24.97	60.37	0.02
Schelle	28.57	60.05	0.02
Temse	46.50	62.92	0.04
Driegoten	55.54	64.78	0.06
Baasrode	53.14	60.88	0.11
Dendermonde	44.37	60.12	0.15
Schoonaarde	22.61	34.26	0.13
Schellebelle	16.08	26.31	0.14
Wetteren	12.13	21.32	0.14
Melle	7.05	15.42	0.15

A0CL runs

Water levels

Table 7 – Statistical parameters of HW, LW and complete time series of water levels (VaG_A0CL - Reference_A0CL)

Stations	Complete Time Series			HW			LW		
	BIAS	RMSE	RMSE_0	BIAS	RMSE	RMSE_0	BIAS	RMSE	RMSE_0
	[m]			[m]			[m]		
Bath	0.000	0.003	0.003	-0.002	0.002	0.000	0.004	0.004	0.000
Zandvliet	0.000	0.003	0.003	-0.002	0.002	0.000	0.005	0.005	0.001
Prosperpolder	0.000	0.003	0.003	-0.002	0.002	0.000	0.005	0.005	0.001
Liefkenshoek	0.000	0.004	0.004	-0.002	0.002	0.000	0.005	0.005	0.001
Kallosluis	0.001	0.005	0.005	-0.003	0.003	0.000	0.006	0.006	0.001
Antwerpen	0.001	0.008	0.008	-0.005	0.005	0.001	0.009	0.009	0.001
Hemiksem	0.002	0.016	0.016	-0.015	0.015	0.002	0.017	0.017	0.003
Schelle	0.003	0.018	0.018	-0.018	0.018	0.002	0.019	0.019	0.004
Temse	0.005	0.029	0.028	-0.027	0.027	0.003	0.028	0.029	0.006
Tielrode	0.005	0.034	0.034	-0.032	0.032	0.004	0.031	0.031	0.007
StAmands	-0.003	0.044	0.044	-0.047	0.048	0.011	0.004	0.005	0.004
Dendermonde	-0.066	0.160	0.145	0.131	0.132	0.016	-0.252	0.255	0.036
Schoonaarde	-0.059	0.166	0.155	0.129	0.130	0.018	-0.244	0.245	0.025
Wetteren	-0.027	0.110	0.106	0.109	0.111	0.020	-0.131	0.131	0.007
Melle	-0.033	0.109	0.103	0.112	0.114	0.019	-0.121	0.121	0.008

Harmonic components

Figure 80 – M2 amplitude in VaG_A0CL and Reference_A0CL

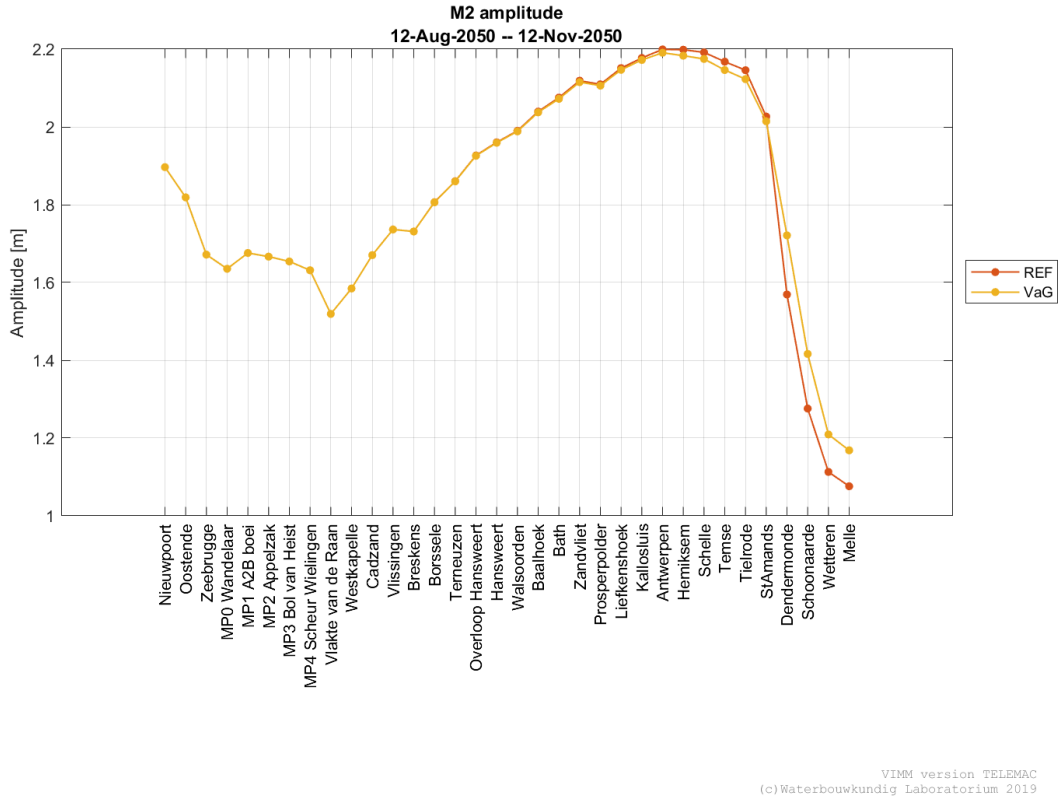

Figure 81 – M2 phase in VaG_A0CL and Reference_A0CL

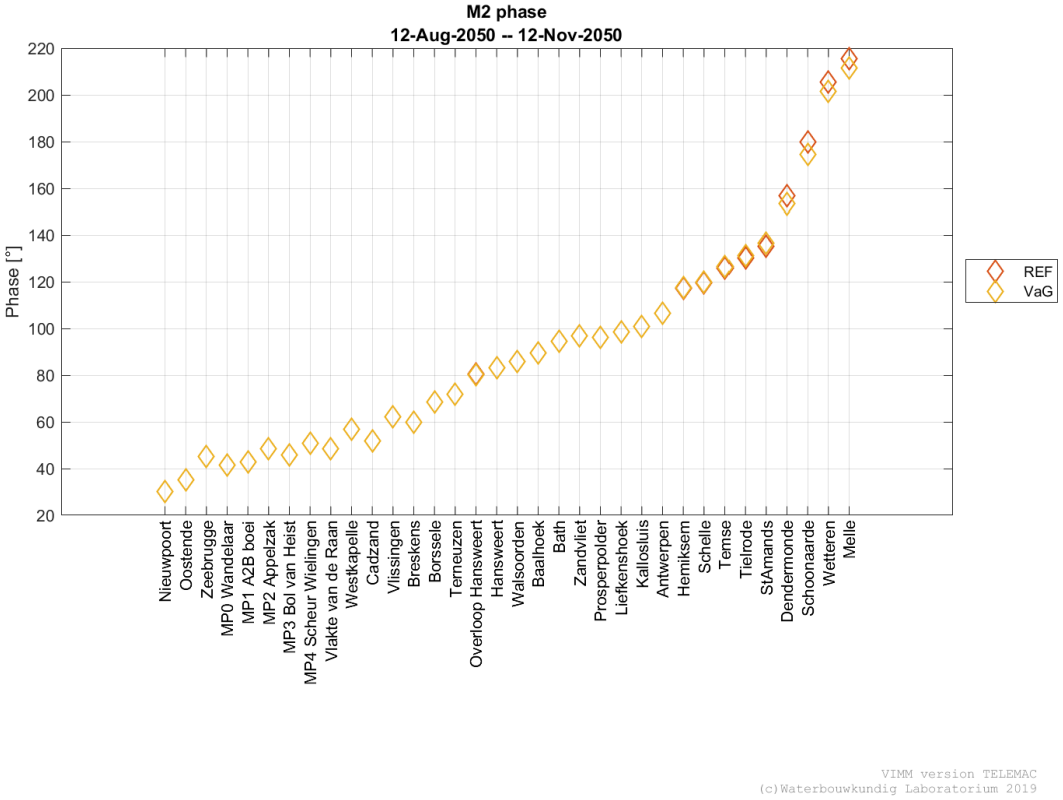

Figure 82 – M4 amplitude in VaG_A0CL and Reference_A0CL

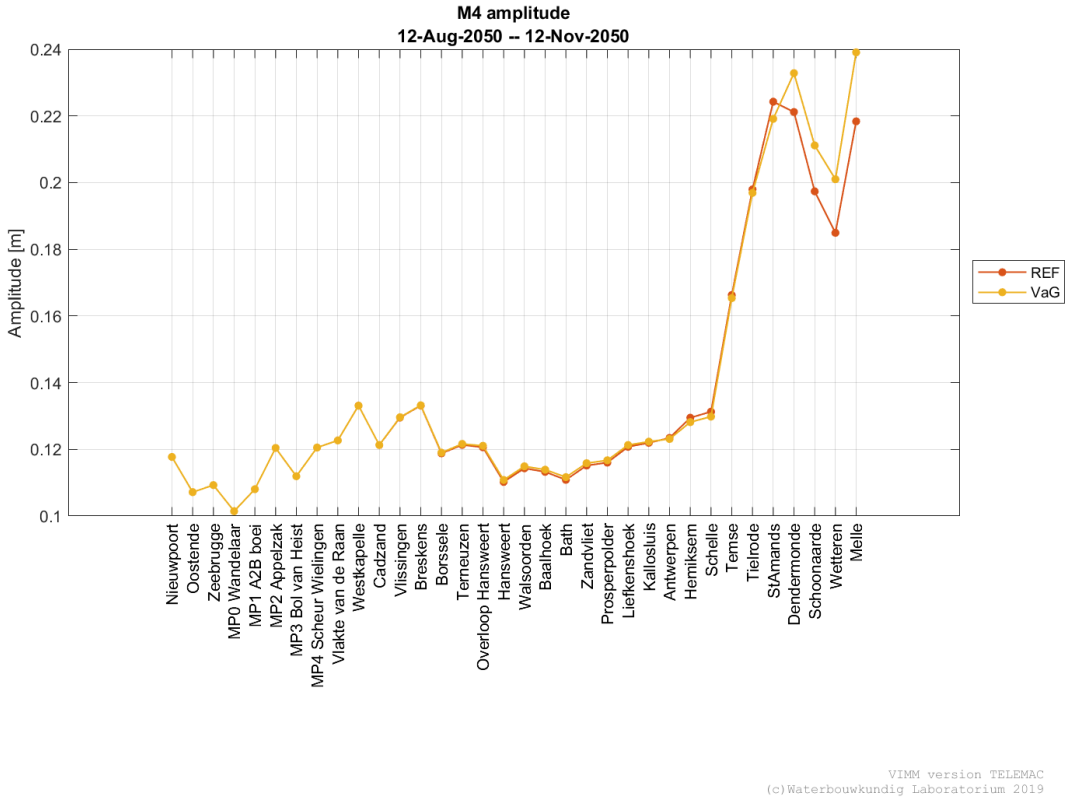

Figure 83 – M4 phase in VaG_A0CL and Reference_A0CL

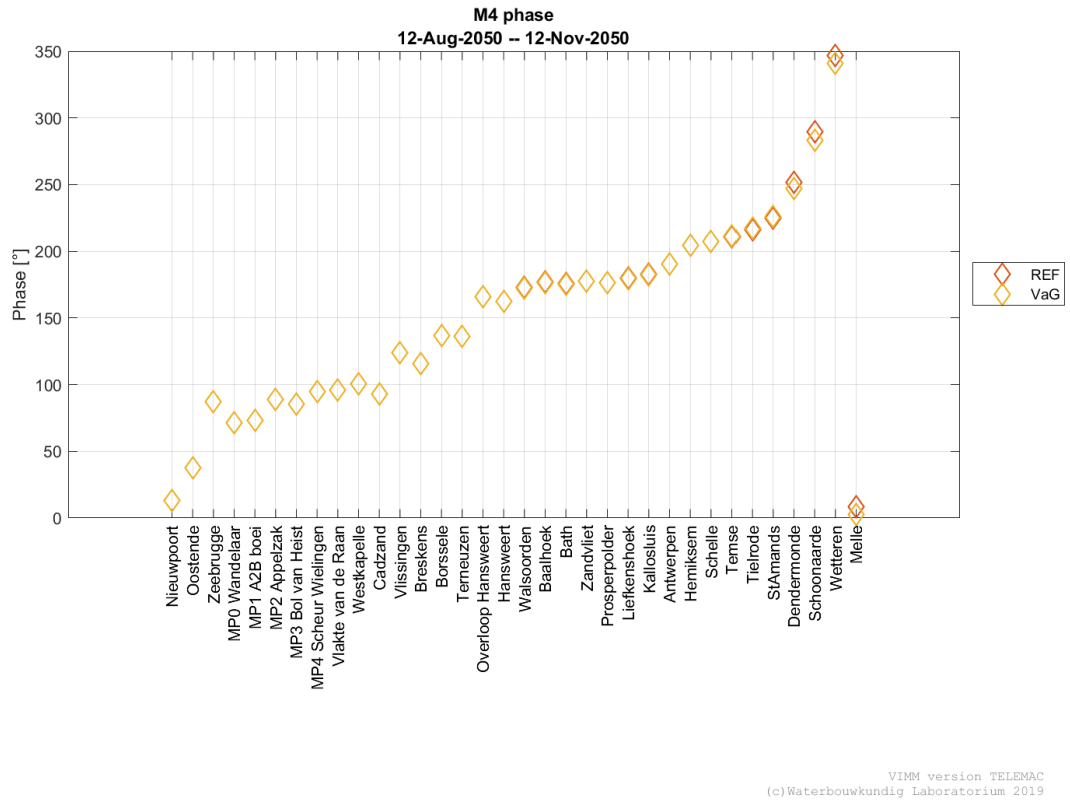

Figure 84 – S2 amplitude in VaG_A0CL and Reference_A0CL

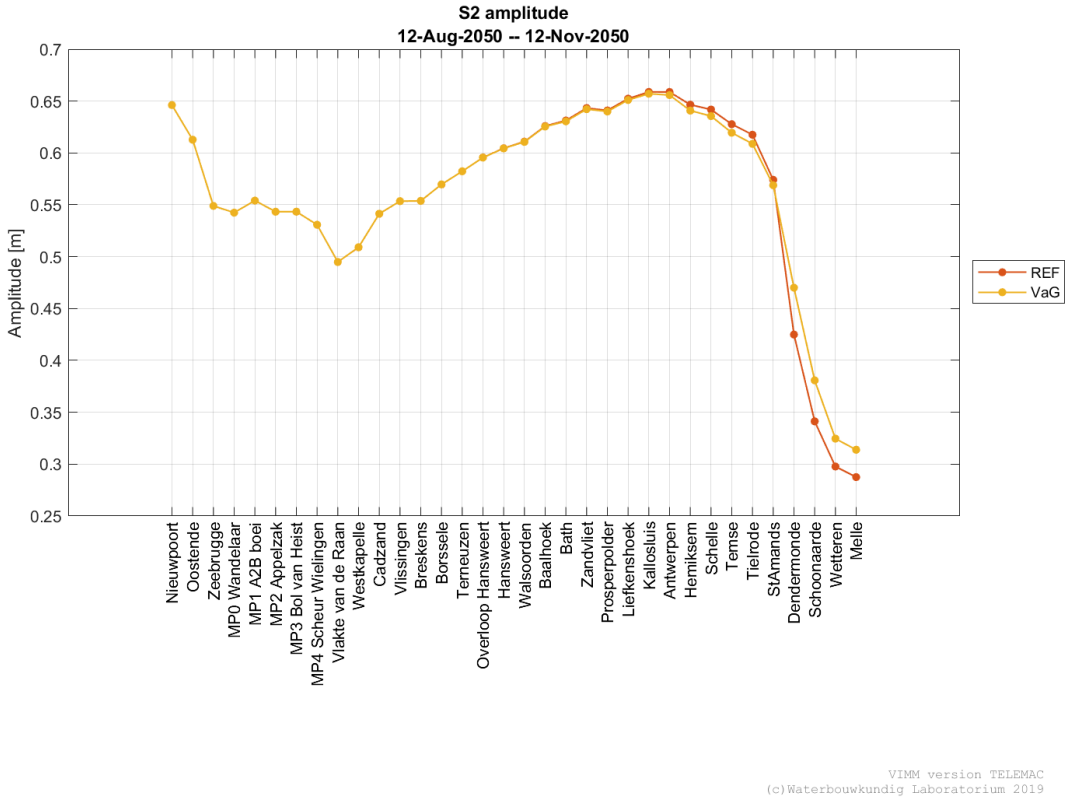

Figure 85 – S2 phase in VaG_A0CL and Reference_A0CL

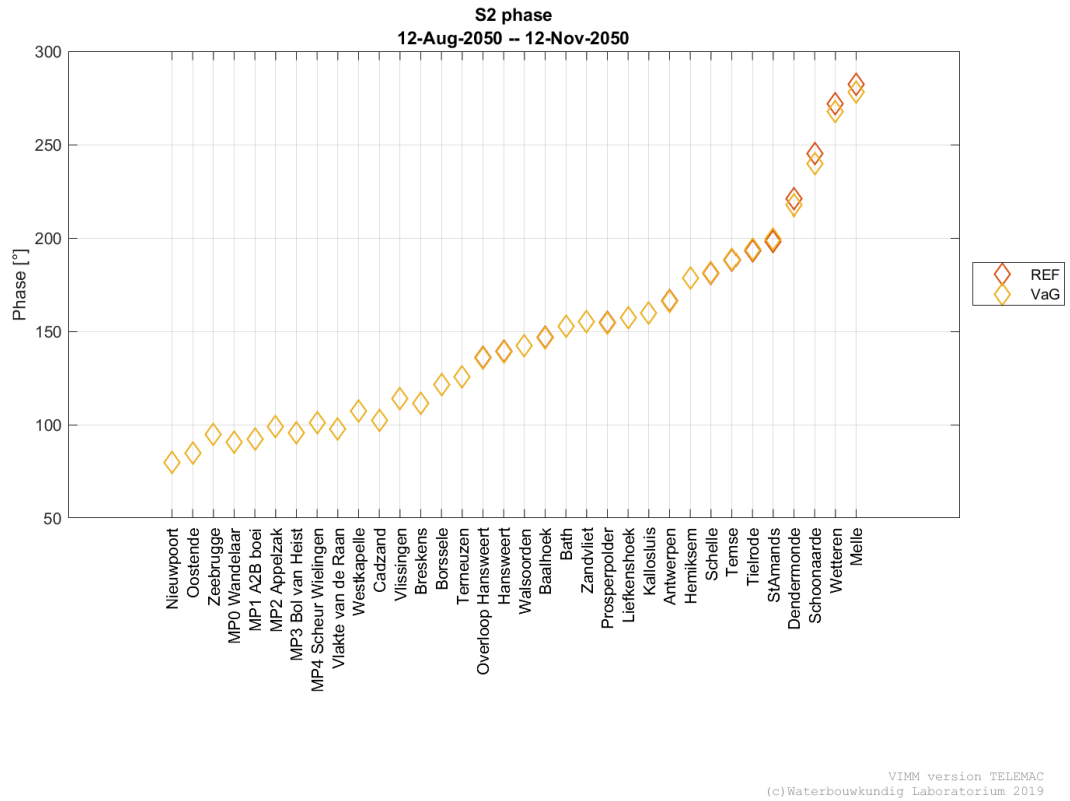

Discharges

Table 8 – Statistical parameters of complete discharge time series VaG A0CL vs Reference A0CL

Stations	VaG - Ref		
	BIAS TS	RMSE TS	RRMSE TS
	[m³/s]	[m³/s]	[-]
R3 Overloop van Valkenisse	-17.82	53.87	0.00
R3 Zimmermangeul	-0.91	3.36	0.01
R2 Nauw van Bath	-7.36	29.98	0.01
R2 Schaar van de Noord	-7.27	28.20	0.00
R1 Vaarwater boven Bath	-7.47	53.52	0.01
R1 Ballastplaat	-0.82	6.66	0.01
Liefkenshoek	1.47	59.25	0.01
Oosterweel	12.34	58.79	0.01
Kruibeke	23.26	57.44	0.02
Schelle	26.82	57.15	0.02
Temse	43.89	60.70	0.04
Driegoten	52.40	61.26	0.06
Baasrode	49.64	57.61	0.10
Dendermonde	41.37	57.46	0.15
Schoonaarde	20.25	31.61	0.13
Schellebelle	15.28	23.21	0.14
Wetteren	11.47	18.89	0.14
Melle	6.73	12.96	0.15

AplusCH runs

Water levels

Table 9 – Statistical parameters of HW, LW and complete time series of water levels (VaG_AplusCH - Reference_AplusCH)

Stations	Complete Time Series			HW			LW		
	BIAS	RMSE	RMSE_0	BIAS	RMSE	RMSE_0	BIAS	RMSE	RMSE_0
	[m]			[m]			[m]		
Bath	0.000	0.003	0.003	-0.002	0.002	0.000	0.004	0.004	0.001
Zandvliet	0.000	0.003	0.003	-0.002	0.002	0.000	0.005	0.005	0.001
Prosperpolder	0.000	0.003	0.003	-0.002	0.002	0.000	0.005	0.005	0.001
Liefkenshoek	0.000	0.004	0.004	-0.002	0.002	0.000	0.006	0.006	0.001
Kallosluis	0.001	0.005	0.005	-0.003	0.003	0.000	0.007	0.007	0.001
Antwerpen	0.001	0.008	0.008	-0.006	0.006	0.001	0.010	0.011	0.002
Hemiksem	0.003	0.018	0.017	-0.015	0.015	0.002	0.019	0.020	0.004
Schelle	0.003	0.020	0.020	-0.016	0.017	0.002	0.022	0.022	0.005
Temse	0.006	0.031	0.031	-0.028	0.029	0.005	0.032	0.033	0.007
Tielrode	0.006	0.037	0.037	-0.033	0.034	0.006	0.035	0.036	0.008
StAmands	-0.002	0.047	0.047	-0.045	0.045	0.008	0.006	0.008	0.005
Dendermonde	-0.068	0.168	0.153	0.130	0.131	0.015	-0.273	0.275	0.037
Schoonaarde	-0.058	0.170	0.160	0.119	0.120	0.016	-0.261	0.262	0.026
Wetteren	-0.022	0.114	0.112	0.117	0.119	0.022	-0.139	0.140	0.008
Melle	-0.027	0.113	0.109	0.121	0.123	0.024	-0.126	0.126	0.009

Harmonic components

Figure 86 – M2 amplitude in VaG AplusCH and Reference AplusCH

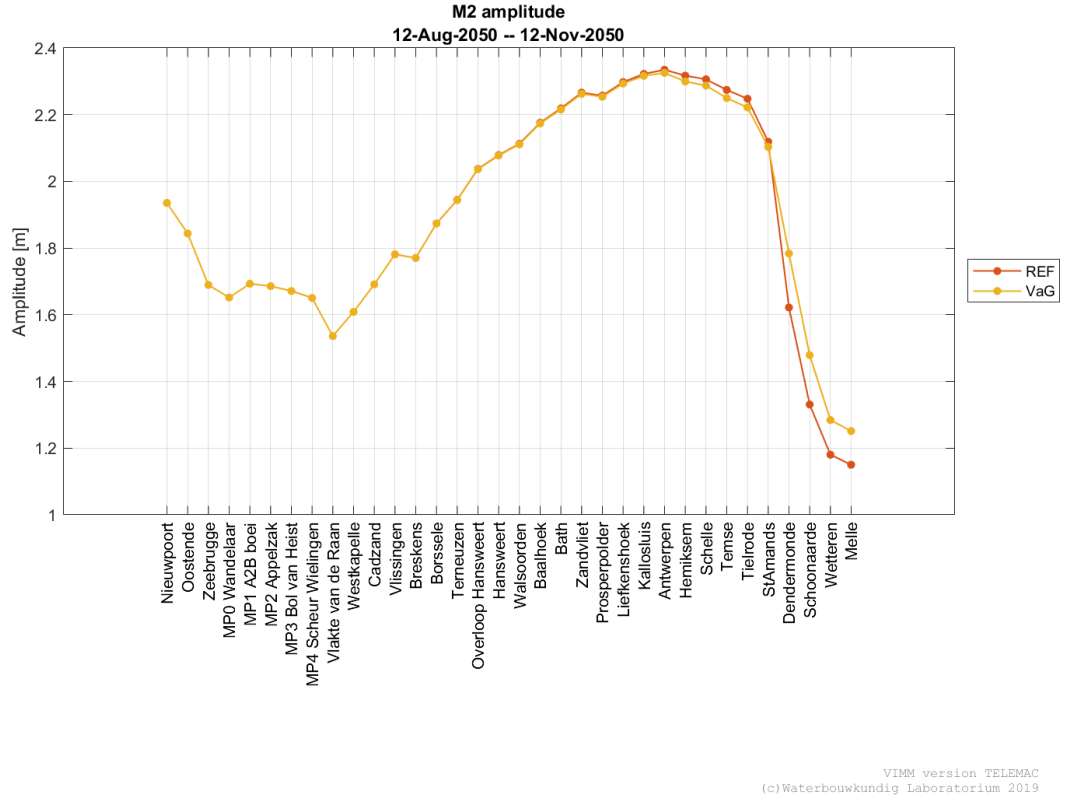

Figure 87 – M2 phase in VaG AplusCH and Reference AplusCH

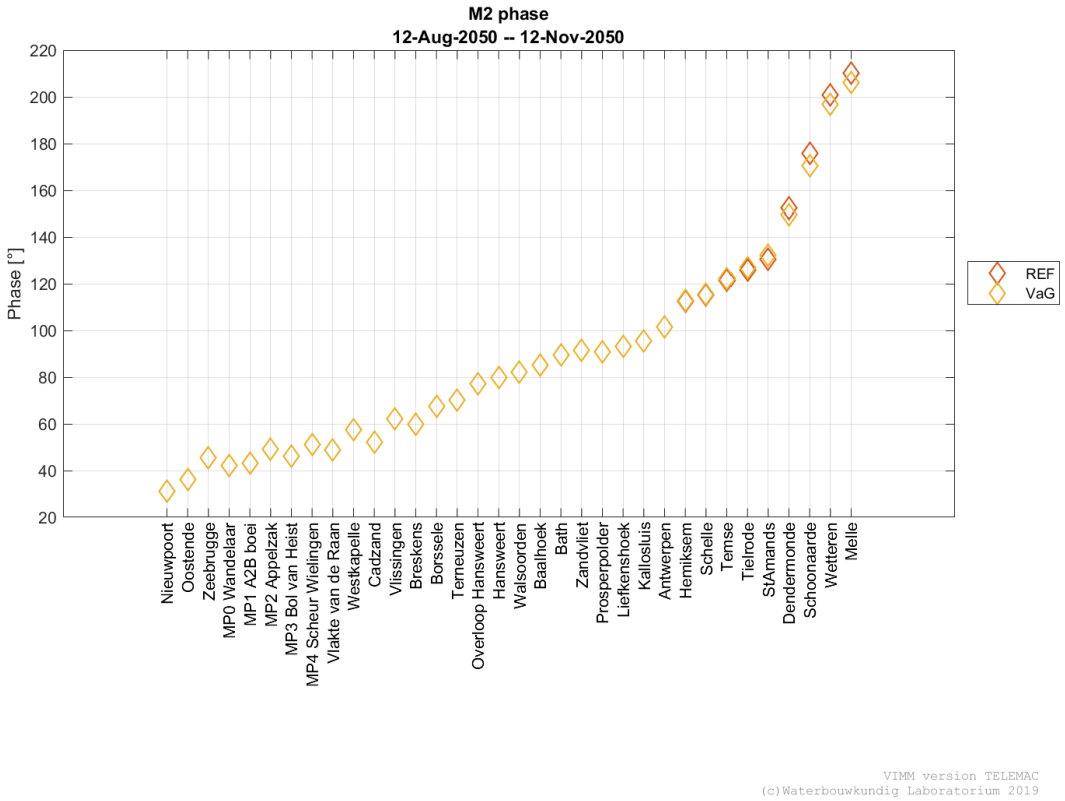

Figure 88 – M4 amplitude in VaG AplusCH and Reference AplusCH

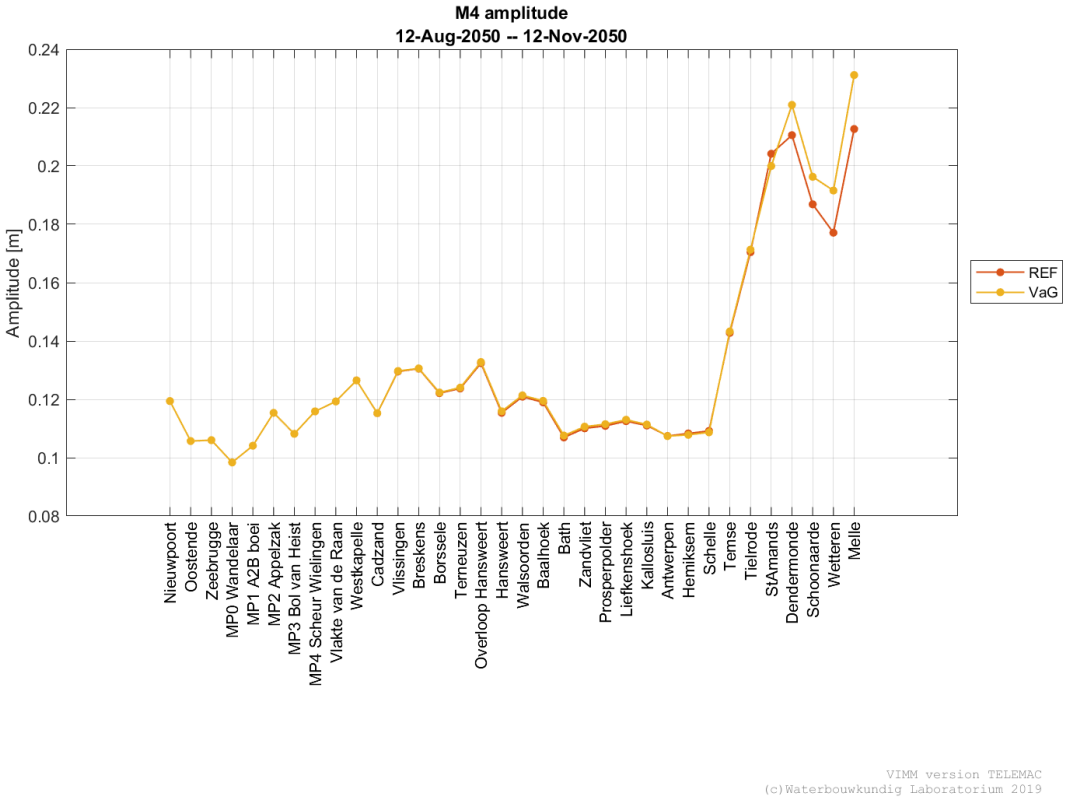

Figure 89 – M4 phase in VaG AplusCH and Reference AplusCH

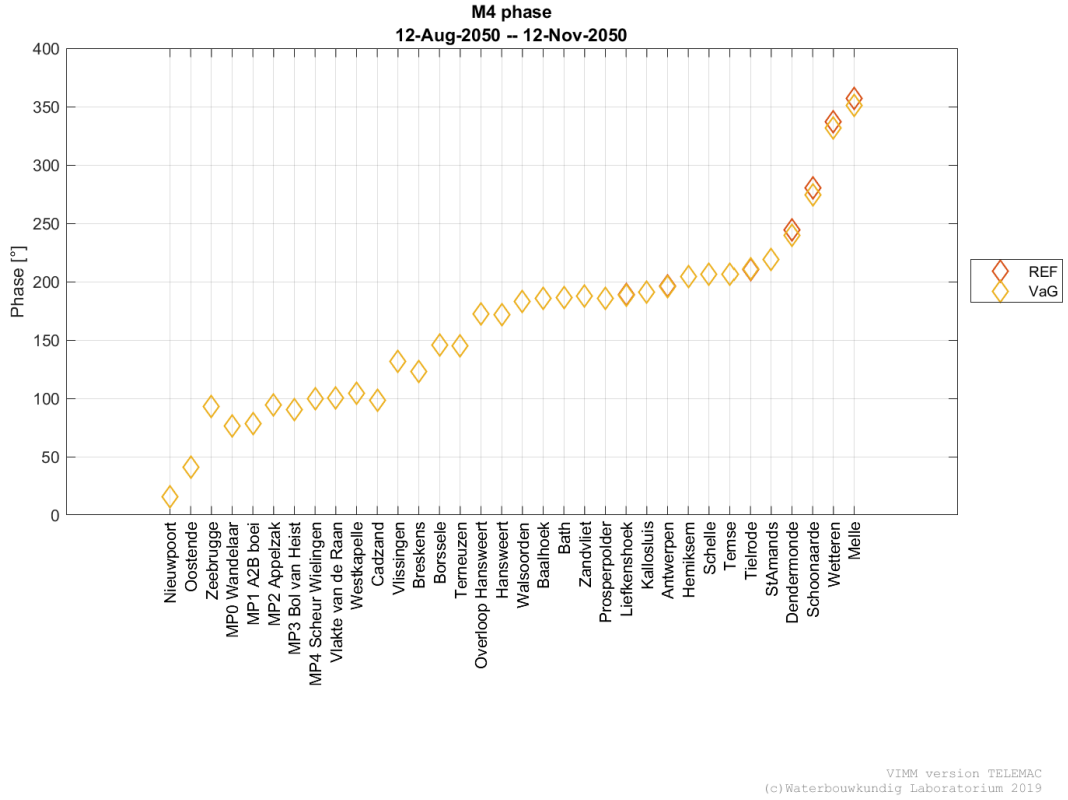

Figure 90 – S2 amplitude in VaG AplusCH and Reference AplusCH

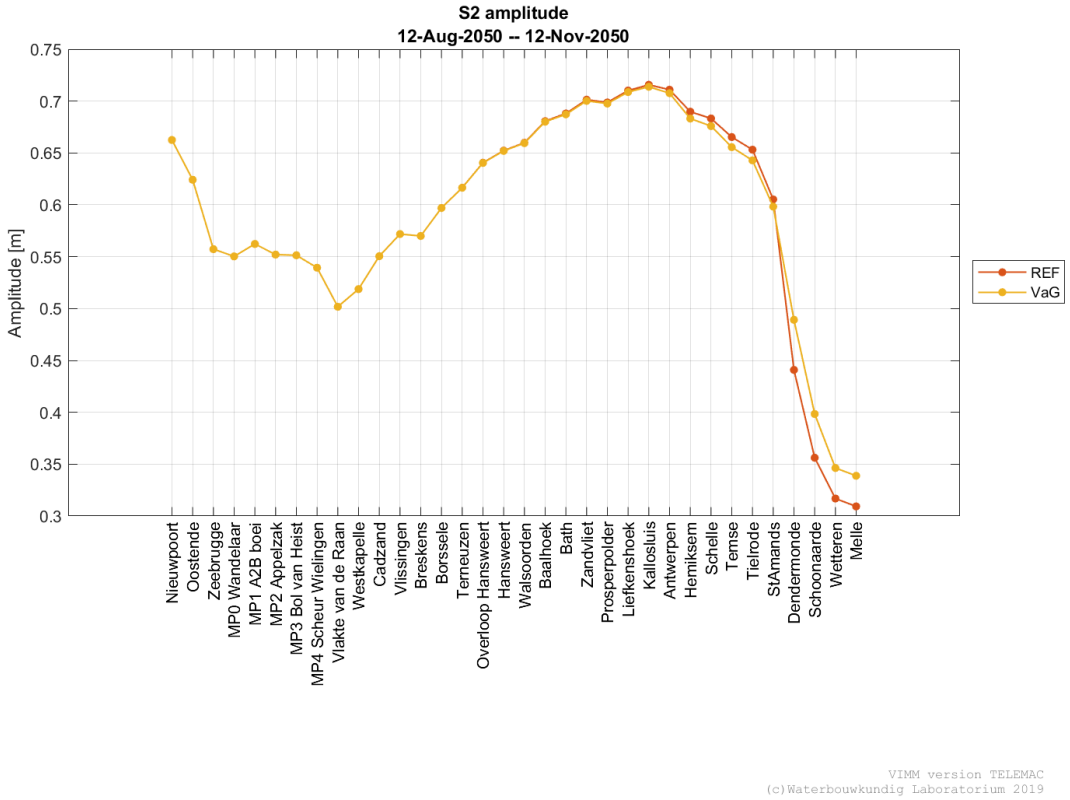

Figure 91 – S2 phase in VaG AplusCH and Reference AplusCH

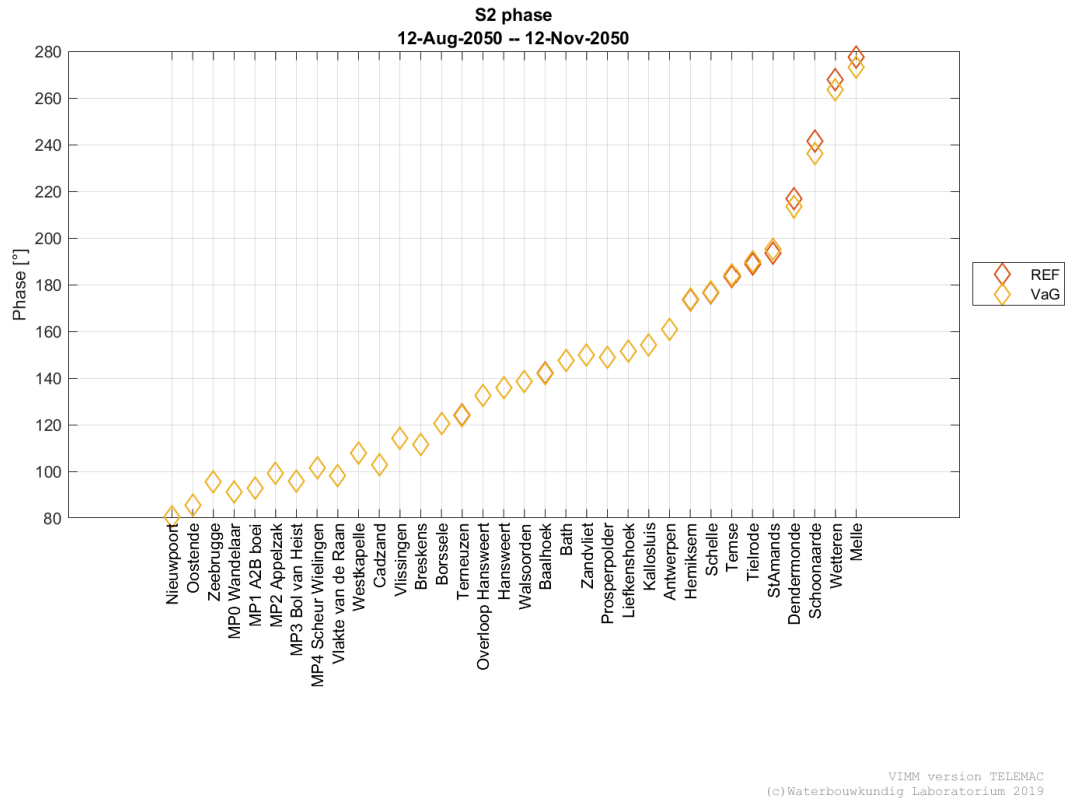

Discharges

Table 10 – Statistical parameters of complete discharge time series VaG AplusCH vs Reference AplusCH

Stations	VaH - Ref		
	BIAS TS	RMSE TS	RRMSE TS
	[m³/s]	[m³/s]	[-]
R3 Overloop van Valkenisse	-20.33	60.57	0.00
R3 Zimmermangeul	-1.10	4.22	0.01
R2 Nauw van Bath	-8.00	33.83	0.01
R2 Schaar van de Noord	-8.45	32.60	0.00
R1 Vaarwater boven Bath	-8.95	58.62	0.01
R1 Ballastplaat	-0.91	8.45	0.01
Liefkenshoek	0.89	64.56	0.01
Oosterweel	12.92	63.48	0.01
Kruibeke	24.52	61.98	0.02
Schelle	28.62	61.63	0.02
Temse	47.63	65.93	0.04
Driegoten	57.32	67.49	0.06
Baasrode	56.01	64.98	0.11
Dendermonde	46.32	62.50	0.15
Schoonaarde	23.99	35.87	0.13
Schellebelle	16.63	24.37	0.14
Wetteren	12.60	19.89	0.14
Melle	7.27	13.37	0.14

AminCL runs

Water levels

Table 11 – Statistical parameters of HW, LW and complete time series of water levels (VaG_AminCL - Reference_AminCL)

Stations	Complete Time Series			HW			LW		
	BIAS	RMSE	RMSE_0	BIAS	RMSE	RMSE_0	BIAS	RMSE	RMSE_0
	[m]			[m]			[m]		
Bath	0.000	0.003	0.003	-0.002	0.002	0.000	0.004	0.004	0.000
Zandvliet	0.000	0.004	0.004	-0.002	0.002	0.000	0.005	0.005	0.000
Prosperpolder	0.000	0.003	0.003	-0.002	0.002	0.000	0.004	0.005	0.000
Liefkenshoek	0.000	0.004	0.004	-0.002	0.002	0.000	0.005	0.005	0.001
Kallosluis	0.000	0.004	0.004	-0.003	0.003	0.000	0.006	0.006	0.001
Antwerpen	0.001	0.007	0.007	-0.005	0.005	0.001	0.008	0.008	0.001
Hemiksem	0.002	0.015	0.014	-0.015	0.015	0.002	0.014	0.015	0.003
Schelle	0.002	0.017	0.017	-0.018	0.018	0.002	0.016	0.016	0.003
Temse	0.004	0.026	0.025	-0.027	0.027	0.004	0.024	0.024	0.005
Tielrode	0.004	0.032	0.031	-0.031	0.031	0.005	0.026	0.027	0.006
StAmands	-0.003	0.040	0.040	-0.042	0.043	0.010	0.003	0.005	0.004
Dendermonde	-0.062	0.150	0.136	0.126	0.127	0.017	-0.233	0.235	0.032
Schoonaarde	-0.058	0.160	0.149	0.128	0.130	0.018	-0.233	0.234	0.023
Wetteren	-0.028	0.106	0.102	0.098	0.100	0.014	-0.129	0.129	0.007
Melle	-0.035	0.106	0.100	0.106	0.107	0.016	-0.119	0.119	0.008

Harmonic components

Figure 92 – M2 amplitude in VaG AminCL and Reference AminCL

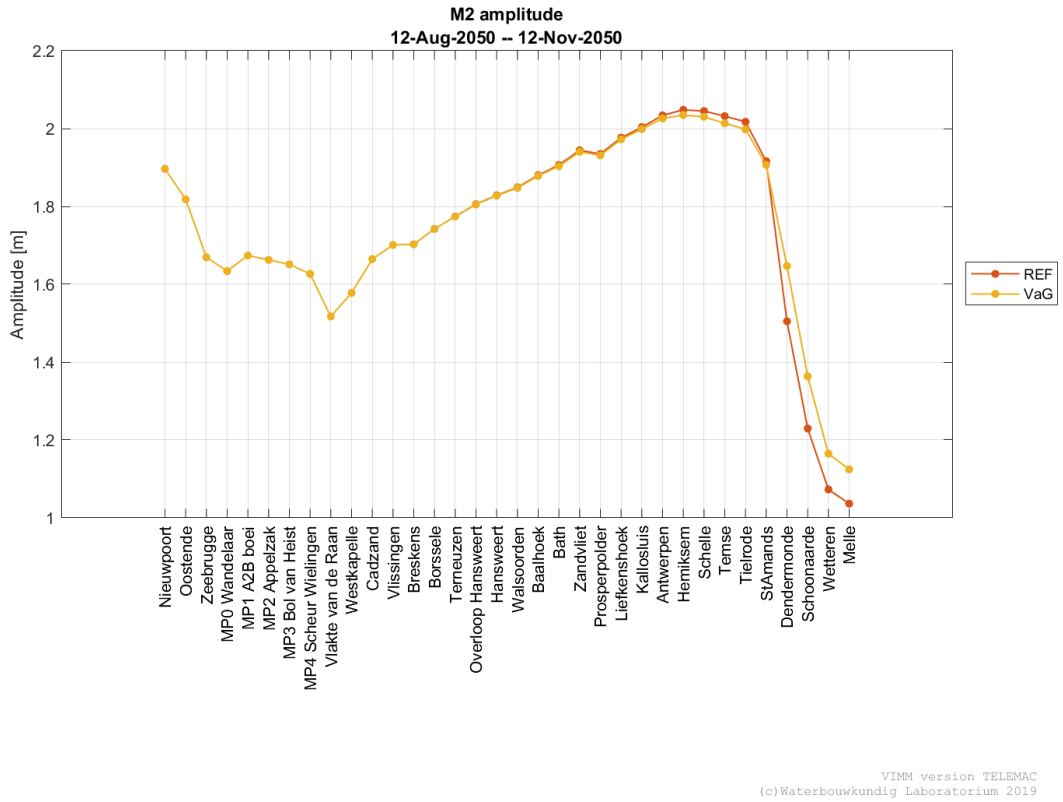

Figure 93 – M2 phase in VaG AminCL and Reference AminCL

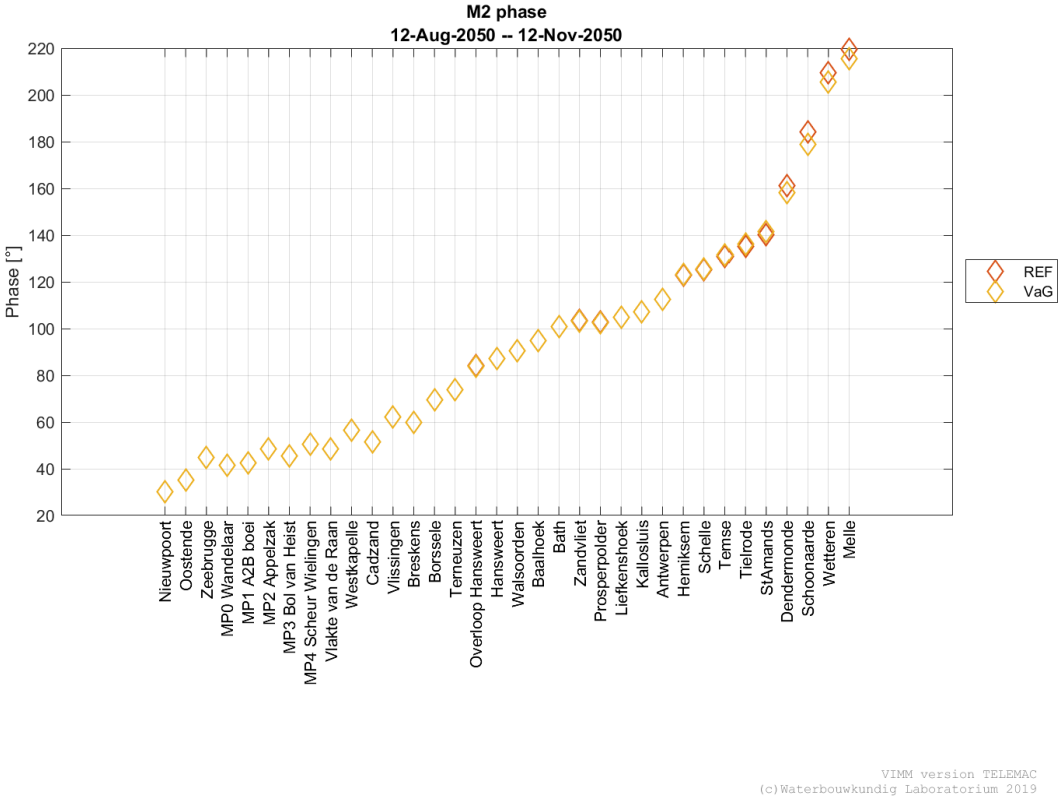

Figure 94 – M4 amplitude in VaG AminCL and Reference AminCL

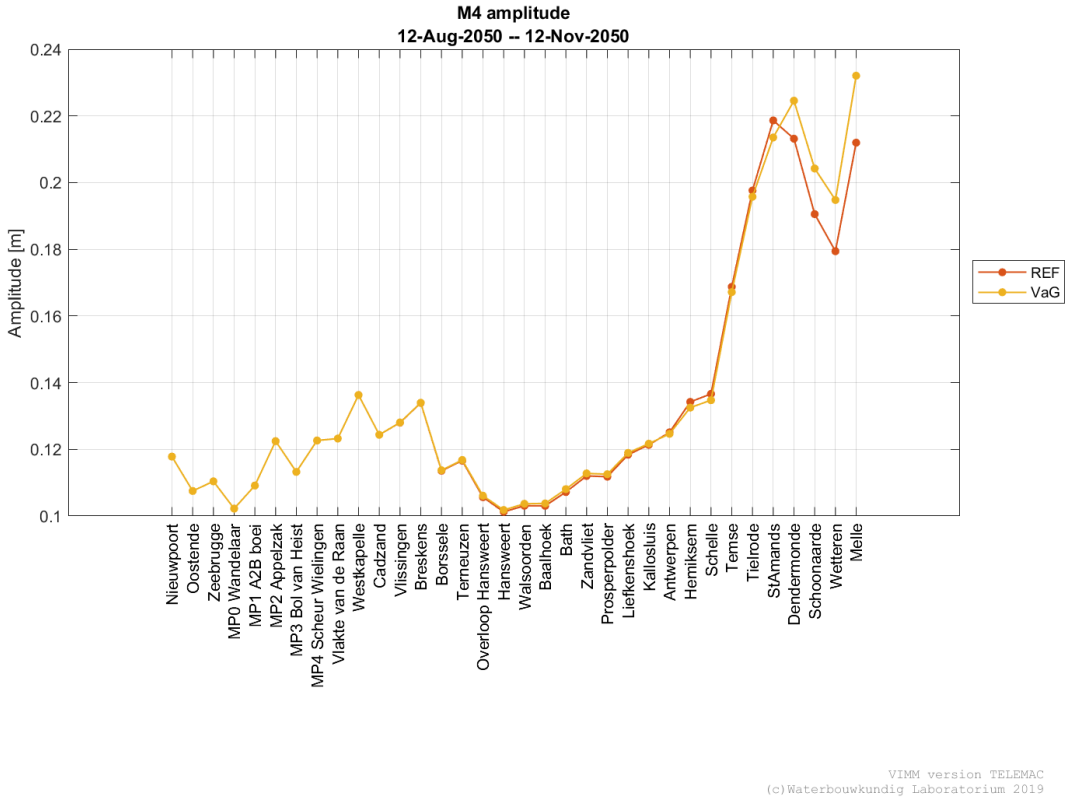

Figure 95 – M4 phase in VaG AminCL and Reference AminCL

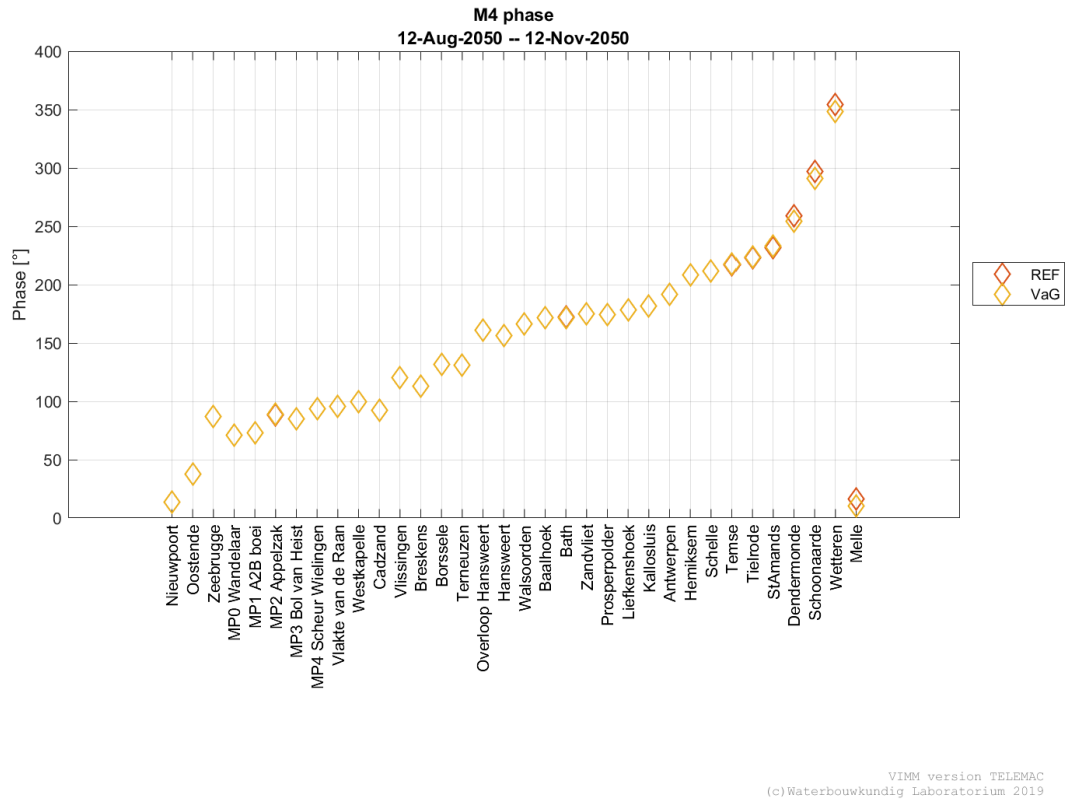

Figure 96 – S2 amplitude in VaG AminCL and Reference AminCL

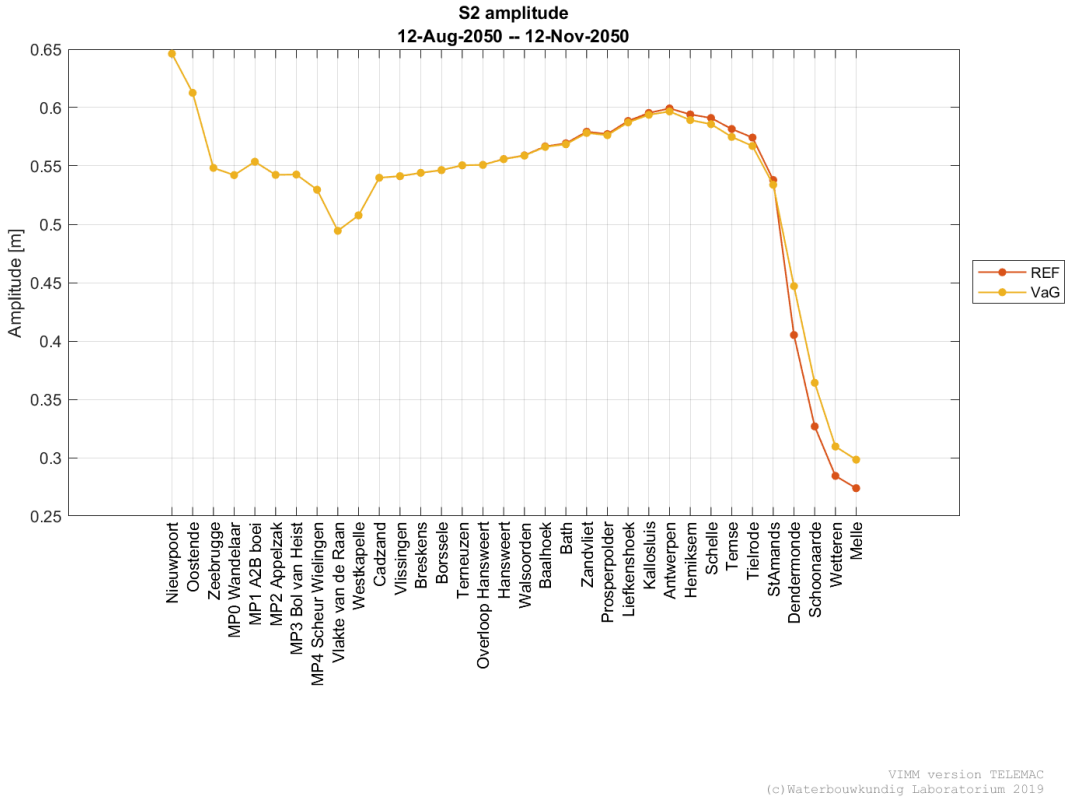

Figure 97 – S2 phase in VaG AminCL and Reference AminCL

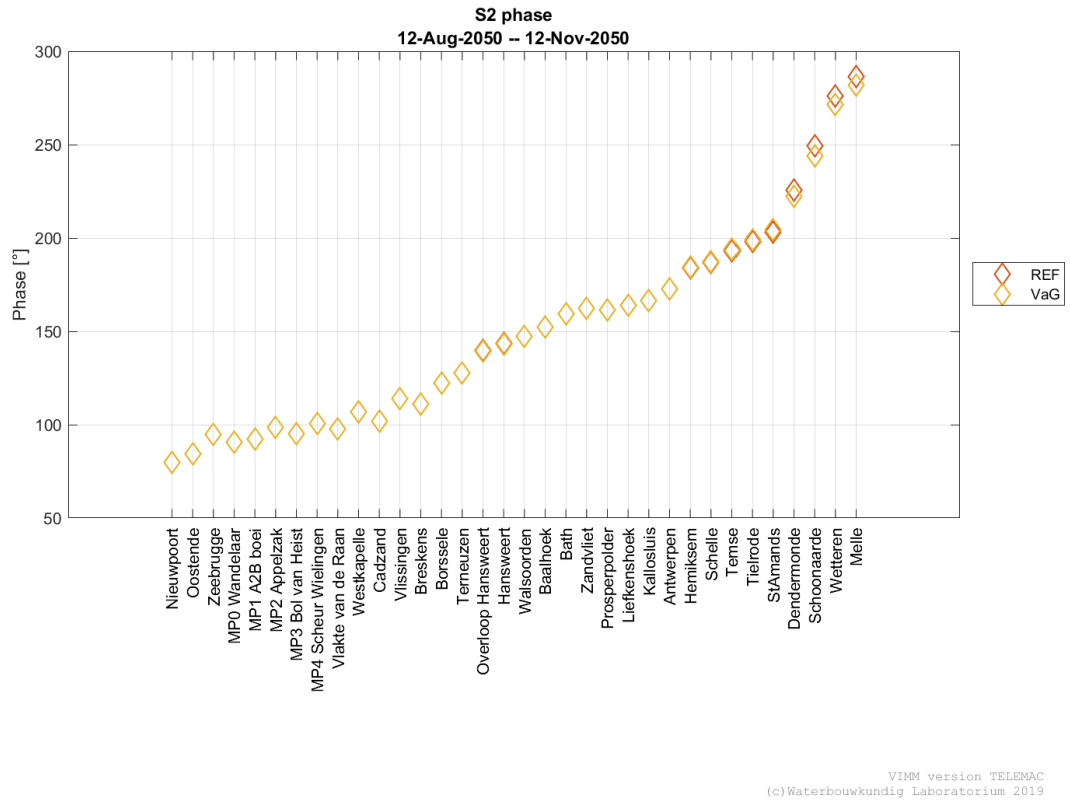

Discharges

Table 12 – Statistical parameters of complete discharge time series VaG AminCL vs Reference AminCL

Stations	**VaG - Ref**		
	BIAS TS	RMSE TS	RRMSE TS
	[m³/s]	[m³/s]	[-]
R3 Overloop van Valkenisse	-14.91	48.97	0.00
R3 Zimmermangeul	-0.76	2.89	0.01
R2 Nauw van Bath	-6.01	27.29	0.01
R2 Schaar van de Noord	-6.12	25.22	0.00
R1 Vaarwater boven Bath	-5.33	50.18	0.01
R1 Ballastplaat	-0.55	5.53	0.01
Liefkenshoek	3.20	56.04	0.01
Oosterweel	13.37	56.13	0.01
Kruibeke	23.34	54.82	0.02
Schelle	26.75	54.47	0.02
Temse	42.16	57.42	0.04
Driegoten	49.27	57.37	0.06
Baasrode	46.41	53.52	0.10
Dendermonde	38.79	54.39	0.15
Schoonaarde	18.77	29.67	0.13
Schellebelle	14.49	22.30	0.14
Wetteren	10.80	18.13	0.14
Melle	6.31	12.38	0.15

Tidal asymmetry in runs with different boundary conditions

Figure 98 – Tidal asymmetry (Tincrease/Tdecrease water level) in VaG and Reference runs

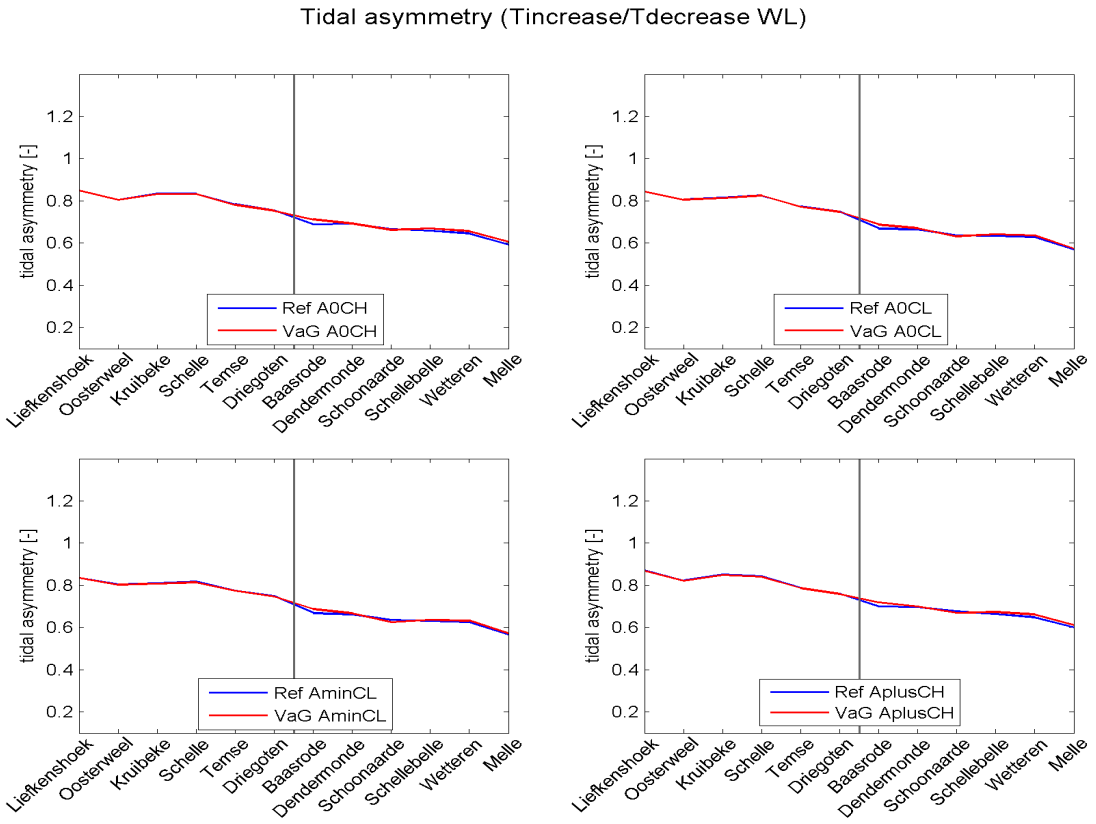

Figure 99 – Tidal asymmetry (Tflood/Tebb) in VaG and Reference runs

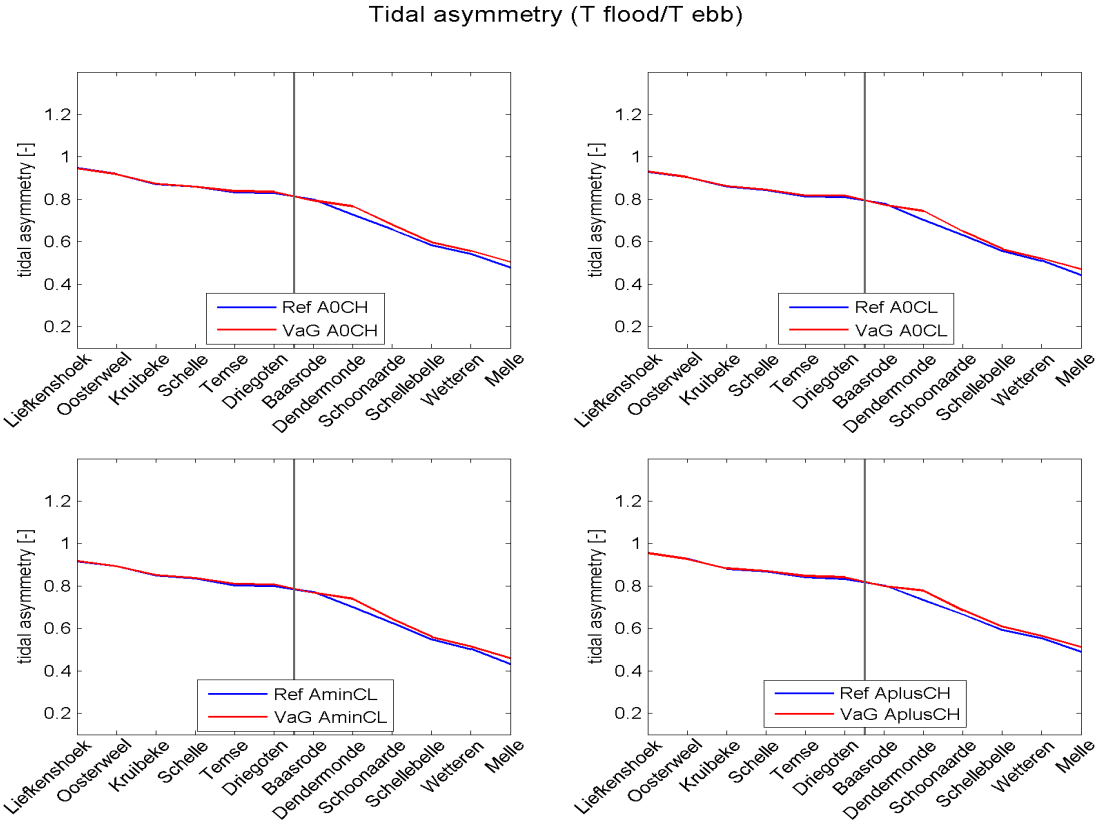

Figure 100 – Tidal asymmetry (Vmax flood/Vmax ebb) in VaG and Reference runs

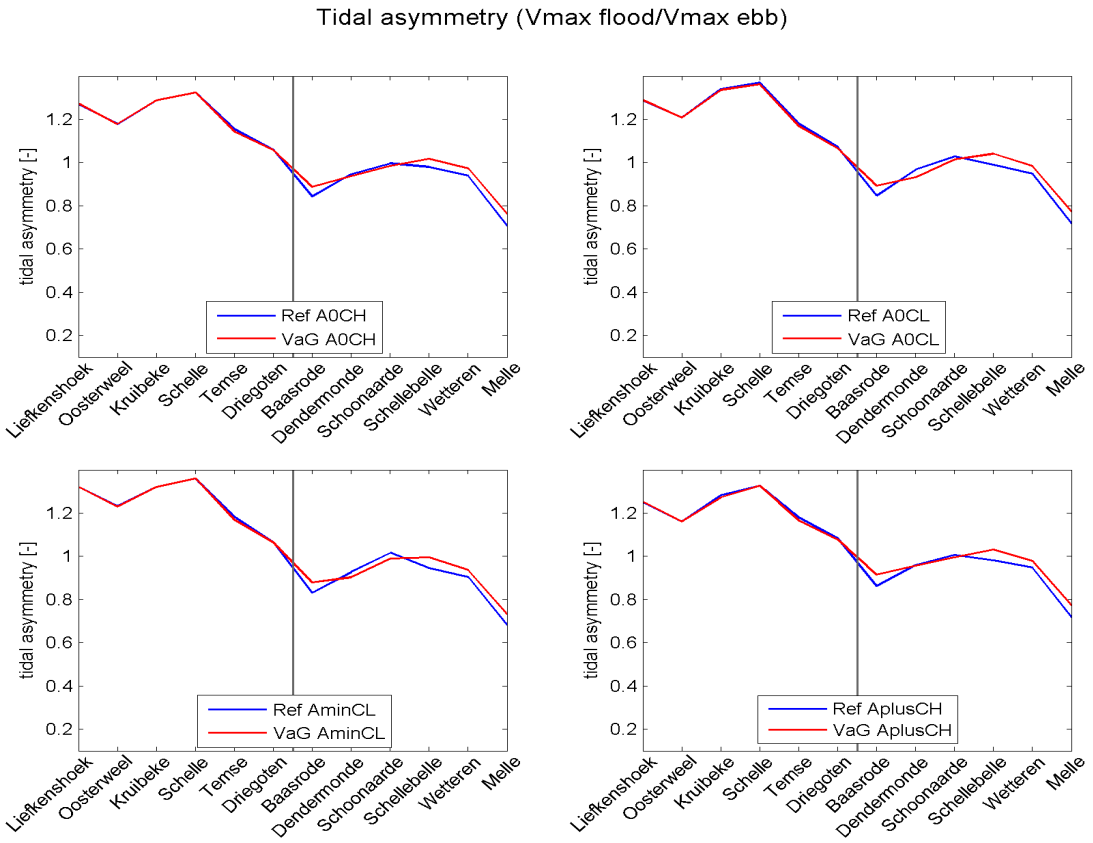

Figure 101 – Tidal asymmetry (based on V^3) in VaG and Reference runs

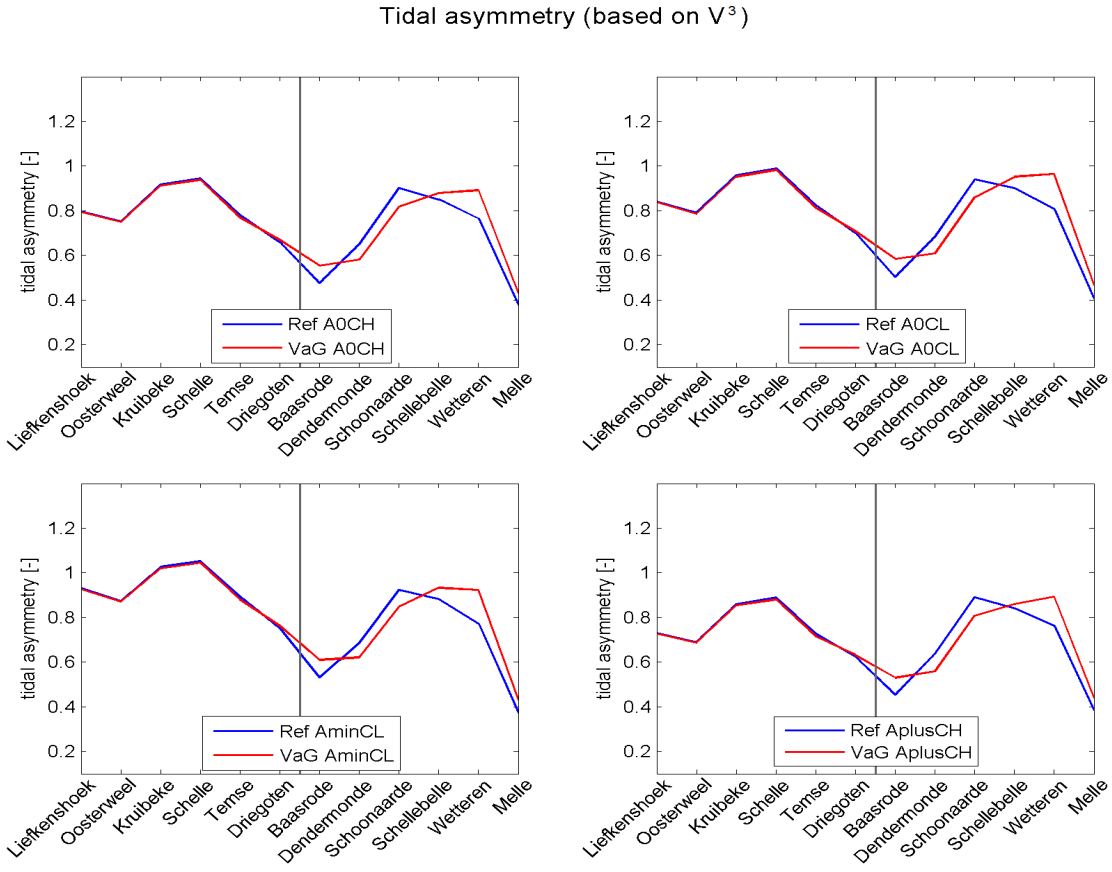

Figure 102 – Tidal asymmetry (based on V^4) in VaG and Reference runs

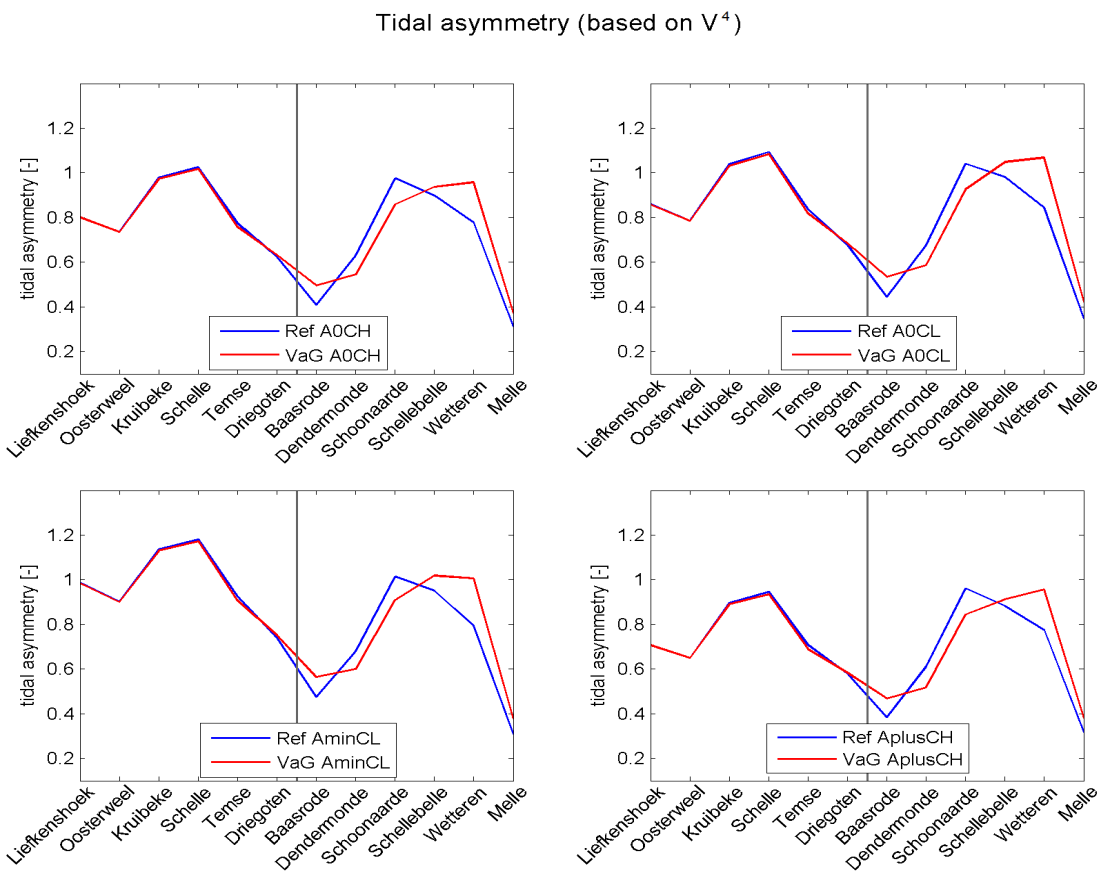

Appendix 3: Effect of VaH

A0CH runs

Water levels

Table 13 – Statistical parameters of HW, LW and complete time series of water levels (VaH_A0CH - Reference_A0CH)

Stations	Complete Time Series			HW			LW		
	BIAS	RMSE	RMSE_0	BIAS	RMSE	RMSE_0	BIAS	RMSE	RMSE_0
	[m]			[m]			[m]		
Bath	0.000	0.001	0.001	0.000	0.000	0.000	0.000	0.001	0.000
Zandvliet	0.000	0.001	0.001	0.000	0.000	0.000	0.001	0.001	0.000
Prosperpolder	0.000	0.001	0.001	0.000	0.000	0.000	0.001	0.001	0.000
Liefkenshoek	0.000	0.001	0.001	0.000	0.000	0.000	0.001	0.001	0.000
Kallosluis	0.000	0.001	0.001	0.000	0.000	0.000	0.001	0.001	0.000
Antwerpen	0.000	0.001	0.001	0.000	0.001	0.000	0.001	0.001	0.000
Hemiksem	0.000	0.002	0.002	-0.002	0.002	0.000	0.003	0.003	0.000
Schelle	0.000	0.002	0.002	-0.002	0.002	0.000	0.004	0.004	0.000
Temse	0.001	0.004	0.004	-0.005	0.005	0.001	0.006	0.006	0.001
Tielrode	0.001	0.005	0.004	-0.005	0.005	0.001	0.007	0.007	0.001
StAmands	0.002	0.009	0.009	-0.008	0.008	0.002	0.014	0.014	0.002
Dendermonde	-0.004	0.008	0.007	0.003	0.004	0.002	-0.014	0.015	0.004
Schoonaarde	-0.003	0.006	0.006	-0.005	0.005	0.001	-0.006	0.007	0.004
Wetteren	-0.018	0.025	0.018	0.010	0.010	0.004	-0.033	0.034	0.006
Melle	-0.023	0.034	0.024	0.012	0.013	0.006	-0.042	0.042	0.008

Harmonic components

Figure 103 – M2 amplitude in VaH A0CH and Reference A0CH

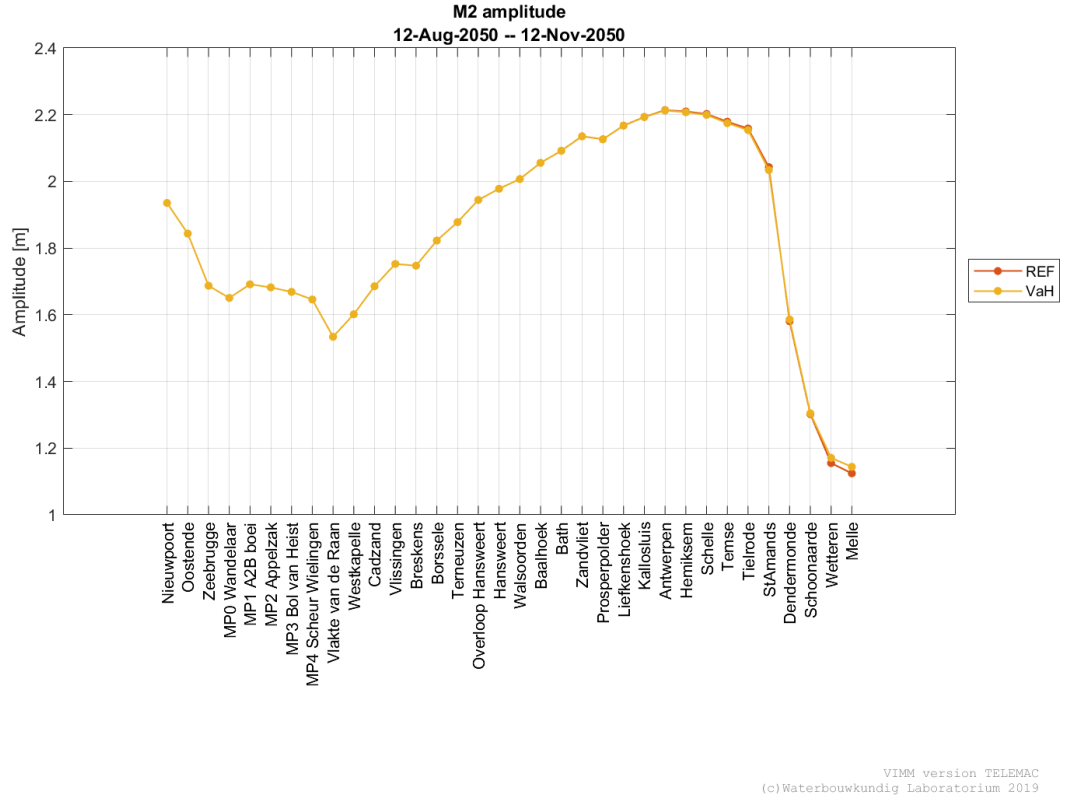

Figure 104 – M2 phase in VaH A0CH and Reference A0CH

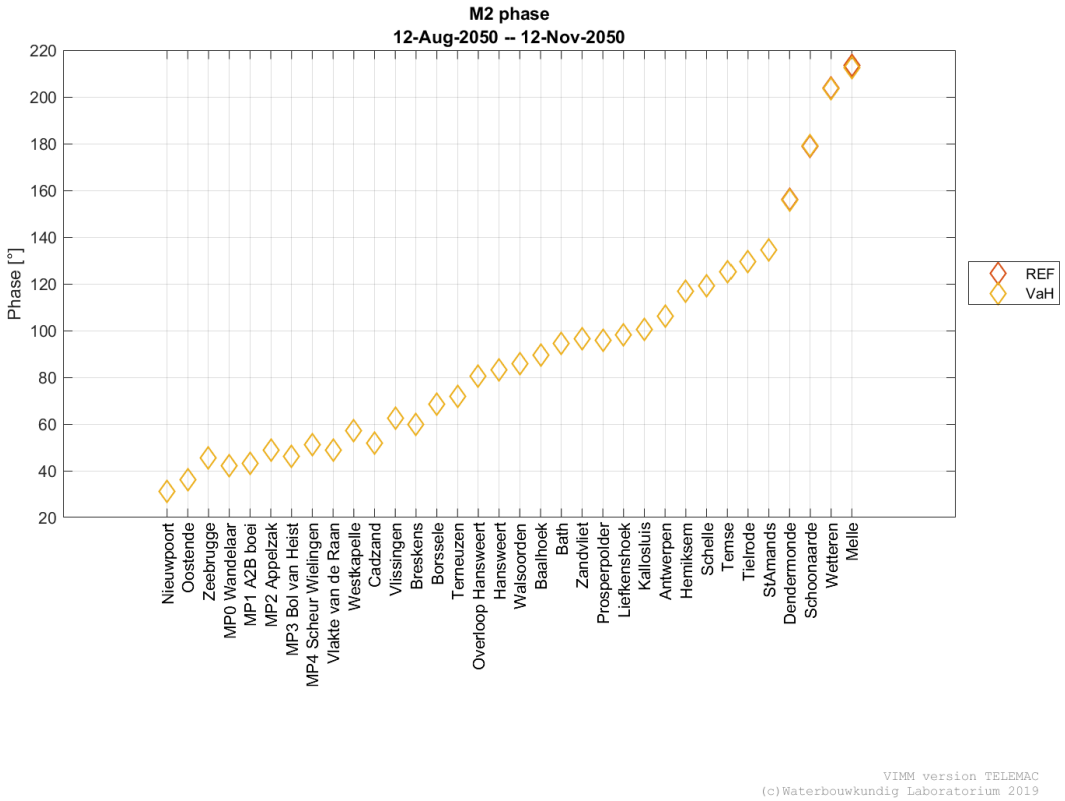

Figure 105 – M4 amplitude in VaH A0CH and Reference A0CH

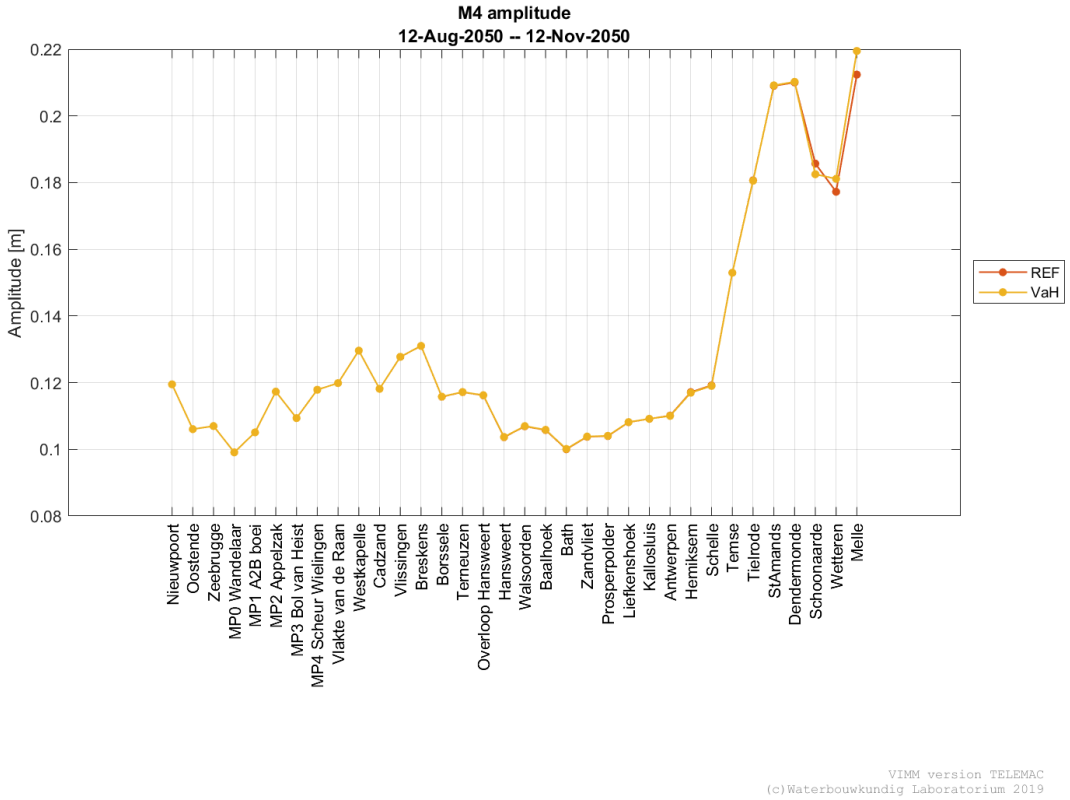

Figure 106 – M4 phase in VaH A0CH and Reference A0CH

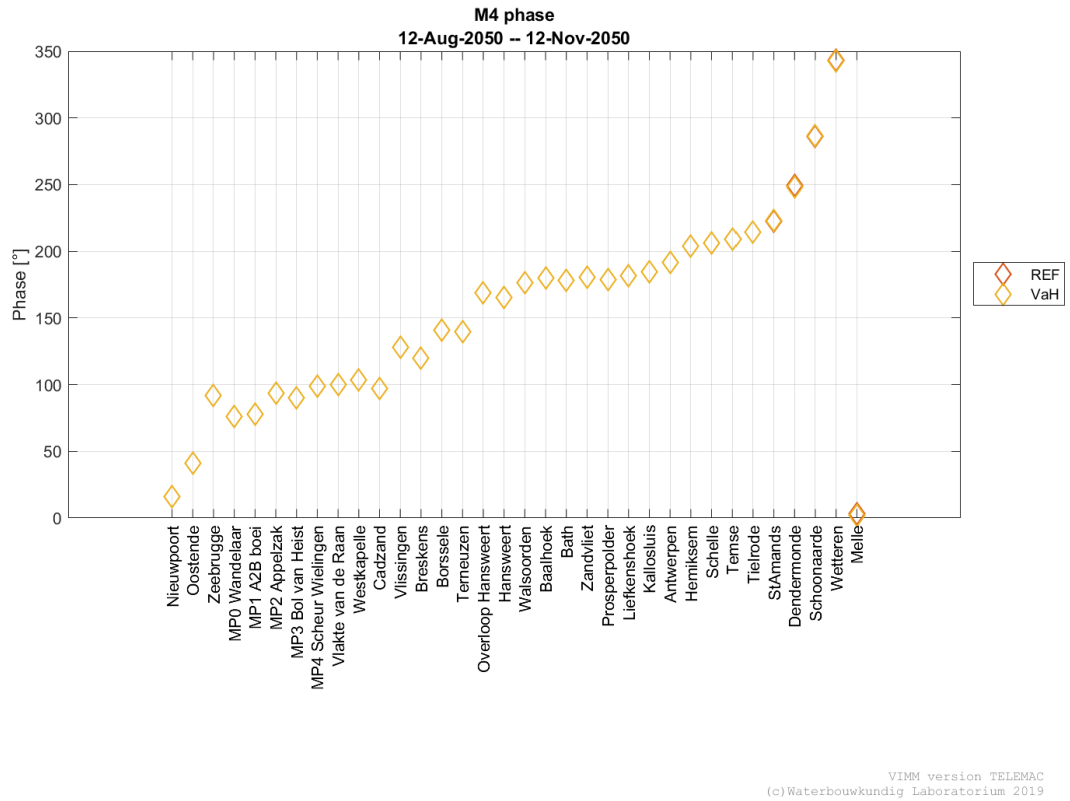

Figure 107 – S2 amplitude in VaH A0CH and Reference A0CH

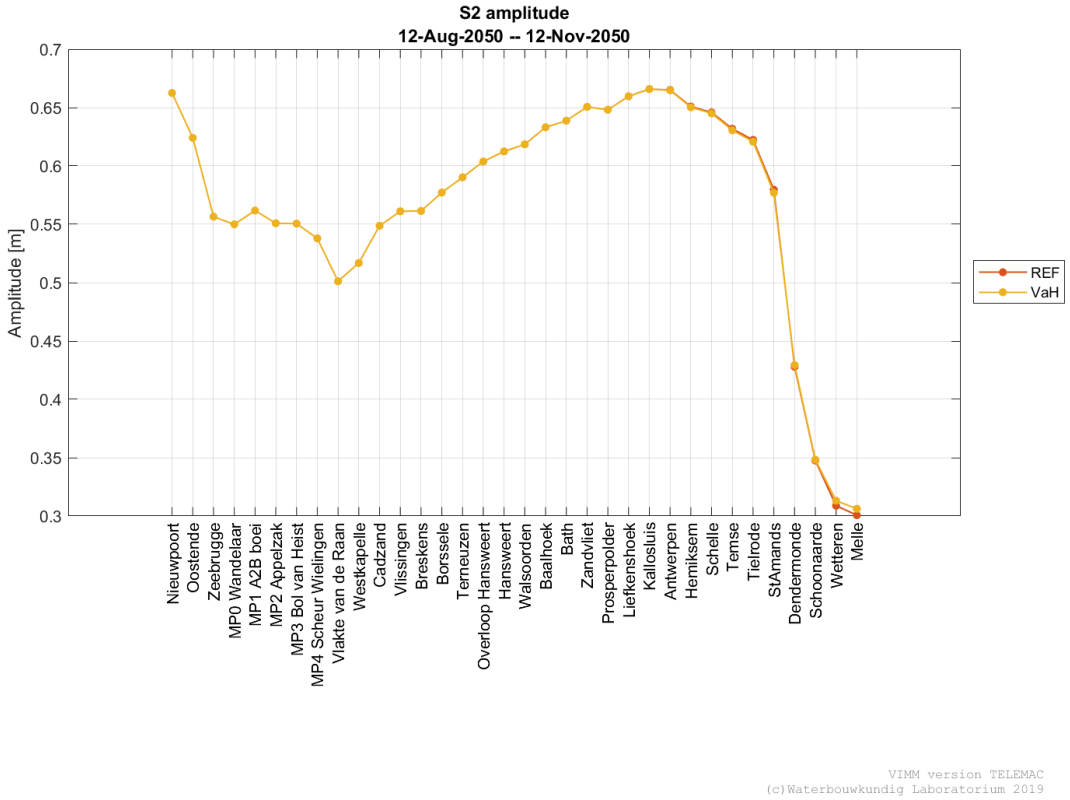

Figure 108 - S2 phase in VaH A0CH and Reference A0CH

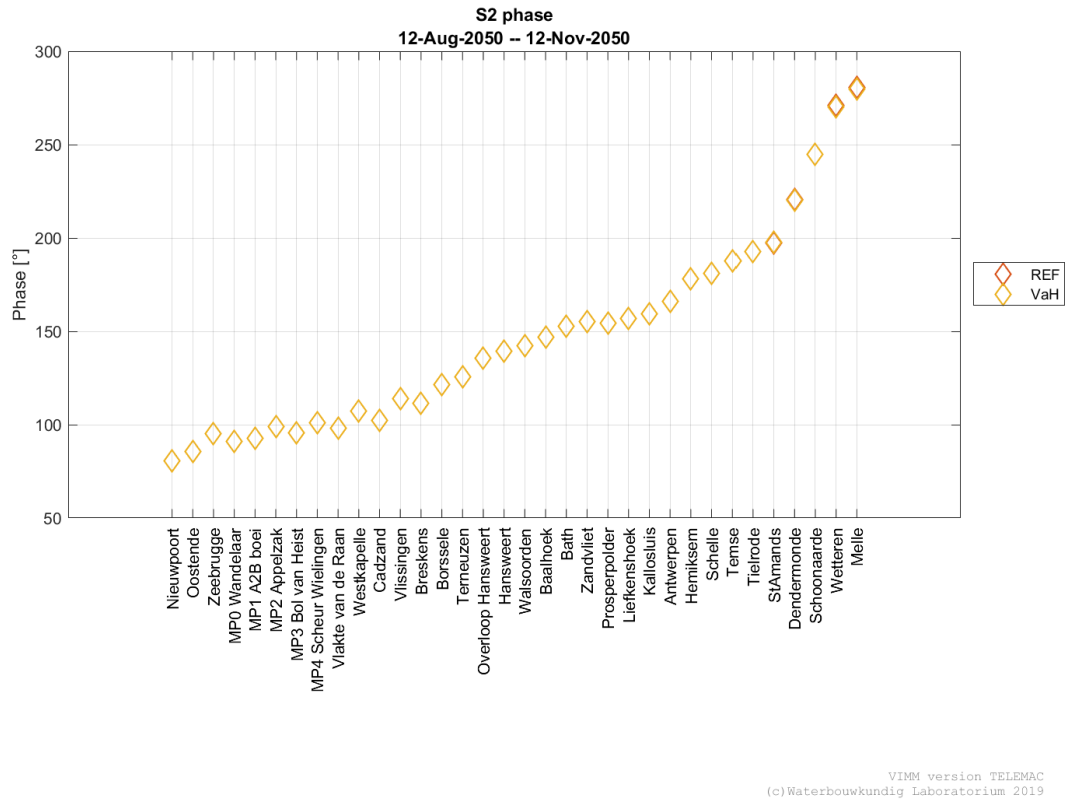

Discharges

Table 14 – Statistical parameters of complete discharge time series VaH A0CH vs Reference A0CH

Stations	VaH - Ref		
	BIAS TS	RMSE TS	RRMSE TS
	[m³/s]	[m³/s]	[-]
R3 Overloop van Valkenisse	-5.01	7.63	0.00
R3 Zimmermangeul	-0.15	0.52	0.00
R2 Nauw van Bath	-2.41	4.22	0.00
R2 Schaar van de Noord	-2.44	4.05	0.00
R1 Vaarwater boven Bath	-4.05	7.59	0.00
R1 Ballastplaat	-0.31	0.95	0.00
Liefkenshoek	-3.28	8.40	0.00
Oosterweel	-1.83	8.32	0.00
Kruibeke	-0.03	8.20	0.00
Schelle	0.36	8.27	0.00
Temse	4.02	9.33	0.01
Driegoten	5.89	9.27	0.01
Baasrode	8.21	9.31	0.02
Dendermonde	5.74	7.05	0.02
Schoonaarde	5.96	6.75	0.03
Schellebelle	5.33	6.47	0.04
Wetteren	4.63	6.05	0.04
Melle	2.63	4.71	0.05

A0CL runs

Water levels

Table 15 – Statistical parameters of HW, LW and complete time series of water levels (VaH_A0CL - Reference_A0CL)

Stations	Complete Time Series			HW			LW		
	BIAS	RMSE	RMSE_0	BIAS	RMSE	RMSE_0	BIAS	RMSE	RMSE_0
	[m]			[m]			[m]		
Bath	0.000	0.001	0.001	0.000	0.000	0.000	0.000	0.000	0.000
Zandvliet	0.000	0.001	0.001	0.000	0.000	0.000	0.000	0.001	0.000
Prosperpolder	0.000	0.001	0.001	0.000	0.000	0.000	0.000	0.000	0.000
Liefkenshoek	0.000	0.001	0.001	0.000	0.000	0.000	0.001	0.001	0.000
Kallosluis	0.000	0.001	0.001	0.000	0.000	0.000	0.001	0.001	0.000
Antwerpen	0.000	0.001	0.001	0.000	0.000	0.000	0.001	0.001	0.000
Hemiksem	0.000	0.002	0.002	-0.002	0.002	0.000	0.003	0.003	0.000
Schelle	0.000	0.002	0.002	-0.002	0.002	0.000	0.004	0.004	0.000
Temse	0.001	0.004	0.004	-0.005	0.005	0.001	0.006	0.006	0.001
Tielrode	0.001	0.005	0.004	-0.006	0.006	0.001	0.007	0.007	0.001
StAmands	0.002	0.010	0.009	-0.010	0.010	0.001	0.014	0.014	0.002
Dendermonde	-0.003	0.008	0.007	0.004	0.005	0.003	-0.012	0.013	0.004
Schoonaarde	-0.002	0.006	0.006	-0.006	0.006	0.001	-0.002	0.005	0.005
Wetteren	-0.019	0.025	0.018	0.008	0.009	0.004	-0.033	0.033	0.006
Melle	-0.025	0.034	0.023	0.011	0.013	0.006	-0.041	0.042	0.008

Harmonic components

Figure 109 – M2 amplitude in VaH A0CL and Reference A0CL

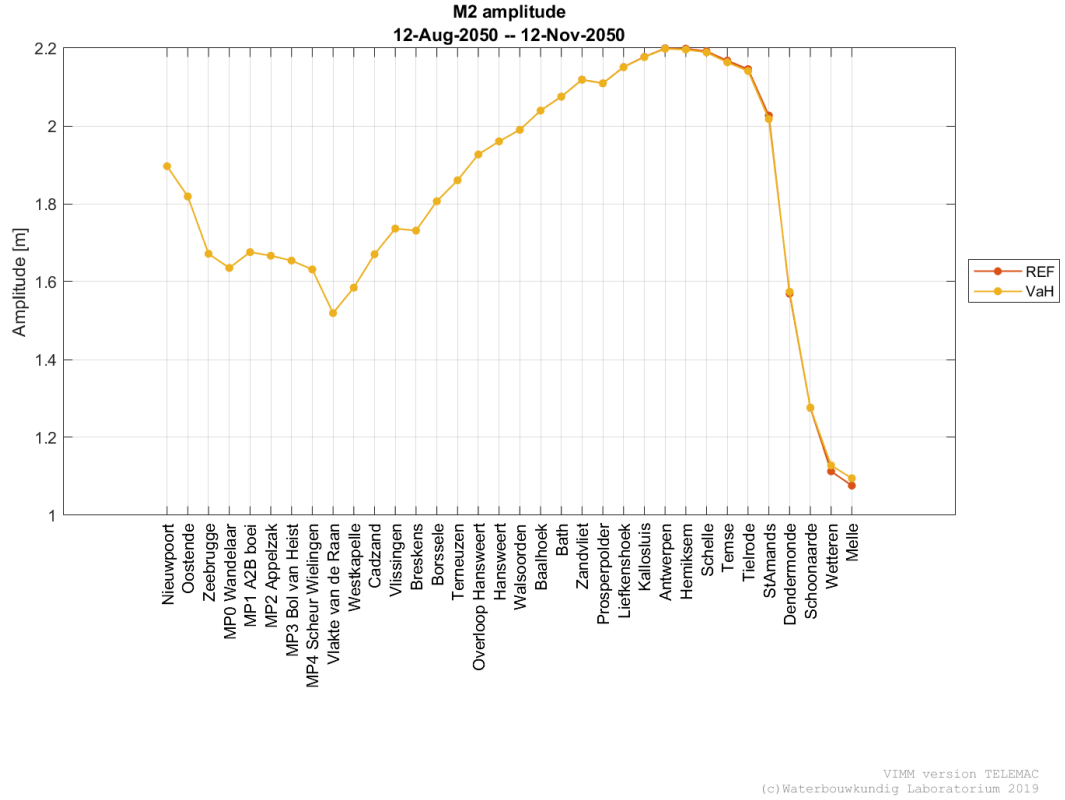

Figure 110 – M2 phase in VaH A0CL and Reference A0CL

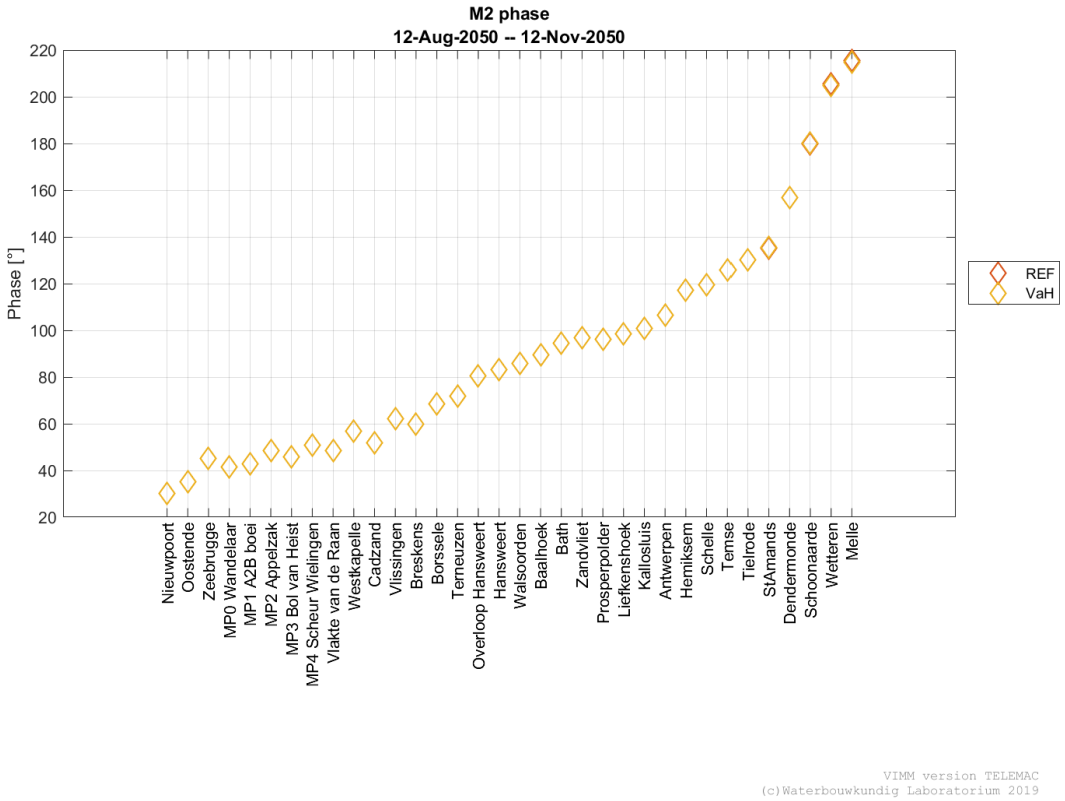

Figure 111 – M4 amplitude in VaH A0CL and Reference A0CL

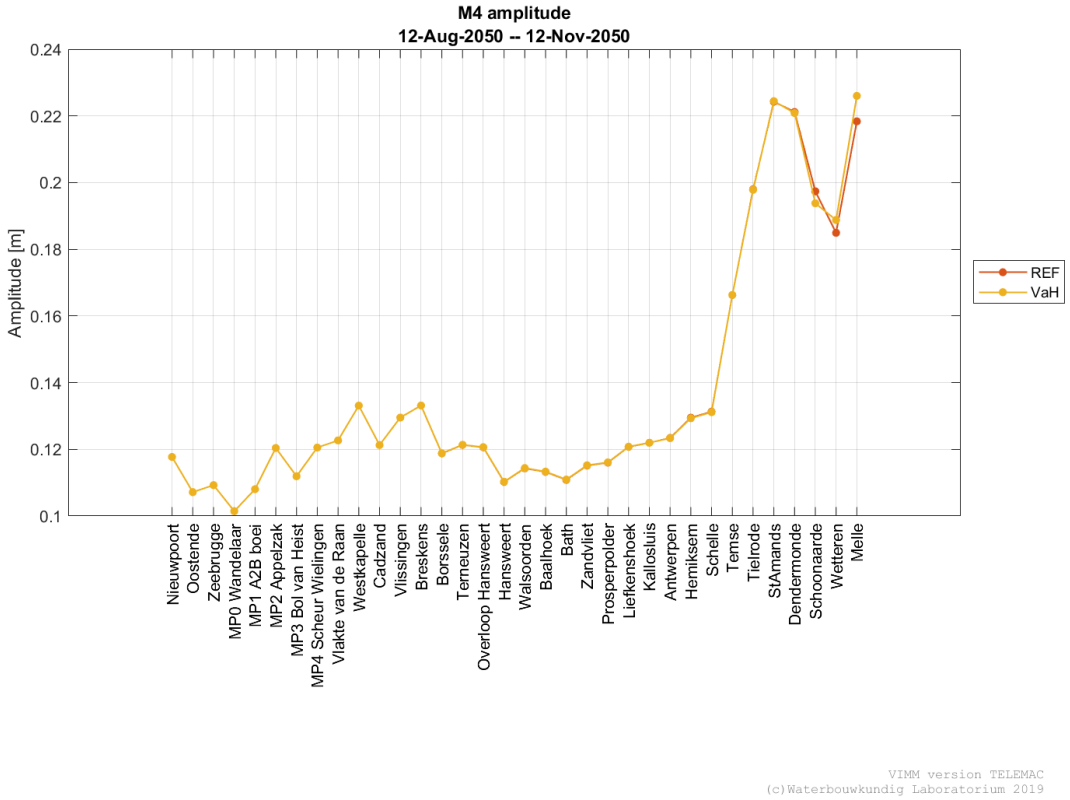

Figure 112 – M4 phase in VaH A0CL and Reference A0CL

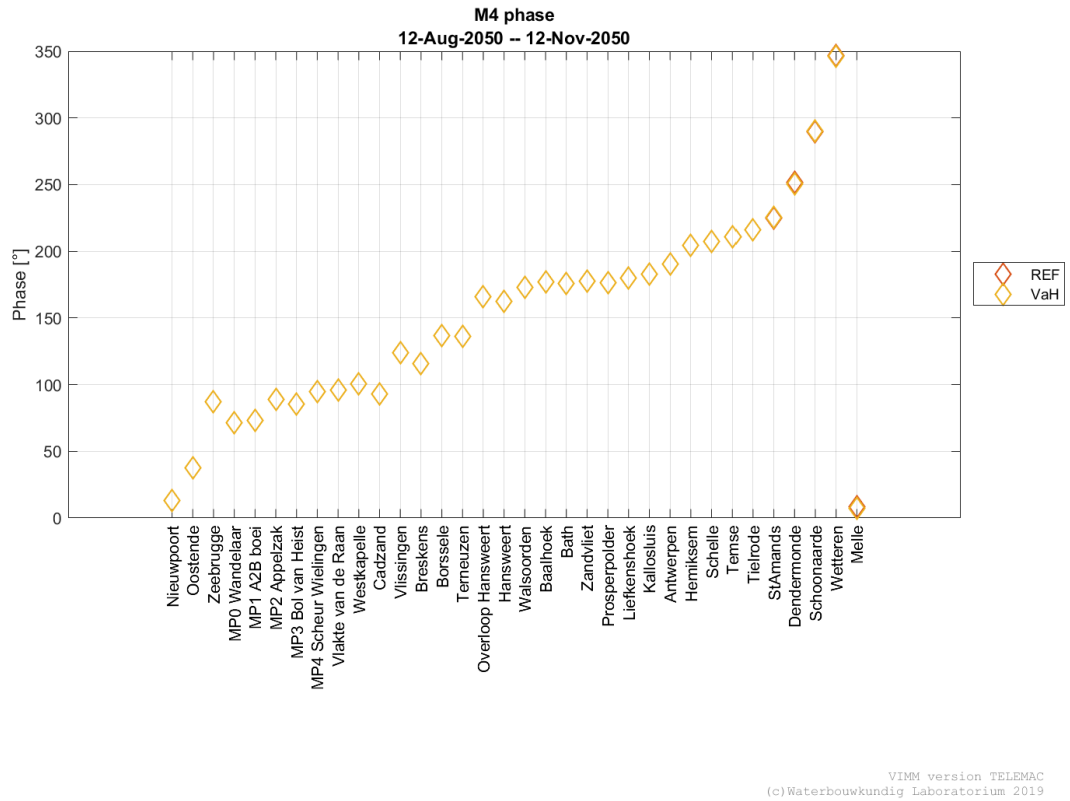

Figure 113 – S2 amplitude in VaH A0CL and Reference A0CL

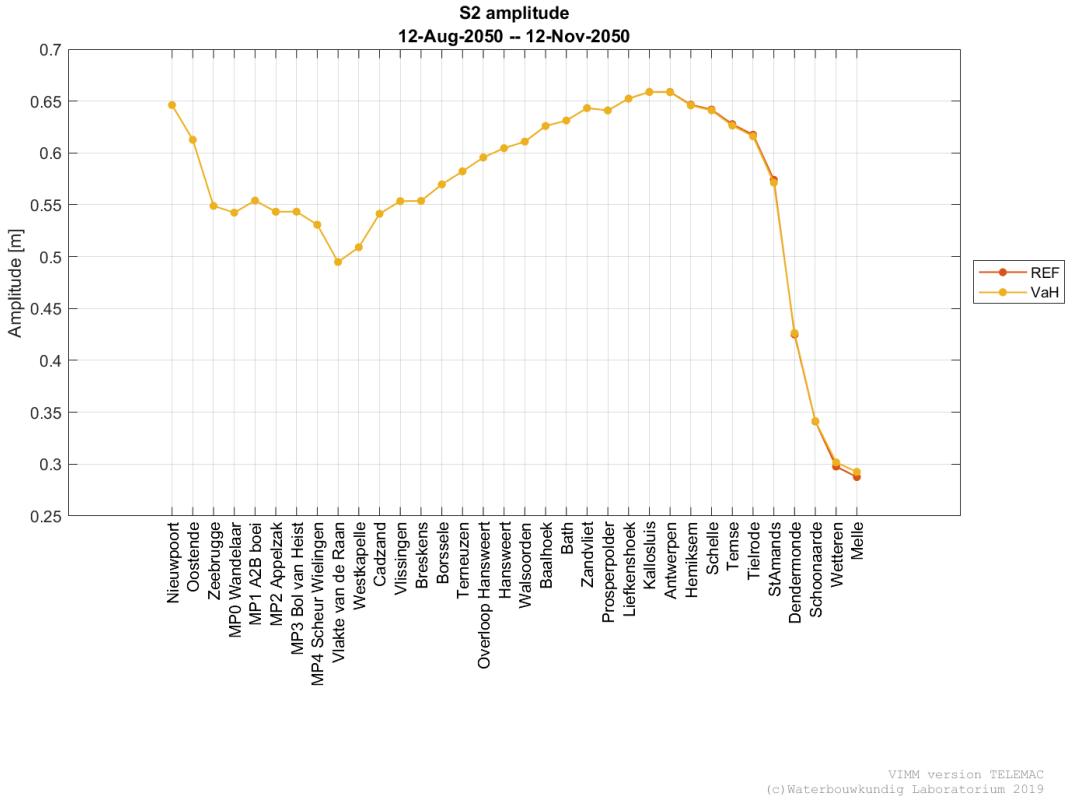

Figure 114 – S2 phase in VaH A0CL and Reference A0CL

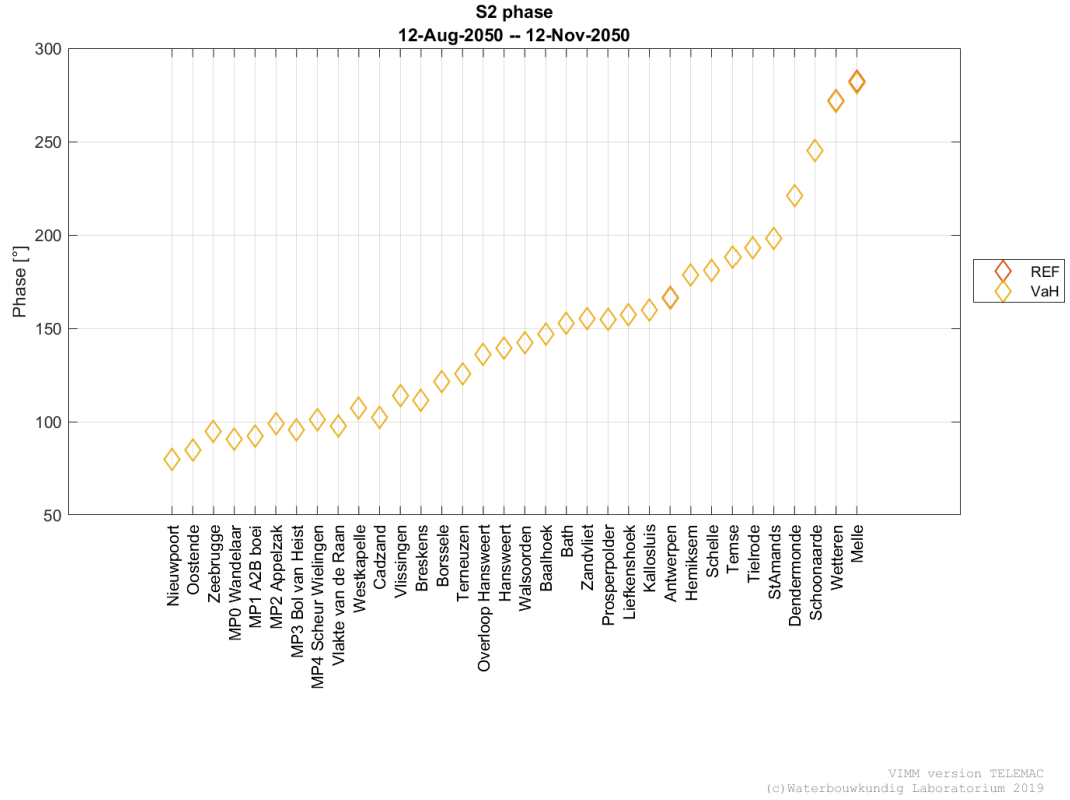

Discharges

Table 16 – Statistical parameters of complete discharge time series VaH_A0CL vs Reference_A0CL

Stations	VaH - Ref		
	BIAS TS	RMSE TS	RRMSE TS
	[m³/s]	[m³/s]	[-]
R3 Overloop van Valkenisse	-5.07	7.55	0.00
R3 Zimmermangeul	-0.14	0.47	0.00
R2 Nauw van Bath	-2.52	4.18	0.00
R2 Schaar van de Noord	-2.41	3.94	0.00
R1 Vaarwater boven Bath	-4.19	7.48	0.00
R1 Ballastplaat	-0.30	0.83	0.00
Liefkenshoek	-3.54	8.20	0.00
Oosterweel	-2.09	8.13	0.00
Kruibeke	-0.31	8.00	0.00
Schelle	0.36	8.00	0.00
Temse	3.84	9.01	0.01
Driegoten	5.56	9.04	0.01
Baasrode	8.02	8.91	0.02
Dendermonde	5.56	6.83	0.02
Schoonaarde	5.76	6.62	0.03
Schellebelle	5.11	6.32	0.04
Wetteren	4.41	5.88	0.04
Melle	2.44	4.68	0.05

AplusCH runs

Water levels

Table 17 – Statistical parameters of HW, LW and complete time series of water levels (VaH_AplusCH - Reference_AplusCH)

Stations	**Complete Time Series**			**HW**			**LW**		
	BIAS	RMSE	RMSE_0	BIAS	RMSE	RMSE_0	BIAS	RMSE	RMSE_0
	[m]			[m]			[m]		
Bath	0.000	0.001	0.001	0.000	0.000	0.000	0.000	0.001	0.000
Zandvliet	0.000	0.001	0.001	0.000	0.000	0.000	0.001	0.001	0.000
Prosperpolder	0.000	0.001	0.001	0.000	0.000	0.000	0.001	0.001	0.000
Liefkenshoek	0.000	0.001	0.001	0.000	0.000	0.000	0.001	0.001	0.001
Kallosluis	0.000	0.001	0.001	0.000	0.000	0.000	0.001	0.001	0.000
Antwerpen	0.000	0.001	0.001	-0.001	0.001	0.000	0.001	0.001	0.000
Hemiksem	0.000	0.002	0.002	-0.002	0.002	0.000	0.003	0.003	0.000
Schelle	0.000	0.002	0.002	-0.002	0.002	0.000	0.004	0.004	0.000
Temse	0.001	0.004	0.004	-0.005	0.005	0.001	0.007	0.007	0.001
Tielrode	0.001	0.005	0.005	-0.005	0.005	0.001	0.007	0.008	0.001
StAmands	0.002	0.010	0.010	-0.008	0.008	0.001	0.015	0.015	0.002
Dendermonde	-0.004	0.008	0.007	0.003	0.004	0.002	-0.015	0.016	0.004
Schoonaarde	-0.003	0.007	0.006	-0.005	0.005	0.002	-0.007	0.008	0.004
Wetteren	-0.018	0.026	0.019	0.010	0.011	0.004	-0.035	0.035	0.005
Melle	-0.024	0.034	0.025	0.013	0.014	0.006	-0.042	0.043	0.008

Harmonic components

Figure 115 – M2 amplitude in VaH AplusCH and Reference AplusCH

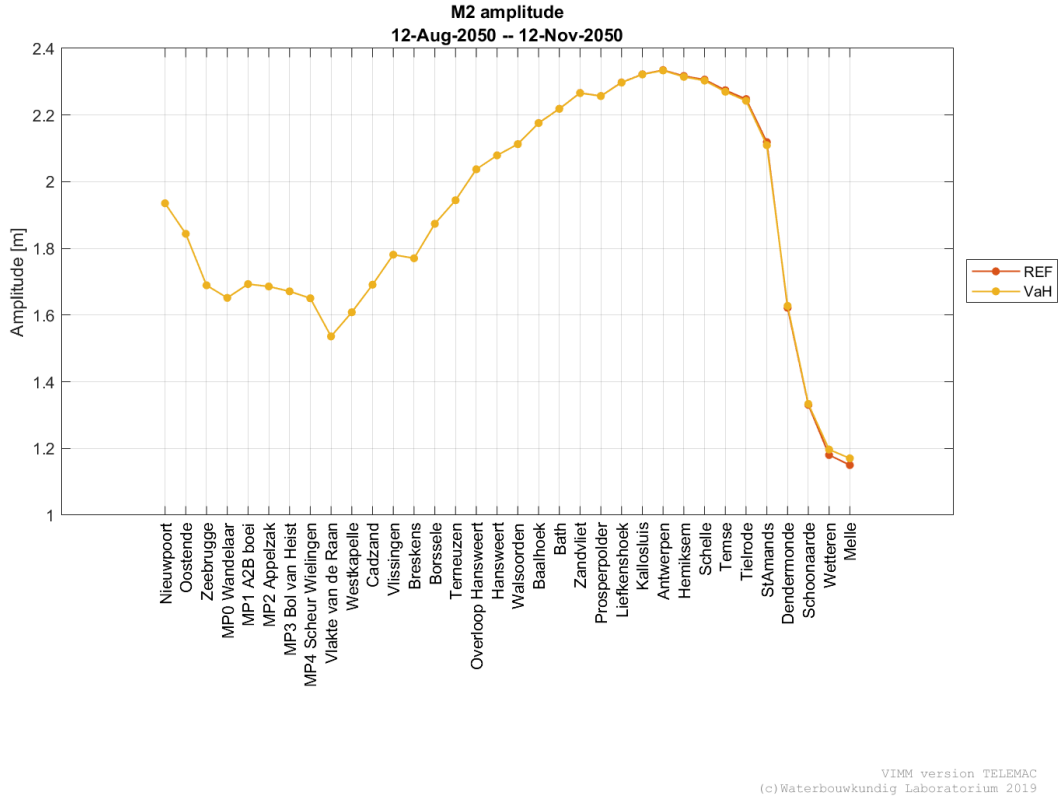

Figure 116 – M2 phase in VaH AplusCH and Reference AplusCH

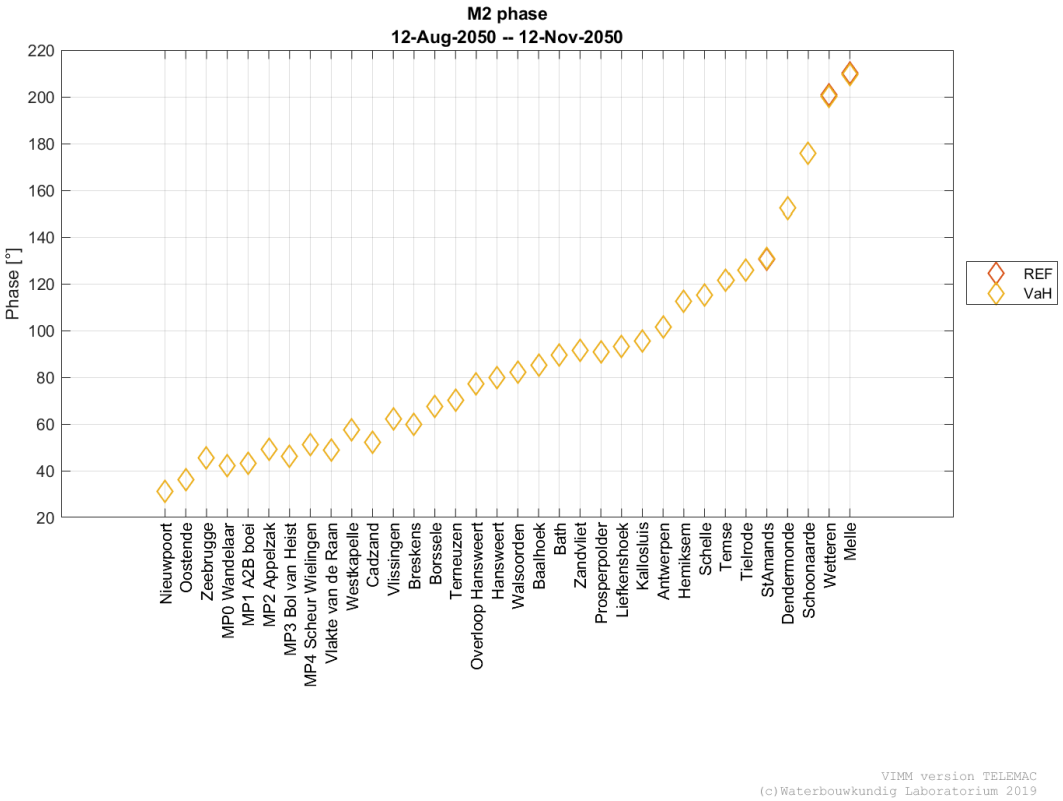

Figure 117 – M4 amplitude in VaH AplusCH and Reference AplusCH

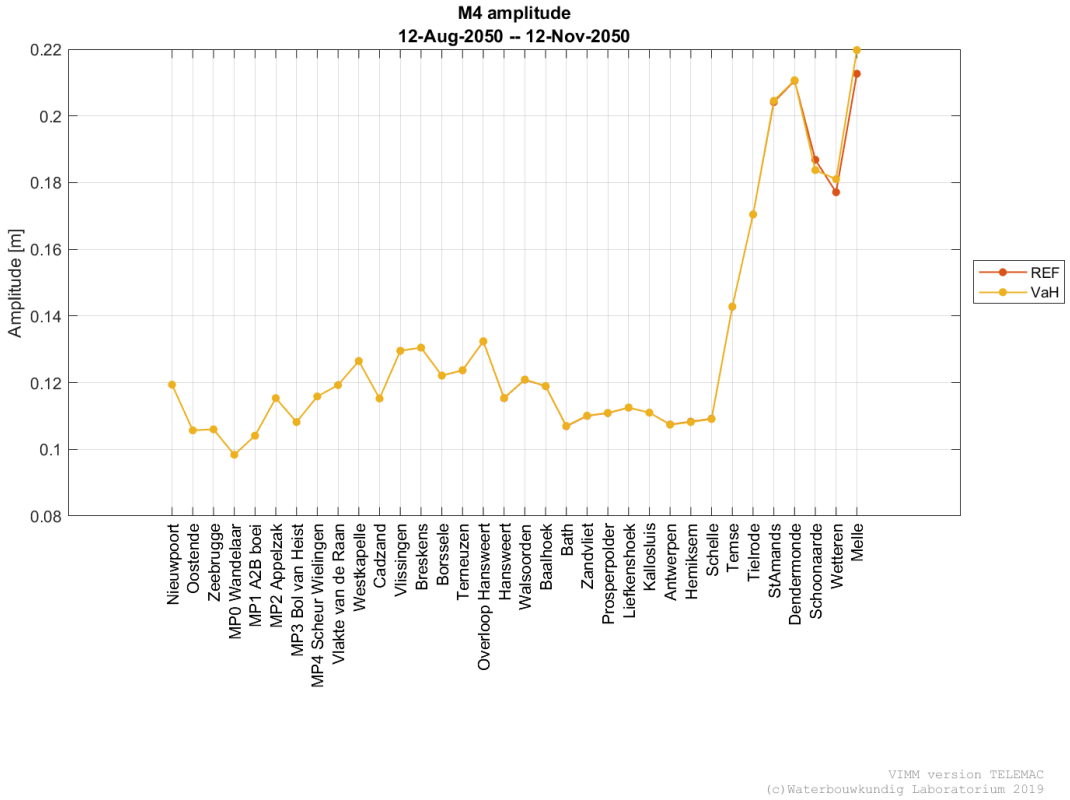

Figure 118 – M4 phase in VaH AplusCH and Reference AplusCH

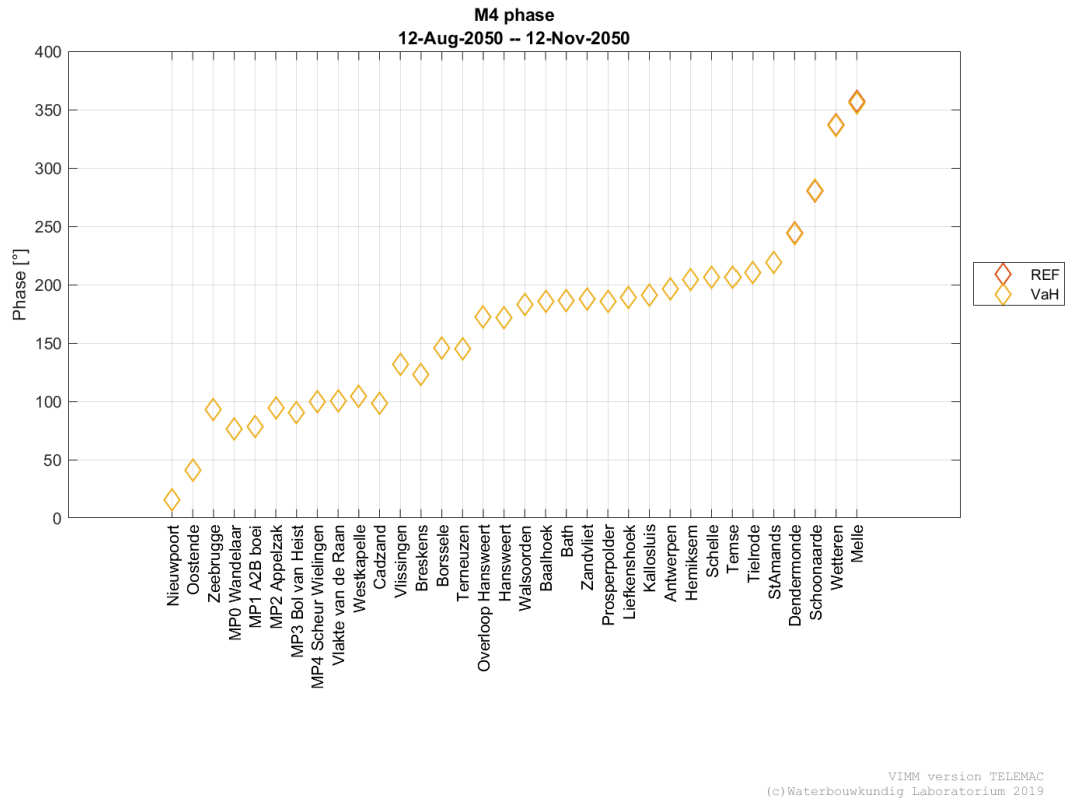

Figure 119 – S2 amplitude in VaH AplusCH and Reference AplusCH

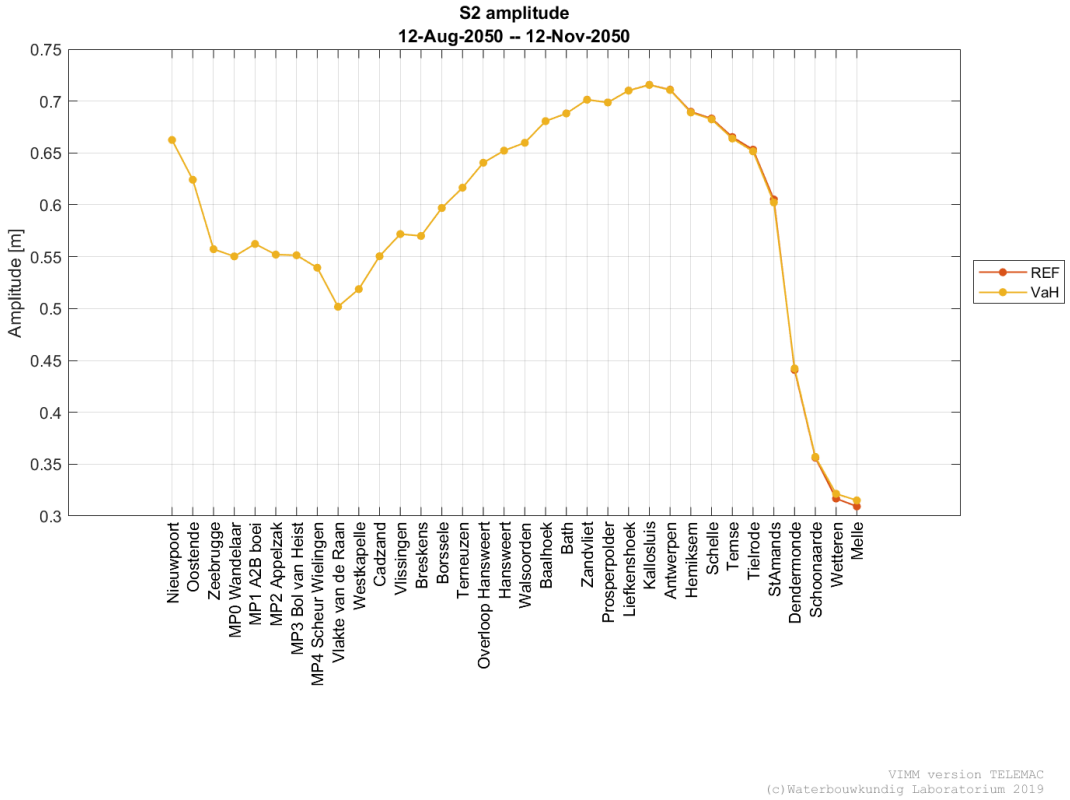

Figure 120 – S2 phase in VaH AplusCH and Reference AplusCH

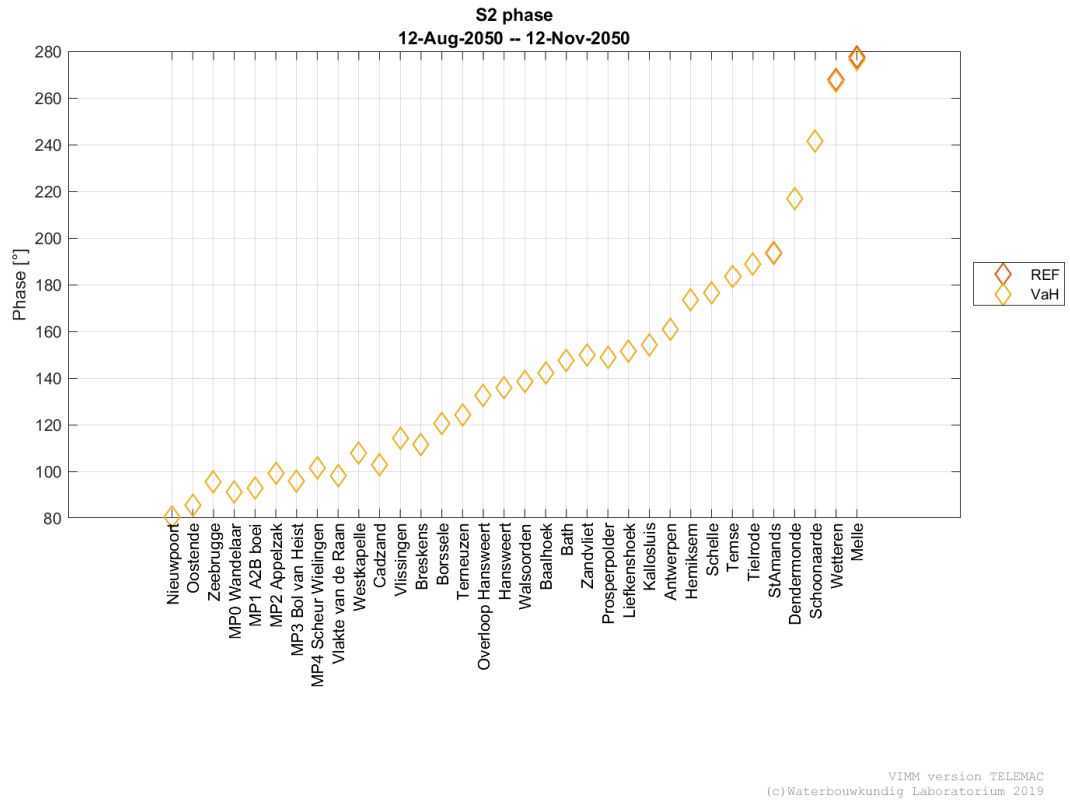

Discharges

Table 18 – Statistical parameters of complete discharge time series VaH AplusCH vs Reference AplusCH

Stations	VaH - Ref		
	BIAS TS	RMSE TS	RRMSE TS
	[m³/s]	[m³/s]	[-]
R3 Overloop van Valkenisse	-5.25	8.03	0.00
R3 Zimmermangeul	-0.17	0.58	0.00
R2 Nauw van Bath	-2.56	4.44	0.00
R2 Schaar van de Noord	-2.51	4.36	0.00
R1 Vaarwater boven Bath	-4.16	7.74	0.00
R1 Ballastplaat	-0.35	1.04	0.00
Liefkenshoek	-3.39	8.48	0.00
Oosterweel	-1.94	8.33	0.00
Kruibeke	-0.06	8.20	0.00
Schelle	0.64	8.19	0.00
Temse	4.20	9.23	0.01
Driegoten	5.91	9.39	0.01
Baasrode	8.68	9.53	0.02
Dendermonde	6.10	7.31	0.02
Schoonaarde	6.04	6.82	0.03
Schellebelle	5.09	6.52	0.04
Wetteren	4.28	5.98	0.04
Melle	2.28	4.72	0.05

AminCL runs

Water levels

Table 19 – Statistical parameters of HW, LW and complete time series of water levels (VaH_AminCL -Reference_AminCL)

Stations	Complete Time Series			HW			LW		
	BIAS	RMSE	RMSE_0	BIAS	RMSE	RMSE_0	BIAS	RMSE	RMSE_0
	[m]			[m]			[m]		
Bath	0.000	0.001	0.001	0.000	0.000	0.000	0.000	0.000	0.000
Zandvliet	0.000	0.001	0.001	0.000	0.000	0.000	0.000	0.000	0.000
Prosperpolder	0.000	0.001	0.001	0.000	0.000	0.000	0.000	0.000	0.000
Liefkenshoek	0.000	0.001	0.001	0.000	0.000	0.000	0.000	0.001	0.000
Kallosluis	0.000	0.001	0.001	0.000	0.000	0.000	0.001	0.001	0.000
Antwerpen	0.000	0.001	0.001	0.000	0.000	0.000	0.001	0.001	0.000
Hemiksem	0.000	0.002	0.002	-0.002	0.002	0.000	0.003	0.003	0.000
Schelle	0.000	0.002	0.002	-0.002	0.002	0.000	0.003	0.003	0.000
Temse	0.001	0.004	0.003	-0.004	0.004	0.001	0.005	0.005	0.001
Tielrode	0.001	0.004	0.004	-0.006	0.006	0.001	0.006	0.006	0.001
StAmands	0.002	0.009	0.009	-0.011	0.011	0.001	0.012	0.012	0.002
Dendermonde	-0.003	0.007	0.006	0.005	0.005	0.003	-0.011	0.012	0.003
Schoonaarde	-0.002	0.006	0.006	-0.007	0.007	0.001	-0.001	0.004	0.004
Wetteren	-0.018	0.025	0.017	0.007	0.008	0.005	-0.032	0.032	0.006
Melle	-0.024	0.033	0.022	0.010	0.012	0.007	-0.040	0.041	0.008

Harmonic components

Figure 121 – M2 amplitude in VaH AminCL and Reference AminCL

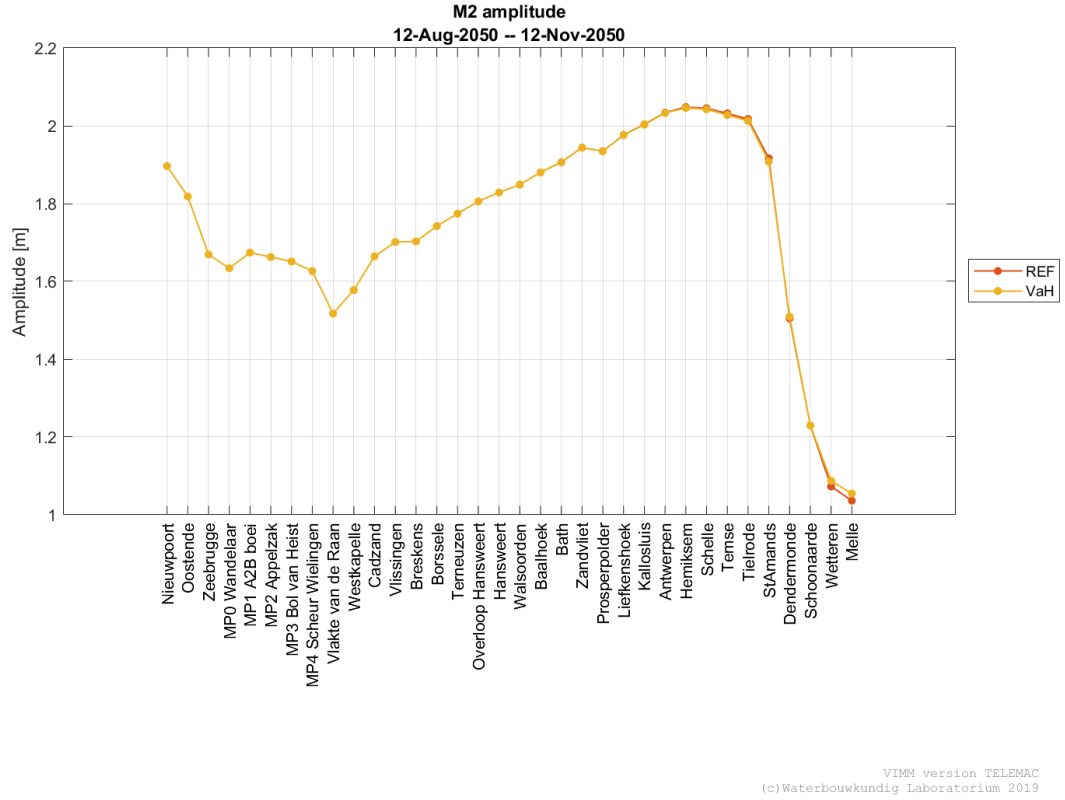

Figure 122 – M2 phase in VaH AminCL and Reference AminCL

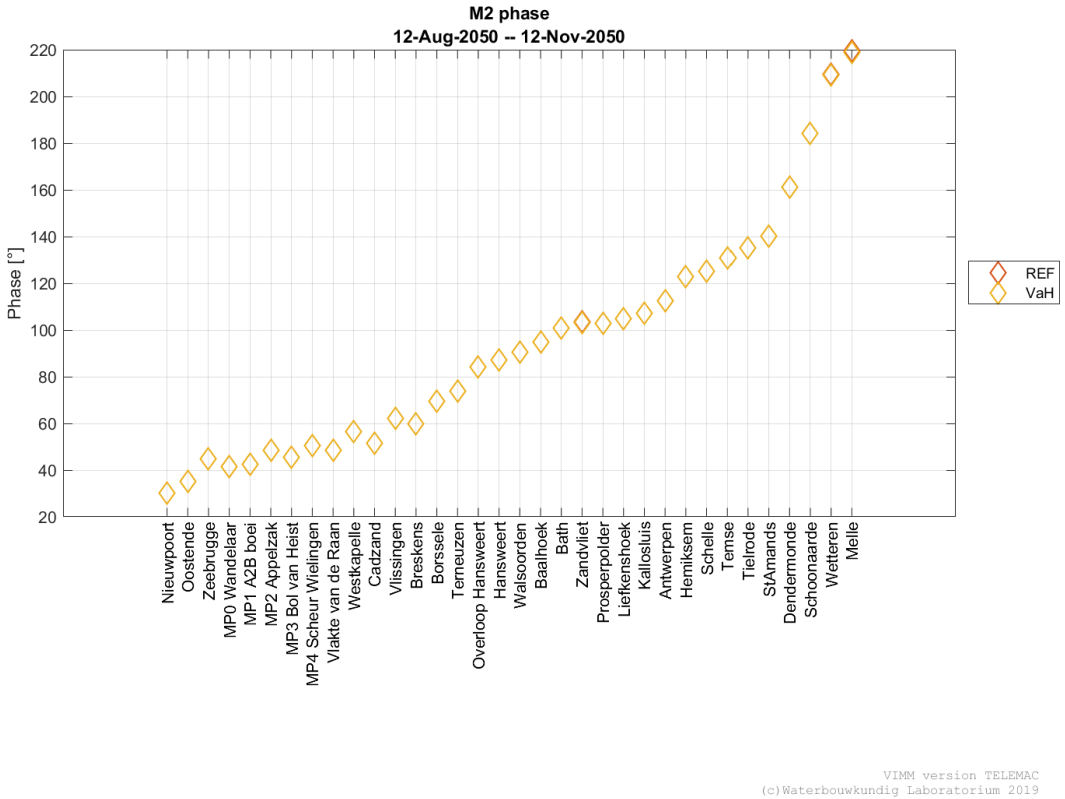

Figure 123 – M4 amplitude in VaH AminCL and Reference AminCL

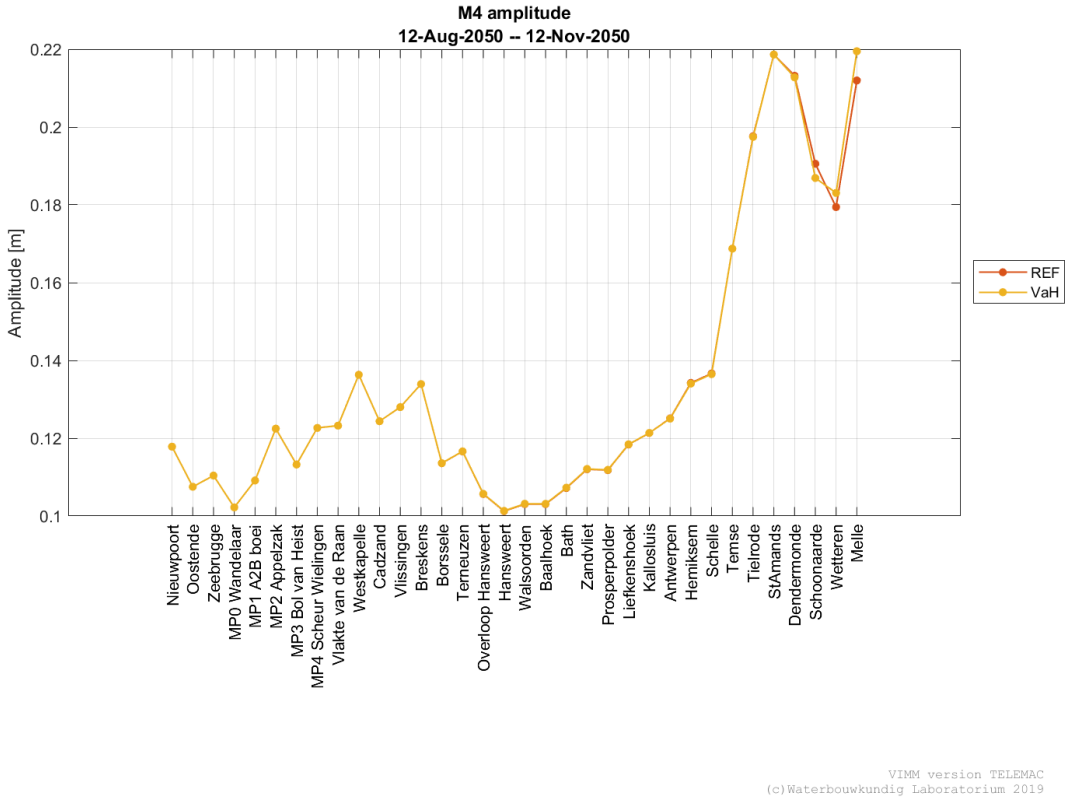

Figure 124 – M4 phase in VaH AminCL and Reference AminCL

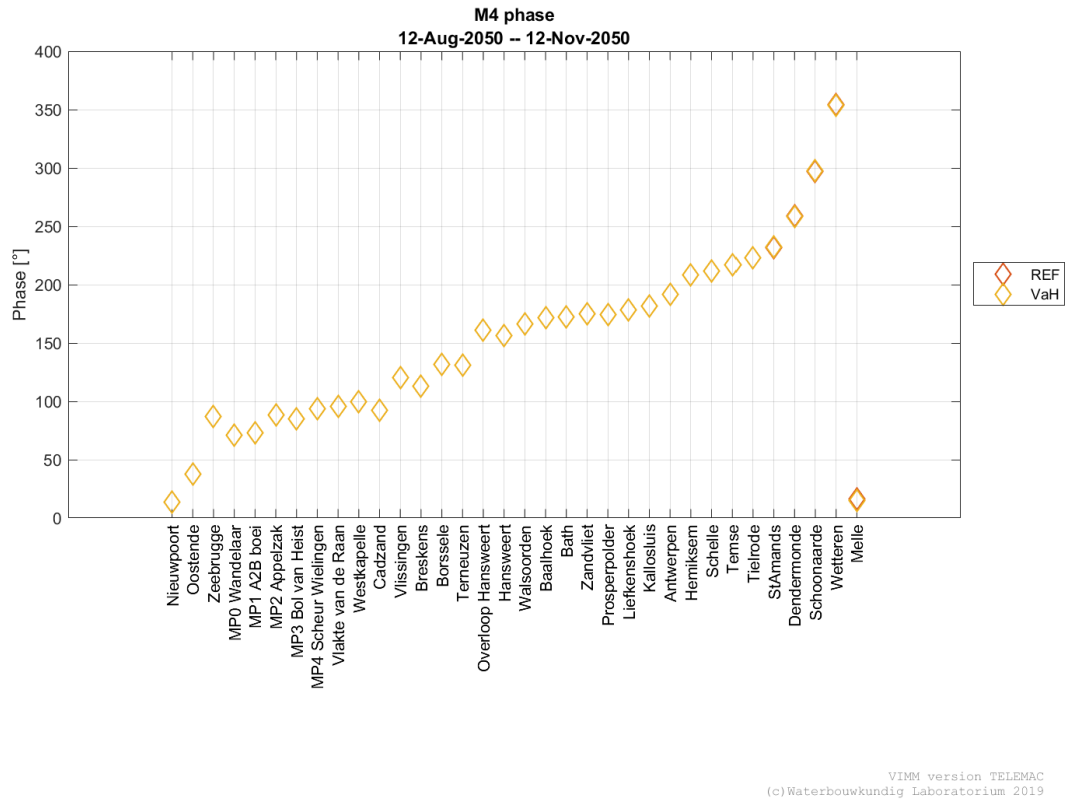

Figure 125 – S2 amplitude in VaH AminCL and Reference AminCL

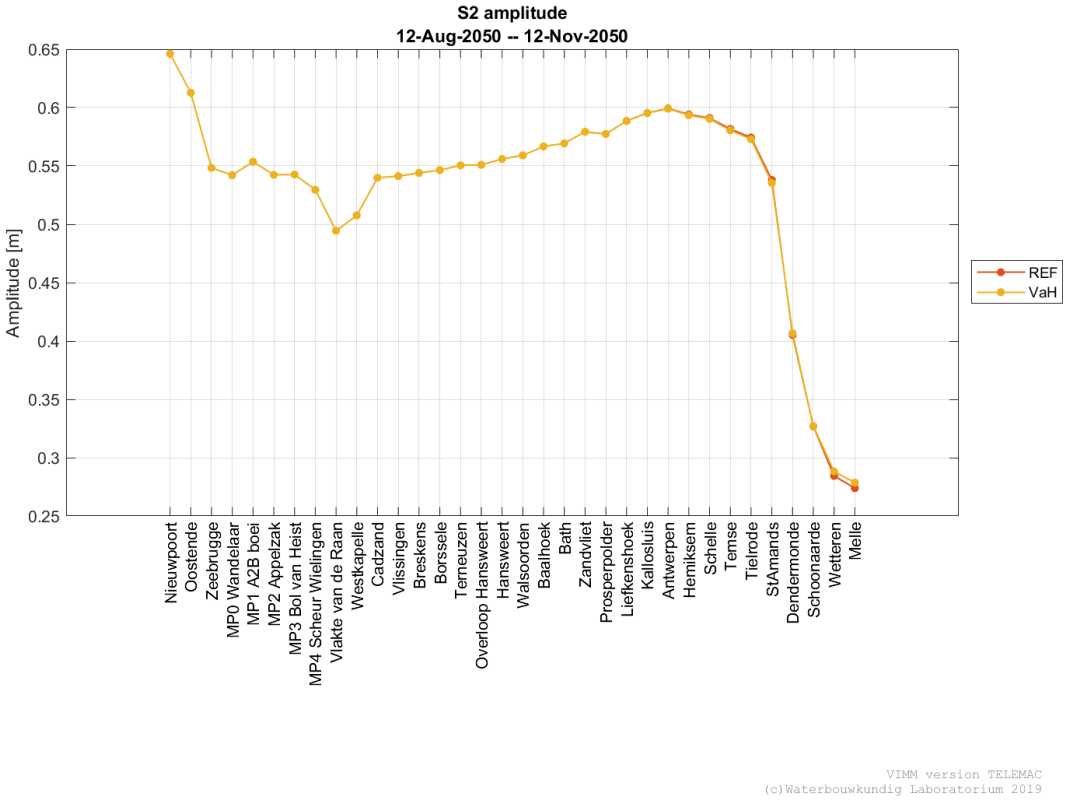

Figure 126 – S2 phase in VaH AminCL and Reference AminCL

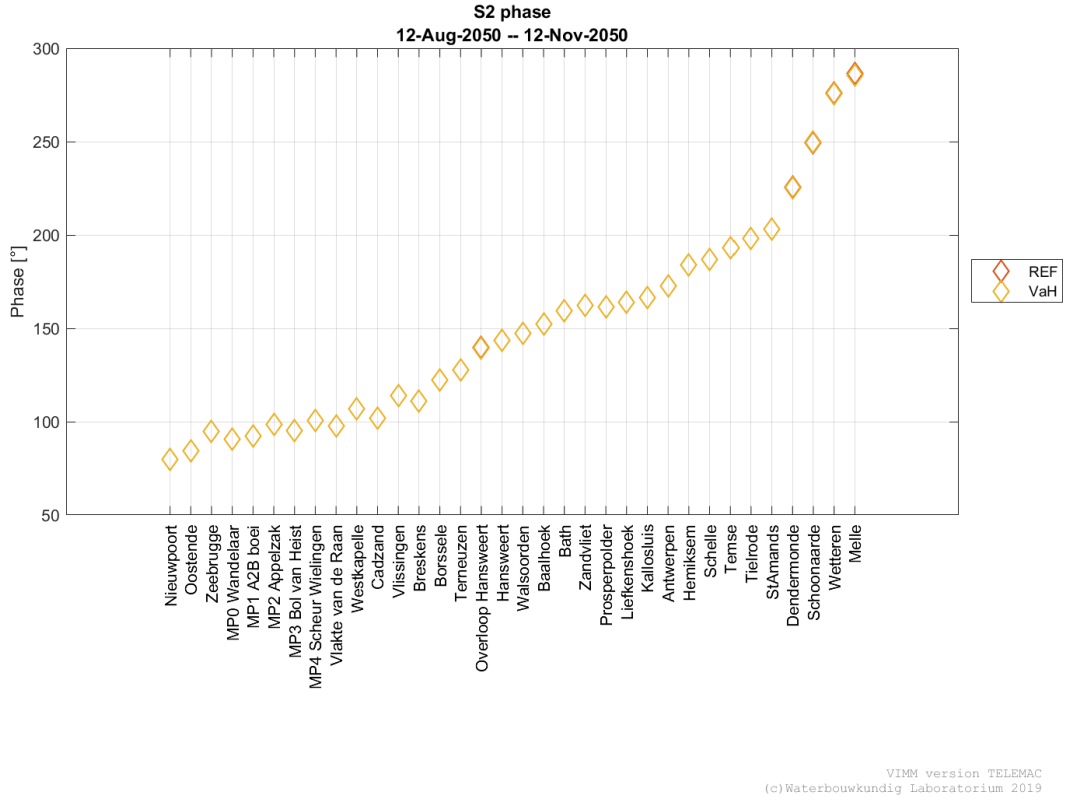

Discharges

Table 20 – Statistical parameters of complete discharge time series VaH AminCL vs Reference AminCL

Stations	**VaH - Ref**		
	BIAS TS	RMSE TS	RRMSE TS
	[m³/s]	[m³/s]	[-]
R3 Overloop van Valkenisse	-4.90	7.17	0.00
R3 Zimmermangeul	-0.16	0.40	0.00
R2 Nauw van Bath	-2.44	3.96	0.00
R2 Schaar van de Noord	-2.36	3.65	0.00
R1 Vaarwater boven Bath	-3.99	7.29	0.00
R1 Ballastplaat	-0.26	0.68	0.00
Liefkenshoek	-3.40	8.01	0.00
Oosterweel	-1.96	8.00	0.00
Kruibeke	-0.30	7.88	0.00
Schelle	0.33	7.86	0.00
Temse	3.65	8.84	0.01
Driegoten	5.30	8.80	0.01
Baasrode	7.69	8.55	0.02
Dendermonde	5.36	6.58	0.02
Schoonaarde	5.61	6.46	0.03
Schellebelle	5.02	6.14	0.04
Wetteren	4.37	5.73	0.05
Melle	2.43	4.58	0.05

Tidal asymmetry in runs with different boundary conditions

Figure 127 – Tidal asymmetry (T increase/Tdecrease water level) in VaH and Reference runs

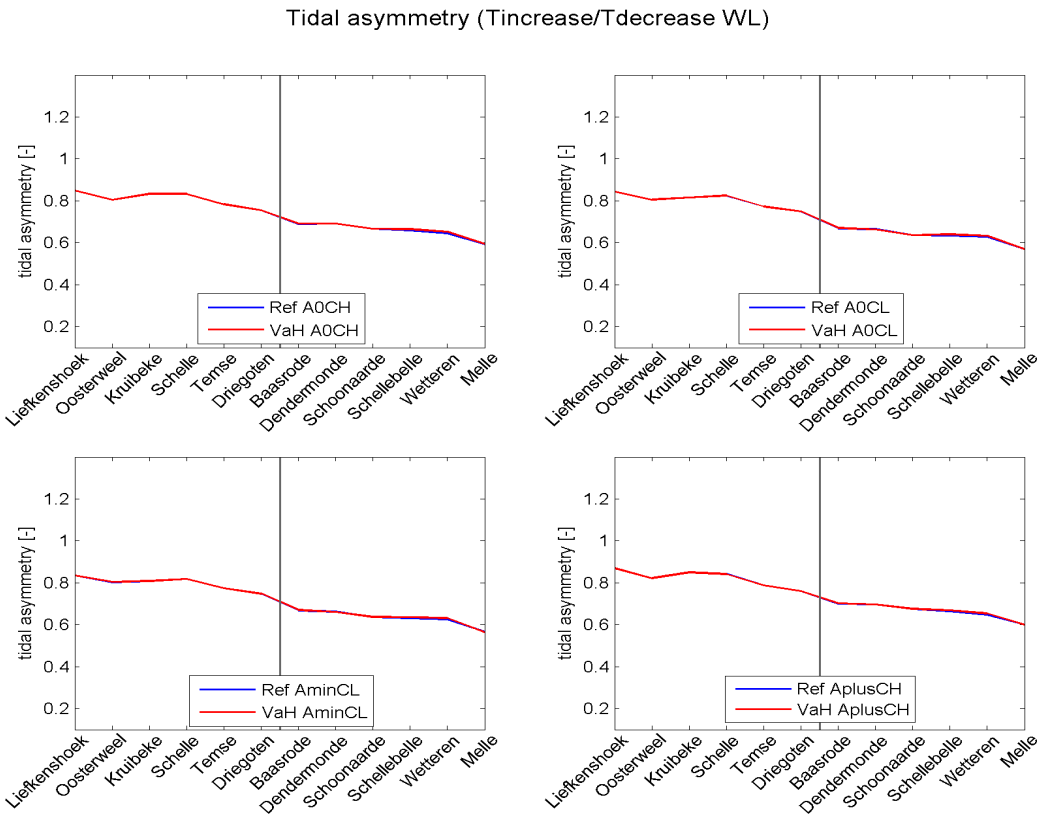

Figure 128 – Tidal asymmetry (T flood/T ebb) in VaH and Reference runs

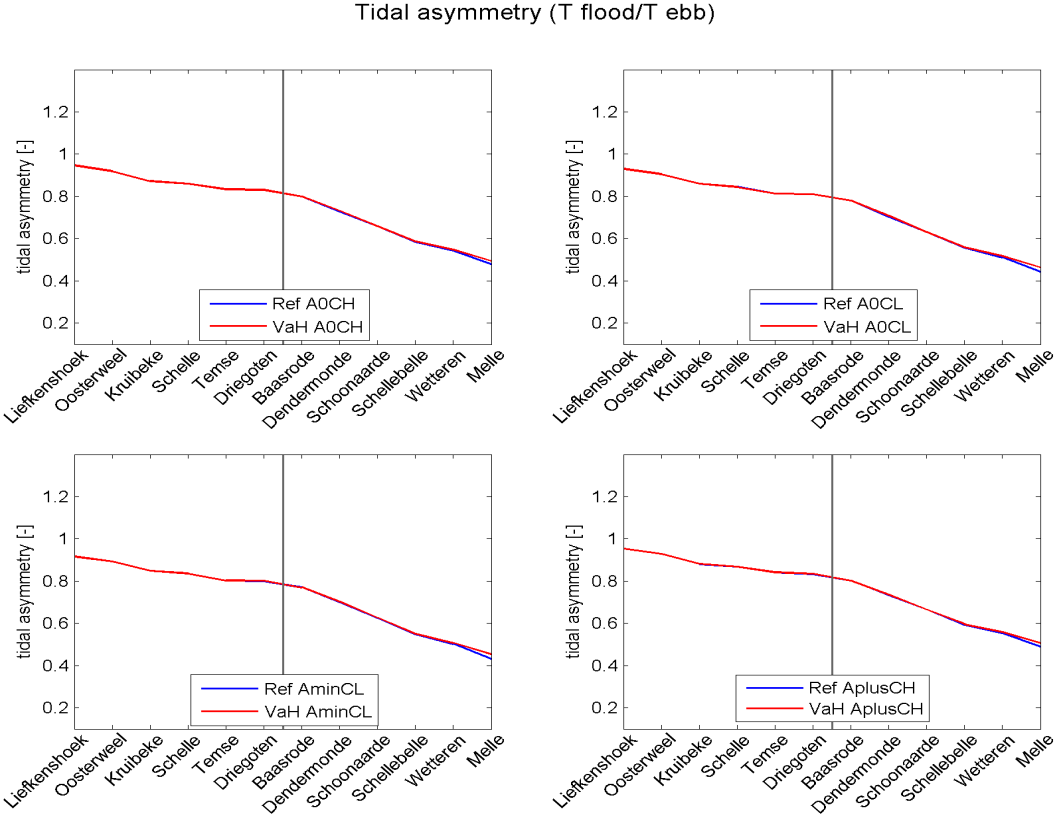

Figure 129 – Tidal asymmetry (V max flood/Vmax ebb) in VaH and Reference runs

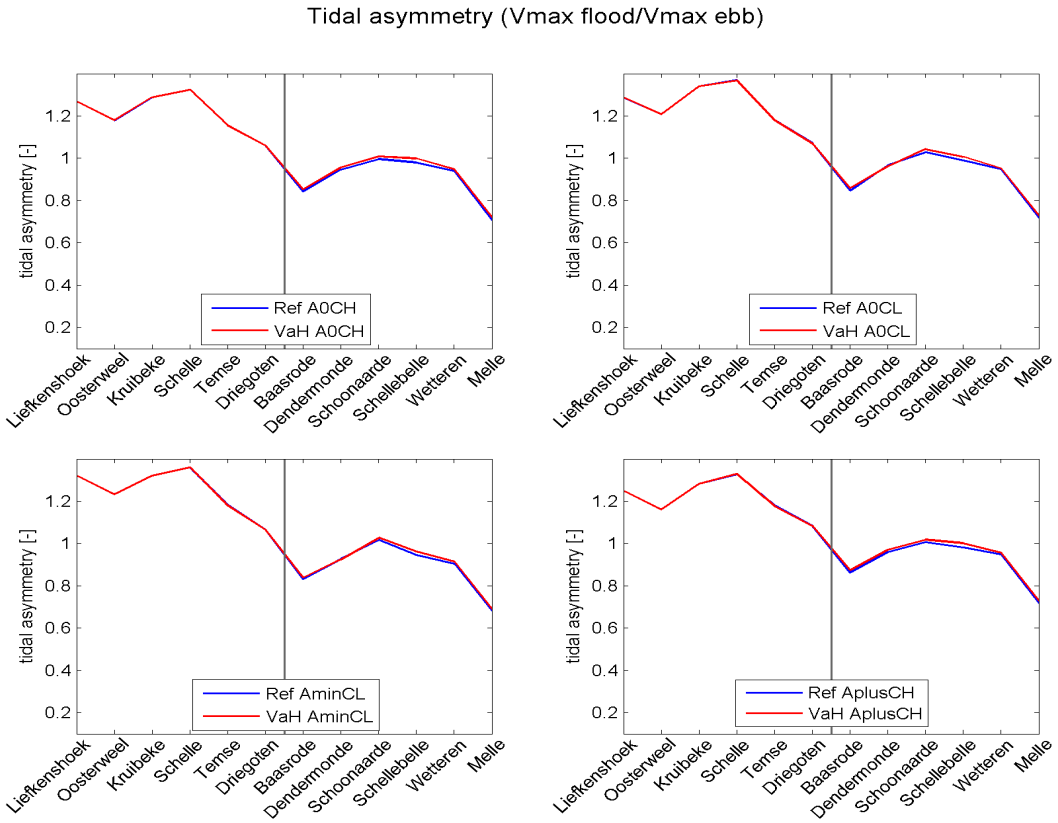

Figure 130 – Tidal asymmetry (based on V^3) in VaH and Reference runs

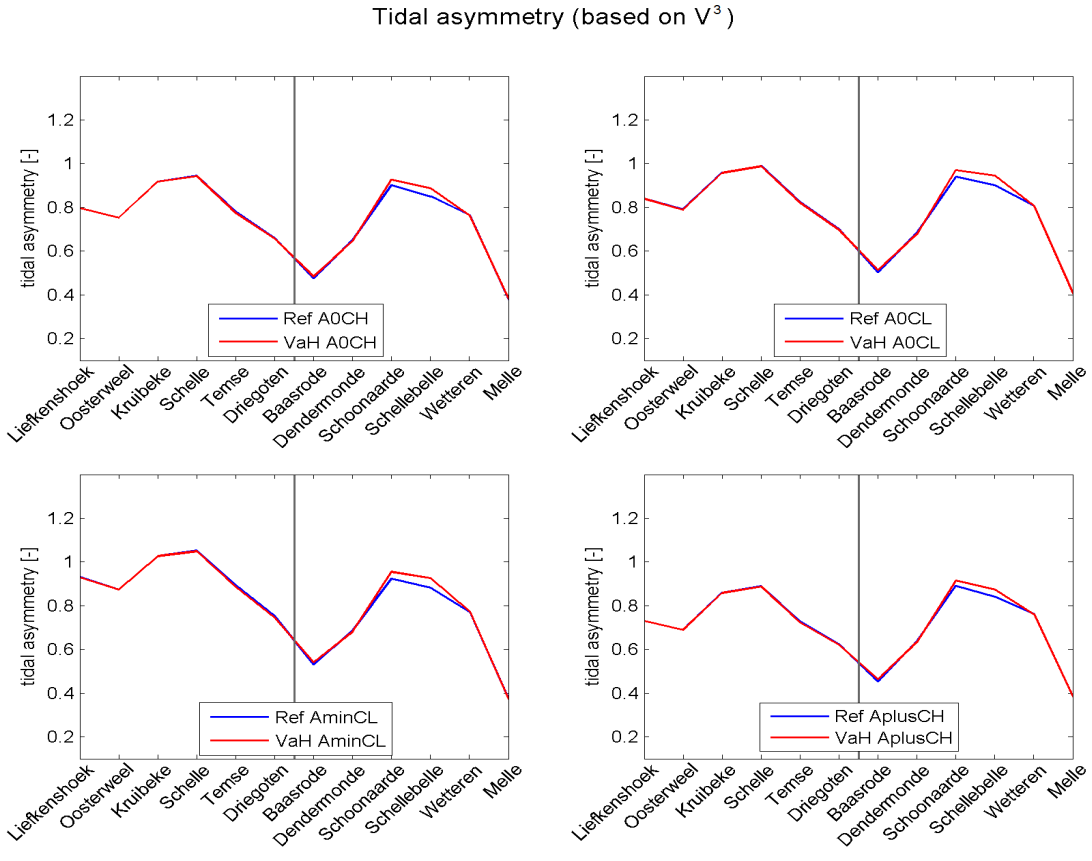

Figure 131 – Tidal asymmetry (based on V^4) in VaH and Reference runs

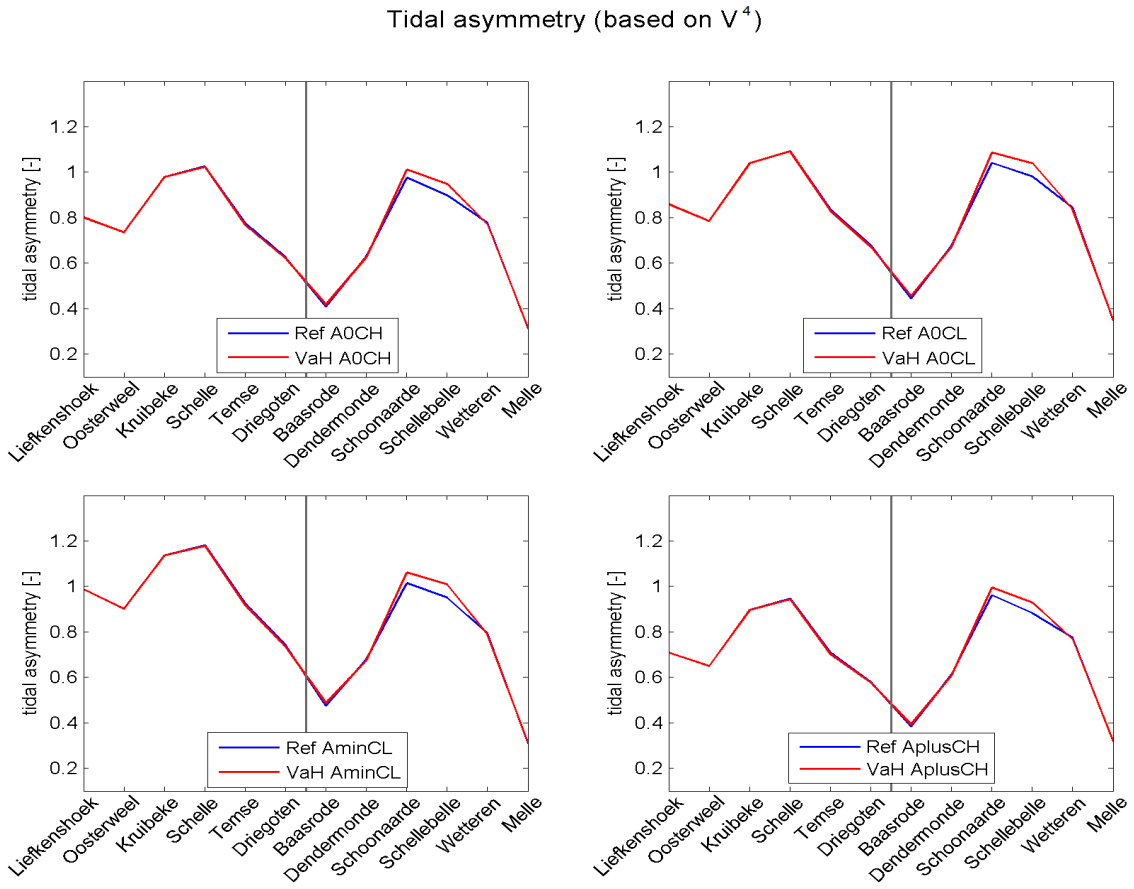

Appendix 4: Effect of Chafing

A0CH runs

Water levels

Table 21 – Statistical parameters of HW, LW and complete time series of water levels (Chafing_A0CH- Reference_A0CH)

Stations	Complete Time Series			HW			LW		
	BIAS	RMSE	RMSE_0	BIAS	RMSE	RMSE_0	BIAS	RMSE	RMSE_0
	[m]			[m]			[m]		
Bath	0.000	0.000	0.000	0.000	0.000	0.000	0.000	0.001	0.000
Zandvliet	0.000	0.000	0.000	0.000	0.000	0.000	0.001	0.001	0.000
Prosperpolder	0.000	0.000	0.000	0.000	0.000	0.000	0.000	0.001	0.000
Liefkenshoek	0.000	0.001	0.001	0.000	0.000	0.000	0.001	0.001	0.000
Kallosluis	0.000	0.001	0.001	0.000	0.000	0.000	0.001	0.001	0.000
Antwerpen	0.000	0.001	0.001	-0.001	0.001	0.000	0.001	0.001	0.000
Hemiksem	0.000	0.002	0.002	-0.002	0.002	0.000	0.003	0.003	0.000
Schelle	0.000	0.002	0.002	-0.002	0.002	0.000	0.003	0.003	0.000
Temse	0.001	0.004	0.004	-0.004	0.004	0.001	0.005	0.005	0.001
Tielrode	0.001	0.004	0.004	-0.005	0.005	0.001	0.006	0.006	0.001
StAmands	0.001	0.009	0.009	-0.007	0.007	0.001	0.011	0.011	0.002
Dendermonde	-0.005	0.012	0.011	0.009	0.009	0.002	-0.024	0.024	0.003
Schoonaarde	-0.005	0.013	0.012	0.009	0.009	0.002	-0.020	0.021	0.004
Wetteren	-0.005	0.011	0.009	0.007	0.007	0.002	-0.008	0.009	0.003
Melle	-0.003	0.010	0.010	0.009	0.009	0.002	0.002	0.004	0.004

Harmonic components

Figure 132 – M2 amplitude in Chafing A0CH and Reference A0CH

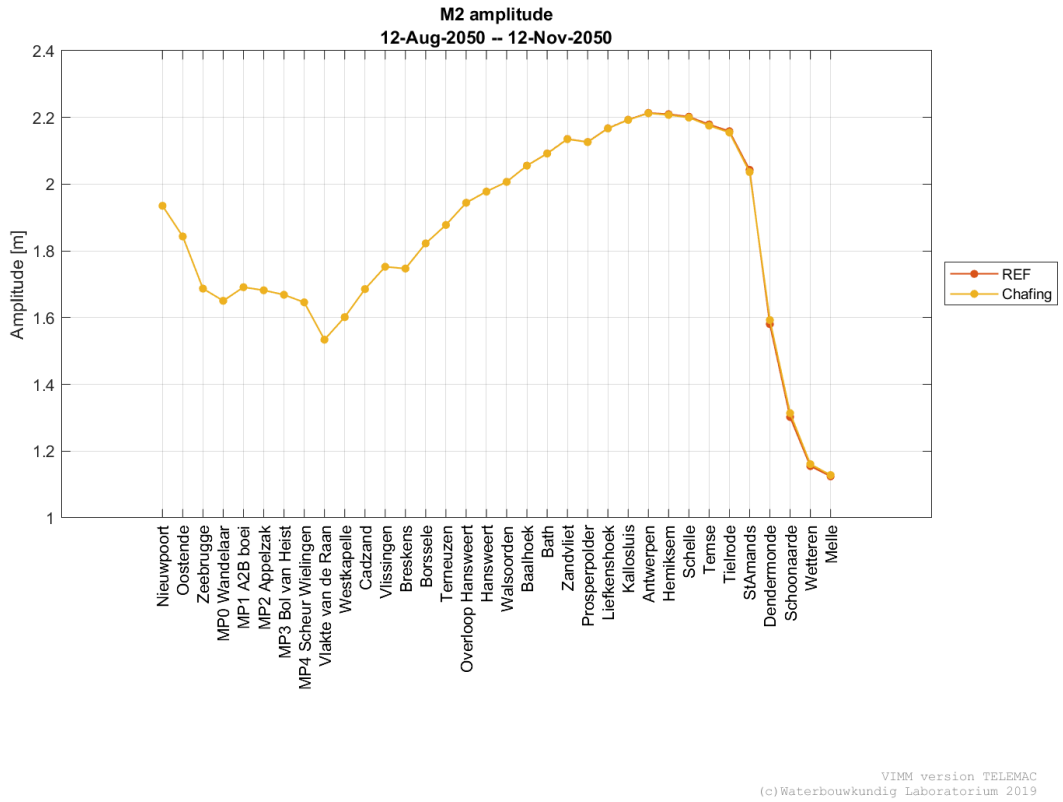

Figure 133 - M2 phase in Chafing A0CH and Reference A0CH

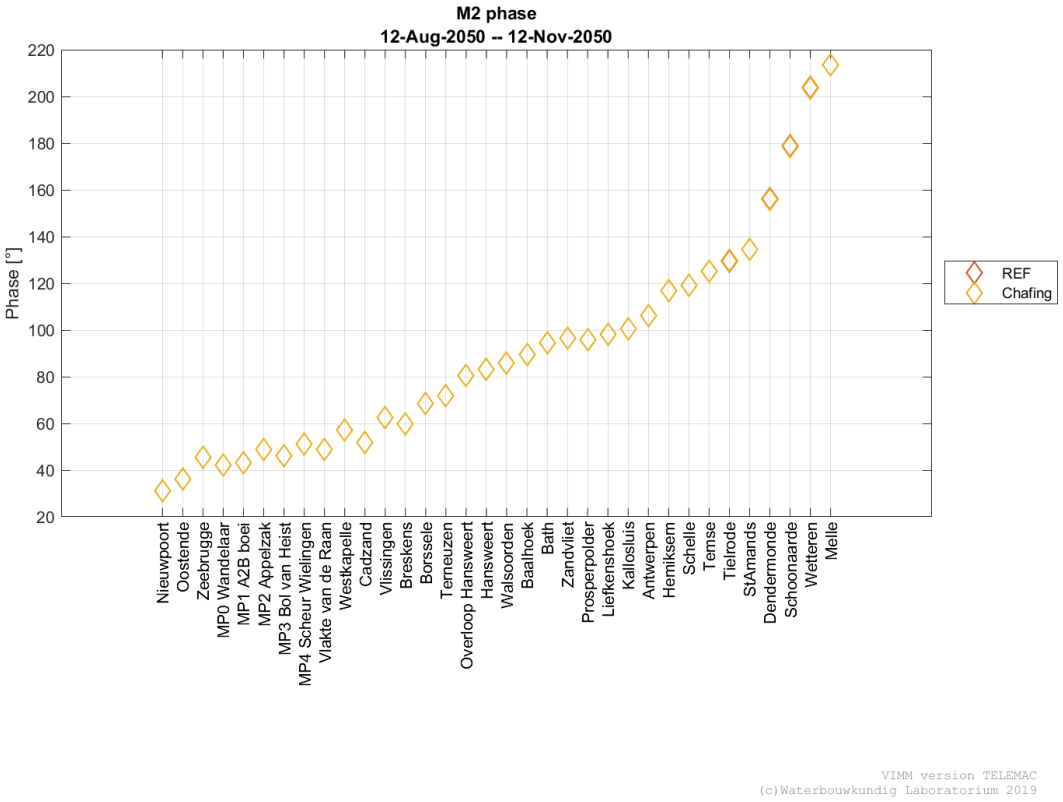

Figure 134 – M4 amplitude in Chafing A0CH and Reference A0CH

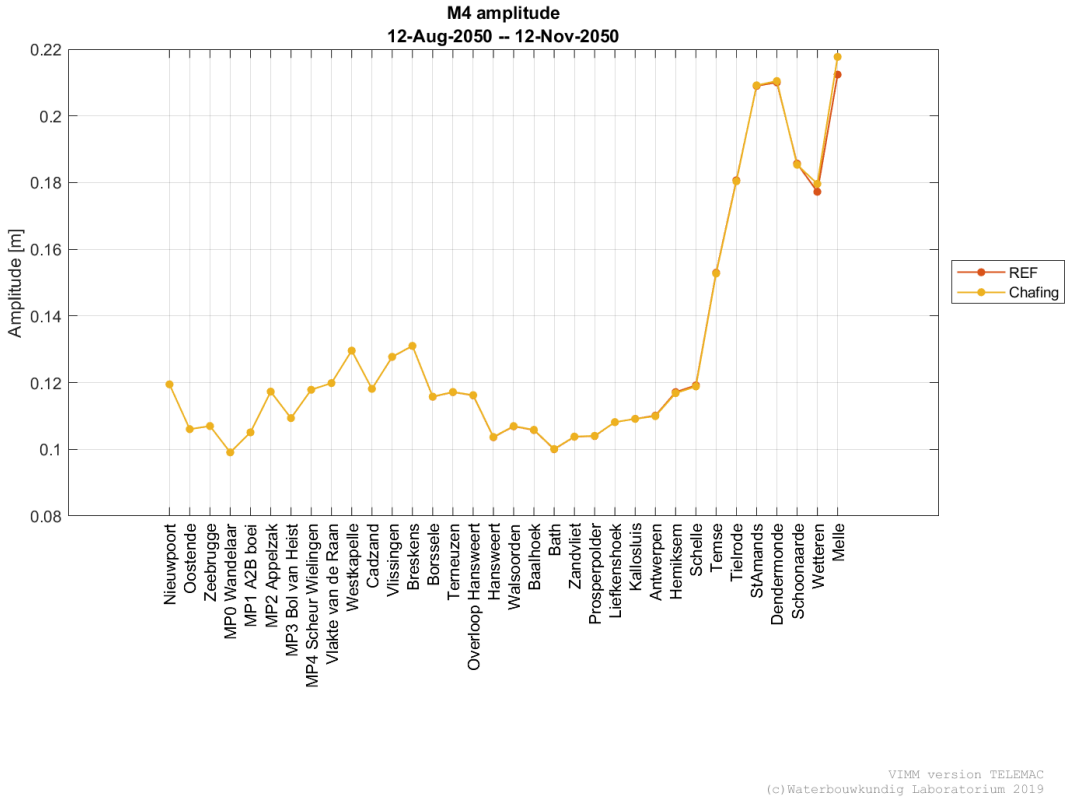

Figure 135 – M4 phase in Chafing A0CH and Reference A0CH

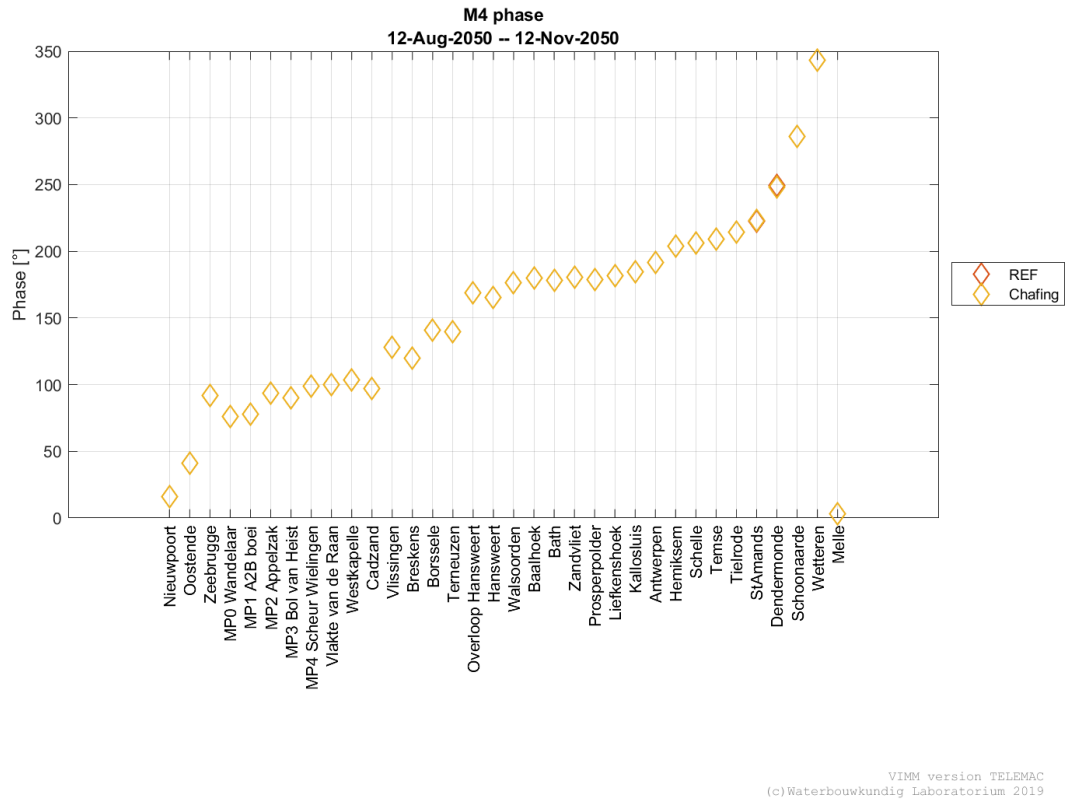

Figure 136 – S2 amplitude in Chafing A0CH and Reference A0CH

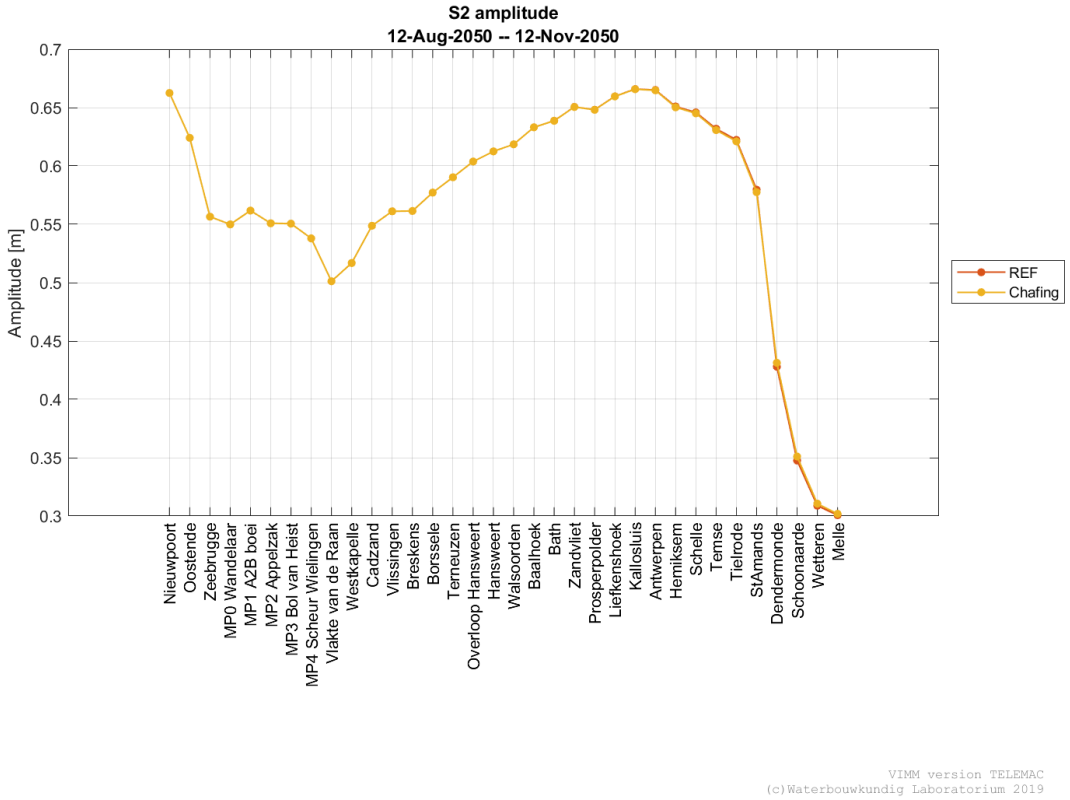

Figure 137 – S2 phase in Chafing A0CH and Reference A0CH

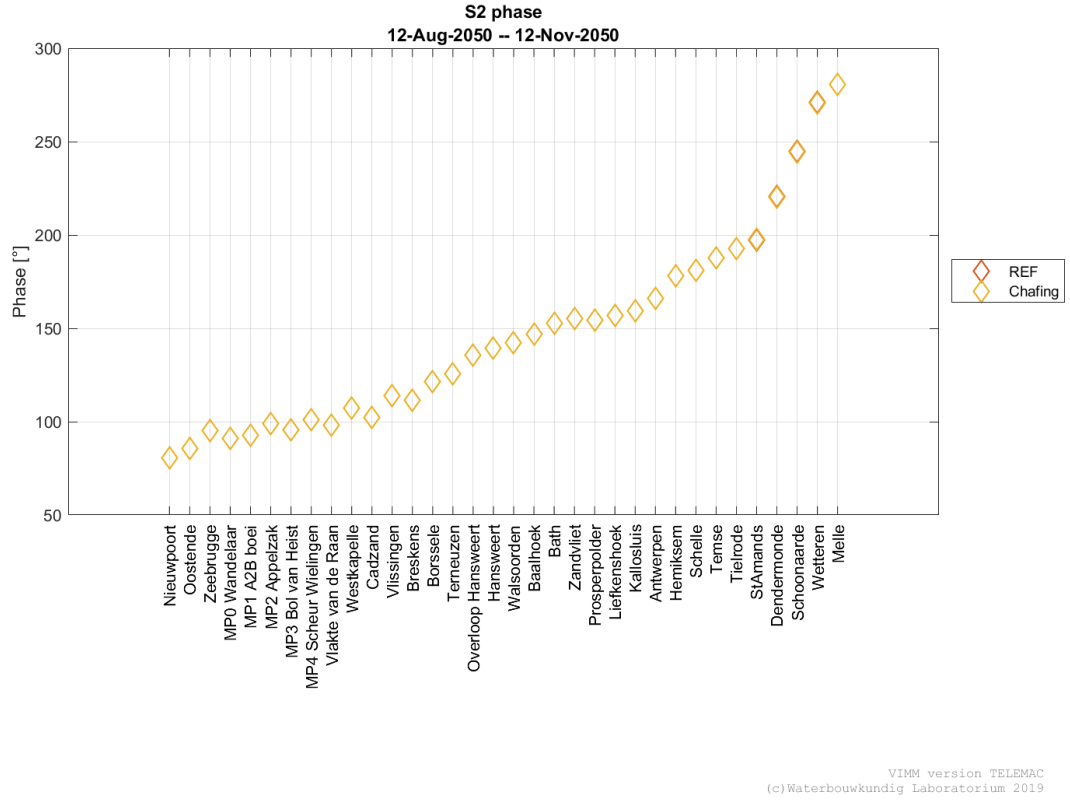

Discharges

Table 22 – Statistical parameters of complete discharge time series Chafing A0CH vs Reference A0CH

Stations	Chafing - Ref		
	BIAS TS	RMSE TS	RRMSE TS
	[m³/s]	[m³/s]	[-]
R3 Overloop van Valkenisse	-3.62	7.09	0.00
R3 Zimmermangeul	-0.16	0.57	0.00
R2 Nauw van Bath	-1.65	3.89	0.00
R2 Schaar van de Noord	-1.67	3.86	0.00
R1 Vaarwater boven Bath	-2.45	7.05	0.00
R1 Ballastplaat	-0.21	0.98	0.00
Liefkenshoek	-1.48	7.90	0.00
Oosterweel	-0.15	7.79	0.00
Kruibeke	1.45	7.65	0.00
Schelle	1.92	7.62	0.00
Temse	4.58	8.21	0.01
Driegoten	6.40	8.55	0.01
Baasrode	7.91	8.49	0.01
Dendermonde	4.32	5.52	0.01
Schoonaarde	2.95	3.68	0.01
Schellebelle	2.53	3.15	0.02
Wetteren	2.42	3.11	0.02
Melle	1.79	3.12	0.03

A0CL runs

Water levels

Table 23 – Statistical parameters of HW, LW and complete time series of water levels (Chafing_A0CL - Reference_A0CL)

Stations	Complete Time Series			HW			LW		
	BIAS	RMSE	RMSE_0	BIAS	RMSE	RMSE_0	BIAS	RMSE	RMSE_0
	[m]			[m]			[m]		
Bath	0.000	0.000	0.000	0.000	0.000	0.000	0.000	0.001	0.000
Zandvliet	0.000	0.001	0.000	0.000	0.000	0.000	0.001	0.001	0.000
Prosperpolder	0.000	0.000	0.000	0.000	0.000	0.000	0.001	0.001	0.000
Liefkenshoek	0.000	0.001	0.001	0.000	0.000	0.000	0.001	0.001	0.000
Kallosluis	0.000	0.001	0.001	0.000	0.000	0.000	0.001	0.001	0.000
Antwerpen	0.000	0.001	0.001	-0.001	0.001	0.000	0.001	0.001	0.000
Hemiksem	0.000	0.002	0.002	-0.002	0.002	0.000	0.003	0.003	0.000
Schelle	0.000	0.002	0.002	-0.002	0.002	0.000	0.003	0.003	0.000
Temse	0.001	0.004	0.004	-0.004	0.004	0.001	0.005	0.005	0.001
Tielrode	0.001	0.004	0.004	-0.005	0.005	0.001	0.006	0.006	0.001
StAmands	0.002	0.009	0.009	-0.009	0.009	0.001	0.011	0.011	0.002
Dendermonde	-0.005	0.012	0.011	0.010	0.010	0.002	-0.023	0.023	0.004
Schoonaarde	-0.004	0.013	0.012	0.010	0.010	0.002	-0.017	0.017	0.004
Wetteren	-0.005	0.010	0.009	0.005	0.005	0.002	-0.007	0.007	0.002
Melle	-0.003	0.011	0.010	0.008	0.008	0.002	0.005	0.007	0.004

Harmonic components

Figure 138 – M2 amplitude in Chafing A0CL and Reference A0CL

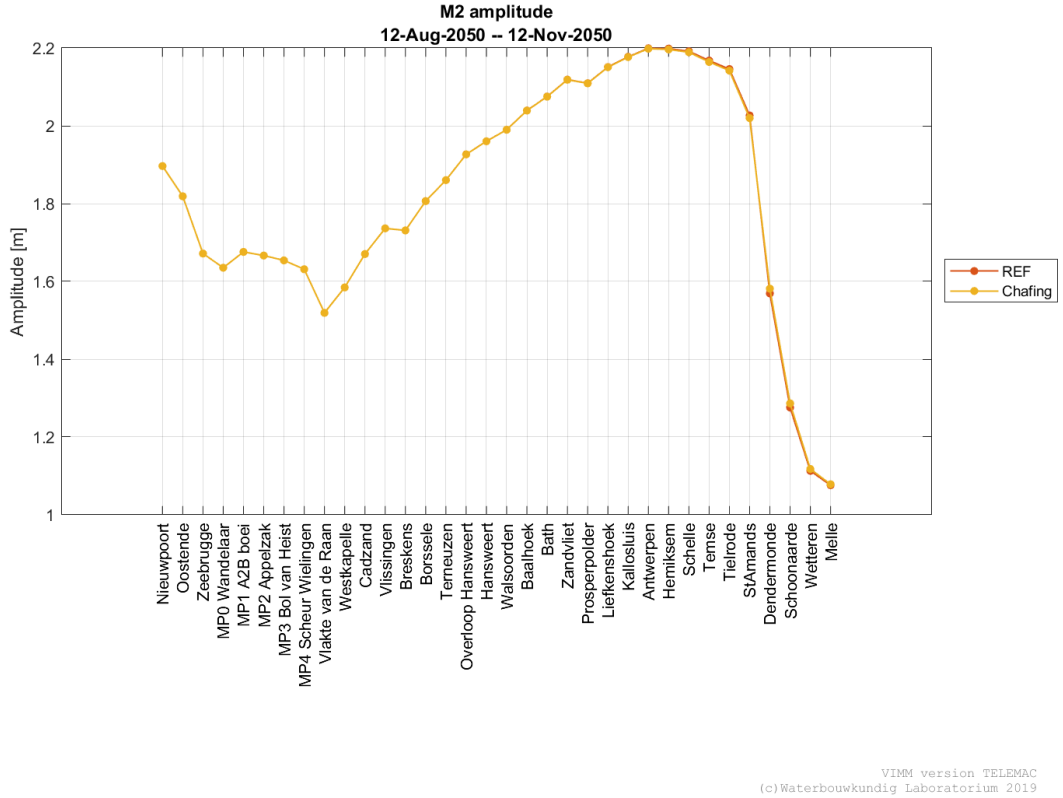

Figure 139 – M2 phase in Chafing A0CL and Reference A0CL

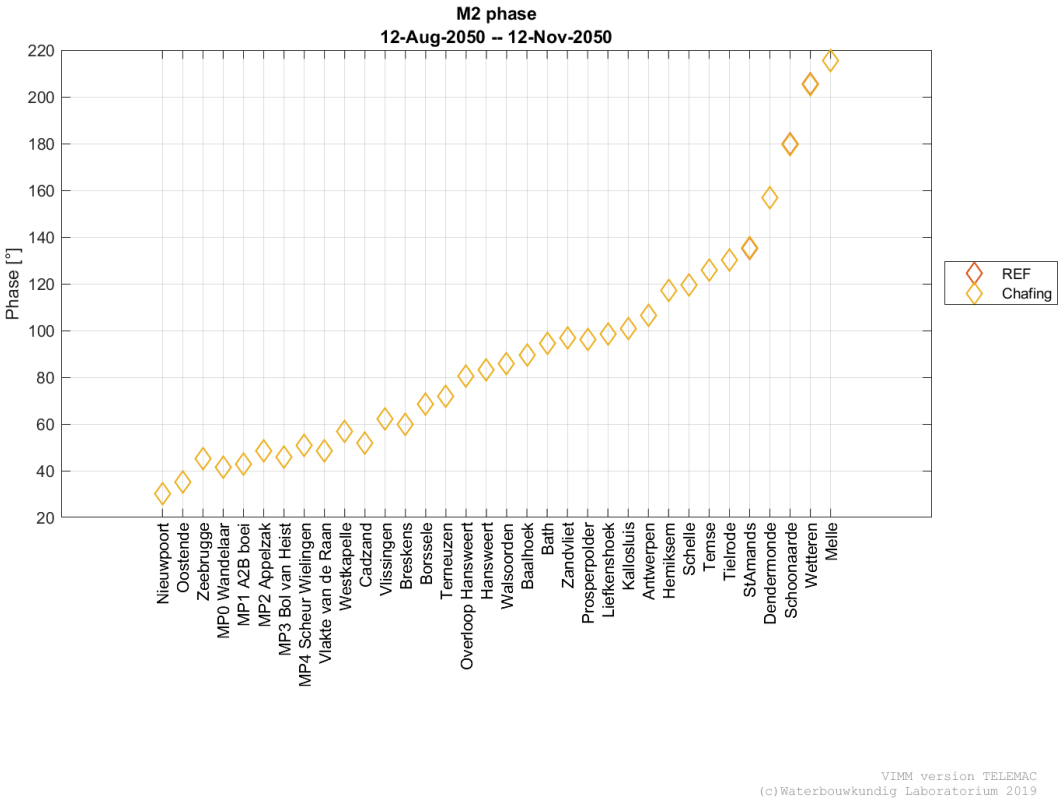

Figure 140 – M4 amplitude in Chafing A0CL and Reference A0CL

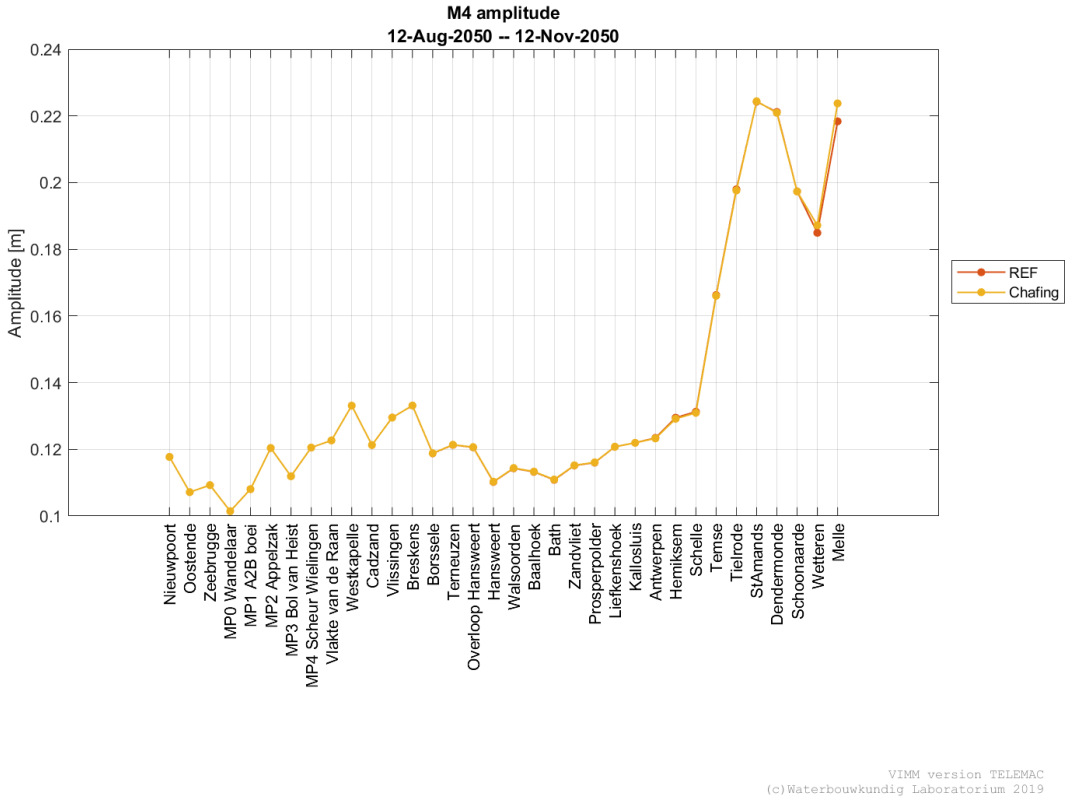

Figure 141 – M4 phase in Chafing A0CL and Reference A0CL

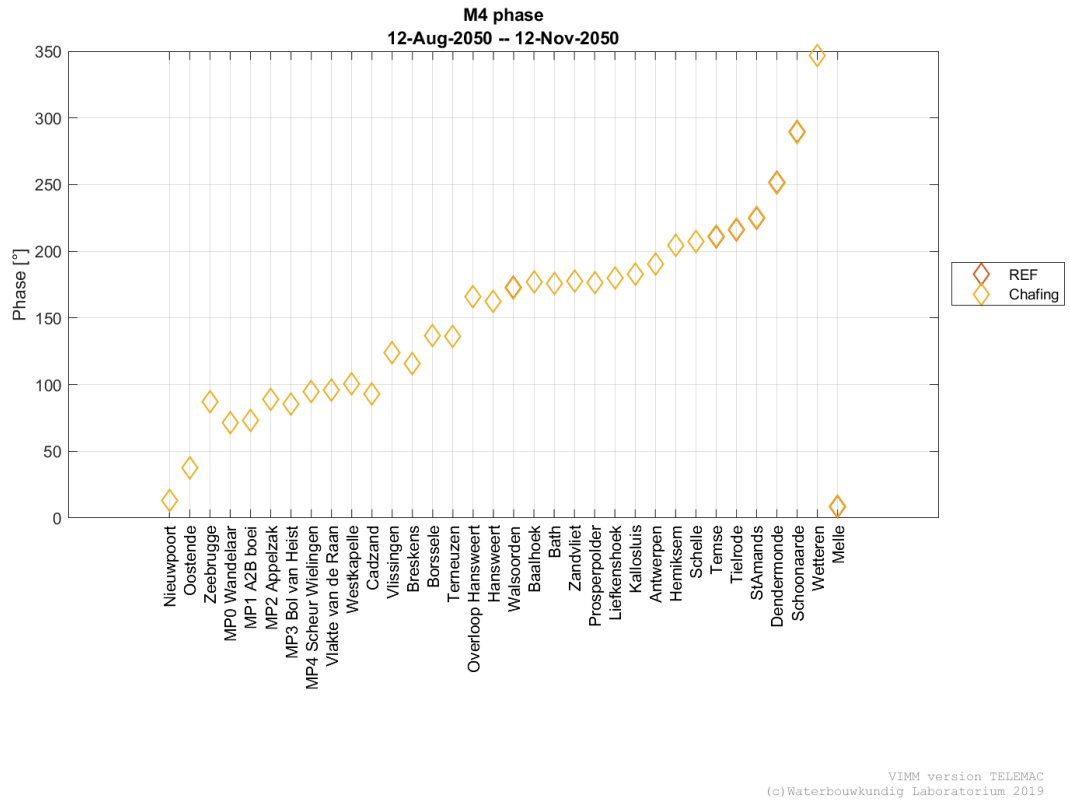

Figure 142 – S2 amplitude in Chafing A0CL and Reference A0CL

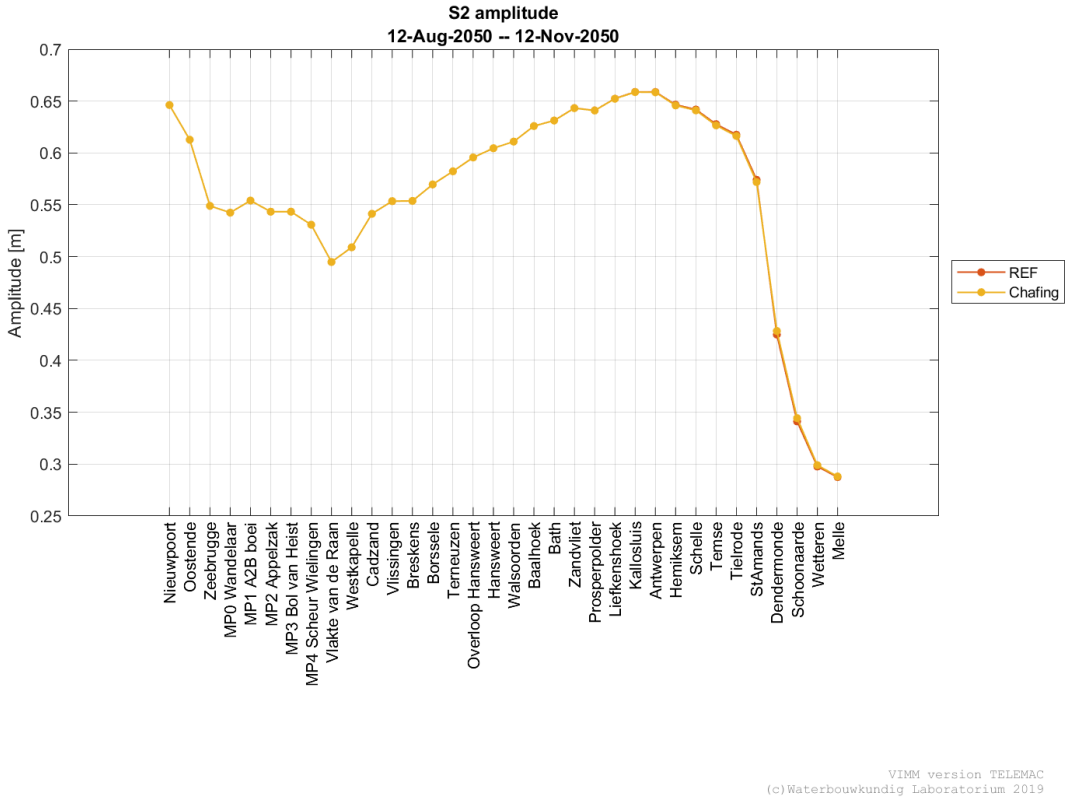

Figure 143 – S2 phase in Chafing A0CL and Reference A0CL

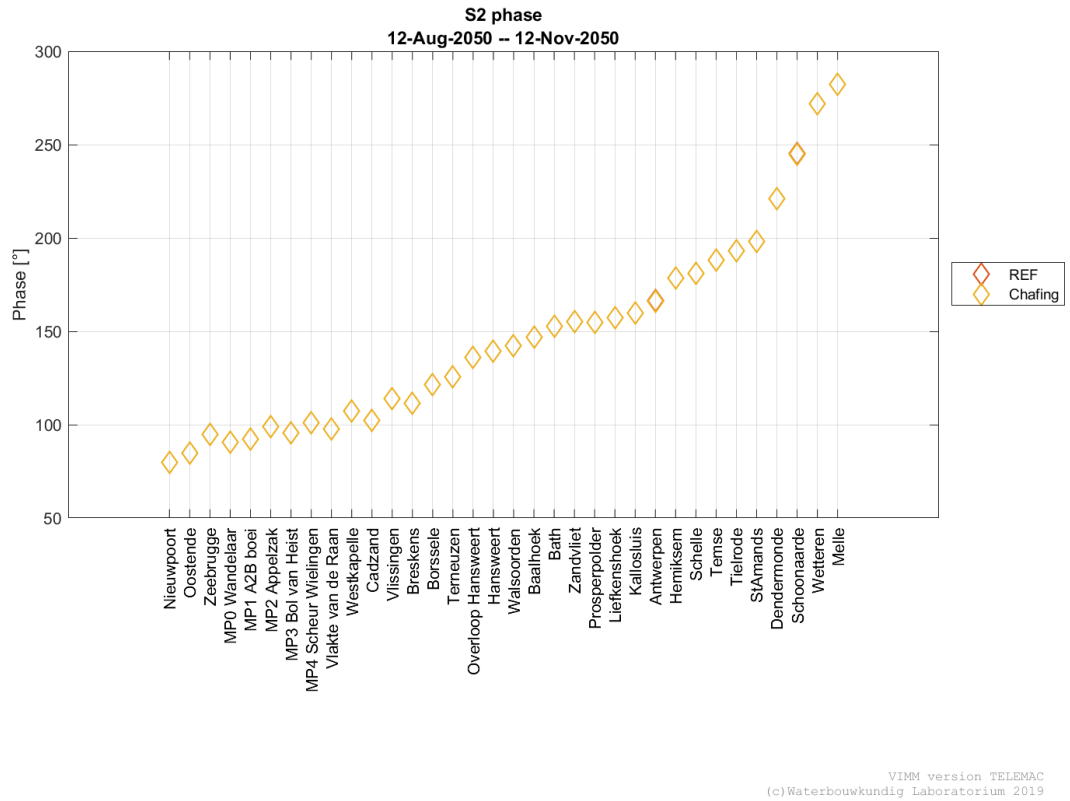

Discharges

Table 24 – Statistical parameters of complete discharge time series Chafing A0CL vs Reference A0CL

Stations	**Chafing - Ref**		
	BIAS TS	RMSE TS	RRMSE TS
	[m³/s]	[m³/s]	[-]
R3 Overloop van Valkenisse	-3.65	6.97	0.00
R3 Zimmermangeul	-0.12	0.51	0.00
R2 Nauw van Bath	-1.70	3.85	0.00
R2 Schaar van de Noord	-1.68	3.73	0.00
R1 Vaarwater boven Bath	-2.66	6.98	0.00
R1 Ballastplaat	-0.19	0.93	0.00
Liefkenshoek	-1.78	7.77	0.00
Oosterweel	-0.37	7.71	0.00
Kruibeke	1.20	7.56	0.00
Schelle	1.77	7.53	0.00
Temse	4.39	8.13	0.01
Driegoten	6.22	8.43	0.01
Baasrode	7.73	8.36	0.02
Dendermonde	4.17	5.32	0.01
Schoonaarde	2.75	3.46	0.01
Schellebelle	2.24	2.90	0.02
Wetteren	2.22	2.88	0.02
Melle	1.65	2.89	0.03

AplusCH runs

Water levels

Table 25 – Statistical parameters of HW, LW and complete time series of water levels (Chafing_AplusCH - Reference_AplusCH)

Stations	**Complete Time Series**			**HW**			**LW**		
	BIAS	RMSE	RMSE_0	BIAS	RMSE	RMSE_0	BIAS	RMSE	RMSE_0
	[m]			[m]			[m]		
Bath	0.000	0.000	0.000	0.000	0.000	0.000	0.000	0.001	0.000
Zandvliet	0.000	0.000	0.000	0.000	0.000	0.000	0.001	0.001	0.000
Prosperpolder	0.000	0.000	0.000	0.000	0.000	0.000	0.000	0.001	0.000
Liefkenshoek	0.000	0.001	0.001	0.000	0.000	0.000	0.001	0.001	0.000
Kallosluis	0.000	0.001	0.001	0.000	0.000	0.000	0.001	0.001	0.000
Antwerpen	0.000	0.001	0.001	-0.001	0.001	0.000	0.001	0.001	0.000
Hemiksem	0.000	0.002	0.002	-0.002	0.002	0.000	0.003	0.003	0.000
Schelle	0.000	0.002	0.002	-0.002	0.002	0.000	0.003	0.003	0.000
Temse	0.001	0.004	0.004	-0.004	0.004	0.001	0.005	0.005	0.001
Tielrode	0.001	0.005	0.004	-0.004	0.005	0.001	0.006	0.006	0.001
StAmands	0.002	0.009	0.009	-0.007	0.007	0.001	0.012	0.012	0.002
Dendermonde	-0.006	0.012	0.011	0.009	0.009	0.002	-0.025	0.026	0.004
Schoonaarde	-0.005	0.014	0.013	0.009	0.009	0.002	-0.022	0.022	0.004
Wetteren	-0.005	0.011	0.010	0.008	0.008	0.003	-0.009	0.010	0.003
Melle	-0.004	0.011	0.010	0.010	0.010	0.003	0.002	0.004	0.004

Harmonic components

Figure 144 – M2 amplitude in Chafing AplusCH and Reference AplusCH

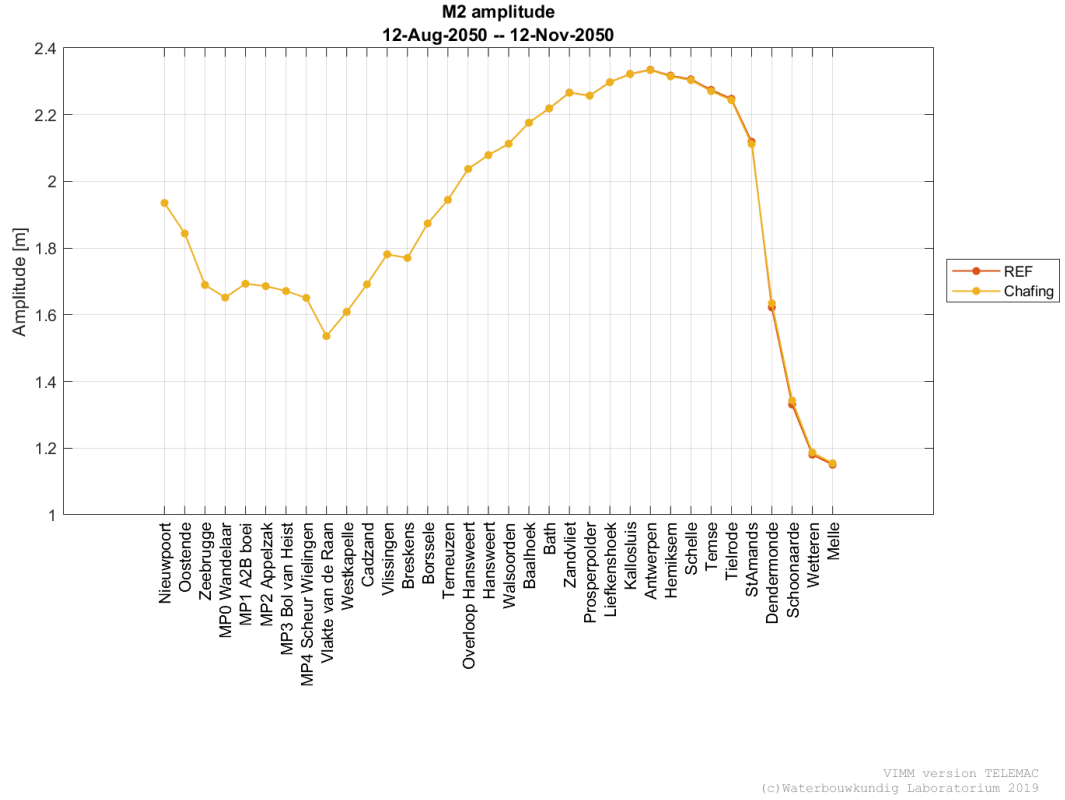

Figure 145 – M2 phase in Chafing AplusCH and Reference AplusCH

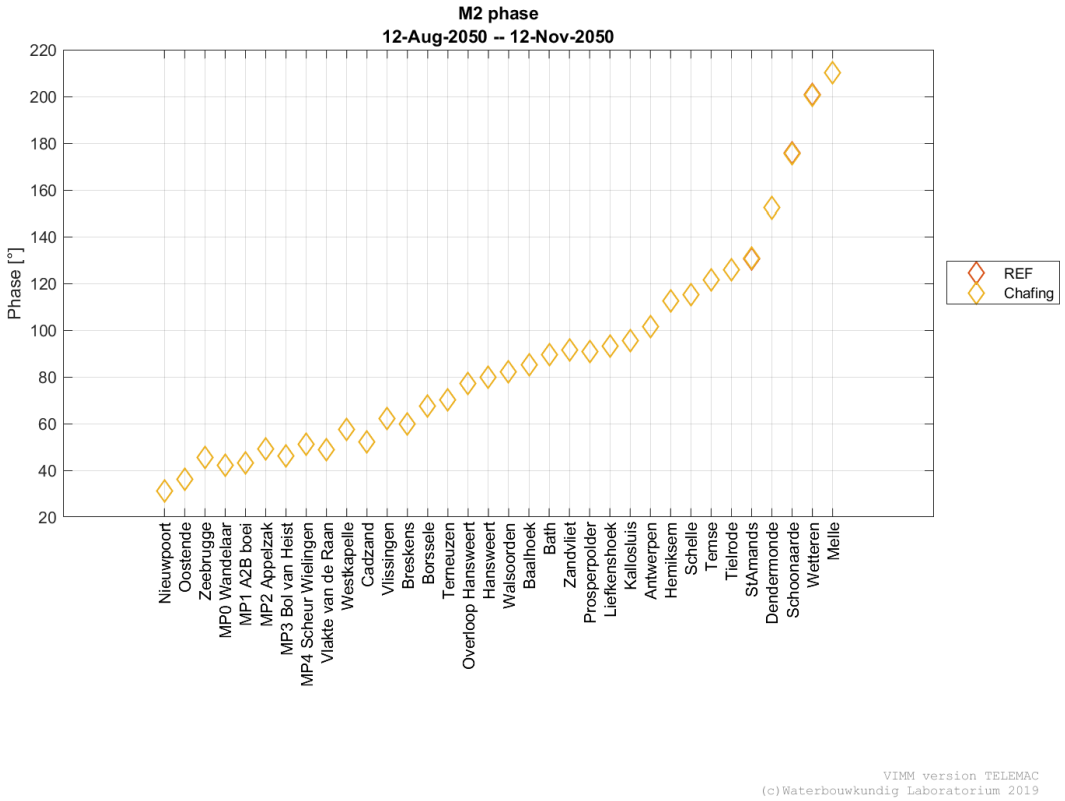

Figure 146 – M4 amplitude in Chafing AplusCH and Reference AplusCH

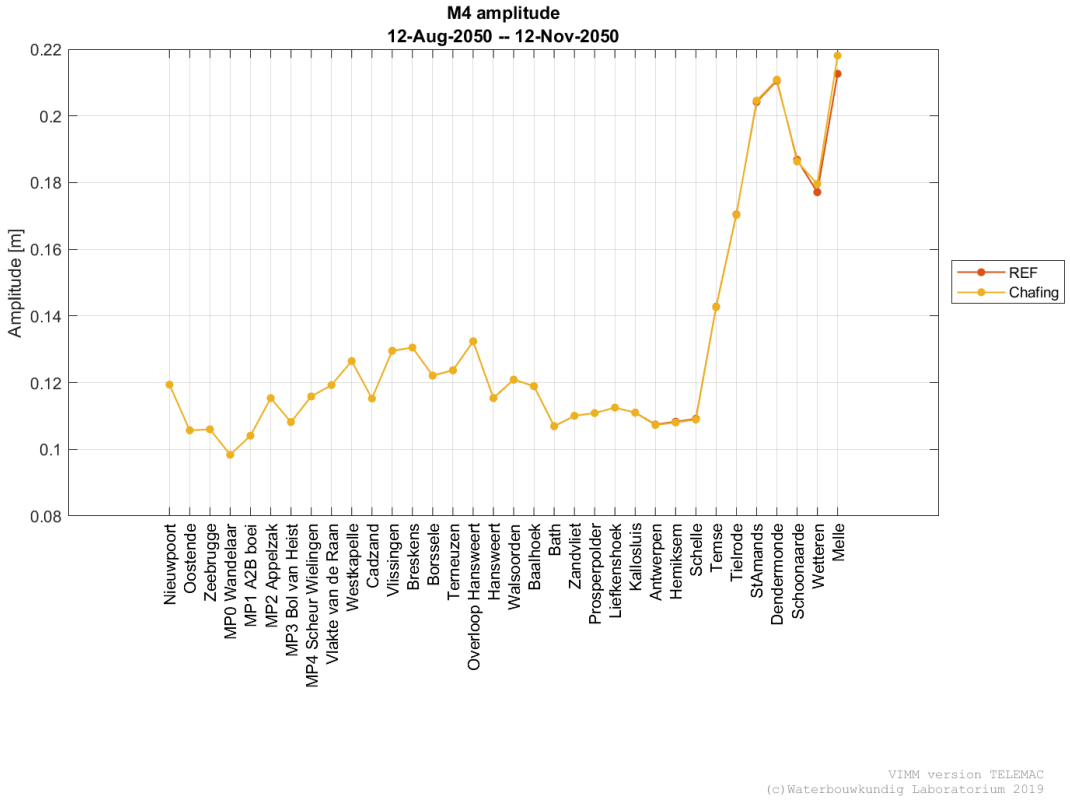

Figure 147 – M4 phase in Chafing AplusCH and Reference AplusCH

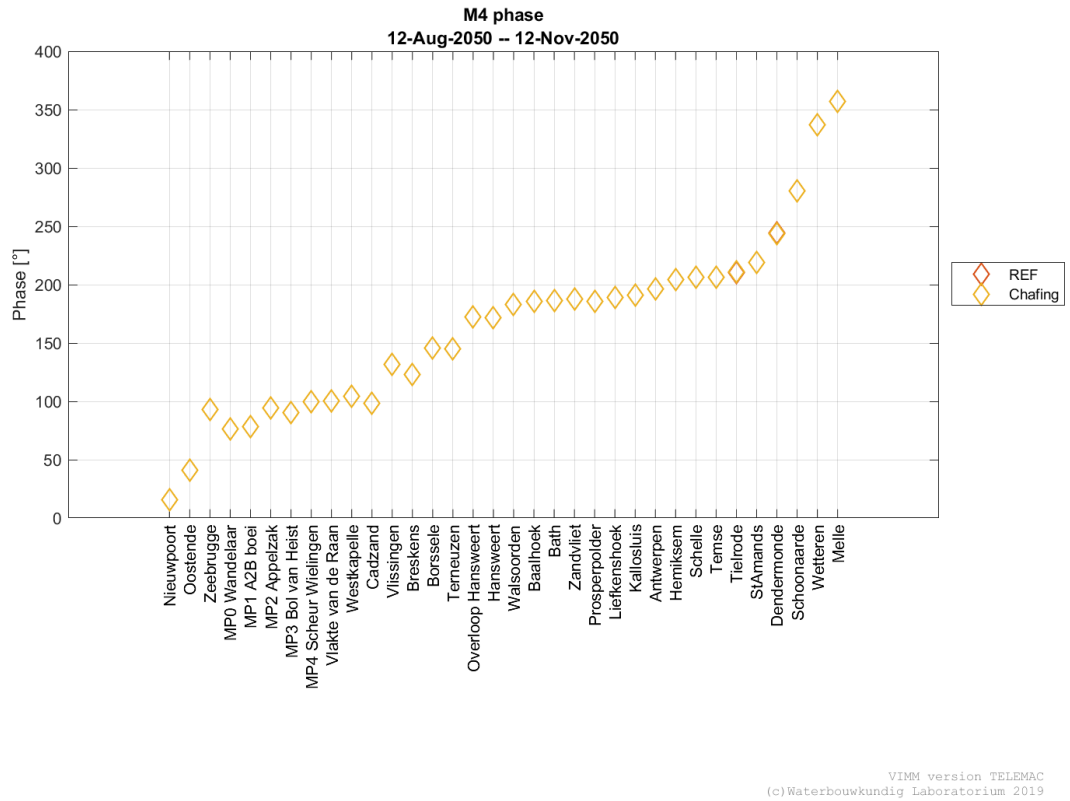

Figure 148 – S2 amplitude in Chafing AplusCH and Reference AplusCH

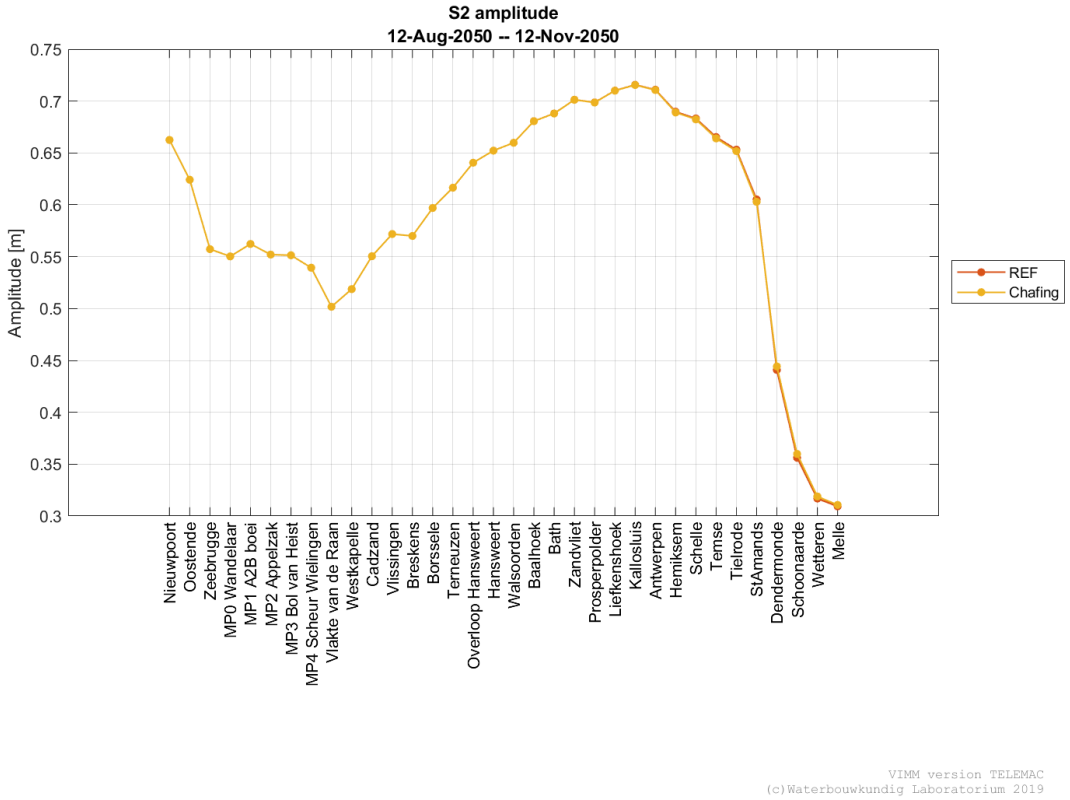

Figure 149 – S2 phase in Chafing AplusCH and Reference AplusCH

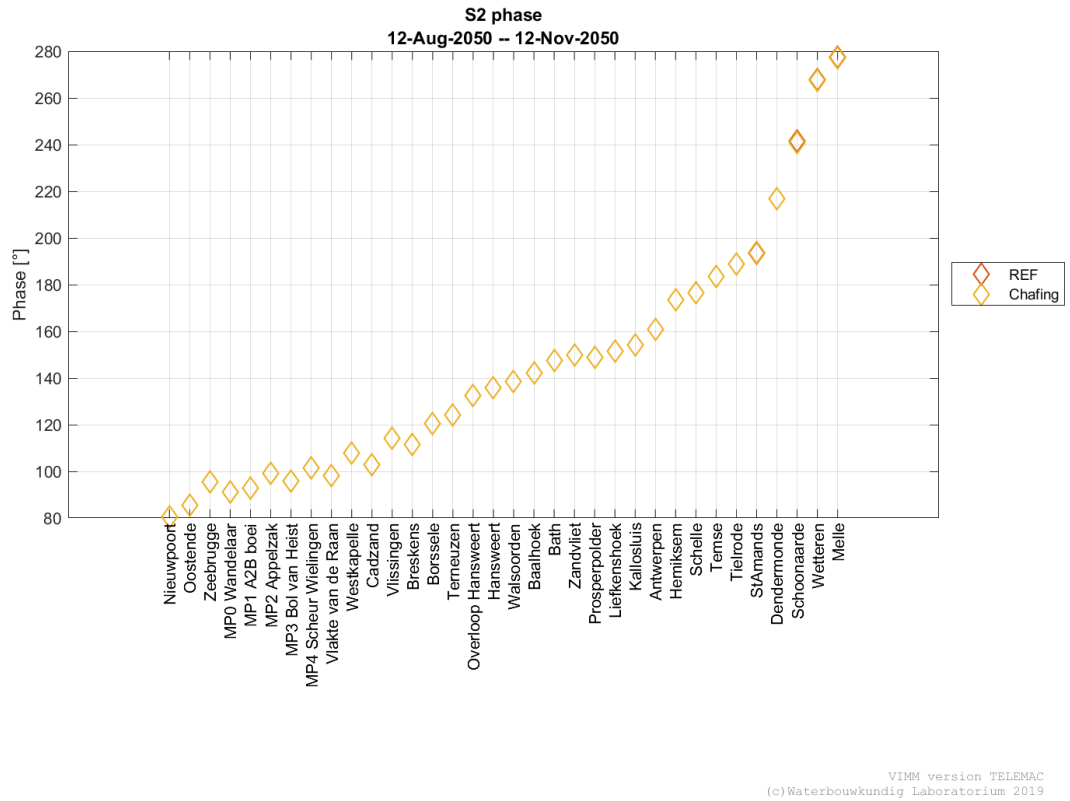

Discharges

Table 26 – Statistical parameters of complete discharge time series Chafing AplusCH vs Reference AplusCH

Stations	**Chafing - Ref**		
	BIAS TS	RMSE TS	RRMSE TS
	[m³/s]	[m³/s]	[-]
R3 Overloop van Valkenisse	-3.77	7.41	0.00
R3 Zimmermangeul	-0.18	0.63	0.00
R2 Nauw van Bath	-1.73	4.04	0.00
R2 Schaar van de Noord	-1.72	4.13	0.00
R1 Vaarwater boven Bath	-2.52	7.14	0.00
R1 Ballastplaat	-0.23	1.07	0.00
Liefkenshoek	-1.56	7.93	0.00
Oosterweel	-0.23	7.78	0.00
Kruibeke	1.39	7.62	0.00
Schelle	1.99	7.59	0.00
Temse	4.61	8.23	0.01
Driegoten	6.44	8.68	0.01
Baasrode	8.24	8.89	0.01
Dendermonde	4.61	5.84	0.01
Schoonaarde	3.00	3.76	0.01
Schellebelle	2.17	2.95	0.02
Wetteren	2.10	2.87	0.02
Melle	1.46	2.81	0.03

AminCL runs

Water levels

Table 27 – Statistical parameters of HW, LW and complete time series of water levels (Chafing_AminCL - Reference_AminCL)

Stations	Complete Time Series			HW			LW		
	BIAS	RMSE	RMSE_0	BIAS	RMSE	RMSE_0	BIAS	RMSE	RMSE_0
	[m]			[m]			[m]		
Bath	0.000	0.000	0.000	0.000	0.000	0.000	0.000	0.000	0.000
Zandvliet	0.000	0.001	0.001	0.000	0.000	0.000	0.000	0.000	0.000
Prosperpolder	0.000	0.001	0.001	0.000	0.000	0.000	0.000	0.000	0.000
Liefkenshoek	0.000	0.001	0.001	0.000	0.000	0.000	0.000	0.000	0.000
Kallosluis	0.000	0.001	0.001	0.000	0.000	0.000	0.001	0.001	0.000
Antwerpen	0.000	0.001	0.001	-0.001	0.001	0.000	0.001	0.001	0.000
Hemiksem	0.000	0.002	0.002	-0.002	0.002	0.000	0.002	0.003	0.000
Schelle	0.000	0.002	0.002	-0.002	0.002	0.000	0.003	0.003	0.000
Temse	0.001	0.003	0.003	-0.004	0.004	0.001	0.004	0.005	0.001
Tielrode	0.001	0.004	0.004	-0.005	0.005	0.001	0.005	0.005	0.001
StAmands	0.001	0.008	0.008	-0.009	0.010	0.002	0.010	0.010	0.002
Dendermonde	-0.005	0.011	0.010	0.010	0.011	0.002	-0.021	0.022	0.003
Schoonaarde	-0.004	0.012	0.011	0.010	0.010	0.002	-0.015	0.016	0.004
Wetteren	-0.005	0.010	0.008	0.004	0.004	0.002	-0.006	0.007	0.002
Melle	-0.003	0.011	0.010	0.007	0.007	0.002	0.006	0.007	0.004

Harmonic components

Figure 150 – M2 amplitude in Chafing AminCL and Reference AminCL

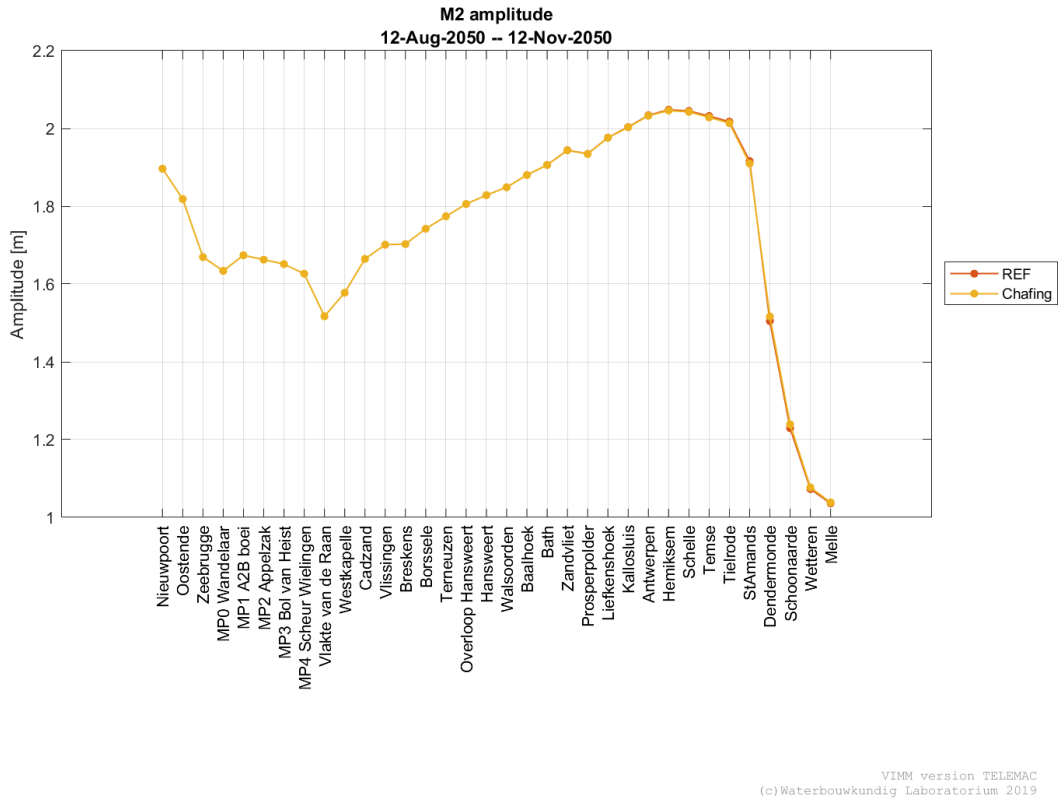

Figure 151 – M2 phase in Chafing AminCL and Reference AminCL

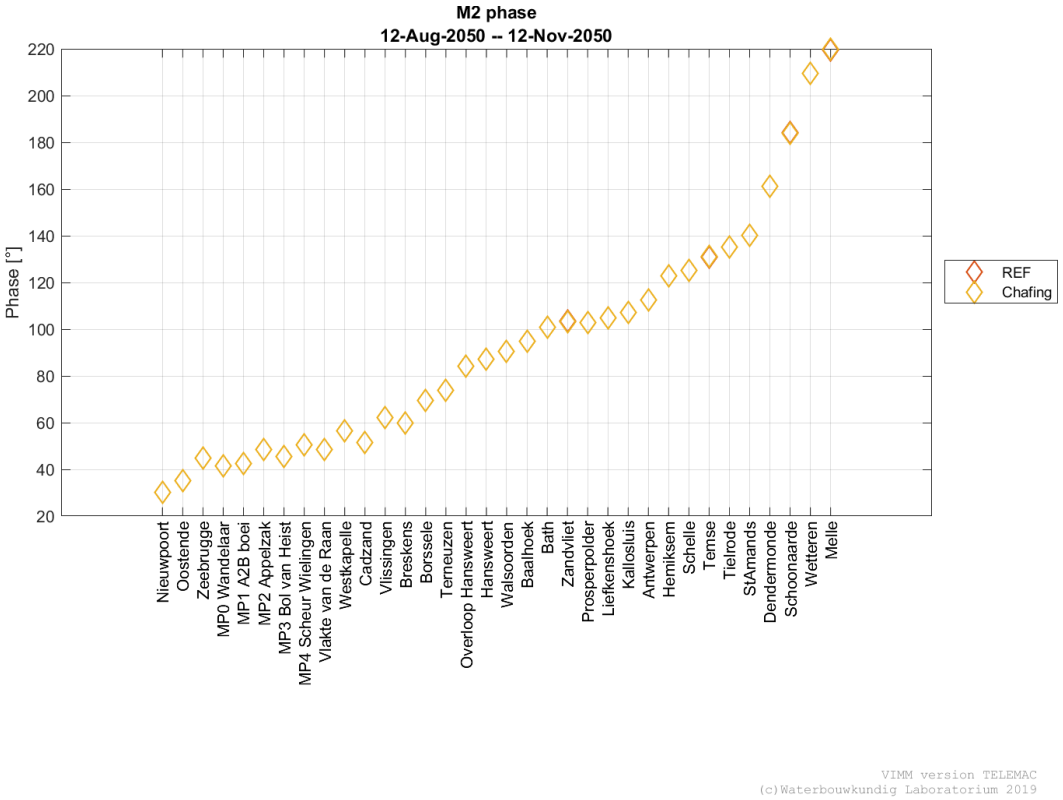

Figure 152 – M4 amplitude in Chafing AminCL and Reference AminCL

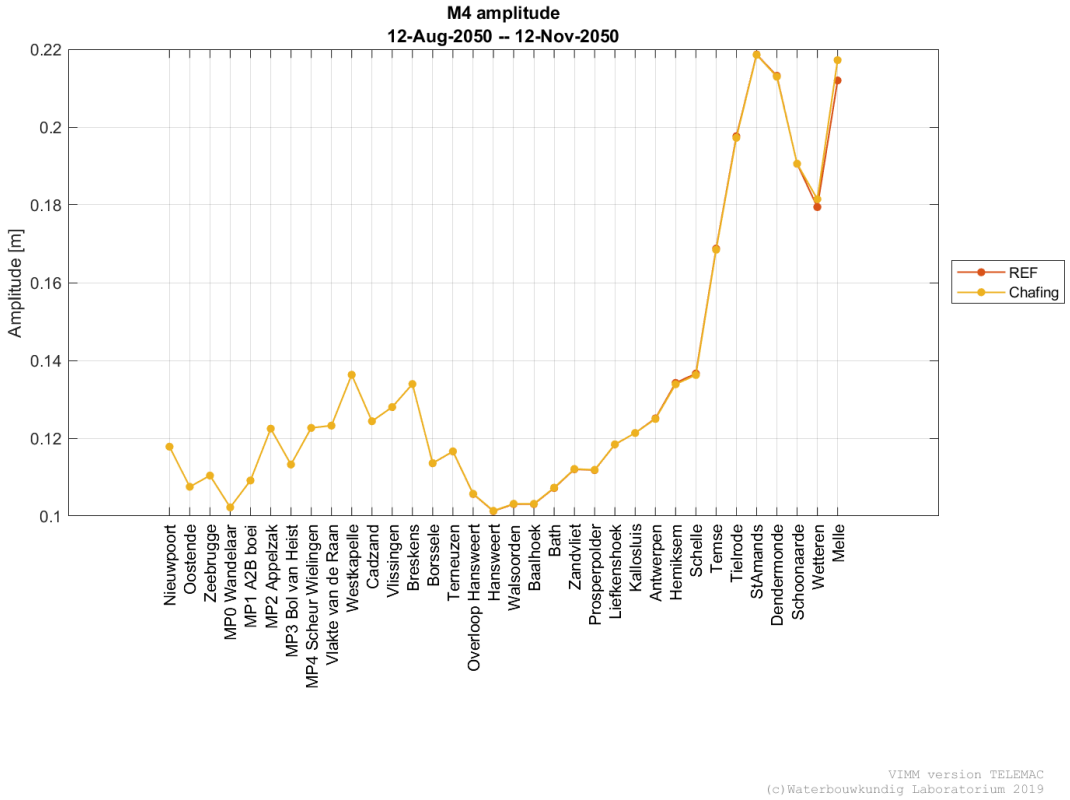

Figure 153 – M4 phase in Chafing AminCL and Reference AminCL

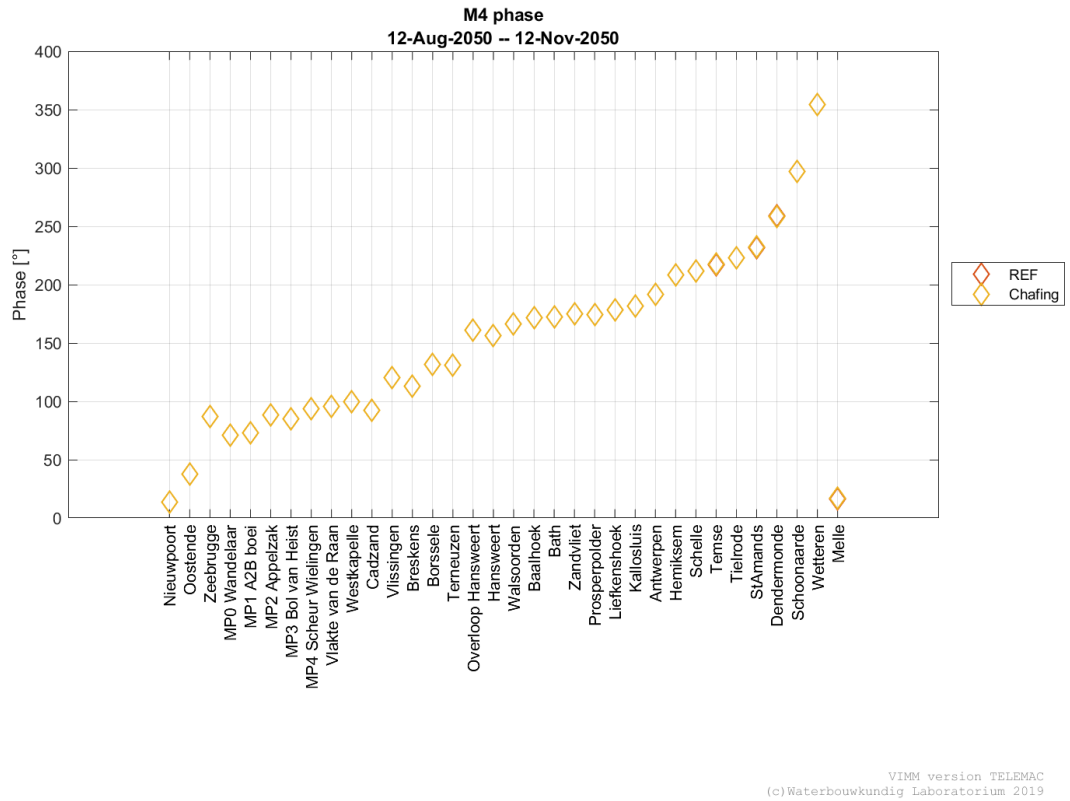

Figure 154 – S2 amplitude in Chafing AminCL and Reference AminCL

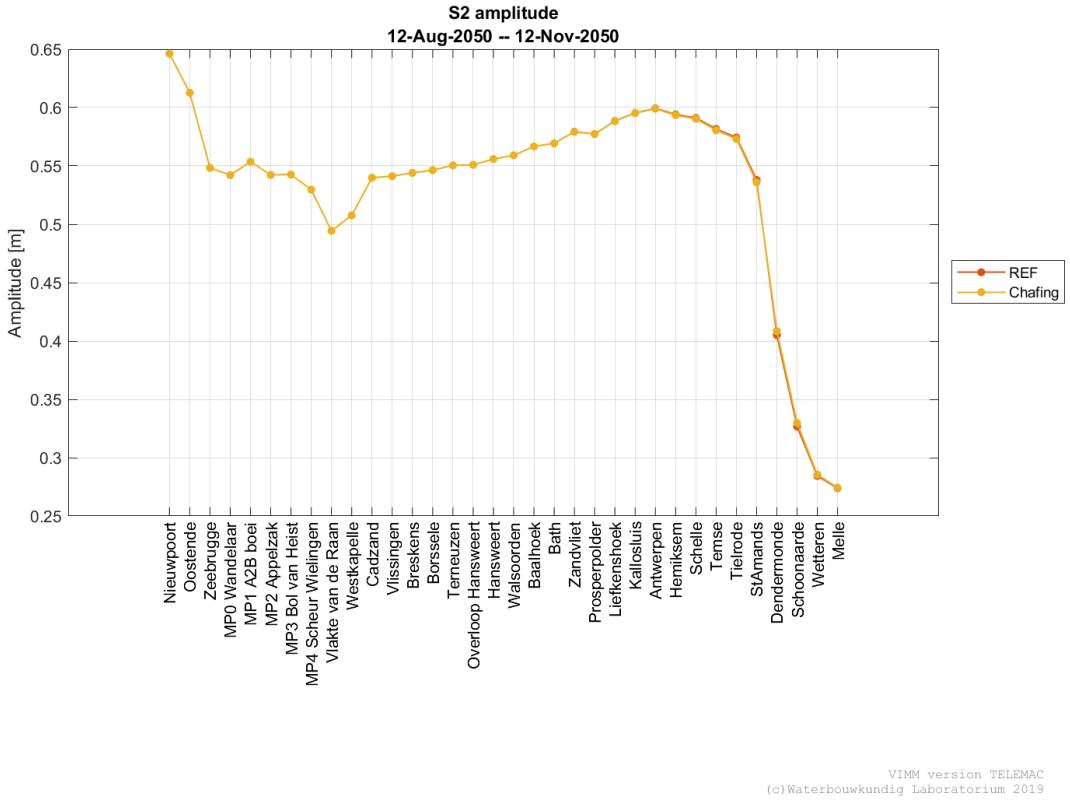

Figure 155 – S2 phase in Chafing AminCL and Reference AminCL

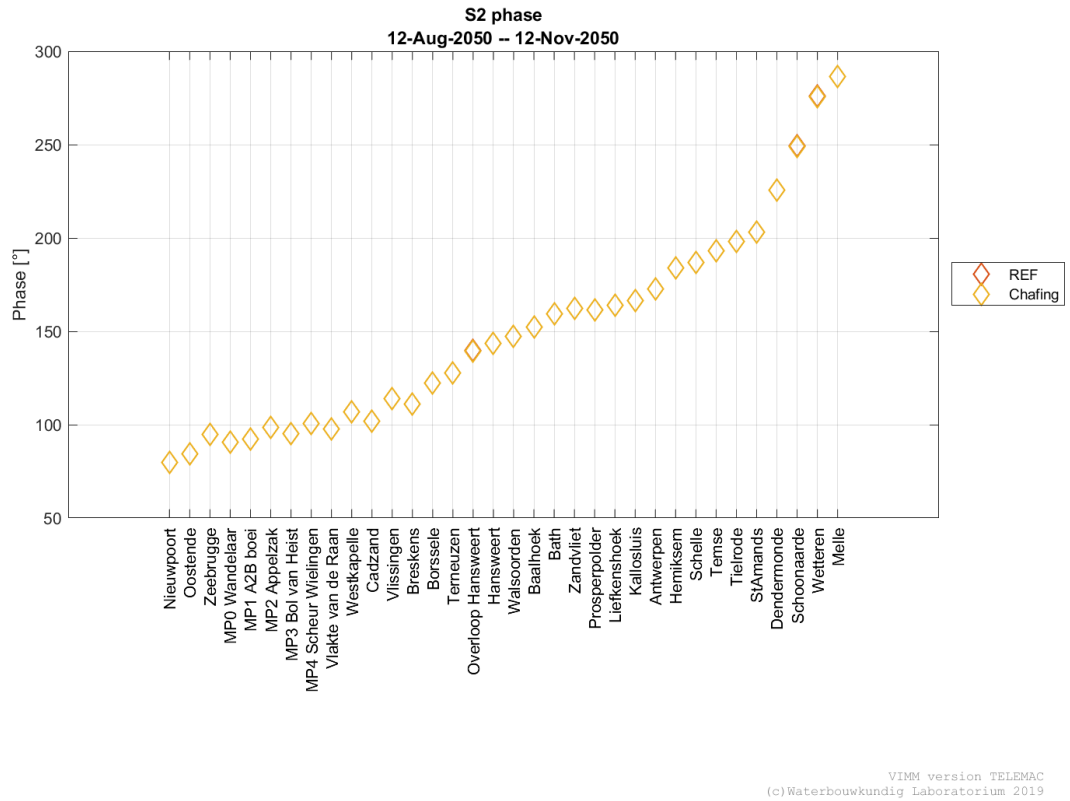

Discharges

Table 28 – Statistical parameters of complete discharge time series Chafing AminCL vs Reference AminCL

Stations	**Chafing - Ref**		
	BIAS TS	RMSE TS	RRMSE TS
	[m³/s]	[m³/s]	[-]
R3 Overloop van Valkenisse	-3.47	6.59	0.00
R3 Zimmermangeul	-0.14	0.43	0.00
R2 Nauw van Bath	-1.64	3.66	0.00
R2 Schaar van de Noord	-1.61	3.39	0.00
R1 Vaarwater boven Bath	-2.46	6.79	0.00
R1 Ballastplaat	-0.17	0.69	0.00
Liefkenshoek	-1.64	7.55	0.00
Oosterweel	-0.27	7.54	0.00
Kruibeke	1.18	7.40	0.00
Schelle	1.72	7.36	0.00
Temse	4.21	7.95	0.01
Driegoten	5.94	8.16	0.01
Baasrode	7.42	7.97	0.02
Dendermonde	4.00	5.05	0.01
Schoonaarde	2.66	3.34	0.01
Schellebelle	2.24	2.86	0.02
Wetteren	2.23	2.86	0.02
Melle	1.68	2.88	0.03

Tidal asymmetry in runs with different boundary conditions

Figure 156 – Tidal asymmetry (T increase/Tdecrease water level) in Chafing and Reference runs

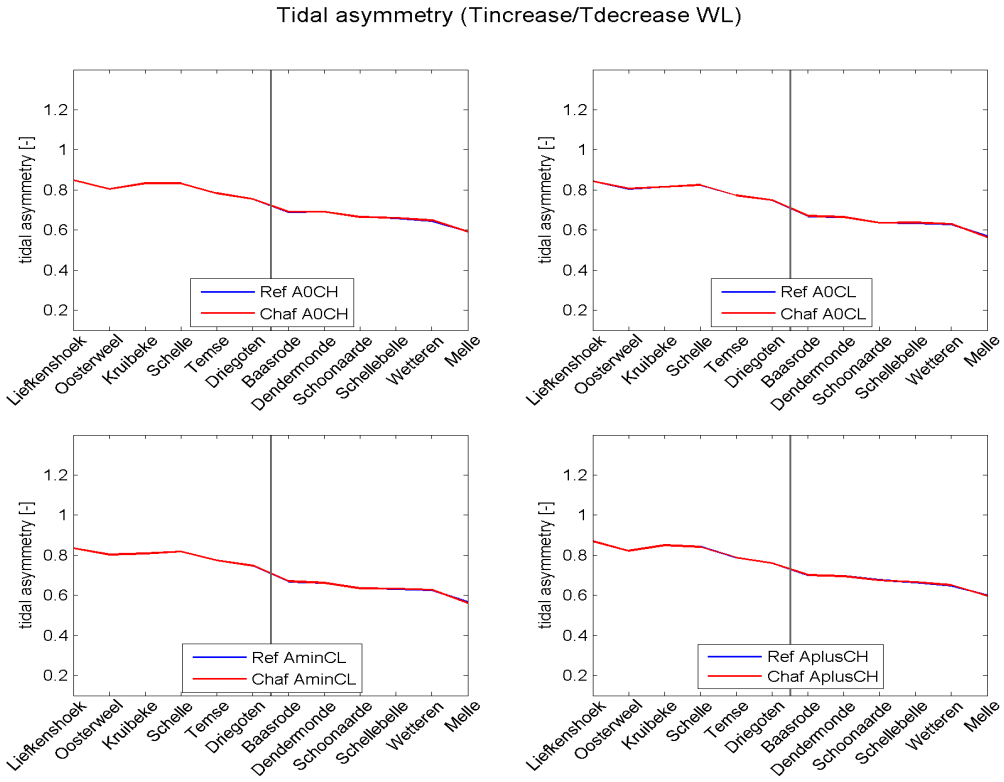

Figure 157 – Tidal asymmetry (T flood/T ebb) in Chafing and Reference runs

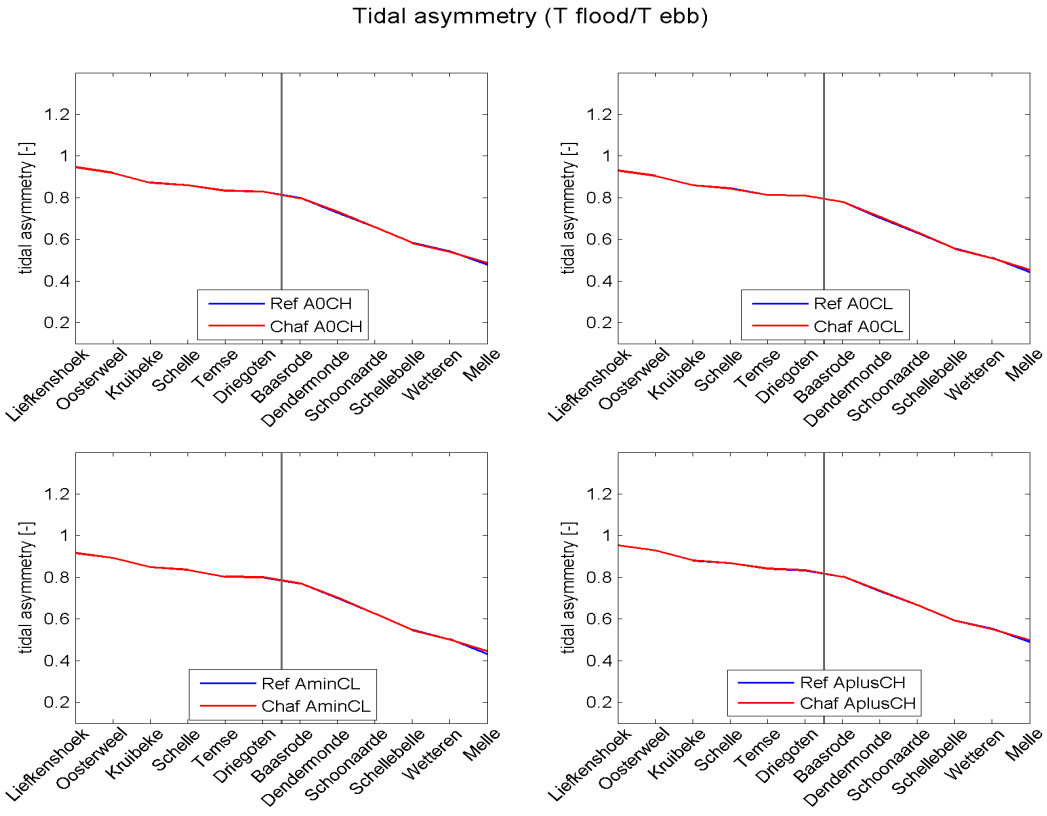

Figure 158 – Tidal asymmetry (V max flood/Vmax ebb) in Chafing and Reference runs

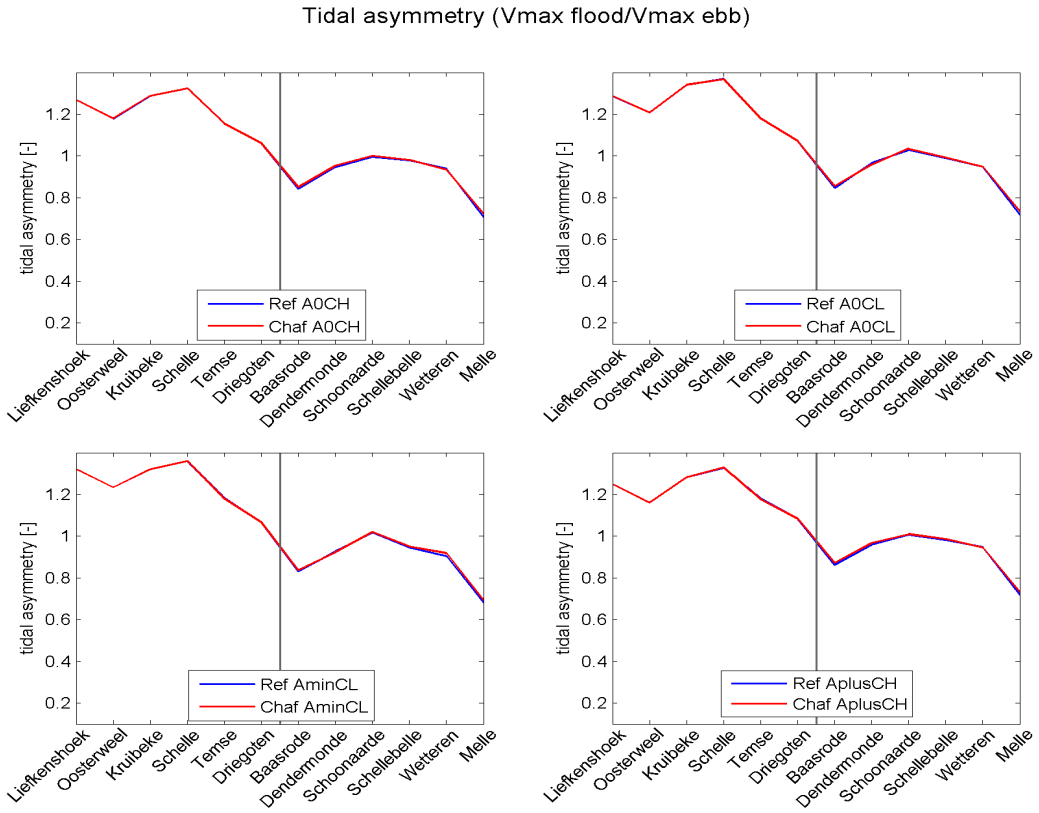

Figure 159 – Tidal asymmetry (based on V^3) in Chafing and Reference runs

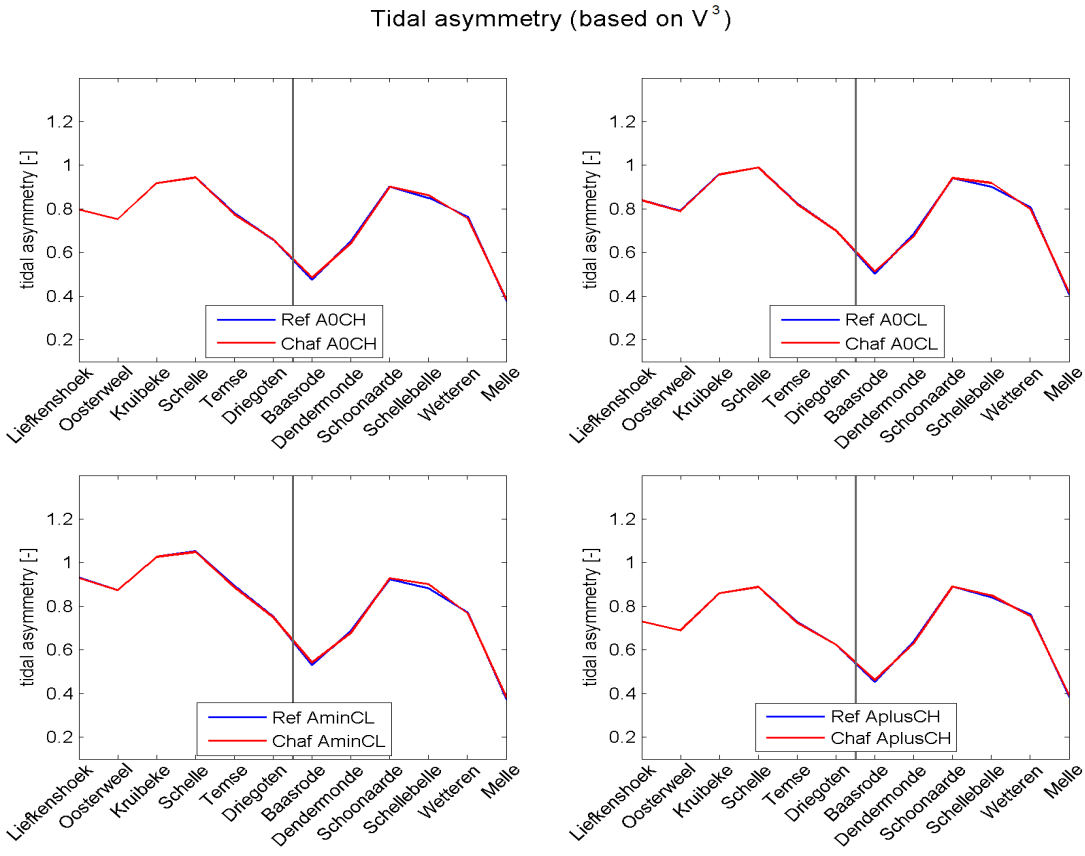

Figure 160 – Tidal asymmetry (based on V^4) in Chafing and Reference runs

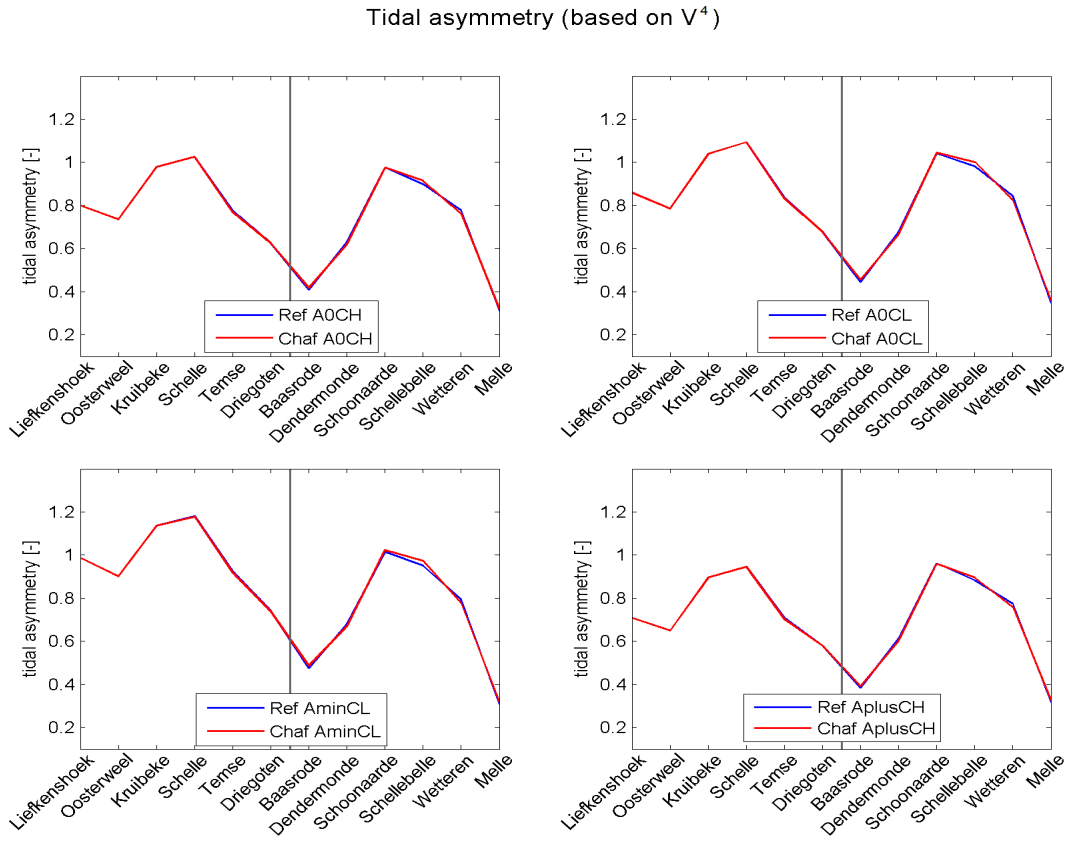

DEPARTMENT **MOBILITY & PUBLIC WORKS**
Flanders hydraulics Research

Berchemlei 115, 2140 Antwerp
T +32 (0)3 224 60 35
F +32 (0)3 224 60 36
waterbouwkundiglabo@vlaanderen.be
www.flandershydraulicsresearch.be